

**X-RAY STUDIES ON Pt/Re
AND OTHER COMPOUNDS**

A thesis submitted in partial fulfilment
for the degree of Doctor of Philosophy
in the University of Glasgow

by

sayyed Ali Asghar Torabi

Chemistry Department

Glasgow University

June 1996

© A. A. Torabi 1996

ProQuest Number: 13833393

All rights reserved

INFORMATION TO ALL USERS

The quality of this reproduction is dependent upon the quality of the copy submitted.

In the unlikely event that the author did not send a complete manuscript and there are missing pages, these will be noted. Also, if material had to be removed, a note will indicate the deletion.



ProQuest 13833393

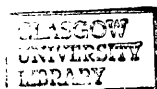
Published by ProQuest LLC (2019). Copyright of the Dissertation is held by the Author.

All rights reserved.

This work is protected against unauthorized copying under Title 17, United States Code
Microform Edition © ProQuest LLC.

ProQuest LLC.
789 East Eisenhower Parkway
P.O. Box 1346
Ann Arbor, MI 48106 – 1346

Theris
10481
Copy 1



ACKNOWLEDGEMENTS

I wish to express my sincere thanks to my supervisor Dr. K. W. Muir for his great encouragement and guidance throughout the course of this work and, in particular, for his theoretical and practical teaching of the work undertaken. His assistance during of the writing of this thesis has been very much appreciated.

I would also especially like to thank Dr Lj. Manojlovic-Muir for her unfailing help and encouragement, particularly with platinum rhenium cluster work.

My thanks go to Professor R. J. Puddephatt, Professor G. Kirby, Professor D. Robins, Dr. Knox and Dr. Davidson and their respective research groups for providing me with the crystals for my research.

I would also like to thank all friends met over the years I have spent in Glasgow.

I thank my wife Nahid for her patience and encouragement during my stay in the UK.

Finally, I am grateful to Zanzan University and the Ministry of Culture and Higher Education of Iran for their financial support which enabled me to carry out this work.

CONTENTS

	Page No.
SUMMARY	1
SECTION 1 - X-ray crystal structure analysis	3
Introduction	3
Crystal	3
Intensity	7
Measurements and diffractometers	8
Data processing	9
The polarisation factor	9
Absorption and related corrections	10
Extinction	11
Structure analysis	11
Atomic scattering factor	12
Temperature factor	13
Structure solution	14
Direct methods	14
Heavy atom method	16
Refinement	17
The residual index	18
Computer programs	18
CAD4EXPRESS	18
The GX package	19
SHELX programs	19
Drawing programs	20
Geometry	20

References	21
SECTION 2 - The structures of Pt/Re heterometallic cluster compounds and related complexes stabilised by diphosphine ligands	22
Chapter 2.1 - Stabilisation of metal cluster complexes by diphosphine ligands	23
2.1.1. Diphosphine ligands	23
2.1.2. Bonding mode of the bis(diphenylphosphino)methane ligand	25
2.1.3. A bimetallic ruthenium complex $[\text{Ru}_2\text{Cl}_3\text{H}(\text{CO})_2(\mu\text{-dppm})_2]$	30
Introduction	30
Results and discussion	30
Experimental	32
Caption to Figures	34
Chapter 2.2- The structures of Pt_3Re cluster complexes	40
2.2.1. Introduction	40
2.2.2. The structure of $[\text{Pt}_3(\text{ReO}_3)(\mu\text{-dppm})_3][\text{ReO}_4]$	41
Experimental	44
Captions to Figures	45
2.2.3. The structure of $[\text{Pt}_3(\text{ReO}_3)(\mu\text{-dppm})_3][\text{PF}_6]$	54
Experimental	56
Captions to Figures	58
2.2.4. The structure of $[\text{Pt}_3\{\text{Re}(\text{CO})_3\text{P}(\text{OPh})_3\}(\mu\text{-dppm})_3][\text{PF}_6]$	65
Experimental	67
Captions to Figures	68
2.2.5. The structure of $[\text{Pt}_3\text{IRe}(\text{CO})_3(\mu\text{-dppm})_3]$	78
Experimental	80
Captions to Figures	81
2.2.6. The structure of $[\text{Pt}_3\text{Re}(\text{CO})_2\{\text{P}(\text{OMe})_3\}(\mu\text{-O})_2(\mu\text{-dppm})_3][\text{AsF}_6]$	90

Experimental	92
Captions to Figures	93
2.2.7. The structure of $[\{\text{Pt}(\text{PPr}_3^i)_3\}_3(\mu\text{-CO})_3(\mu_3\text{-ReO}_3)]^+$	102
Chapter 2.3 - Chemistry of binuclear Pt-Re complexes	104
2.3.1. Introduction	104
2.3.2. Chemical reactions	104
2.3.3. Current views on bonding in Pt/Re Clusters	112
2.2.4. Bimetallic Pt/Re catalysis	117
Use of Pt/Re	117
Conclusion	119
References	120
SECTION 3 - Stereochemical studies of some organic compounds	126
Introduction	127
Chapter 3.1- Cycloadducts of chiral acylnitroso compounds	128
3.1.1. Introduction	128
3.1.2. Results and discussion	131
3.1.3. Experimental	134
Captions to Figures	137
Chapter 3.2 - Normal and catalysed Diels-Alder reaction of ferrocenylethylenes	151
3.2.1. Introduction	151
3.2.2. Results and discussion	152
3.2.3. Experimental	155
Captions to Figures	157
Chapter 3.3 - The conformations of some anti-cancer drugs	172
3.3.1. Introduction	172
3.3.2. Results and discussion	173
3.3.3. Experimental	176

Captions to Figures	177
SECTION 4 - Miscellaneous compounds	187
Chapter 4.1 - o-Tetramethoxy calix[4]arene silver(I) nitrate	188
4.1.1. Introduction	188
4.1.2. Results and discussion	190
4.1.3. Experimental	193
4.1.4. Captions to Figures	194
Chapter 4.2 - The structure of seven co-ordinate tungsten complex	201
4.2.1. Introduction	201
4.2.2. Results and discussion	201
4.2.3. Experimental	203
Caption to Figure	204

LIST OF TABLES

	Page No.
Table 1.1.1. The seven crystal systems	5
Table 2.1.1. Atomic fractional and isotropic displacement parameters (\AA^2) for compound 2	37
Table 2.1.2 Selected bond distances (\AA) and bond angles ($^\circ$)	38
Table 2.1.3. Crystallographic data of the structure analysis of compound 2	39
Table 2.2.1. Atomic fractional and isotropic displacement parameters (\AA^2) for compound 6	49
Table 2.2.2 Selected bond distances (\AA) and bond angles ($^\circ$)	51
Table 2.2.3. Crystallographic data of the structure analysis of compound 6	53
Table 2.2.4. Atomic fractional and isotropic displacement parameters (\AA^2) for compound 7	62
Table 2.2.5 Selected bond distances (\AA) and bond angles ($^\circ$)	63
Table 2.2.6. Crystallographic data of the structure analysis of compound 7	64
Table 2.2.7. Atomic fractional and isotropic displacement parameters (\AA^2) for compound 8	71
Table 2.2.8 Selected bond distances (\AA) and bond angles ($^\circ$)	74
Table 2.2.9. Crystallographic data of the structure analysis of compound 7	77
Table 2.2.10. Atomic fractional and isotropic displacement parameters (\AA^2) for compound 9	84
Table 2.2.11. Selected bond distances (\AA) and bond angles ($^\circ$)	87
Table 2.2.12. Crystallographic data of the structure analysis of compound 9	89

Table 2.2.13. Atomic fractional and isotropic displacement parameters (\AA^2) for compound 10	96
Table 2.2.14 Selected bond distances (\AA) and bond angles ($^\circ$)	99
Table 2.1.15. Crystallographic data of the structure analysis of compound 10	101
Table 2.2.16. Crystallographic data of the structure analysis of compound 16	103
Table 2.3.1. Mean Pt-Pt & Pt-Re bond length (\AA)	116
Table 3.1.1. Stereochemistry chemical parameters for compounds 1 - 6 (\AA , $^\circ$)	135
Table 3.1.2. Characteristic hydrogen bonds (\AA) and angles ($^\circ$) in 1 and 2	136
Table 3.1.3 Selected bond lengths in the ONC(O)R unit of 1 - 6 (\AA)	136
Table 3.1.4. Crystallographic data of the structure analysis of compound 1 and 2	143
Table 3.1.5. Crystallographic data of the structure analysis of compound 3 and 4	144
Table 3.1.6. Crystallographic data of the structure analysis of compound 5 and 6	145
Table 3.1.7. Atomic fractional and isotropic displacement parameters (\AA^2) for compound 1 - 6	146
Table 3.2.1 Selected bond length in the isobenzofuran units of 10 - 13 (\AA)	162
Table 3.2.2. Selected torsion angles for compound 10 - 13 ($^\circ$)	163
Table 3.2.3. Selected bond distances in the ferrocenyl units 10 - 13 (\AA)	163
Table 3.2.4. Crystallographic data of the structure analysis of compound 10 - 11	164
Table 3.2.5. Crystallographic data of the structure analysis of compound 12 - 13	165

Table 3.2.6. Atomic fractional and isotropic displacement parameters (\AA^2) for compound 10 - 13	166
Table 3.3.1. Selected torsion and bond angles and bond distances for compounds 14 - 16 ($^\circ$, \AA)	176
Table 3.3.2. Crystallographic data of the structure analysis of compound 14 - 16	182
Table 3.3.3. Atomic fractional and isotropic displacement parameters (\AA^2) for compound 14 - 16	183
Table 4.1.1. Atomic fractional and isotropic displacement parameters (\AA^2) for compound 1	197
Table 4.1.2 Selected bond distances (\AA) and bond angles ($^\circ$)	198
Table 4.1.3. Crystallographic data of the structure analysis of compound 1	200
Table 4.2.1. Atomic fractional and isotropic displacement parameters (\AA^2) for compound 2	206
Table 4.2.2 Selected bond distances (\AA) and bond angles ($^\circ$)	207
Table 4.2.3. Crystallographic data of the structure analysis of compound 2	208

LIST OF SCHEME

Scheme 2.3.1. Reaction with dioxygen ligands	108
Scheme 2.3.2. Reaction with neutral ligands	109
Scheme 2.3.3. Reaction with halide ligands	110
Scheme 2.3.4. Reaction with sulphur ligands	111
Scheme 3.1.1.	129

Summary

In this thesis X-ray diffraction analysis is applied to the study of molecular structure and conformation. The contents are divided into four sections.

The first section is a brief review of the theory and practical aspects of the X-ray diffraction methods used in sections two, three and four.

Section two is concerned with the structure of ruthenium and platinum complexes stabilised by the diphosphine ligand $\text{Ph}_2\text{PCH}_2\text{PPh}_2$ (dppm). First, earlier work on binuclear complexes, on triangular $\text{M}_3(\text{dppm})_3$ species and on platinum cluster complexes is reviewed and the structure of the binuclear species $[\text{Ru}_2\{\mu\text{-Cl}(\mu\text{-H})\text{Cl}_2(\text{CO})_2\}(\mu\text{-dppm})_2]$ is described. Then the structures of five large heterometallic clusters derived from $[\text{Pt}_3\{\mu_3\text{-Re}(\text{CO})_3\}(\mu\text{-dppm})_3]^+$ are presented. These clusters are obtained by reaction of the parent cluster with dioxygen, halide or neutral ligand. Their structures have been of critical importance to this new field of cluster chemistry. The characterisation of $[\text{Pt}_3(\mu_3\text{-ReO}_3)(\mu\text{-dppm})_3]^+$, which contains Pt(0) stabilised by phosphine and Re(VII) stabilised by oxide, is of particular significance. The section concludes with a summary of current knowledge of the chemistry of and bonding in platinum-rhenium clusters. Platinum-rhenium catalysts, for which the clusters are models, are also briefly described.

Section three is concerned with the stereochemistry of newly synthesized organic compounds. The formation of oxazines by Diels-Alder addition of acylnitroso compounds is described in Chapter 3.1. The reaction typically involves the creation of chiral centres. The structural work has been directed at predicting the stereochemistry of the preferred diastereoisomer. In Chapter 3.2 the stereochemistry of Diels-Alder addition of ferrocene derivatives to 1, 3-diphenylisobenzofuran is considered, with emphasis on the effect of AlCl_3 catalysis

on the nature of the product. In Chapter 3.3 the stereochemistry of cis and trans ArCH=CHAr molecules, and its relationship to their biological activity, is discussed.

Section four describes the structure of tetramethoxycalix[4]arene silver(I) nitrate. The ability of calix[4]arenes to act as hosts has led to major developments in supramolecular chemistry. The attachment of silver(I) to the calixarene is of a novel type. The section also deals with the structures of mononuclear tungsten(II) complexes in which the metal atom could be six or seven co-ordinate.

Section 1

X-ray crystal structure analysis

Introduction

The main experimental techniques and equations used for crystal structure analyses will be discussed briefly in this section.

Crystals

Crystals have been a subject of study for many years. A solid having a regularly repeating internal arrangement of atoms is called a crystal. The repetition of such a pattern can be considered by replacing each unit of the pattern by a point. This leads to a crystal lattice or space lattice, which is a three-dimensional arrangement of points, and the view in a given direction from each point in this lattice is identical with the view in the same direction from any other point. The crystal lattice is not the same as the structure, which is an array of objects (atoms, molecules, ions) rather than merely of (imaginary) points. Thus the lattice defines the translational repetition of the contents of the unit cell which gives rise to the regularly repeating structure of the crystal. The combination of a lattice with an object gives the crystal structure (Glusker & Trueblood, 1985).

The faces of a crystal are planes enclosing a three-dimensional solid. The planes in the crystal are then described by the intercepts on the axes, a/h , b/k and c/l , where h , k and l are small whole numbers called Miller indices. Miller indices used to describe planes and faces are usually enclosed in parentheses, e.g. (hkl) .

The geometry of the unit cell is defined by three lengths a , b and c , which are the edges of the cell, and three inter-axial angles α , β and γ . A unit cell belongs to one of seven possible three-dimensional crystal systems, according to the shape and relative dimensions of unit cell, both of which depend on its symmetry properties. Table 1.1.1 illustrates the seven possible crystal systems (Stout & Jensen, 1989).

Table 1.1.1. The seven crystal systems

Crystal System	Number of Independent Parameters	Parameters	Lattice Symmetry	Bravais Lattice
Triclinic	6	$a \neq b \neq c; \alpha \neq \beta \neq \gamma^\circ$	$\bar{1}$	P
Monoclinic	4	$a \neq b \neq c; \alpha = \gamma = 90^\circ; \beta \neq 90^\circ$	2/m	P and C
Orthorhombic	3	$a \neq b \neq c; \alpha = \beta = \gamma = 90^\circ$	mmm	P, C, F, and I
Tetragonal	2	$a = b \neq c; \alpha = \beta = \gamma = 90^\circ$	4/mmm	P and I
Trigonal				
rhombohedral lattice	2	$a = b = c; \alpha = \beta = \gamma \neq 90^\circ$	$\bar{3}m$	R
hexagonal lattice	2	$a = b \neq c; \alpha = \beta = 90^\circ; \gamma = 120^\circ$	6/mmm	
Hexagonal	2	$a = b \neq c; \alpha = \beta = 90^\circ; \gamma = 120^\circ$	6/mmm	P
Cubic	1	$a = b = c; \alpha = \beta = \gamma = 90^\circ$	m3m	P, F, and I

In three-dimensions there are 14 distinct space lattices known as Bravais lattices. There are seven different lattices based on the unit-cell shapes appropriate to the seven crystal systems, and called primitive (P). The primitive rhombohedral lattice is usually denoted by R. In some crystal systems non-primitive lattices, such as A, B, C or F-face centring or I-body centring, occur.

Point groups describe the symmetry existing about a point, and are important in descriptions of the symmetry of the physical properties of crystals and of the atomic or molecular arrangements. There are 32 crystallographic point groups, derived from the symmetry operations consistent with a lattice structure (Glusker & Trueblood, 1985):

- a. centre of symmetry ($\bar{1}$)
- b. mirror plane (m)
- c. rotation axes (2, 3, 4 and 6)
- d. inversion axes ($\bar{3}$, $\bar{4}$ and $\bar{6}$).

Combination of point group symmetry operations with translations gives space-symmetry operations:

- a. glide planes (a, b, c, n and d)
- b. screw axes (2_1 , 3_1 , 3_2 , 4_1 , 4_2 , 4_3 , 6_1 , 6_2 , 6_4 , 6_5).

The smallest part of a crystal structure from which the complete structure can be obtained from the space group symmetry operations is called the asymmetric unit (Glusker & Trueblood, 1985). The operation of the symmetry elements on it will generate the entire contents of the primitive unit cell. Combination of the 32 point groups with the 14 Bravais lattices leads to 230 arrangements of points in space. These 230 space groups describe identical objects arranged in an infinite lattice and they are listed and described in volume A of the International Tables for Crystallography (1983).

Symmetry concerned with the unit cell is revealed to some extent by the symmetry of the diffraction pattern and by the systematically absent reflections. The probable space group of the crystal can be deduced from this information. Systematic absences of reflections arise from the presence of centred lattices, screw axes or glide planes.

A crystal structure analysis normally proceeds through three distinct stages.

- (i) Measurements of the intensities of Bragg reflections which are then corrected for various geometrical and physical factors to yield a set of structure amplitudes.
- (ii) The solution of the phase problem. The phases of the diffracted beams cannot be measured directly and yet they must be derived in some way before the structure can be solved.
- (iii) The approximate atomic parameters must be refined to obtain the best agreement between the observed and calculated structure amplitudes.

Intensity

X-rays are part of the electromagnetic spectrum. To generate X-rays, electrons are accelerated by an electric field and directed against a metal target. The most common target material is probably molybdenum, although copper is also often used. In all experiments described here the intensity measurements were carried out with molybdenum radiation. A graphite monochromator crystal and pulse height analyser were used to get monochromatic X-rays.

The electron cloud of an atom scatters an X-ray beam: the scattering is dependent on the number of electrons and their positions in the clouds. The scattered X-rays can be detected in various way but only intensities (not the phases) of the diffracted beams can be measured.

The diffracted beam will only occur when the angle of the incident beam satisfies the Bragg equation. In the Bragg equation each diffracted beam is considered as a reflection from a lattice plane. All unit cells scatter in phase when

$$2d \sin\theta = \lambda$$

where λ is the wavelength of the radiation used and the incident and diffracted beams each make angle θ with the lattice planes of spacing d (Figure 1.1.1).

In order to describe the relationship between crystal structure and diffraction pattern it is possible to construct a reciprocal lattice. Any point of the real lattice is taken as an origin. Lines of length $1/d$ are drawn perpendicular to each set of real lattice planes. The termini of these lines (or diffraction vectors, see Figure 1.1.1) map out the reciprocal lattice of the crystal.

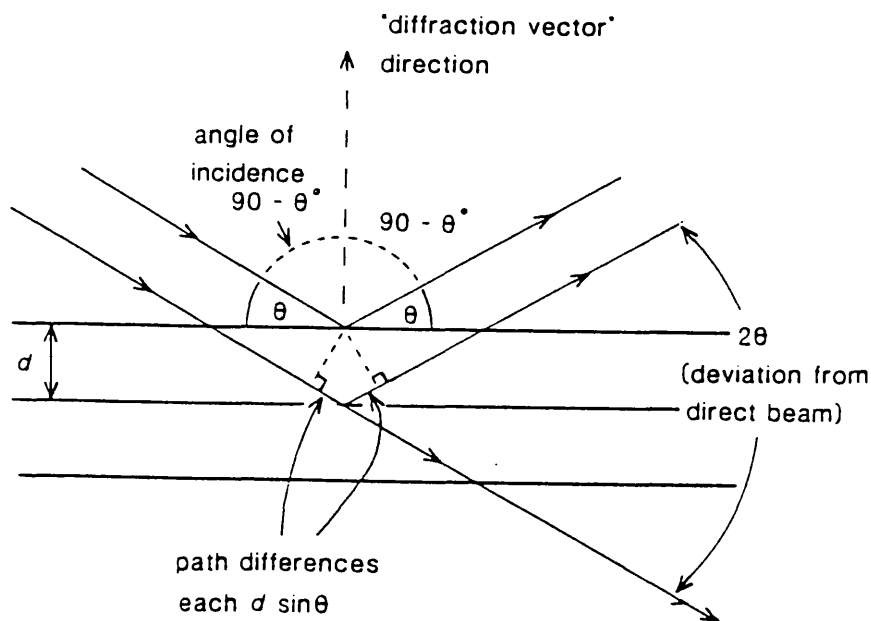


Figure 1.1.1. Diagram of reflection of x-ray by imaginary plane

Measurements and diffractometers

All the structure analyses described in this thesis were performed on an Enraf-Nonius CAD4 diffractometer. This diffractometer allows the crystal to be oriented by rotation about three independent axes and the counter to be swung about the crystal specimen so that a high proportion of all accessible Bragg reflections can be observed. In a typical experiment 15-25 Bragg reflections were located and their setting angles carefully measured. The unit cell and its orientation were then deduced from the setting angles. The shape of the unit cell indicates which crystal systems are possible. The final choice of system was made by comparing the intensities of reflections which could be related by symmetry, thereby establishing the Laue group. If necessary, the reduced cell was derived and then the

conventional cell by the methods of International Tables for Crystallography, volume A, section 9.

Final intensity measurements, $I(hkl)$, would then be made out of to as high an angle as possible using the $\omega/2\theta$ scan method and an ω scan width of $0.8 - 1.0^\circ$, increased by 25% at each end to allow for background.

Data processing

Structure amplitudes were determined from the expression:

$$I(hkl) = KLP A^2(hkl)$$

K is a scale factor for the experiment. Lorentz factor, L, and polarisation factor, P, are functions of Bragg angle and depend on the experimental conditions.

The intensity of a reflection is proportional to the time during which the corresponding reciprocal point is close to the surface of the reflection sphere. The Lorentz factor arises because this time varies with the position of the reciprocal lattice point and the direction in which it passes through the sphere of reflection.

$$L = 1/\sin 2\theta$$

The polarisation factor

When the X-ray is reflected by a plane in the crystal, a reduction in the intensity of the reflected beam occurs as a result of polarisation. The form of the polarisation correction when the diffraction planes at monochromator and specimen are normal to one another is:

$$P = \frac{\cos^2 2\theta + \cos^2 2\theta_M}{1 + \cos^2 2\theta_M}$$

where θ is the Bragg angle of the reflection and θ_M is the angle of the reflection of the monochromator crystal which was used to select the wavelength (Giacovazzo, Monaco, Terbo, Scorari, Gilli, Zanotti & Catti, 1992). When θ_M is nearly zero, the polarisation factor take its simplest form:

$$P = (1 + \cos^2 2\theta) / 2$$

The X-ray beam from standard laboratory sources is unpolarised (Stout & Jensen, 1989)

Absorption and related corrections

During the refinement stage of a crystal structure analysis, some systematic errors may need correction. The most important are absorption and extinction effects. The intensities of both the incident and diffracted X-ray beams are weakened in the crystal by absorption. If I is the observed intensity and I_0 the value it would have in the absence of absorption, then

$$I = I_0 e^{-\mu x}$$

where x is the distance traveled in the crystal by the X-ray beam and μ is the linear absorption coefficient which depends on the composition of the substance, its density, and the wavelength of the X-rays. If the crystal shape can be defined the transmission factor, I/I_0 , can be calculated by integration of $\exp(-\mu x)$ over the

volume of the crystal, usually by Gaussian quadrature. Alternatively, an empirical transmission surface can be derived from Ψ scans (Molen, 1990) or ΔF values (Walker & Stuart, 1983).

In cases where crystal decomposition was a problem the mean of intensity standards was used to apply a linear decay correction to segments of data.

Extinction

X-rays reflected from a crystal plane may be reflected again. The doubly scattered beam is in the same direction as the original beam but is exactly out of phase with it. This enhanced attenuation of the diffracted beam from a perfect crystal is called primary extinction.

However, some crystals behave as mosaics of small blocks of perfect crystals not accurately fitted together; for such crystals the beam is attenuated by diffraction as it passes through the crystal and some parts of the crystal see a substantially weakened incident beam. This effect is called secondary extinction. For mosaic crystals the effects of primary extinction are small and can be neglected. In contrast, the effects of secondary extinction are often large. Reflections affected by secondary extinction can be recognized in the final stage of crystal structure refinement when for some high-intensity reflection $F_o < F_c$ (Giacovazzo, Monaco, Terbo, Scorari, Gilli, Zanotti & Catti, 1992) and modern least squares programs allow empirical correction for the effect.

Structure analysis

The wave scattered from a single unit cell during Bragg reflection from the (hkl) plane is defined by the structure factor.

$$\begin{aligned}
F(hkl) &= \sum_{j=1}^N f_j \exp 2\pi i(hx_j + ky_j + zl_j) \\
&= |F(hkl)| \exp i\alpha(hkl) \\
&= A(hkl) + iB(hkl)
\end{aligned}$$

The summation is over the N atoms in the unit cell, f_j , x_j , y_j and z_j , are respectively the scattering factor and the fractional co-ordinates of the jth atom and $|F(hkl)|$ represents the amplitude of the scattered wave and $\alpha(hkl)$ its phase.

For space groups with a centre of symmetry B(hkl) is zero.

In this case,

$$\begin{aligned}
F(hkl) &= A, \text{ and} \\
\alpha &= 0 \text{ or } 180^\circ
\end{aligned}$$

Atomic scattering factor

For atoms or ions at rest the scattering factor, f_j , can be calculated from suitable electronic wave functions which usually assume a spherical distribution of electron density. The scattering factor for a spherical charge distribution is real and a function of $\sin \theta/\lambda$ only. The maximum value of the scattering factor of an atom is equal to Z, the atomic number, and is attained when $\sin \theta/\lambda=0$. As $\sin \theta/\lambda$ increases, the scattering factor decreases, because X-rays scattered from an electron in one part of an atom would be to an increasing extent out of phase with those scattered in another part of the electron cloud (Stout & Jensen, 1989).

The scattering factor, f_j , is usually calculated for a spherical distribution of classical electrons. Such a calculation ignores the effect of the atomic nucleus on the

scattering process. When allowance is made the scattering factor is of the form $f + f' + if''$ where f and f'' are the anomalous dispersion corrections to the classical scattering factor, f .

In non-centrosymmetric space groups anomalous dispersion leads to inequivalence of $|F(hkl)|$ and $|F(\bar{h} \bar{k} \bar{l})|$ and thus implies that the chirality of the crystal structure can be determined. In the GX package (Mallinson & Muir, 1985) the parameter η , a multiplier for f'' corrections, is used to determine chirality; SHELXL-93 (Sheldrick, 1993) uses a related method.

Temperature factor

The magnitude of the thermal vibration depends on the temperature, the mass of the atom and its crystalline environment. In general, the higher the temperature, the greater the vibrational motion. The effect of such thermal motion is to spread the electron cloud over a larger volume and thus to cause the scattering power of the vibrating atom to fall down more rapidly with $\sin \theta/\lambda$ than would that of the atom at rest. The change in scattering power can be expressed as

$$t = \exp[-8\pi^2 U (\sin\theta/\lambda)^2]$$

where U is the mean-square amplitude of vibration normal to the Bragg plane. For anisotropic vibration this temperature factor is defined by six independent U_{ij} parameters in the expression:

$$\exp -2\pi^2 (h^2 a^{*2} U_{11} + k^2 b^{*2} U_{22} + \dots \dots 2hka^* b^* U_{12} \dots \dots)$$

where a^* , b^* and c^* are the reciprocal cell parameters.

Structure solution

The electron density at the point with fractional coordinates x, y, z is given by

$$\rho(xyz) = V^{-1} \sum_h \sum_k \sum_l F(hkl) \exp -2\pi i(hx+ky+lz)$$

where V is the cell volume. This expression can also be written as:

$$\rho(xyz) = V^{-1} \sum_h \sum_k \sum_l |F(hkl)| \exp -2\pi i[(hx+ky+lz)-\alpha(hkl)]$$

where α is the phase angle.

The summation is over all possible sets of Miller indices hkl .

To calculate the electron density function both the structure amplitude and the phase angle are required. The structure amplitude is experimentally available. If atomic positions are known it is possible to calculate phase angles but normally the purpose of the experiment is to determine the atomic positions.

Two methods frequently used to overcome the phase problem are:

- (1) direct methods, and
- (2) the heavy atom method.

Direct methods

Direct methods are a group of analytical techniques for the determination of a set of phases from the structure amplitudes which then yields an approximation to the electron density map (Glusker & Trueblood, 1985). They are especially important for structures containing no heavy atoms.

The electronic density must be positive or zero but never negative. This requirement, together with the information that there are peaks at atomic positions but that elsewhere the map is near zero, implies that there are mathematical constraints on a possible phase angle (see Karle and Hauptman, 1950). In these methods the phases are chosen to give the least negative electron density map. The simplest case is that of a centrosymmetric structure where the phase problem reduces to that of determining the sign of each $A(hkl)$. The direct determination of phases is based on a relationship between the signs of reflections in centrosymmetric structures of the form:

$$S(hkl) \cdot S(h'k'l') \sim S(h-h', k-k', l-l')$$

where S means the sign of a reflection. The probability that this relationship is true is greater if the reflections involved are intense. If two of these signs are known, it is possible to determine the third. From such relationships it is often possible to derive phases for almost all intense Bragg reflections, and, since it is the intense Bragg reflections that dominate the electron density map, to obtain a good approximation to that map (Glusker & Domenicano, 1992). Analogous methods are used for non-centrosymmetric structures. The structure amplitudes are normalised by removing the effects of the fall-off of the scattering factor and the temperature factor, so that only the geometric component, $E(hkl)$, is left. Usually only the highest of E values are used and high weight is given to high angle reflections. An analysis of the statistical distribution of E values shows whether the structure is centrosymmetric or non-centrosymmetric. The average E value for a non-centrosymmetric crystal (0.888) is larger than for a centrosymmetric one (0.798) (Glusker, Lewis and Rossi, 1994). When the intensity data have been converted to E values, one of the first things that must be checked is whether the crystal is centrosymmetric or not. Direct methods were carried out using SHELX-86 in this thesis (Sheldrick, 1986).

Heavy atom method

This method uses the positions of the heavy atoms to phase the first approximate electron density map. If necessary, successive approximate electron density maps are carried out until all the non-hydrogen atoms had been located. In this method, one or two atoms in the structure have atomic number, Z_i , considerably greater than those of the other atoms present. Such an atom has surprisingly large effects on the phases of the structure factors, even though it represents a relatively small fraction of the total electron count of the cell. Heavy atoms can usually be located by analysis of a Patterson map. Once it has been located the assumption is then made that it dominates the diffraction pattern, and the phase angle for each diffracted beam for the whole structure is approximated by that for the heavy atom.

Certain portions of the Patterson map, depending on the space group, contain a large proportion of the readily interpretable structural information because they contain many vectors between space group-equivalent atoms. These portions are known as Harker lines and planes. The heavy atom coordinates were deduced from the location of the peaks in the Patterson map, including those on Harker lines or Harker planes. Fourier syntheses were calculated using only the heavy atom coordinates to calculate phases, enabling the scattering matter in the vicinity of the heavy atom to be located. Further Fourier syntheses, including the newly located atomic coordinates in the phasing calculations, were carried out until all the non-hydrogen atoms had been located [Glusker & Trueblood, 1985; Stout & Jenson 1989].

The Patterson function is expressed by

$$P(uvw) = \sum_h \sum_k \sum_l |F_{hkl}|^2 \cos 2\pi(hu + kv + lw)$$

where $P(uvw)$ is the value of the function at the position with fractional coordinates u , v and w . The summation is over all Bragg reflections and $|F(hkl)|$ is the observed structure amplitude. In order to find the position of the heavy atoms it is necessary to locate them with respect to the symmetry elements. Atoms at the positions (x_1, y_1, z_1) and (x_2, y_2, z_2) give rise to a peak in $P(uvw)$ at $u=x_2-x_1$, $v=y_2-y_1$, $w=z_2-z_1$ whose height is roughly proportional to $Z_1 Z_2$ (the atomic numbers).

Refinement

After all or most of the atoms have been located, the analysis is completed by the process of refinement. This involves the method of least squares, a common technique for finding the best values for the parameters which describe the model, and also requires the detecting and removal of systematic errors in the observed structure amplitudes. The mathematical basis of this method is the proposition that the best agreement between sets of experimental and calculated quantities is obtained when the sum of the squares of the discrepancies between them is a minimum.

Structure parameters (normally, scale, atomic co-ordinates and U_{ij} values) are most commonly varied to minimise

$$D = \sum w (|F_o|^n - |F_c|^n)^2$$

where the w is the weight of the observation, normally equal to $1/\sigma^2(|F_o|^n)$, the sum is over all measurements and n is either 1 (refinement on F) or 2 (refinement on F^2). D is minimised if :

$$\frac{\delta D}{\delta P_j} = 0 \quad (j=1,2,\dots,N)$$

where P_j is one of the N parameters which are used to calculate $|F_c|$ and whose values are to be refined. Refinement is continued until the ratio of the maximum shift over standard deviation is substantially less than unity.

The residual index, R

Structure factor agreement is compared by

$$R = \frac{\sum ||F_o| - |F_c||}{\sum |F_o|}$$

$$R_w = \left[\frac{\sum w (|F_o|^n - |F_c|^n)^2}{\sum w (F_o^2)^n} \right]^{1/2}$$

when $n=2$

$$w = 1.0 / [\sum \sigma^2 (F_o^2) + (aP)^2 + bP]$$

$$P = (F_o^2 + 2F_c^2) / 3$$

a and b are chosen to give a satisfactory analysis of variance.

The summations are over the reflections actually employed in the analysis.

Final values of R and R_w for satisfactory analyses are typically 0.02-0.07 and 0.04-0.08 respectively when $n=1$; R_w is bigger when $n=2$. They depend on a great variety of factors and are thus not an especially reliable guide to the relative accuracy of a particular structure determination.

Computer programs

CAD4 EXPRESS

The CAD4 diffractometer can be controlled by rather primitive software developed during the 1970s. In this laboratory this software is itself controlled by the CAD4EXPRESS shell which allows automatic control of the experiment. CAD4EXPRESS performed the following tasks.

1. Searching for up to 25 reflections for determination of cell dimensions and crystal system.
2. Measurement of slightly more than an asymmetric unit of intensities.
3. Ψ -scan measurements for 9 reflections for absorption correction.
4. Determination of accurate cell dimensions from high angle reflections.

The GX package (Mallinson & Muir, 1985)

This package has been designed for refining structures interactively with VAX or PC machines. The heart of the system is the crystal model file, containing the parameters of the crystal model. The package consists of independent programs that communicate via a standard set of data files, principally the model and reflection files. All the main types of calculation performed during structure analysis, such as absorption correction, checking of weighting schemes, least-squares refinement, geometry calculation and preparation of structures for publication, are available. This program refines the crystal structure against F . Most compounds found in this thesis were refined with the GX package.

There is no direct phasing program in this package. To solve a structure heavy atom methods or direct methods (Sheldrick, 1986) are used. The size of some structures led to problems with the GX program package because there is a limit of 200 atoms per asymmetric unit.

SHELX Programs

SHELXS (Sheldrick, 1986) has been used for solving non-heavy structures in this thesis. This widely used direct methods program is designed to solve structures automatically with a minimum of data (usually just composition, cell dimensions, space group and structure amplitudes). Most of the heavy atom

compounds have been solved from the Patterson function using non-automatic methods. The PATT option of SHELXS was used for some structures.

The SHELXL-93 (Sheldrick, 1993) program for the refinement of crystal structures is designed for single crystal X-ray data. This program offers refinement based on F^2 values rather than traditional crystal structures refinement against F which ignores the weaker data. For weakly diffracting crystals refinement against all data can give good results. The errors (standard deviations) are reduced because more experimental information is used (Sheldrick, 1993).

Drawing programs

Three graphics programs were used in this thesis (ORTEP, CAMERON & PLUTON). ORTEP has been developed by Dr. P. R. Mallinson from the original program for drawing atoms and bonds. CAMERON is another program for drawing: it is controlled by either typing commands at the keyboard or by mouse. This program was used on a PC machine, it is especially helpful in studying packing. PLUTON has mainly been used for spacefilling figures. It can run on PC machines.

Geometry

The geometry program used here (GEOM) is part of the GX package (Mallinson & Muir, 1985). It reads fractional coordinates and their standard deviations from a model file and then calculates the bond lengths, bond angles, torsion angles, intermolecular and interamolecular contacts. Throughout this thesis observed bond lengths have been compared with mean values from International Tables for Crystallography, Volume C, Tables 9.5.1.1- 9.6.3.3. These standard distances are derived from database studies.

References

- Giacovazzo, C., Monaco, H. L., Vitero, D., Scordari, F., Gilli, G. & Zanotti, G. & Catti, M. (1992). *Fundamentals of Crystallography*, IUCr, Oxford Science Publications.
- Glusker, J. P. & Domenicano, A. (1992). *Accurate molecular structures, their determination and importance*, Edited by Domenicano, A. & Hargittai, I., IUCr, Oxford University Press.
- Glusker, J. P., Lewis, M. & Rossi, M. (1994). *Crystal structure analysis for chemists and biologists*, VCH Publishers Inc., New York.
- Glusker, J. P. & Trueblood, K. N. (1985). *Crystal structure analysis: a primer*, Oxford University Press, Oxford.
- International Tables for Crystallography*. (1983). D. Reidel publishing company, Volume A, Dordrecht, The Netherlands.
- International Tables for Crystallography*. (1992). Kluwer academic publishers, Volume C, Dordrecht, The Netherlands.
- Karle, J. & Hauptman, H. (1950). *Acta Cryst.* 3, 181-187.
- Mallinson, P. & Muir, K. W. (1985). *J. Appl. Cryst.* 18, 51-53.
- Molen. (1990). *Crystallography program package*, Enraf-Nonius, Delft, The Netherlands.
- Sheldrick, G. M. SHELXL-93. (1993). A program for refining crystal structures. University of Gottingen, Germany.
- Sheldrick, G. M. SHELXS-86. (1986). A program for solving crystal structures. University of Gottingen, Germany.
- Stout, G. H. & Jensen, L. H. (1989). *X-ray structure determination*, John Wiley & Sons, New York, U.S.A.
- Walker, N. & Stuart, D. (1983). *Acta Cryst.* A39, 158-166.

Section 2

The structures of platinum-rhenium heterometallic cluster compounds and related complexes stabilised by diphosphine ligands

Chapter 2.1. Stabilisation of metal cluster complexes by diphosphine ligands

2.1.1. Diphosphine ligands

A survey of the Cambridge structural database shows that several hundred complexes stabilised by diphosphine ligands have been characterised. The discovery of the ligand $\text{Ph}_2\text{PCH}_2\text{PPh}_2$ (dppm) in particular has led to development of a rich coordination chemistry of transition metals, especially of platinum.

In the following three chapters the structures of new platinum-rhenium cluster complexes are discussed. The present chapter reviews some aspects of diphosphine chemistry because all clusters in section two contain $\text{Ph}_2\text{PCH}_2\text{PPh}_2$. The structure of a binuclear ruthenium complex is also discussed here.

The main topic of this section is, however, that of platinum-rhenium cluster chemistry which is discussed in Chapter 2.2. This work has involved:

- (i) characterisation of new triplatinum rhenium compounds,
- (ii) provision of the experimental basis for the assessment of the structure, bonding and catalytic properties,
- (iii) an attempt at understanding the behaviour of heterogeneous Pt/Re/ Al_2O_3 catalysts which are widely used in the petroleum industry.

The chemistry, bonding theory and catalytic properties of the complexes are discussed in Chapter 2.3.

The starting point for phosphine-stabilised platinum clusters was the work of Chatt and Chini (1970). They described, for example, the first preparation of trinuclear phosphine carbonyl cluster compounds. In 1985 Mingos and Wardle published a comprehensive review of platinum cluster chemistry (Mingos & Wardle, 1985). They showed that most triangulo- M_3 ($\text{M}=\text{Pt}, \text{Pd}$) clusters are 42 electron M_3P_6 species. Such a 42 electron unsaturated cluster can add small molecules, such

as alkyne, phosphite or cyanide and also provides a starting point for the synthesis of heteronuclear compounds by the addition of other metals, notably gold and tin. In 1990 a comprehensive review of tripalladium and triplatinum cluster compounds by Puddephatt, Manojlovic-Muir & Muir appeared: it focused on the development of tripalladium and triplatinum chemistry by the synthesis of new types of cluster derived from the parent cation $[\text{Pt}_3(\text{CO})(\mu\text{-dppm})_3]^{+2}$ by addition of extra metal atoms. They stressed that a 42 electron M_3P_6 unsaturated cluster can react with sulphur or halide as well as ligands containing metals such as Sn, Hg and Au.

In the new work discussed here on heteronuclear clusters containing platinum and rhenium, ReO_3 , $\text{Re}(\text{CO})_3$ or $\text{Re}(\text{CO})_2\text{P}(\text{OPh})_3$ units have been added to the basic skeleton of Pt_3P_6 to give a 54 electron cluster. In a search of the Cambridge database for platinum rhenium cluster compounds only three published papers were found, all from this laboratory (Xiao, Puddephatt, Manojlovic-Muir & Muir, 1993; Xiao, Puddephatt, Manojlovic-Muir, Muir & Torabi, 1994; Xiao, Hao, Puddephatt, Manojlovic-Muir, Muir & Torabi, 1995). This new departure arose from the synthesis in 1992 of the bimetallic cluster $[\text{Pt}_3\text{Re}(\text{CO})_3(\mu\text{-dppm})_3]^{+1}$ by Professor Puddephatt's group at the University of Western Ontario (Xiao, Vittal, Puddephatt, Manojlovic-Muir & Muir, 1993). This synthesis and subsequent work has allowed Puddephatt's group to develop new area, the chemistry of triplatinum-rhenium species. The six structure analyses described in Chapter 2.2 have been an integral part of this development.

2.1.2. Bonding mode of the bis(diphenylphosphino)methane ligand

The ligand dppm and its relatives show a strong tendency to stabilize dinuclear complexes, as may be seen in the review by Puddephatt (1983). Tertiary phosphine ligands have been widely used to stabilize the lower oxidation states of transition metals (McAuliffe & Levason, 1979). The structural literature on transition metal phosphine complexes is extensive, as can be seen from the Cambridge Structural Database which contains several thousand entries only for triphenylphosphine-stabilized species. These ligands can be easily synthesized with a variety of substituents on phosphorus and are thus capable of displaying a wide range of electronic and steric properties (Tolman, 1977). With diphosphines, $\text{R}_2\text{P}(\text{CH}_2)_n\text{PR}_2$, the length of carbon chain between the phosphorus atoms is a further factor in determining ligand behaviour. In all compounds to be discussed in this section, n is one and R is phenyl. Nowadays there is a substantial structural literature available on diphosphinomethane complexes, especially for dppm ($n=1$, $R=\text{Ph}$), but also for other members of the family. By replacing phosphorus by other group 5 elements, for example arsenic and antimony, the ligands $\text{Ph}_2\text{AsCH}_2\text{AsPh}_2$ and $\text{Ph}_2\text{SbCH}_2\text{SbPh}_2$ are obtained. They have also been studied in some depth (Colton, 1976; Okawara & Matsumura, 1976).

Four models of ligation are known for the dppm ligand:

- (a) incorporation in a four-membered chelate ring, as in $\text{trans}[\text{RhHCl}(\mu\text{-dppm})_2]^+$ (Cowie & Dwight, 1979) - see Figure 2.1.1(i),
- (b) bridging a metal-metal bond, as in $[\text{Pt}_2\text{Cl}_2(\mu\text{-dppm})_2]$ (Manojlovic-Muir, Muir & Solomun, 1979) - see Figure 2.1.1(ii),
- (c) bridging two metal atoms which are not directly bonded to each other, as in $[\text{Rh}_2(\text{CO})_4(\text{CN})_2(\mu\text{-dppm})_2]^{+2}$ (Sanger, 1981) - see Figure 2.1.1(iii),
- (d) coordination through only one phosphorus atoms, as in $\text{trans-Pd}(\text{Bu}^t\text{NC})_2(\mu\text{-dppm})_2]^{+2}$ (Olmstead, Lee & Balch, 1982) - see Figure 2.1.1(iv).

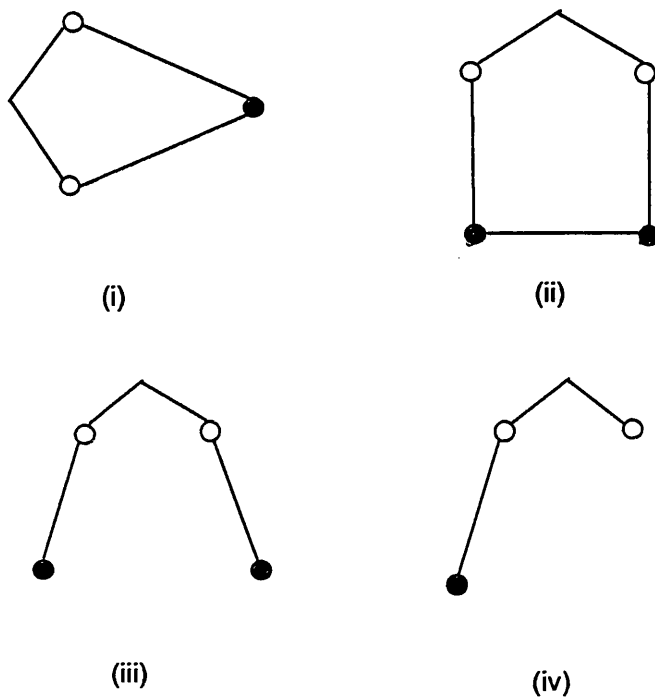
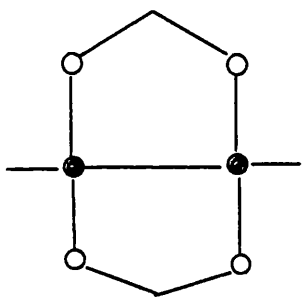


Figure 2.1.1. Models of bonding of diphosphinomethane to a metal atom, $\text{M}=\bullet$ and $\text{P}=\text{O}$.

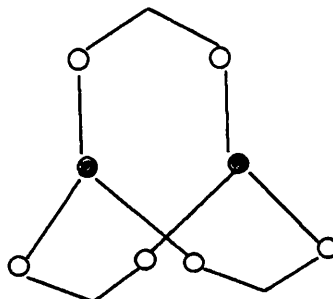
In binuclear complexes bonding modes (ii) and (iii) (Figure 2.1.1) predominate. Some of the commonly found structural classes exhibited by binuclear complexes of the dppm are shown in Figure 2.1.2.

In Figure 2.1.2(v) two metals with square-planar coordination are directly bonded to one another and are also linked by a pair of bridging diphosphine ligands, as in $[\text{Pt}_2\text{Cl}_2(\mu\text{-dppm})_2]$ (Manojlovic-Muir, Muir & Solomun, 1979), a so-called side-by-side binuclear compound (see page 900, Cotton & Wilkinson, 1985), Figure 2.1.2(vi) is the only type of binuclear complex with three $\mu\text{-dppm}$ ligands and is exemplified by $[\text{Pd}_2(\mu\text{-dppm})_3]$ (Stern & Maples, 1972) and $[\text{Pt}_2(\mu\text{-dppm})_3]$ (Manojlovic-Muir & Muir, 1982).

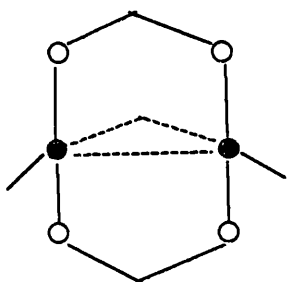
Figure 2.1.2(vii) shows M_2P_4 complexes with a $(\mu\text{-H})$ bridged M-M bond, such as was found in $[\text{Pt}_2\text{Me}_2(\mu\text{-H})(\mu\text{-dppm})_2]^+$ (Brown, Cooper, Frew, Manojlovic-Muir, Muir, Puddephatt & Thomson, 1979). Formally this kind of bridged bond arises from protonation and consequent weakening of the Pt-Pt bond. In Figure 2.1.2(viii) $(\mu\text{-H})$ is replaced by a larger bridging group, which can be neutral, anionic or cationic (Hoffman & Hoffmann, 1981) to make A-frame compounds (see page 900, Cotton & Wilkinson, 1985).



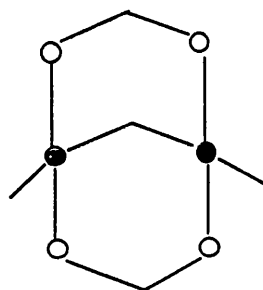
(v)



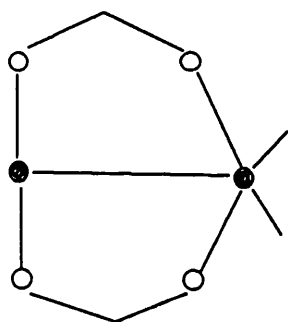
(vi)



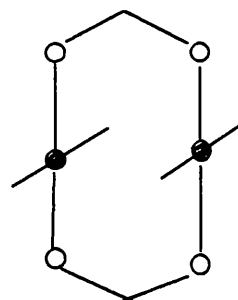
(vii)



(viii)



(ix)



(x)

Figure 2.1.2. Structural arrangements of the nucleus M_2L_2 , $M=\bullet$ and $L=dppm=O$.

Bridging dppm ligands can also stabilize donor-acceptor metal-metal bonds: $[\text{Pt}_2\text{Me}_3(\mu\text{-dppm})_2]^+$ (Brown, Cooper, Frew, Manojlovic-Muir, Muir, Pudddephatt & Seddon, 1981) has the skeleton shown in Figure 2.1.1(ix), the electron-rich PtMe_2 centre donating an electron-pair to the PtMe centre. Binuclear complexes, $[\text{X}_2\text{M}(\mu\text{-dppm})_2\text{MX}_2]$, in which a pair of $\mu\text{-dppm}$ ligands is the only link between the metal atoms, can have *cis* or *trans* co-ordination at the metal atoms: in $[\text{Pt}_2\text{Me}_4(\mu\text{-dppm})_2]$ the *cis* stereochemistry (Pudddephatt, Thomson, Manojlovic-Muir, Muir, Frew & Brown, 1981) occurs, whereas in $[\text{Pt}_2(\text{C}\equiv\text{CR})_4(\mu\text{-dppm})_2]$ (Pringle & Shaw, 1982) there is a *trans* co-ordination of the metal atoms. Figure 2.1.2(x) shows the *trans* co-ordination for such so-called face-to-face compounds (see page 900, Cotton & Wilkinson, 1985).

The addition of one bridging ligand per metal atom to 2.1.2(x) gives M_2L_{10} complexes such as $[\text{Mo}_2\text{Cl}_6(\mu\text{-dppm})_2]$ and $[\text{Ru}_2\text{Cl}_6(\mu\text{-dppm})_2]$ (Chakravarty, Cotton, Diebold, Lewis & Roth, 1986) in which two metal octahedra share a common edge. In the course of this work the structure of the ruthenium complex, $[\text{Ru}_2(\mu\text{-H})(\mu\text{-Cl})\text{Cl}_2(\text{CO})_2(\mu\text{-dppm})_2]$, **2**, was shown to display this arrangement. Its structure will be discussed later in this chapter.

2.1.3. A bimetallic ruthenium complex $[\text{Ru}_2\text{Cl}_3\text{H}(\text{CO})_2(\mu\text{-dppm})_2]$

Introduction

A primary reason for the extensive synthetic and structural research on dinuclear dppm complexes just discussed was the hope that these complexes could either function as homogeneous catalysts for various organic reactions or that they could be employed under mild conditions as precursors in the synthesis of generally inaccessible products. For catalytic activity it is believed that the cluster requires coordinative unsaturation; this can be produced by loss of a ligand or by metal-metal bond scission. Therefore, for effective catalysis a compromise (as discussed above) must be reached between the stability and reactivity of the cluster framework. One approach is to use bridging ligands to maintain the integrity of the polymetallic core. During an attempt to apply this strategy by using bis(diphenylphosphino)methane (dppm) ligands to stabilise binuclear ruthenium compounds $[\text{Ru}_2(\text{CO})_4(\mu\text{-CO})(\mu\text{-dppm})_2]$, **1**, was dissolved in benzene and the solution was stirred under ethylene. After one day a yellow-orange solid was obtained. It was recrystallized from $\text{CH}_2\text{Cl}_2/\text{ethanol}$ by slow diffusion to give complex **2** (Puddephatt, private communication). The nature of this product has been established by an X-ray crystal structure analysis. Preparation, crystallization and spectroscopic characterisation of complex **2** were performed by Professor Puddephatt and his co-workers at the University of Western Ontario, Canada. Although **2** has now been adequately characterised the reaction sequence which gives rise to it remains obscure.

Results and discussion

The molecular structure of **2** is shown in Figure 2.1.4. It displays exact C_2 symmetry, the diad axis passing through the bridging H(1) and Cl(1) atoms and bisecting the Ru-Ru vector. Compound **2** thus contains two $\text{RuCl}(\text{CO})$ fragments

bridged by two dppm ligands to form a $\text{Ru}_2\text{Cl}_2(\text{CO})_2(\mu\text{-dppm})_2$ skeleton. The metal atoms are further bridged by chloride and hydride to complete an edge-sharing bioctahedral M_2L_{10} -type structure (Chakravarty, Cotton, Diehold, Lewis and Roth, 1986) which has two types of terminal ligands, equatorial (e) and axial (a), in addition to bridging (b) groups (Figure 2.1.3).

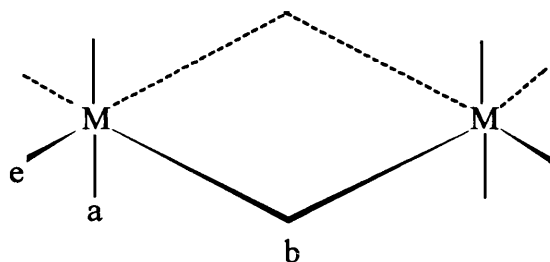


Figure 2.1.3. A model for M_2L_{10} complexes

The maximum symmetry is D_{2h} (Shaik, Hoffmann, Fisel & Summerville, 1980). Real complexes may depart from D_{2h} symmetry in many ways, but even within the D_{2h} constraint there is a wide range of deformations. The e-M-e and a-M-a angles may change from their idealized octahedral values of 90° and 180° , respectively. In 2 the largest departures from octahedral co-ordination at the metal involve the carbonyl ligand: Cl(2)-Ru-C(1) opens to $98.8(6)^\circ$ at the expense of C(1)-Ru-H(1) which closes to $78.0(4)^\circ$, and the C(1)-Ru-Cl(1) angle is $167.3(6)^\circ$ (see Table 2.1.2). Each $\text{Ru}_2\text{P}_2\text{C}$ ring adopts an envelope conformation, with the carbon atom at the flap which is folded towards the hydrido and carbonyl ligands. Such a conformation brings the equatorial phenyl substituents [rings C(3)-C(8) and C(15)-C(20)] to the carbonyl side of the $\text{Ru}_2\text{P}_4\text{C}_2$ core (see Figure 2.1.4). There are some intramolecular contacts involving the carbonyl ligands [C(1)...Cl(2) 3.24(2), C(1)...H(1) 2.29(3), C(1)...P(1) 2.86(2) and C(1)...P(2) 2.94(2) Å].

The Ru-Ru distance [2.931(3) Å] lies towards the upper end of the range of values previously observed for Ru-Ru single bonds [2.67 - 3.10 Å] (Johnson & Gladfelter, 1992; Lugan, Bonnet & Ibers, 1985; Clucas, Harding, Nicholls & Smith, 1985; Colombie, Bonnet, Fompeyrine, Lavigne & Sunshine, 1986). The Ru-H distances are in agreement with those found in the Ru₂(μ-H) bridges of other binuclear and cluster complexes [1.7 - 1.9 Å] (Bruce, Humphrey, Snow, Tiekink & Wallis, 1986; Manojlovic-Muir, Brandes & Puddephatt, 1987; Mirza, Vittal & Puddephatt, 1993). The bridging Ru-Cl bond [Ru-Cl(1) 2.453(5) Å] is about 0.02 Å longer than the terminal one [Ru-Cl(2) 2.435(4) Å] (see Table 2.1.1), but both bonds are much longer than the bridging Ru-Cl bond lengths in Ru₂Cl₆(μ-dppm)₂ [2.353(2) - 2.334(2) Å] (Chakraverty, Cotton, Diebold, Lewis & Roth, 1986).

The arrangement of the molecules in the crystal (Figure 2.1.5) shows two features of interest. First, when viewed down the c-axis there is a narrow slit, roughly 6 Å long by 2 Å wide, centred on x=y=1/2, which is free of atomic nuclei. This slit is too small to contain solvent molecules: it disappears when a space-filling model of the unit cell is viewed down c and the final difference synthesis (Table 2.1.3) does not contain any unexpected peaks. Second, a search of the CSD reveals ten binuclear diphosphine complexes, containing a variety of metals, which are isomorphous with the present structure. It is also worth noting that P₄2₁2 (or P₄3₂2) is the most common tetragonal space group in the CSD.

Experimental

A red prismatic crystal of Ru₂Cl₂(CO)₂(μ-H)(μ-Cl)(μ-dppm)₂, **2**, was sealed in a glass capillary, together with some mother liquor/nujol and apiezon grease, and mounted on a CAD4-diffractometer. The positions of the ruthenium atoms were determined from a Patterson function and those of the remaining non-hydrogen atoms from difference electron density syntheses. The position of the hydrido ligand,

H(1), was determined from a low angle difference map which showed a peak of 0.62 eÅ⁻³ at a co-ordination site on the *a* axis which relates the two ruthenium atoms; the displacement parameter of H(1) was constrained at U(H)=1.2 U(Ru), the equivalent isotropic displacement parameter of the ruthenium atom. The positions of the hydrogen atoms of the dppm ligands were calculated assuming standard stereochemistry at C_{sp}³ and C_{sp}² atoms. Isotropic displacement parameters were refined for phenyl carbon atoms. The structure was refined by full matrix least squares, minimizing the function $\sum w(|F_o| - |F_c|)^2$, where $w = 1 / \{1 + [(|F_o| - FB) / FA]^2\}^2$, with FA=95.0 and FB=56.0.

The choice of the space group P4₁2₁2₁ rather than the enantiomeric P4₃2₁2₁ was justified by refinement of the chirality parameter η (Rodgers, 1981); its final value was 1.1(2), satisfactory close to +1.

The atomic fractional co-ordinates are shown in Table 2.1.1 and crystallographic data are given for compound 2 in Table 2.1.3. All calculations were performed using the GX program package (Mallinson, Muir, 1985).

Captions to Figures

Figure 2.1.4. A view of the molecular structure of $[\text{Ru}_2\text{Cl}_2(\text{CO})_2(\mu\text{-H})(\mu\text{-Cl})(\mu\text{-dppm})_2]$, **2**, with the thermal ellipsoids displaying 50% probability. In the phenyl rings the carbon atoms are in the sequence C(n), C(n+1)...C(n+5), starting at the atom bonded to phosphorus. Only the C(n+1) atoms are labelled and all hydrogen atoms of the dppm atoms are omitted for clarity. The structure has crystallographically imposed C_2 symmetry, the two-fold axis passing through the H(1) and Cl(1) atoms and bisecting the Ru-Ru vector.

Figure 2.1.5. A view of the molecular packing of $[\text{Ru}_2\text{Cl}_2(\text{CO})_2(\mu\text{-H})(\mu\text{-Cl})(\mu\text{-dppm})_2]$, **2**, in projection down the c-axis.

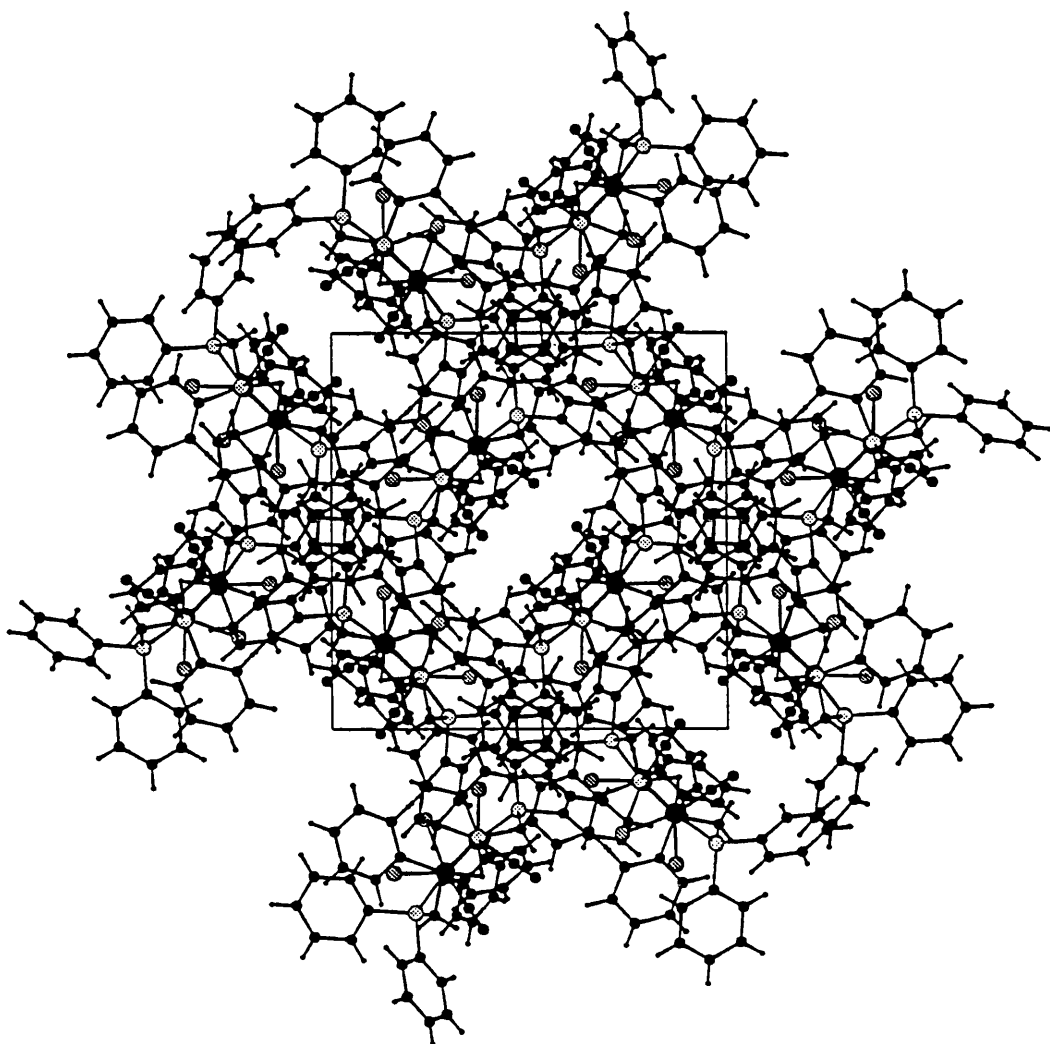


Figure 2.1.5

Table 2.1.1. Atomic fractional co-ordinates and isotropic displacement parameters(\AA^2) for compound 2

Atom	x	y	z	U
Ru(1)	0.21728(7)	0.13360(7)	0.95571(4)	0.041
P(1)	0.1331(3)	0.2238(2)	0.8990(1)	0.046
P(2)	0.2925(3)	0.0304(2)	1.0091(1)	0.047
Cl(1)	0.2680(3)	0.2680	1.0000	0.061
Cl(2)	0.3457(3)	0.1313(3)	0.8993(2)	0.069
O(1)	0.1209(10)	-0.0115(9)	0.9109(6)	0.123
C(1)	0.1567(12)	0.0422(10)	0.9290(6)	0.068
C(2)	0.0245(9)	0.2447(9)	0.9255(5)	0.050
C(3)	0.1036(14)	0.1726(12)	0.8382(4)	0.052(4)
C(4)	0.0236(12)	0.1889(6)	0.8129(7)	0.072(5)
C(5)	0.0076(6)	0.1499(12)	0.7656(6)	0.080(5)
C(6)	0.0715(11)	0.0947(10)	0.7437(3)	0.090(6)
C(7)	0.1514(10)	0.0784(8)	0.7689(7)	0.091(6)
C(8)	0.1675(8)	0.1174(14)	0.8162(6)	0.070(5)
C(9)	0.1731(9)	0.3313(5)	0.8780(5)	0.060(4)
C(10)	0.2627(7)	0.3526(11)	0.8844(7)	0.065(4)
C(11)	0.2948(7)	0.4348(11)	0.8680(6)	0.091(6)
C(12)	0.2374(8)	0.4956(5)	0.8451(4)	0.087(6)
C(13)	0.1478(6)	0.4744(11)	0.8387(7)	0.091(6)
C(14)	0.1156(8)	0.3922(11)	0.8551(5)	0.068(5)
C(15)	0.2837(14)	-0.0825(9)	0.9857(6)	0.052(3)
C(16)	0.2280(13)	-0.1462(8)	1.0076(6)	0.072(4)
C(17)	0.2161(6)	-0.2283(6)	0.9839(3)	0.091(5)
C(18)	0.2598(12)	-0.2468(8)	0.9383(5)	0.110(7)
C(19)	0.3154(10)	-0.1832(7)	0.9164(5)	0.086(5)
C(20)	0.3273(8)	-0.1010(7)	0.9401(3)	0.075(5)
C(21)	0.4107(7)	0.0380(13)	1.0202(7)	0.052(4)
C(22)	0.4565(6)	0.1181(11)	1.0143(8)	0.064(4)
C(23)	0.5457(8)	0.1240(6)	1.0285(5)	0.084(5)
C(24)	0.5892(6)	0.0498(11)	1.0485(6)	0.090(5)
C(25)	0.5434(7)	-0.0302(9)	1.0543(7)	0.091(6)
C(26)	0.4542(9)	-0.0361(8)	1.0402(4)	0.077(5)
H(1)	0.124(7)	0.124	1.000	0.041

Table 2.1.2. Selected bond distances (Å) and bond angles(°)**(a) bond distances**

Ru(1) - Ru(1)'	2.931(2)	Ru(1) - P(1)	2.380(4)	Ru(1) - P(2)	2.378(4)
Ru(1) - Cl(1)	2.453(2)	Ru(1) - Cl(2)	2.435(5)	Ru(1) - C(1)	1.791(17)
P(1) - C(2)	1.803(14)	P(1) - C(3)	1.829(14)	P(1) - C(9)	1.811(10)
P(2) - C(2)	1.866(15)	P(2) - C(15)	1.811(14)	P(2) - C(21)	1.804(12)
O(1) - C(1)	1.08(3)	Ru(1) - H(1)	1.83(9)		

(b) bond angles

Ru(1)' - Ru(1) - P(1)	91.5(1)	Ru(1)' - Ru(1) - P(2)	90.9(1)
Ru(1)' - Ru(1) - Cl(1)	53.3(1)	Ru(1)' - Ru(1) - Cl(2)	146.2(2)
Ru(1)' - Ru(1) - C(1)	115.0(6)	Ru(1)' - Ru(1) - H(1)	36.9(11)
P(1) - Ru(1) - P(2)	173.9(2)	P(1) - Ru(1) - Cl(1)	89.6(2)
P(1) - Ru(1) - Cl(2)	92.7(2)	P(1) - Ru(1) - C(1)	85.5(6)
P(1) - Ru(1) - H(1)	92.1(19)	P(2) - Ru(1) - Cl(1)	96.3(2)
P(2) - Ru(1) - Cl(2)	88.5(2)	P(2) - Ru(1) - C(1)	8.4(6)
P(2) - Ru(1) - H(1)	86.4(18)	Cl(1) - Ru(1) - Cl(2)	93.1(2)
Cl(1) - Ru(1) - C(1)	167.3(6)	Cl(1) - Ru(1) - H(1)	90.2(11)
Cl(2) - Ru(1) - C(1)	98.8(6)	Cl(2) - Ru(1) - H(1)	174.1(10)
C(1) - Ru(1) - H(1)	78.3(14)	Ru(1) - P(1) - C(2)	109.8(5)
Ru(1) - P(1) - C(3)	116.0(6)	Ru(1) - P(1) - C(9)	121.6(5)
C(2) - P(1) - C(3)	101.1(8)	C(2) - P(1) - C(9)	105.2(7)
C(3) - P(1) - C(9)	100.9(7)	Ru(1) - P(2) - C(2)	113.1(5)
Ru(1) - P(2) - C(15)	112.1(6)	Ru(1) - P(2) - C(21)	121.5(7)
C(2) - P(2) - C(15)	103.9(7)	C(2) - P(2) - C(21)	103.5(7)
C(15) - P(2) - C(21)	100.8(10)	Ru(1) - Cl(1) - Ru(1)	73.4(1)
Ru(1) - C(1) - O(1)	176.8(17)	P(1) - C(2) - P(2)	112.4(8)
P(1) - C(3) - C(4)	123.5(14)	P(1) - C(3) - C(8)	116.4(13)
P(1) - C(9) - C(10)	119.2(10)	P(1) - C(9) - C(14)	120.8(10)
P(2) - C(15) - C(16)	123.1(13)	P(2) - C(15) - C(20)	116.4(11)
P(2) - C(21) - C(22)	121.5(12)	P(2) - C(21) - C(26)	118.1(12)
Ru(1) - H(1) - Ru(1)'	106.3(38)		

The primed labels identify atoms at symmetry-equivalent position y, z, 2-z.

Table 2.1.3. Crystallographic data of the structure analysis of compound 2

Formula	$C_{52}H_{45}Cl_3O_2P_4Ru_2$
Formula wt	1134.3
Crystal system	tetragonal
Space group	$P4_12_12$
a Å	15.033(9)
c Å	26.300(7)
V Å ³	5844(5)
Z	4
F(0 0 0)	2288
D calc g cm ⁻³	1.267
T K	294
Crystal colour and habit	red prismatic
Crystal size mm	0.40 x 0.25 x 0.23
Cell: reflections used θ range(°)	10 reflections $8 < \theta < 11$
μ (Mo-K α) cm ⁻¹	7.73
Measured reflections	5226
Unique reflections	4663
Observed reflections $I \geq 3\sigma(I)$	2751
θ range °	2.5 - 24
Miller indices h	0 \rightarrow 17
k	-2 \rightarrow 17
l	-2 \rightarrow 30
Decay in mean standard (%)	4
R _{int}	0.038
No. of parameters	119
R(F)	0.0584
R _w (F)	0.0799
S	4.27
$\Delta\rho_{max}$ and $\Delta\rho_{min}$ eÅ ⁻³	0.79 \rightarrow -0.50
Δ/σ_{max}	0.036

Chapter 2.2. The structures of Pt₃Re cluster complexes

2.2.1. Introduction

In this chapter the structures are presented of six platinum-rhenium cluster complexes, all of which are stabilized by dppm ligands. Each structure is considered individually here. The relevant crystallographic details are contained in Tables 2.2.1-2.2.16 and Figures 2.2.1-2.2.12.

The chemical implications of this work are discussed fully in the next chapter (Chapter 2.3). It should, however, be noted here that the structural analyses discussed here were essential to the interpretation of the chemistry and reactivity of the Pt/Re systems. Such systems are interesting as potential models for the behaviour of industrially important Pt-Re/Al₂O₃ heterogeneous catalysts (see Xiao & Puddephatt, 1995).

Perhaps the most interesting and unexpected result from this work was the discovery of clusters containing low-valent platinum stabilised by π -acceptors, such CO or phosphine, attached to high-valent rhenium stabilised by π -donor oxide. Previously, low-valent metal clusters were regarded as a distinct class of compound, as were high-valent oxide- or halide-containing clusters, (see chapter 2 of Shriver, Kaesz, & Adams, 1990) and mixed types were unknown.

The following chapters will not discuss in detail the Pt-P and P-C bond distances because these distances, which are in the ranges 2.253(3) - 2.307(2) and 1.780(4) - 1.858(9) Å for the new platinum-rhenium cluster complexes, are much the same as those found in the previous work on triplatinum complexes derived from [Pt₃(CO)(μ -dppm)₃]⁺² (Douglas, Jennings, Manojlovic-Muir, Muir & Puddephatt, 1989).

2.2.2. The structure of $[\text{Pt}_3(\text{ReO}_3)(\mu\text{-dppm})_3][\text{ReO}_4]$, **6**

The cluster cation $[\text{Pt}_3(\mu\text{-ReO}_3)(\mu\text{-dppm})_3]^+$, in **6** contains both a high oxidation state Re(VII)O_3^+ fragment and a low oxidation state $\text{Pt}^0_3(\mu\text{-dppm})_3$ unit. The compound is formed by reaction of dioxygen with $[\text{Pt}_3\{\text{Re}(\text{CO})_3\}(\mu\text{-dppm})_3]^+$, **4**, under forcing conditions. Complex **4** can be obtained by reacting the parent cluster $[\text{Pt}_3(\mu\text{-CO})(\mu\text{-dppm})_3]^{+2}$ with $[\text{Re}(\text{CO})_5]^-$ (see Scheme 2.3.1 in the following chapter). More detail about the chemical behaviour of the compound **6** will be presented in chapter 2.3.

The structure of **6** has been determined by X-ray diffraction and the results are presented in Tables 2.2.1 - 2.2.3 and Figures 2.2.1 -2.2.3. The crystals contain $[\text{Pt}_3(\text{ReO}_3)(\mu\text{-dppm})_3]^+$ cluster cations based on a tetrahedral Pt_3Re core and $[\text{ReO}_4]^-$ anions.

Each Pt-Pt edge is bridged by a dppm ligand, forming the well known latitudinal $\text{Pt}_3(\mu\text{-dppm})_3$ moiety. A face of the Pt_3 triangle is μ_3 -bridged by the Re(1)O_3 unit. Re(1) thereby adopts a highly distorted octahedral coordination which retains local C_3 symmetry, with Pt-Re(1)-Pt angles of $56.7(1)$ - $57.4(1)^\circ$ and O-Re-O angles of $104(1)$ - $110(1)^\circ$ (see Table 2.2.2). Thus, the cation in **6** is closely related structurally to $[\text{Pt}_3\text{Re}(\text{CO})_3(\mu\text{-dppm})_3]^+$, **4**, with oxo ligands replacing carbonyl.

Each $\text{Pt}_2\text{P}_2\text{C}$ ring adopts a distorted envelope conformation with a CH_2 group at the flap position. Two of the methylene carbon atoms lie on the same side of the Pt_3 triangle as Re(1) and the third methylene carbon [C(2)] is displaced to the other side of the Pt_3 triangle. The conformation of the $\text{Pt}_3\text{P}_6\text{C}_3$ unit brings two axial and four equatorial phenyl substituents to the side of the two CH_2 groups, affording a cavity which is occupied by the ReO_3 group. The cavity on the other side of the $\text{Pt}_3(\mu\text{-dppm})_3$ fragment, defined by four axial (A, D, I, L) and two equatorial (F, G) phenyl

substituents, encloses a loosely bound $[\text{ReO}_4]^-$ anion (see Figure 2.2.1). The ability of the $\text{M}_3(\mu\text{-dppm})_3$ fragment in related complexes to attach and loosely bind an anion to one face of the M_3 triangle has been observed previously (Ferguson, Lloyd, Manojlovic-Muir, Muir & Puddephatt, 1986; Manojlovic-Muir, Muir, Lloyd & Puddephatt, 1983). Thus, for example, the short Pd-O distances [2.77(1)-2.92(2) Å] involving the $\mu\text{-CF}_3\text{CO}_2^-$ anion in $[\text{Pd}_3(\mu_3\text{-CO})_3(\mu\text{-CF}_3\text{CO}_2)(\mu\text{-dppm})_3][\text{CF}_3\text{CO}_2]$ (Ferguson, Lloyd, Manojlovic-Muir, Muir & Puddephatt, 1986) and the Pt-I distances [3.113(1)-3.341(1) Å] in $[\text{Pt}_3(\mu_3\text{-I})\{(\mu_3\text{-Re}(\text{CO})_3)(\mu\text{-dppm})_3\}]$ (Xiao, Hao, Puddephatt, Manojlovic-Muir, Muir and Torabi, 1995a) are considered indicative of some degree of covalency. In **6**, however, the shortest Pt-O distances [3.37(3), 3.41(3), 3.98(3) Å] (see Table 2.2.2) are too long to indicate a covalent bonding interaction.

The Pt-Pt distances in **4** are nearly constant [2.593(1)-2.611(1) Å] (Xiao, Vittal, Puddephatt, Manojlovic-Muir & Muir, 1993) and virtually identical values are found in **6** [2.598(2)-2.609(3) Å] (see Table 2.2.2). The Pt-Re distances in each cluster are rather less regular; the values in **6** (see Table 2.2.2) are slightly longer than those found in the parent compound **4** (Xiao, Vittal, Puddephatt, Manojlovic-Muir & Muir, 1993). The Re(1)-O distances in **6** are in the range of 1.70(3)-1.77(3) Å (see Table 2.2.2) and compare well with corresponding values in the compounds $[\text{C}_9\text{H}_{10}\text{N}_6\text{BReO}_3]$ [1.707(2)-1.720(2) Å] (Degnan, Herrmann & Herdtweck, 1990), $[\text{C}_{10}\text{H}_{18}\text{NReO}_3]$ [1.678(5)-1.705(4) Å] (Herrmann, Kuhn, Romao, Huy, Wang, Fischer, Kirprof & Scherer, 1993), $[\text{ReO}_2(\text{O}_2\text{C}_6\text{H}_4)_2]$ - [1.681(7) Å] (Dilworth, Ibrahim, Khan, Hursthouse & Karaulov, 1990) and $[\text{Re}_2\text{O}_6(\mu_2\text{-OH})_2\text{C}_4\text{H}_8\text{O}_2]$ [1.694(6)-1.720(5) Å] (Fischer, Krebs, Hoppe, 1982). The O-Re(1)-O angles in **6** [104.4(12)-109.9(12)°] lie between the values found in the compound $\text{C}_9\text{H}_{10}\text{N}_6\text{BReO}_3$ [103.9(1)-104.3(1)°] and those in $\text{C}_{10}\text{H}_{18}\text{NReO}_3$ [119.1(3)-119.5(1)°]. Bond distances and angles in the perrhenate anion are normal and agree with previous studies (Tsany, Reibenspies & Martell, 1993).

Each cation in **6** has closely associated with it an $[\text{ReO}_4]^-$ anion which blocks the free face of the Pt_3 triangle: the $\text{Re}(2)$ atom is nearly equidistant from $\text{Pt}(2)$ and $\text{Pt}(3)$ [4.97(8) & 4.96(2) Å respectively] and is slightly further [5.29(2) Å] from $\text{Pt}(1)$. The anion is oriented so that the $\text{Re}(2)\text{-O}(7)$ vector points towards the midpoint of $\text{Pt}(2)\text{-Pt}(3)$. The resulting short $\text{O}(7)\dots\text{Pt}$ contacts, as mentioned before, are however clearly nonbonding.

The overall transformation of **4** to **6** involves the replacement of the three carbonyl ligands in **4** by the three terminal oxo ligands in **6**. Since both CO and the terminal oxo ligand are formally two-electron donors, the overall cluster count in **4** and **6** are the same. Both are coordinatively unsaturated 54-electron clusters and the similarity displayed by the cluster cores of the two cations is therefore to be expected.

The bonding in both **6** and **4** can be understood in terms of the donation of electron density from three filled Pt-Pt bonding orbitals, having a_1+e symmetry, of the $\text{Pt}_3(\mu\text{-dppm})_3$ fragment to the three vacant acceptor orbitals, also having a_1+e symmetry, of an $\text{Re}(=\text{O})_3^+$ or $\text{Re}(\text{CO})_3$ fragment. In this formulation, the platinum and rhenium atoms in **6** may be considered as $\text{Pt}(0)$ and $\text{Re}(\text{VII})$. Even through this is an extreme interpretation, the oxidation states of platinum and rhenium in **6** are clearly very different, to an extent which is unprecedented in transition metal cluster chemistry.

The ReO_3 fragment is present in several other unusual compounds, such as MeReO_3 , $[(\eta^5\text{-C}_5\text{Me}_5)\text{ReO}_3]$ and $[\text{Me}_2\text{PCH}_2\text{PMe}_2]_2\text{Cl}_2\text{Re-ReO}_3$. The first two of these are considered as $\text{Re}(\text{VII})$ complexes (Ara, Fanwick & Walton, 1992 ; Herrmann, Serrano & Bock, 1984). There is a useful analogy between complexes **6** and $[(\eta^5\text{-C}_5\text{Me}_5)\text{ReO}_3]$, since the donor orbitals of both the $\text{Pt}_3(\mu\text{-dppm})_3$ fragment and C_5Me_5 -ligand have a_1+e symmetry and so may be considered to be isolobal (see chapter 20 of Albright, Burdett & Whangbo, 1985). The analogy, together with proven compatibility between the ReO_3^+ and $\text{Pt}_3(\mu\text{-dppm})_3$ fragments, suggests

several other possibilities for preparing clusters, by substitution of $\text{Pt}_3(\mu\text{-dppm})_3$ units for C_5Me_5 -ligands derived from known $(\text{C}_5\text{Me}_5)\text{MX}_n$ complexes. Since the vast majority of organometallic oxo complexes contain cyclopentadienyl ligands (Bottomley & Sutin, 1988), the preparation of other Pt_3 fragments based on oxide clusters should be feasible.

Experimental

All X-ray measurements were made at 23°C using a small block-shaped crystal. The accuracy of the analysis has been adversely affected by the high mosaicity and low diffracting power of the crystal specimen. Three reflections, (-1 7 1, 4 5 10 and -7 -1 4), were used to monitor the stability of the crystal and diffractometer. Their mean intensity showed a linear decline of up to 7.3% over the 144 hours of data collection. Empirical absorption corrections were made by the method of Walker & Stuart (1985) at the end of the isotropic refinement. The internal agreement factor, R_{int} , for merging 566 duplicate intensities was 0.039 before and after correction for absorption. The structure was solved by the heavy atom method. The positions of the non-hydrogen atoms were obtained using Patterson and difference Fourier methods. The isotropic U_{ij} parameters (see Table 2.2.1) are extremely large for some of the carbon atoms of rings B and K; this suggests positional disorder of these rings although alternative atomic sites were not obvious from difference maps. The final atomic parameters and anisotropic displacement parameters for all compounds except hydrogen atoms are given in Table 2.2.1. Crystallographic data for compound 6 is given in Table 2.2.3.

Captions to Figures

Figure 2.2.1. A view of the $[\text{Pt}_3(\text{ReO}_3)(\mu\text{-dppm})_3]^+$ cation in **6** and its associated $[\text{ReO}_4]^-$ anion. 50% probability ellipsoids are displayed. For clarity hydrogen atoms are omitted, as are all but the ipso carbon atoms of each of the twelve phenyl rings.

Figure 2.2.2. Space-filling diagram for the $[\text{Pt}_3(\text{ReO}_3)(\mu\text{-dppm})_3]^+$ cation in **6**. Here and in Figure 2.2.3 the platinum atoms are shown in black and the oxygen atoms are dotted. The cation is viewed along the normal to the Pt_3 plane from the side containing the $[\text{ReO}_4]^-$ anion which is not shown.

Figure 2.2.3. Space-filling diagram for the cation in **6**. viewed normal to the Pt_3 plane from the ReO_3 side.

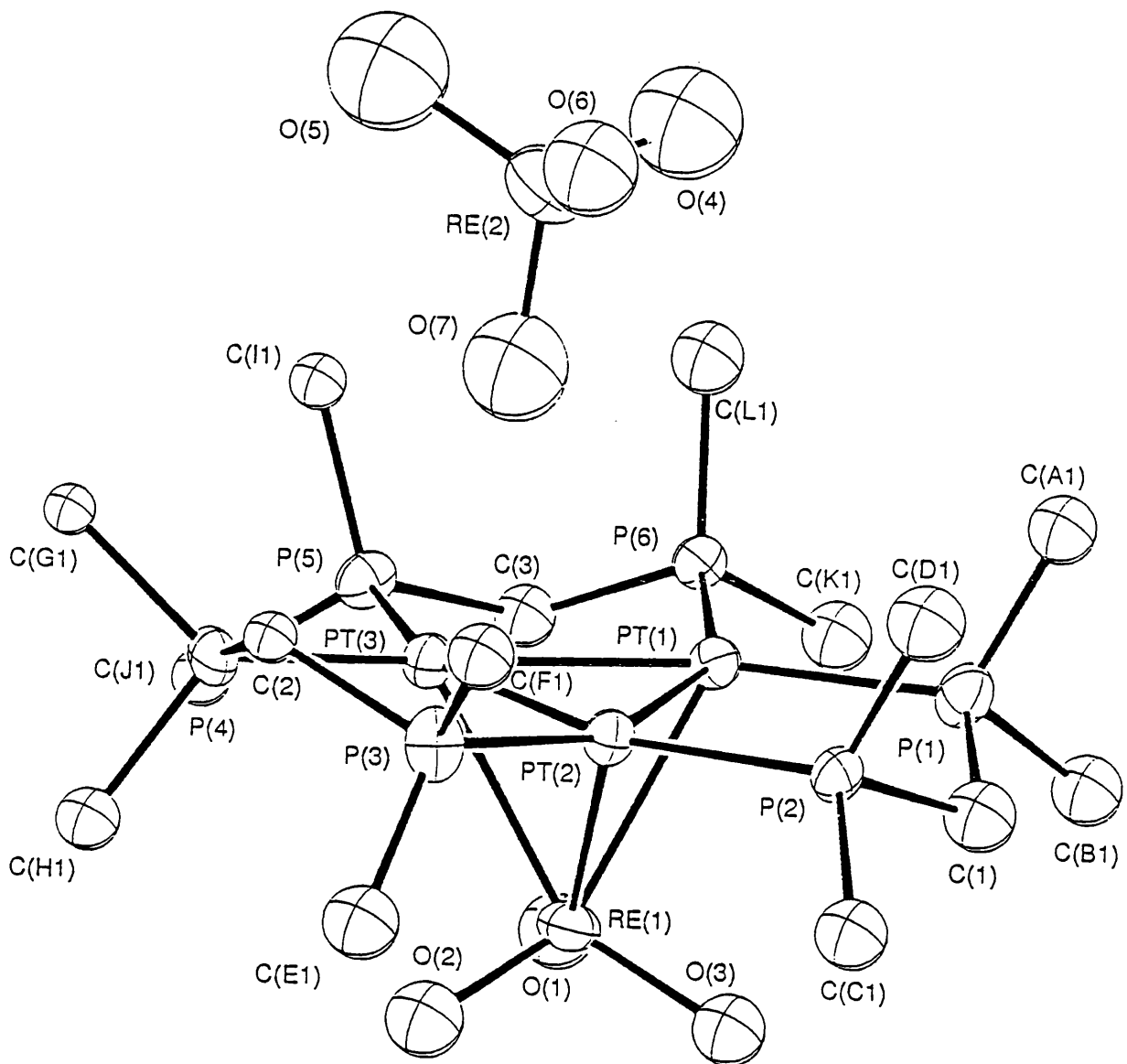


Figure 2.2.1

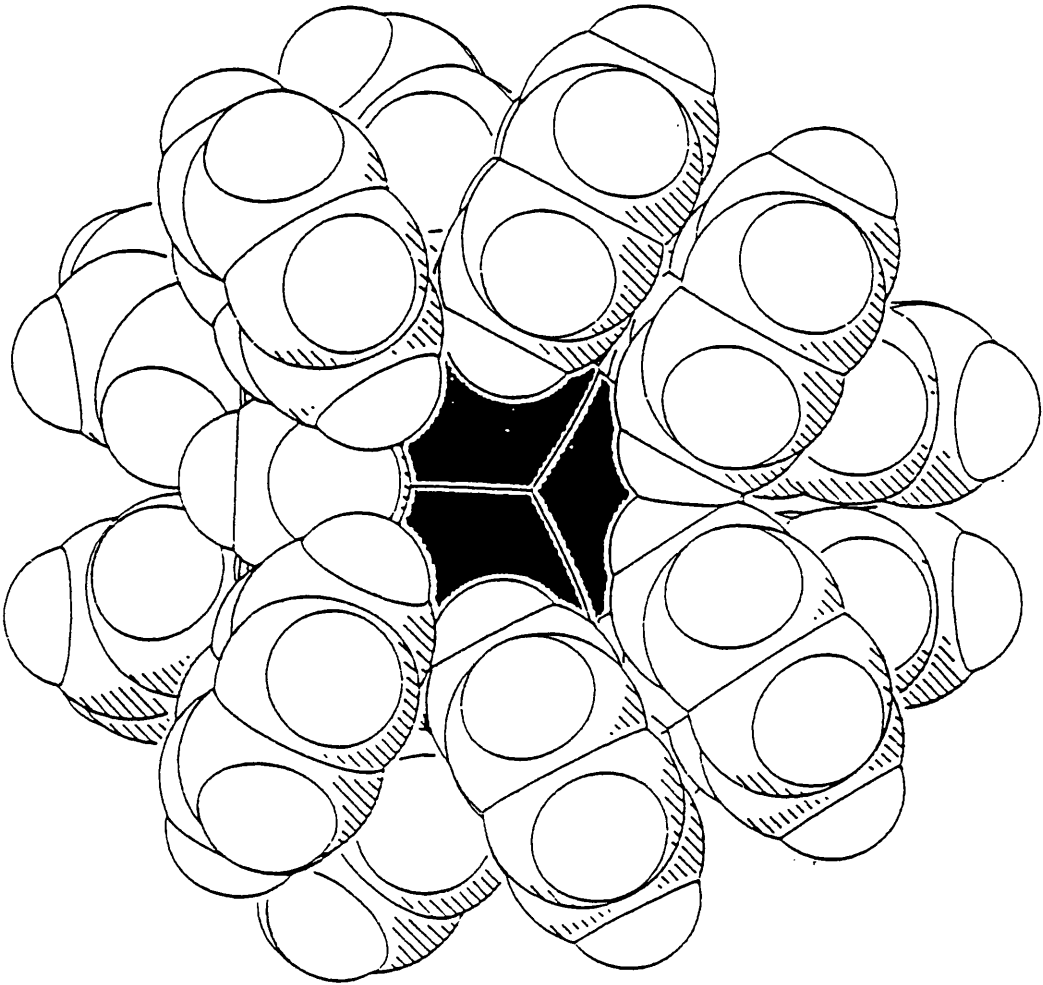


Figure 2.2.2

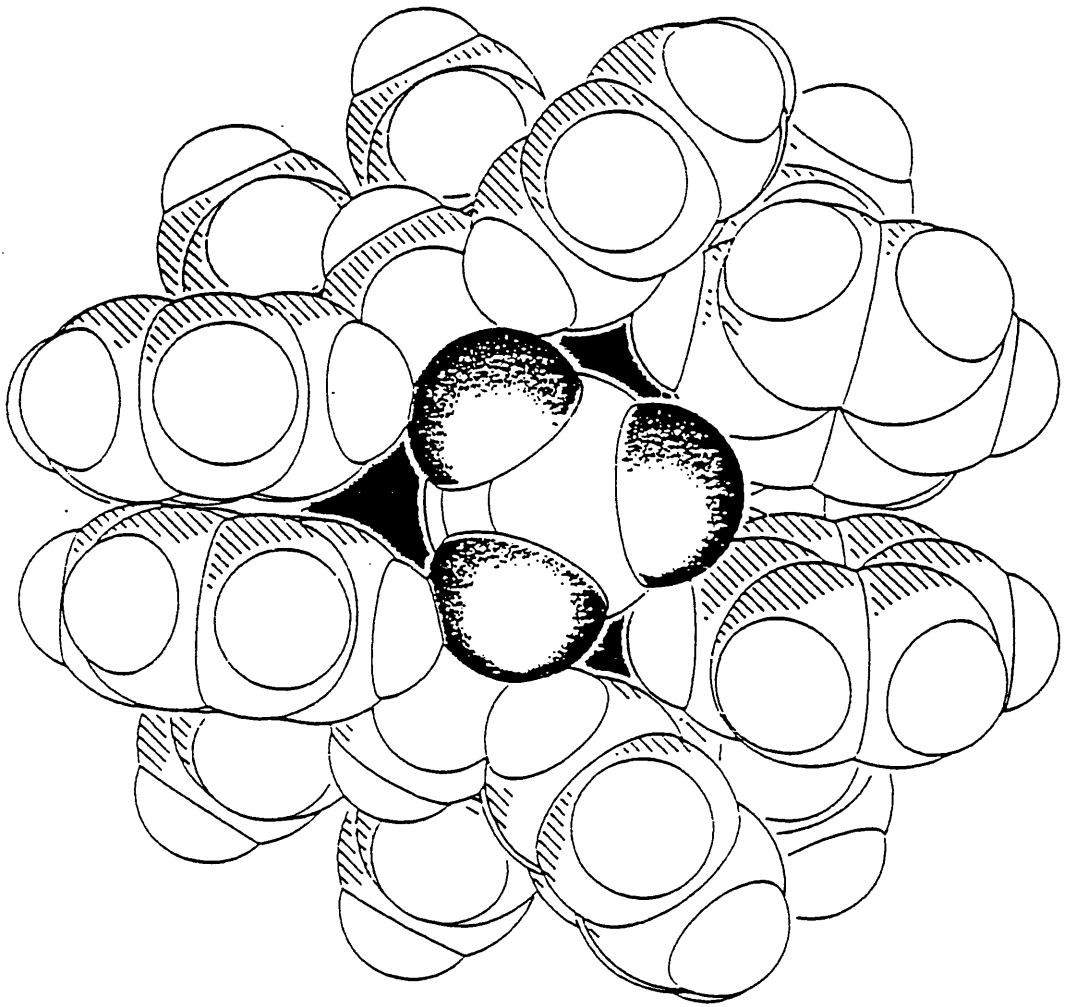


Figure 2.2.3

Table

2.2.1

Table 2.2.1. Atomic fractional co-ordinates and isotropic replacement parameters (\AA^2) for compound 6

Atom	x	y	z	U
Pt(1)	0.84518(11)	0.18573(11)	0.27266(7)	0.024
Pt(2)	0.74350(12)	0.19395(11)	0.18130(7)	0.025
Pt(3)	0.77417(12)	0.35490(11)	0.20632(7)	0.025
Re(1)	0.93211(13)	0.23029(12)	0.14029(7)	0.033
Re(2)	0.45749(16)	0.31020(15)	0.36417(9)	0.058
P(1)	0.8736(8)	0.0189(7)	0.3019(5)	0.033
P(2)	0.7497(8)	0.0295(7)	0.1976(4)	0.029
P(3)	0.6332(8)	0.2686(7)	0.1129(5)	0.035
P(4)	0.6695(7)	0.4593(7)	0.1409(5)	0.031
P(5)	0.8324(7)	0.4457(7)	0.2611(5)	0.029
P(6)	0.9037(7)	0.2521(7)	0.3449(4)	0.027
O(1)	1.0205(19)	0.2710(19)	0.1671(12)	0.050(7)
O(2)	0.9162(19)	0.2914(18)	0.0629(12)	0.049(7)
O(3)	0.9834(18)	0.1064(18)	0.1262(11)	0.043(7)
O(4)	0.504(3)	0.253(3)	0.434(2)	0.11(1)
O(5)	0.403(3)	0.434(3)	0.383(2)	0.12(1)
O(6)	0.376(2)	0.254(2)	0.350(1)	0.08(1)
O(7)	0.554(3)	0.308(2)	0.298(2)	0.10(1)
C(1)	0.858(3)	-0.038(3)	0.234(2)	0.04(1)
C(2)	0.583(2)	0.394(2)	0.129(1)	0.022(8)
C(3)	0.933(3)	0.365(3)	0.301(2)	0.033(9)
C(A1)	0.786(3)	-0.026(2)	0.373(1)	0.04(1)
C(A2)	0.709(3)	0.041(2)	0.407(2)	0.07(1)
C(A3)	0.640(4)	0.008(2)	0.461(2)	0.09(2)
C(A4)	0.649(2)	-0.092(2)	0.482(1)	0.07(1)
C(A5)	0.726(3)	-0.158(2)	0.448(2)	0.11(2)
C(A6)	0.794(4)	-0.125(2)	0.394(3)	0.12(2)
C(B1)	0.999(3)	-0.047(4)	0.313(3)	0.04(1)
C(B2)	1.074(3)	-0.049(4)	0.256(2)	0.07(1)
C(B3)	1.172(4)	-0.090(3)	0.261(2)	0.08(2)
C(B4)	1.195(3)	-0.129(3)	0.324(3)	0.09(2)
C(B5)	1.120(3)	-0.127(4)	0.381(2)	0.20(4)
C(B6)	1.022(4)	-0.086(2)	0.376(2)	0.14(3)
C(C1)	0.771(4)	-0.026(3)	0.121(1)	0.04(1)
C(C2)	0.862(3)	-0.035(3)	0.076(2)	0.05(1)
C(C3)	0.873(3)	-0.067(2)	0.014(2)	0.07(1)
C(C4)	0.793(3)	-0.091(3)	-0.001(1)	0.06(1)
C(C5)	0.702(2)	-0.082(3)	0.044(2)	0.12(2)
C(C6)	0.691(3)	-0.049(1)	0.105(2)	0.06(1)
C(D1)	0.649(2)	-0.019(2)	0.256(1)	0.05(1)
C(D2)	0.567(2)	0.049(2)	0.284(1)	0.030(9)
C(D3)	0.488(3)	0.017(2)	0.329(2)	0.09(2)
C(D4)	0.491(2)	-0.082(2)	0.346(1)	0.07(1)
C(D5)	0.573(3)	-0.150(2)	0.318(2)	0.07(1)
C(D6)	0.652(3)	-0.118(2)	0.273(2)	0.05(1)
C(E1)	0.679(4)	0.275(3)	0.022(1)	0.05(1)

C(E2)	0.622(4)	0.327(2)	-0.024(3)	0.08(1)
C(E3)	0.660(2)	0.322(3)	-0.093(2)	0.08(1)
C(E4)	0.753(3)	0.264(3)	-0.114(1)	0.08(1)
C(E5)	0.809(3)	0.212(2)	-0.067(3)	0.10(2)
C(E6)	0.772(3)	0.218(4)	0.001(2)	0.08(1)
C(F1)	0.519(2)	0.223(3)	0.126(2)	0.04(1)
C(F2)	0.514(3)	0.163(2)	0.082(2)	0.09(2)
C(F3)	0.432(4)	0.122(3)	0.093(1)	0.10(2)
C(F4)	0.355(2)	0.142(3)	0.1482(15)	0.08(1)
C(F5)	0.360(3)	0.201(2)	0.192(2)	0.06(1)
C(F6)	0.442(4)	0.242(3)	0.182(1)	0.05(1)
C(G1)	0.585(3)	0.571(2)	0.169(2)	0.022(8)
C(G2)	0.508(2)	0.558(2)	0.223(2)	0.029(9)
C(G3)	0.445(2)	0.638(2)	0.252(1)	0.08(1)
C(G4)	0.458(3)	0.732(2)	0.225(2)	0.07(1)
C(G5)	0.5349(18)	0.7451(15)	0.1707(12)	0.09(2)
C(G6)	0.598(3)	0.665(2)	0.142(2)	0.06(1)
C(H1)	0.728(2)	0.511(2)	0.056(1)	0.033(9)
C(H2)	0.820(2)	0.532(3)	0.049(2)	0.04(1)
C(H3)	0.8591(19)	0.5873(27)	-0.0096(16)	0.07(1)
C(H4)	0.8065(19)	0.6209(18)	-0.0611(10)	0.07(1)
C(H5)	0.715(2)	0.599(3)	-0.054(2)	0.07(1)
C(H6)	0.6752(18)	0.5444(24)	0.0045(16)	0.06(1)
C(I1)	0.744(4)	0.510(2)	0.329(2)	0.026(8)
C(I2)	0.649(4)	0.493(3)	0.350(1)	0.05(1)
C(I3)	0.5861(19)	0.5307(24)	0.4058(16)	0.06(1)
C(I4)	0.618(3)	0.585(2)	0.441(2)	0.08(2)
C(I5)	0.714(3)	0.602(3)	0.420(1)	0.08(2)
C(I6)	0.777(2)	0.564(2)	0.364(2)	0.07(1)
C(J1)	0.8863(16)	0.5433(18)	0.2043(10)	0.028(9)
C(J2)	0.827(3)	0.637(2)	0.195(2)	0.06(1)
C(J3)	0.864(3)	0.708(2)	0.147(2)	0.07(1)
C(J4)	0.9597(15)	0.6860(16)	0.1087(10)	0.05(1)
C(J5)	1.019(3)	0.592(2)	0.118(2)	0.05(1)
C(J6)	0.982(3)	0.521(2)	0.166(2)	0.06(1)
C(K1)	1.018(3)	0.178(5)	0.366(4)	0.04(1)
C(K2)	1.016(4)	0.135(2)	0.432(4)	0.19(3)
C(K3)	1.104(4)	0.083(4)	0.452(2)	0.28(5)
C(K4)	1.193(3)	0.075(4)	0.405(4)	0.13(2)
C(K5)	1.195(4)	0.119(3)	0.338(3)	0.14(3)
C(K6)	1.107(4)	0.170(5)	0.319(3)	0.13(2)
C(L1)	0.822(4)	0.283(2)	0.425(2)	0.04(1)
C(L2)	0.731(4)	0.258(3)	0.446(1)	0.06(1)
C(L3)	0.666(2)	0.287(3)	0.504(2)	0.09(2)
C(L4)	0.694(4)	0.342(2)	0.542(2)	0.07(1)
C(L5)	0.786(3)	0.367(3)	0.522(1)	0.07(1)
C(L6)	0.850(2)	0.337(2)	0.463(2)	0.09(2)

Table 2.2.2. Selected bond distances (Å) and bond angles(°).

(a) bond distances

Pt(1) - Pt(2)	2.598(2)	Pt(1) - Pt(3)	2.609(3)	Pt(1) - Re(1)	2.720(3)
Pt(1) - P(1)	2.286(10)	Pt(1) - P(6)	2.306(9)	Pt(2) - Pt(3)	2.600(3)
Pt(2) - Re(1)	2.748(3)	Pt(2) - P(2)	2.278(9)	Pt(2) - P(3)	2.275(10)
Pt(3) - Re(1)	2.711(3)	Pt(3) - P(4)	2.295(10)	Pt(3) - P(5)	2.274(9)
Re(1) - O(1)	1.74(3)	Re(1) - O(2)	1.70(3)	Re(1) - O(3)	1.77(3)
Re(2) - O(4)	1.71(4)	Re(2) - O(5)	1.80(4)	Re(2) - O(6)	1.67(3)
Re(2) - O(7)	1.68(4)	P(1) - C(1)	1.83(4)	P(1) - C(A1)	1.81(4)
P(1) - C(B1)	1.83(5)	P(2) - C(1)	1.83(4)	P(2) - C(C1)	1.82(3)
P(2) - C(D1)	1.81(3)	P(3) - C(2)	1.80(4)	P(3) - C(E1)	1.80(4)
P(3) - C(F1)	1.83(4)	P(4) - C(2)	1.80(4)	P(4) - C(G1)	1.82(4)
P(4) - C(H1)	1.84(3)	P(5) - C(3)	1.83(4)	P(5) - C(I1)	1.83(5)
P(5) - C(J1)	1.83(3)	P(6) - C(3)	1.78(4)	P(6) - C(K1)	1.78(6)
P(6) - C(L1)	1.82(5)				

(b) bond angles

Pt(2) - Pt(1) - Pt(3)	59.9(1)	Pt(2) - Pt(1) - Re(1)	62.2(1)
Pt(2) - Pt(1) - P(1)	95.9(3)	Pt(2) - Pt(1) - P(6)	154.3(3)
Pt(3) - Pt(1) - Re(1)	61.1(1)	Pt(3) - Pt(1) - P(1)	155.8(3)
Pt(3) - Pt(1) - P(6)	94.9(3)	Re(1) - Pt(1) - P(1)	109.8(3)
Re(1) - Pt(1) - P(6)	112.4(3)	P(1) - Pt(1) - P(6)	109.1(4)
Pt(1) - Pt(2) - Pt(3)	60.2(1)	Pt(1) - Pt(2) - Re(1)	61.1(1)
Pt(1) - Pt(2) - P(2)	95.2(3)	Pt(1) - Pt(2) - P(3)	155.0(3)
Pt(3) - Pt(2) - Re(1)	60.9(1)	Pt(3) - Pt(2) - P(2)	155.4(3)
Pt(3) - Pt(2) - P(3)	96.2(3)	Re(1) - Pt(2) - P(2)	111.1(3)
Re(1) - Pt(2) - P(3)	116.8(3)	P(2) - Pt(2) - P(3)	107.7(4)
Pt(1) - Pt(3) - Pt(2)	59.8(1)	Pt(1) - Pt(3) - Re(1)	61.5(1)
Pt(1) - Pt(3) - P(4)	154.2(3)	Pt(1) - Pt(3) - P(5)	95.3(3)
Pt(2) - Pt(3) - Re(1)	62.3(1)	Pt(2) - Pt(3) - P(4)	95.5(3)
Pt(2) - Pt(3) - P(5)	155.1(3)	Re(1) - Pt(3) - P(4)	116.2(3)
Re(1) - Pt(3) - P(5)	108.6(3)	P(4) - Pt(3) - P(5)	108.9(4)
Pt(1) - Re(1) - Pt(2)	56.7(1)	Pt(1) - Re(1) - Pt(3)	57.4(1)
Pt(1) - Re(1) - O(1)	88.8(8)	Pt(1) - Re(1) - O(2)	146.7(9)
Pt(1) - Re(1) - O(3)	95.2(8)	Pt(2) - Re(1) - Pt(3)	56.9(1)
Pt(2) - Re(1) - O(1)	142.7(8)	Pt(2) - Re(1) - O(2)	95.7(9)
Pt(2) - Re(1) - O(3)	90.8(8)	Pt(3) - Re(1) - O(1)	94.1(9)
Pt(3) - Re(1) - O(2)	92.9(9)	Pt(3) - Re(1) - O(3)	145.0(8)
O(1) - Re(1) - O(2)	109.9(12)	O(1) - Re(1) - O(3)	107.7(12)
O(2) - Re(1) - O(3)	104.4(12)	O(4) - Re(2) - O(5)	103.5(17)
O(4) - Re(2) - O(6)	111.4(16)	O(4) - Re(2) - O(7)	107.6(17)
O(5) - Re(2) - O(6)	113.5(16)	O(5) - Re(2) - O(7)	110.7(17)
O(6) - Re(2) - O(7)	109.8(15)	Pt(1) - P(1) - C(1)	109.8(13)
Pt(2) - P(2) - C(1)	110.0(13)	Pt(2) - P(3) - C(2)	108.8(11)
Pt(3) - P(4) - C(2)	108.6(11)	Pt(3) - P(5) - C(3)	108.9(12)
Pt(1) - P(6) - C(3)	107.1(12)		

Table 2.2.3. Crystallographic data of the structure analysis of compound 6

Formula	$C_{75}H_{66}O_7P_6Pt_3Re_2$
Formula wt	2222.8
Crystal system	triclinic
Space group	$P \bar{1}$
a Å	14.154(4)
b Å	14.213(3)
c Å	20.522(4)
α °	78.938(14)
β °	75.812(19)
γ °	74.957(22)
V Å ³	3828.9(15)
Z	2
F(0 0 0)	2092
D calc g cm ⁻³	1.928
T K	290
Crystal colour and habit	small block-shaped
Crystal size mm	0.20 x 0.18 x 0.15
Cell: reflections used θ range(°)	23 reflections 20.9< θ <23.5
μ (Mo-K α) cm ⁻¹	88.84
Transmission on F ²	0.78 → 1.32
Measured reflections	13907
Unique reflections	13341
Observed reflections $I \geq 3\sigma(I)$	5414
θ range °	3.14 - 26.27
Miller indices h	-17→17
k	0 →17
l	-25→25
Decay in mean standard (%)	2
R _{int}	0.038
No. of parameters	284
R(F)	0.0685
R _w (F)	0.0773
S	4.18
$\Delta\rho_{max}$ and $\Delta\rho_{min}$. eÅ ⁻³	2.43 → -2.02
Δ/σ_{max} .	0.07

2.2.3. The structure of $[\text{Pt}_3(\text{ReO}_3)(\mu\text{-dppm})_3][\text{PF}_6]$, **7**

The complex cation $[\text{Pt}_3(\text{ReO}_3)(\mu\text{-dppm})_3]^+$ was first crystallized in the form of its $[\text{ReO}_4]^-$ salt. The structure of this salt was described in section 2.2.2. However, the compound $[\text{Pt}_3(\text{ReO}_3)(\mu\text{-dppm})_3][\text{PF}_6]$, **7**, the corresponding $[\text{PF}_6]^-$ salt, gave crystals of somewhat better quality than **6** and of higher, cubic symmetry.

The structure of **7** is shown in Figure 2.2.4. and is characterized by bond distance and angles listed in Table 2.2.5. It contains a triangular Pt_3 unit edge-bridged by the three dppm ligands, yielding a latitudinal $[\text{Pt}_3(\mu\text{-dppm})_3]$ fragment. (Puddephatt, Manojlovic-Muir & Muir, 1990).

The Pt_3 triangle is capped by a ReO_3 group to form a distorted tetrahedral Pt_3Re core (see Table 2.2.5). However, the structure of **7** shows exact C_3 symmetry, the three-fold axis passing through the rhenium atom and the centre of the Pt_3 triangle. In the ReO_3Pt_3 unit the rhenium centre displays a pseudo octahedral coordination symmetry [O-Re-O 108.4(3), Pt-Re-O 83.7(3), 101.7(3), 141.4(3)°]. Each Re-O bond is directed towards one of the symmetrically equivalent P(1) atoms and away from a P(2) atom (see Figure 2.2.4) and the Pt_3O_3 octahedron is therefore distorted towards trigonal prismatic geometry, with a twist angle of 20.3°. This distortion, also apparent from Figure 2.2.4, may be caused by weak attractive interactions involving the polar oxo groups of the ReO_3 unit and the hydrogen atoms of the phenyl substituents in the $[\text{Pt}_3(\mu\text{-dppm})_3]$ fragment, resulting in three short intramolecular O...H distances [O(1)...H(C16B) 2.39(1) Å]. A similar trigonal twist of the co-ordination octahedron around the rhenium centre has been found in the closely related structure of the $[\text{Pt}_3\text{Re}(\text{CO})_3(\mu\text{-dppm})_3]^+$ cation, **4**, (Xiao, Jagadese, Vittal, Puddephatt, 1995) in which the $\text{Re}(\text{CO})_3$ group replaces the ReO_3 group of **7**. The structure of the cation in $[\text{Pt}_3(\text{ReO}_3)(\mu\text{-dppm})_3][\text{PF}_6]$, **7**, described above is

essentially the same as that found in **6**, but there are differences which arise from the conformational change of the $\text{Pt}_3(\mu\text{-dppm})_3$ moiety responding to the different steric and electronic properties of the anions. In the $\text{Pt}_3(\mu\text{-dppm})_3$ fragment in **7** all Pt-P bonds are bent out of the Pt_3 plane, the three Pt-P(2) bonds in the direction towards the ReO_3 group and the other three Pt-P(1) bonds in the opposite direction. The displacements of the P(2), C(1) and P(1) atoms from the Pt_3 face are [0.169(3), 0.403(10) and -0.562(2) Å]. Each $\text{Pt}_2\text{P}_2\text{C}$ unit adopts an envelope conformation with a P(1) atom at the flap position. In the resulting conformation of the $\text{Pt}_3\text{P}_6\text{C}_3$ skeleton all six phenyl substituents on one side of the Pt_3 triangle are equatorial and form a cavity large enough to accommodate the ReO_3 group, while six axial phenyl substituents encase the opposite face of the Pt_3 triangle (see Figure 2.2.5). In **6**, the $\text{Pt}_3\text{P}_6\text{C}_3$ skeleton displays a different conformation; cavities above both faces of the Pt_3 triangle (see the space filling diagrams in Figure 2.2.2-3) permit the ReO_3 and $[\text{ReO}_4]^-$ groups to interact with the Pt atom. In the **7** any association of the anion with the Pt_3 unit is closed off by the conformation of the $[\text{Pt}_3(\mu\text{-dppm})_3]$ fragment, as is evident from Figure 2.2.6.

The Pt-Pt distances in **7** [2.6115(6) Å] (see Table 2.2.5) are indicative of normal single bonds. They are comparable with Pt-Pt bond lengths in **6** [2.598(2)-2.609(3) Å] (see Table 2.2.2) and in $[\text{Pt}_3\text{Re}(\text{CO})_3(\mu\text{-dppm})_3]^+$ [2.5930(9)-2.6114(7) Å] (Xiao, Kristof, Vittal & Puddephatt, 1995) and in all three compounds they are amongst the shortest found in the $[\text{Pt}_3(\mu\text{-CO})(\mu\text{-dppm})_3]^{2+}$ cation and its derivatives (Puddephatt, Manolovic-Muir and Muir, 1990; Ferguson, Lloyd & Puddephatt, 1986). Thus, the replacement of the $\text{Re}(\text{CO})_3$ group in **4** by ReO_3 has no significant effect on Pt-Pt bonding in the Pt_3Re core. The Pt-Re bonds, which are thought to involve donation of three electron pairs from the Pt_3 triangle into three vacant acceptor orbitals of the ReO_3 or $\text{Re}(\text{CO})_3$ group, are longer in **7** [2.7010(6) Å] than in **4** [2.649(1)-2.685(1) Å]. This is unexpected. It may be that the Pt-Re bonds are influenced by the size and electronic properties of the two different capping groups.

In **6** and **7** the O-Re-O angles [104.4(12)-107.7(12) and 108.4(3)°] are much larger than the C-Re-C angles in **4** [88.2(5)-91.0(5)°] and the oxo groups are more polar than the CO groups. This may be a result of interactions of the ReO₃ unit with the hydrogen atoms of the phenyl substituents in the Pt₃(μ-dppm)₃ fragment. For example in **6** O...H distances are in the range of [2.324(2) - 2.590(2) Å] and in **7** [2.39(1) - 2.50(2) Å]. Furthermore, the Pt-Re bonds in **6** [2.711(5), 2.720(3), 2.748(3) Å] (see Table 2.2.2) are longer than those in **7** [2.7010(6) Å]. This can be considered as a reflection of different steric effects in the two compounds, arising from different conformations of the Pt₃(μ-dppm)₃ fragments. In **6** two of the six phenyl substituents on the capped side of the Pt₃ triangles are axial and the cavity enclosing the ReO₃ group is therefore smaller than the corresponding cavity in **7** (see Figures 2.2.2-3, and 2.2.5-6), so the steric effects on the Pt-Re bonds are greater in **6**. The Re-O distances in **7** [1.705(8) Å] are in the range of those found in **6** and other compounds containing the ReO₃ group (Domingos, Marcalo, Parclo, Pires and Sautos, 1993; Okuda, Herdtweck and Hermann, 1988; Manojlovic-Muir, Muir, Rennie, Xiao and Puddephatt, 1993).

Experimental

The atomic fractional co-ordinates are given in Table 2.2.4 and crystal data are summarised in Table 2.2.6. The absorption correction was applied using the Ψ -scan method (Molen, 1991) and correction factors on F^2 were in the range 0.409-0.999, corresponding to a difference in mean path of 0.12 mm. The structure was solved by the direct methods (Sheldrick, 1986) and refined by full matrix least-squares on F^2 , with $\omega=1/[\sigma^2(F^2)+(0.037P)^2+137P]$, where $P=[F^2_{\text{obs}}+2F^2_{\text{calc}}]/3$. All non-hydrogen atoms were assigned anisotropic displacement parameters. All refinement calculations were performed using the SHELXL-93 program package

(Sheldrick, 1993). All the fluorine atoms, and carbon atoms C(44), C(45) and C(46) have large displacement parameters, (see Table 2.2.4.) this suggests positional disorder for these atoms. Attempts to model this disorder were not successful.

Captions to Figures

Figure 2.2.4. A view of the structure of the $[\text{Pt}_3(\text{ReO}_3)(\mu\text{-dppm})_3]^+$ cation in 7. The carbon atoms are represented by spheres of arbitrary radius and the remaining non-hydrogen atoms by 50% probability ellipsoids. Hydrogen atoms are omitted for clarity. Phenyl carbon atoms are numbered in the sequence $\text{Cn}_1\text{-Cn}_6$, where $n= 1\text{-}4$, starting with the *ipso* carbon atom, and labels are shown only for Cn_2 atoms.

Figure 2.2.5. A space filling diagram of the $[\text{Pt}_3(\text{ReO}_3)(\mu\text{-dppm})_3]^+$ cation. The platinum atoms are shown in black and the oxygen atoms are dotted. The cation is viewed along the normal to the Pt_3 plane from the ReO_3 side.

Figure 2.2.6. The corresponding view of the cation in 7 along the normal to the Pt_3 plane from side opposite to ReO_3 .

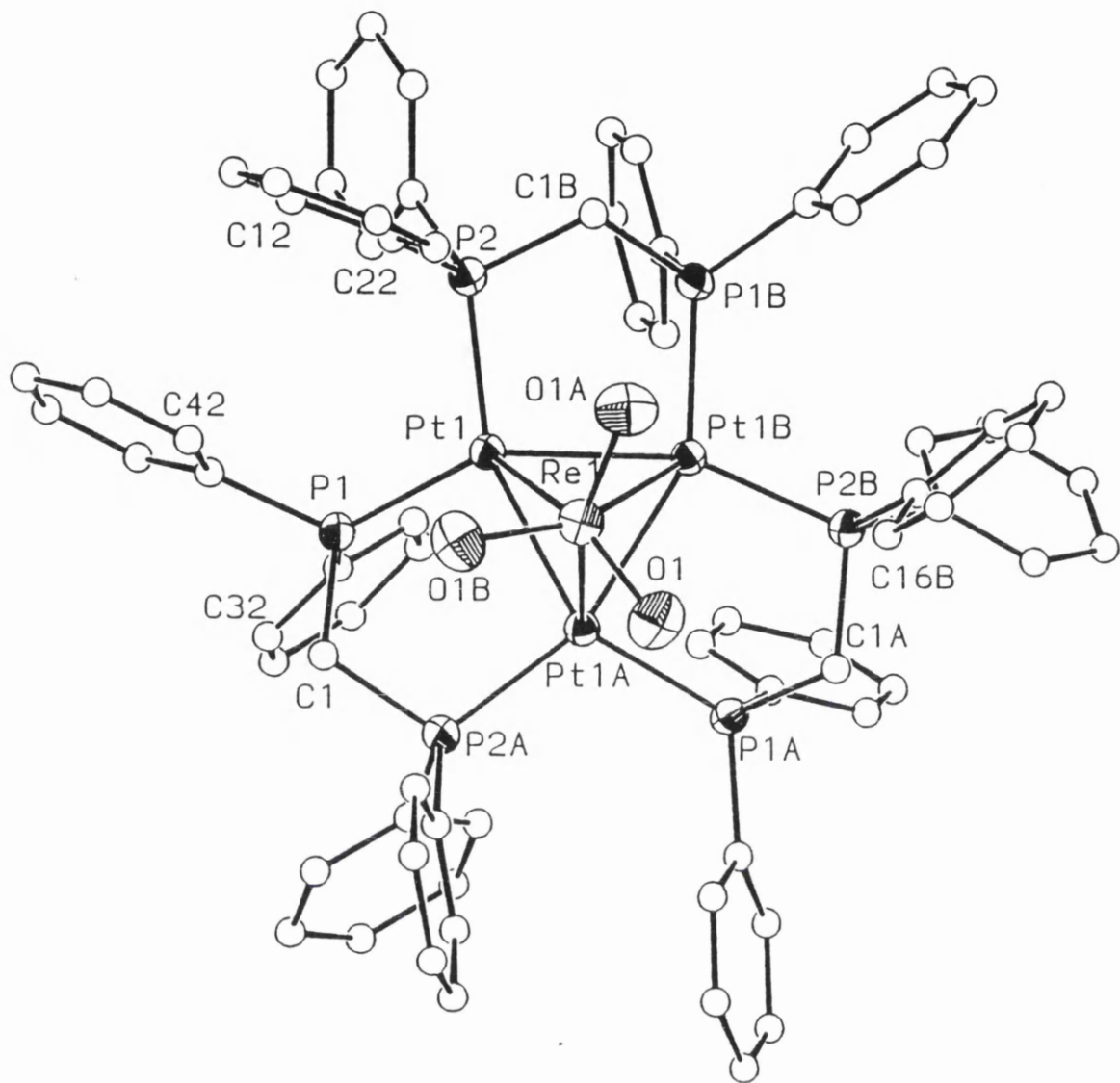


Figure 2.2.4

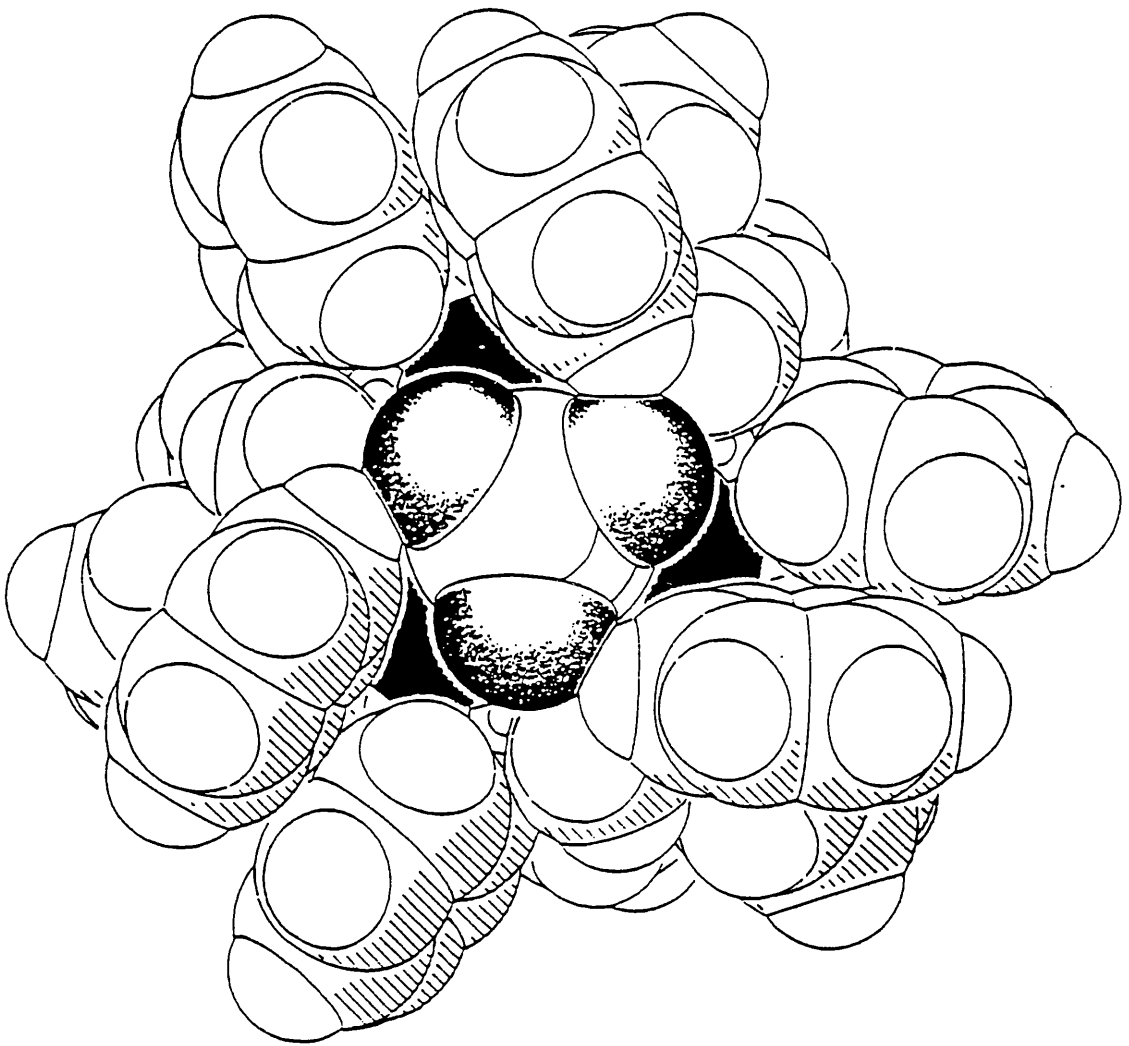


Figure 2.2.5

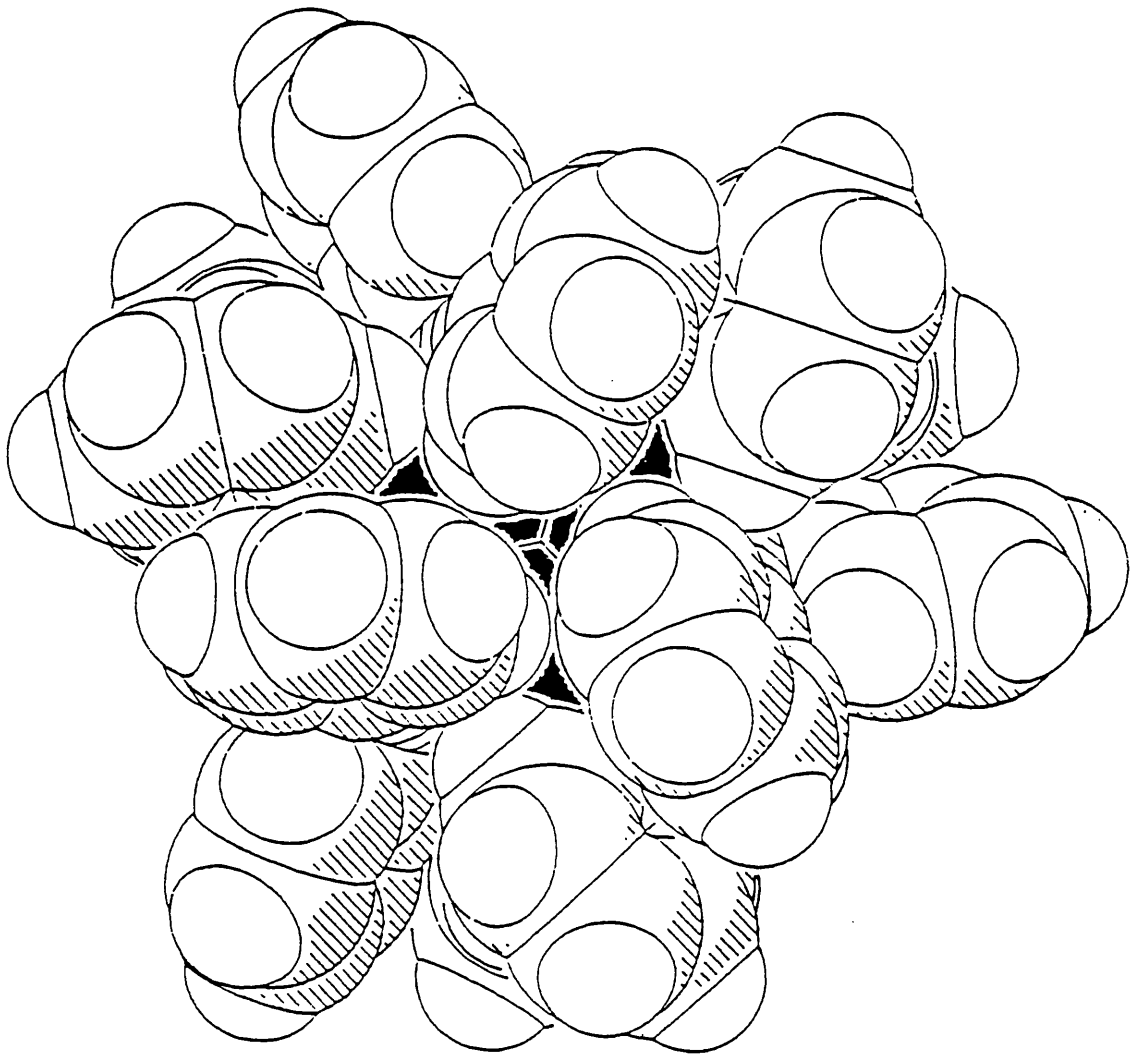


Figure 2.2.6

Table 2.2.4. Atomic fractional co-ordinates and isotropic displacement parameters(\AA^2) for compound 7.

Atom	x	y	z	U
Pt(1)	0.2076(1)	0.2305(1)	0.14631(1)	0.038(1)
Re(1)	0.2476(1)	0.2476(1)	0.2476(1)	0.053(1)
P(1)	0.1415(1)	0.2887(1)	0.1145(1)	0.045(1)
P(2)	0.2810(1)	0.2257(1)	0.0896(1)	0.045(1)
P(3)	0.5000	0.5000	0.0000	0.041(1)
P(4)	0.9396(3)	0.4396(3)	0.0604(4)	0.058(3)
F(3)	0.4862(14)	0.4910(9)	0.0561(7)	0.312(12)
F(4A)	0.9301(11)	0.4531(17)	0.0166(13)	0.248(20)
F(4B)	0.9630(16)	0.4287(12)	0.1055(11)	0.205(13)
O(1)	0.2311(4)	0.2393(4)	0.3147(3)	0.083(3)
C(1)	0.1132(4)	0.3278(4)	0.1719(4)	0.053(3)
C(11)	0.3251(3)	0.2868(2)	0.0897(3)	0.057(3)
C(12)	0.3242(3)	0.3220(3)	0.0457(3)	0.080(4)
C(13)	0.3563(4)	0.3683(3)	0.0460(3)	0.093(4)
C(14)	0.3893(4)	0.3794(3)	0.0903(4)	0.096(5)
C(15)	0.3902(3)	0.3442(4)	0.1343(3)	0.094(4)
C(16)	0.3581(3)	0.2979(3)	0.1340(3)	0.078(4)
C(21)	0.2724(3)	0.2113(3)	0.0171(2)	0.0540(3)
C(22)	0.2203(3)	0.2090(3)	-0.0041(3)	0.068(3)
C(23)	0.2125(4)	0.1968(4)	-0.05855(3)	0.098(5)
C(24)	0.2569(4)	0.1867(3)	-0.0918(2)	0.107(6)
C(25)	0.3090(3)	0.1890(3)	-0.0706(3)	0.101(5)
C(26)	0.3168(3)	0.2013(3)	-0.0161(4)	0.078(4)
C(31)	0.0826(3)	0.2525(3)	0.0858(3)	0.055(3)
C(32)	0.0329(3)	0.2774(3)	0.0767(3)	0.069(3)
C(33)	-0.0102(2)	0.2477(4)	0.0560(3)	0.091(5)
C(34)	-0.0036(3)	0.1930(5)	0.0443(3)	0.101(5)
C(35)	0.0461(4)	0.1680(3)	0.0534(4)	0.095(5)
C(36)	0.0892(3)	0.1978(3)	0.0742(3)	0.065(3)
C(41)	0.1586(3)	0.3428(3)	0.0662(3)	0.057(3)
C(42)	0.2017(3)	0.3768(3)	0.0789(3)	0.081(4)
C(43)	0.2168(4)	0.4175(3)	0.0431(4)	0.090(4)
C(44)	0.1889(5)	0.4243(4)	-0.0054(4)	0.150(9)
C(45)	0.1459(5)	0.3903(4)	-0.0181(13)	0.175(11)
C(46)	0.1307(4)	0.3495(4)	0.0177(3)	0.120(7)

Table 2.2.5. Selected bond distances (Å) and bond angles (°)

(a) bond distances

Pt(1) - Pt(1 ⁱ)	2.6115(6)	Pt(1) - Re(1)	2.7010(6)	Pt(1) - P(1)	2.294(2)
Pt(1) - P(2)	2.275(2)	Re(1) - O(1)	1.705(8)	P(1) - C(1)	1.838(10)
P(1) - C(31)	1.834(6)	P(1) - C(41)	1.824(6)	P(2) - C(1 ⁱⁱ)	1.840(10)
P(2) - C(11)	1.846(6)	P(2) - C(21)	1.823(6)	P(3) - F(3)	1.433(12)

(b) bond angles

Pt(1 ⁱ) - Pt(1) - Re(1)	61.090(8)	Pt(1 ⁱⁱ) - Pt(1) - P(1)	89.75(6)
Pt(1 ⁱ) - Pt(1) - P(2)	157.75(7)	Pt(1 ⁱⁱ) - Pt(1) - P(1)	146.87(6)
Pt(1 ⁱⁱ) - Pt(1) - P(2)	98.12(7)	Re(1) - Pt(1) - P(1)	118.16(6)
Re(1) - Pt(1) - P(2)	106.41(7)	P(1) - Pt(1) - P(2)	112.47(9)
Pt(1 ⁱ) - Re(1) - Pt(1)	57.82(2)	Pt(1 ⁱⁱ) - Re(1) - Pt(1)	57.82(2)
Pt(1) - Re(1) - O(1 ⁱ)	101.7(3)	Pt(1) - Re(1) - O(1)	141.4(3)
Pt(1 ⁱⁱ) - Re(1) - O(1 ⁱ)	83.6(3)	Pt(1) - Re(1) - O(1 ⁱⁱ)	83.7(3)
O(1) - Re(1) - O(1 ⁱⁱ)	108.4(3)	Pt(1) - P(1) - C(1)	109.3(3)
Pt(1) - P(1) - C(31)	112.7(2)	Pt(1) - P(1) - C(41)	120.7(3)
C(1) - P(1) - C(31)	104.3(4)	C(1) - P(1) - C(41)	101.7(4)
C(31) - P(1) - C(41)	106.4(4)	Pt(1) - P(2) - C(1 ⁱⁱ)	109.7(3)
Pt(1) - P(2) - C(11)	114.8(3)	Pt(1) - P(2) - C(21)	120.9(3)
C(1 ⁱⁱ) - P(2) - C(11)	102.5(4)	C(1 ⁱⁱ) - P(2) - C(21)	103.9(4)
C(11) - P(2) - C(21)	103.0(4)		

Symmetry transformations used to generate equivalent atoms:

i z, x, y

ii y, z, x

Table 2.2.6. Crystallographic data of the structure analysis of compound 7

Formula	$C_{75}H_{66}F_6O_3P_7Pt_3Re$
Formula wt	2117.54
Crystal system	cubic
Space group	$Pa\bar{3}$ (No.205)
a Å	24.495(1)
V Å ³	14697(1)
Z	8
F(0 0 0)	8064
D calc g cm ⁻³	1.914
T K	293
Crystal colour and habit	dark red prismatic
Crystal size mm	0.41 x 0.39 x 0.31
Cell: reflections used θ range(°)	25 reflections 20.8< θ <24.7
μ (Mo-K α) cm ⁻¹	75.49
Transmission on F ²	0.4067 - 0.9987
Measured reflections	16677
Unique reflections	5559
Observed reflections $I \geq 3\sigma(I)$	3113
θ range °	2.0 - 27.4
Miller indices h	0 \rightarrow 31
k	-31 \rightarrow 0
l	0 \rightarrow 31
Decay in mean standard (%)	6.8
R _{int}	0.0982
No. of parameters	250
R(F ²)	0.041
R _w (F ²)	0.0883
S	0.93
$\Delta\rho_{max}$ and $\Delta\rho_{min}$ eÅ ⁻³	1.07 \rightarrow -1.14
Δ/σ_{max}	0.277

2.2.4. The structure of $[\text{Pt}_3\{\text{Re}(\text{CO})_3\text{P}(\text{OPh})_3\}(\mu\text{-dppm})_3][\text{PF}_6] \text{C}_2\text{H}_5\text{OH}$, **8**

The complex $[\text{Pt}_3\{\text{Re}(\text{CO})_3\text{P}(\text{OPh})_3\}(\mu\text{-dppm})_3][\text{PF}_6] \text{C}_2\text{H}_5\text{OH}$, **8**, has been characterized by an X-ray crystal structure analysis. Selected bond lengths and angles are listed in Table 2.2.8. The molecular structure of **8**, presented in Figure 2.2.7, shows that addition of phosphite to the parent complex $[\text{Pt}_3\text{Re}(\text{CO})_3(\mu\text{-dppm})_3]^+$, **4**, (Xiao, Vittal, Puddephatt, Manojlovic-Muir & Muir, 1993) occurs selectively at the rhenium atom.

The structure is built of $\text{Re}(\text{CO})_3\text{P}(\text{OPh})_3^+$ and $\text{Pt}_3(\mu\text{-dppm})_3$ fragments, the latter containing a triangular Pt_3 unit edge-bridged by three dppm ligands. The Pt_3 triangle is capped by the $\text{Re}(\text{CO})_3\text{P}(\text{OPh})_3^+$ fragment to form a distorted tetrahedral Pt_3Re cluster with two edges, Pt(1)-Re and Pt(2)-Re weakly semi-bridged by carbonyl ligands [Re-C 1.969(9), 1.998(9) Å and Pt-C 2.428(9), 2.550(9) Å].

The $\text{Pt}_3\{\text{Re}(\text{CO})_3\text{P}(\text{O})_3\}(\mu\text{-PCP})_3$ core approximates to C_s symmetry (see Figure 2.2.7), the mirror plane passing through the atoms Pt(3), Re, P(7), C(1), O(1) and C(4), and bisecting the Pt(1)-Pt(2) vector. Distorted octahedral geometry around the Re atom in the $\text{Re}\{\text{P}(\text{OPh})_3\}(\text{CO})_3^+$ unit, evident from the bond angles shown in Table 2.2.8, is completed by the Pt(3) atom and the mid-point of the Pt(1)-Pt(2) bond. Each Pt atom has 16 and the Re atom 18 valence electrons. The Pt-Re bond lengths in **8** [2.762(1), 2.825(1) and 2.949(1) Å] are longer than those in **4** [2.649(1), 2.684(1) and 2.685(1)]. Addition of phosphite evidently changes the valence electron count of the cluster complex from 54 in **4** to 56 in **8** and weakens the Pt-Re bonding.

In **8** the Pt-Pt bond lengths show some variation [2.603(1), 2.635(1), 2.677(1) Å]. The Pt-Re distances are spread over a considerable range [2.762(1), 2.828(1), 2.942(1) Å], though all three distances lie within the accepted range for Pt-Re bond lengths (2.65-3.00 Å) (Xiao, Vittal, Puddephatt, Manojlovic-Muir &

Muir, 1993; Hao, Xiao, Vittal & Puddephatt, 1994; Xiao, Puddephatt, Manojlovic-Muir, Muir & Torabi, 1995; Xiao, Vittal & Puddephatt, 1993; Powell, Brewer, Gulia & Sawyer, 1992; Ciani, Moret, Sironi, Antogmazza, Beringhelli, D'Alfonso, Pergola & Minoja, 1991; Carr, Fontaine, Shaw & Thornton-Pett, 1988). The average Pt-Pt distance [2.60 Å in **4** (Xiao, Vittal, Puddephatt, Manojlovic-Muir & Muir, 1993) and 2.64 Å in **8**] and mean Pt-Re distance (2.67 Å in **4** and 2.84 Å in **8**) indicate that the phosphite ligand binds to the parent complex **4** at the expense of some cluster bonding, affecting the Pt-Re bonds to a greater extent than the Pt-Pt bonds. The Pt-P, Re-P and P-O bond lengths (see Table 2.2.7) are unexceptional (Puddephatt, Manojlovic-Muir & Muir, 1990; Qi, Fanwick & Walton, 1990).

In the $\text{Pt}_3(\mu\text{-dppm})_3$ fragment the Pt_3P_6 skeleton is severely distorted from the idealized latitudinal geometry (see Figure 2.2.8). All Pt-P bonds are bent out of the Pt_3 plane and away from the bulky $\text{Re}(\text{CO})_3\{\text{P}(\text{OPh})_3\}^+$ fragment. The out-of-plane displacements of the phosphorus atoms [0.088(2)-1.195(2) Å] are particularly large for the P(5) and P(4) atoms [0.969(2) and 1.195(2) Å], presumably arising from steric interactions with semi-bridging carbonyl groups. The conformation of the $\text{Pt}_3\text{P}_6\text{C}_3$ unit differs from that in **4** (Xiao, Vittal, Puddephatt, Manojlovic-Muir & Muir, 1993) where the Pt_3P_6 skeleton is essentially planar and all three $\text{Pt}_2\text{P}_2\text{C}$ rings shows envelope conformations with a carbon atom at the flap. In **8** the three rings adopt envelope conformations, but with carbon atom at the flap only in the Pt(1)Pt(2)P(1)C(1)P(2) ring; in the other two rings the flaps are occupied by phosphorus atoms, P(4) and P(5) (see Figure 2.2.8).

Experimental

The crystal selected for analysis was dark red. The final atomic co-ordinates and displacement parameters are listed in Table 2.2.7. The crystallographic data and the unit cell constants are given in Table 2.2.9. They were determined by a least squares treatment of 25 reflections. The absorption correction was made at the end of isotropic refinement using the empirical method of Walker and Stuart (1983). The positions of the platinum and rhenium atoms were determined from a Patterson function and those of the remaining non-hydrogen atoms from subsequent difference Fourier syntheses.

The structure was refined by full matrix least squares. Each phenyl group was treated as a rigid body with D_{6h} symmetry, C-C=1.38 Å and C-H=0.96 Å. Phenyl carbon atoms and atoms of the solvent molecule were refined with isotropic displacement parameters, and the remaining non-hydrogen atoms with anisotropic displacement parameters. No allowance was made for scattering of the hydrogen atoms in the solvent molecules. All calculations were performed using the GX program package (Mallinson & Muir, 1985).

Captions to Figures.

Figure 2.2.7. A view of the molecular structure of $[\text{Pt}_3\{\text{Re}(\text{CO})_3\text{P}(\text{OPh})_3\}(\mu\text{-dppm})_3]^+$, **8**, with atoms represented by spheres of arbitrary radius. In the phenyl rings atoms are numbered in the sequence $\text{C}(n_1)\dots\text{C}(n_6)$, where $n=\text{A}$ to L and the $\text{C}(n_1)$ atom is P- or O-substituted. The hydrogen atoms are omitted for clarity.

Figure 2.2.8. A view of the inner core of **8**, with displacement ellipsoids showing 50% probability. Only the ipso carbon atoms of the phenyl groups are shown.

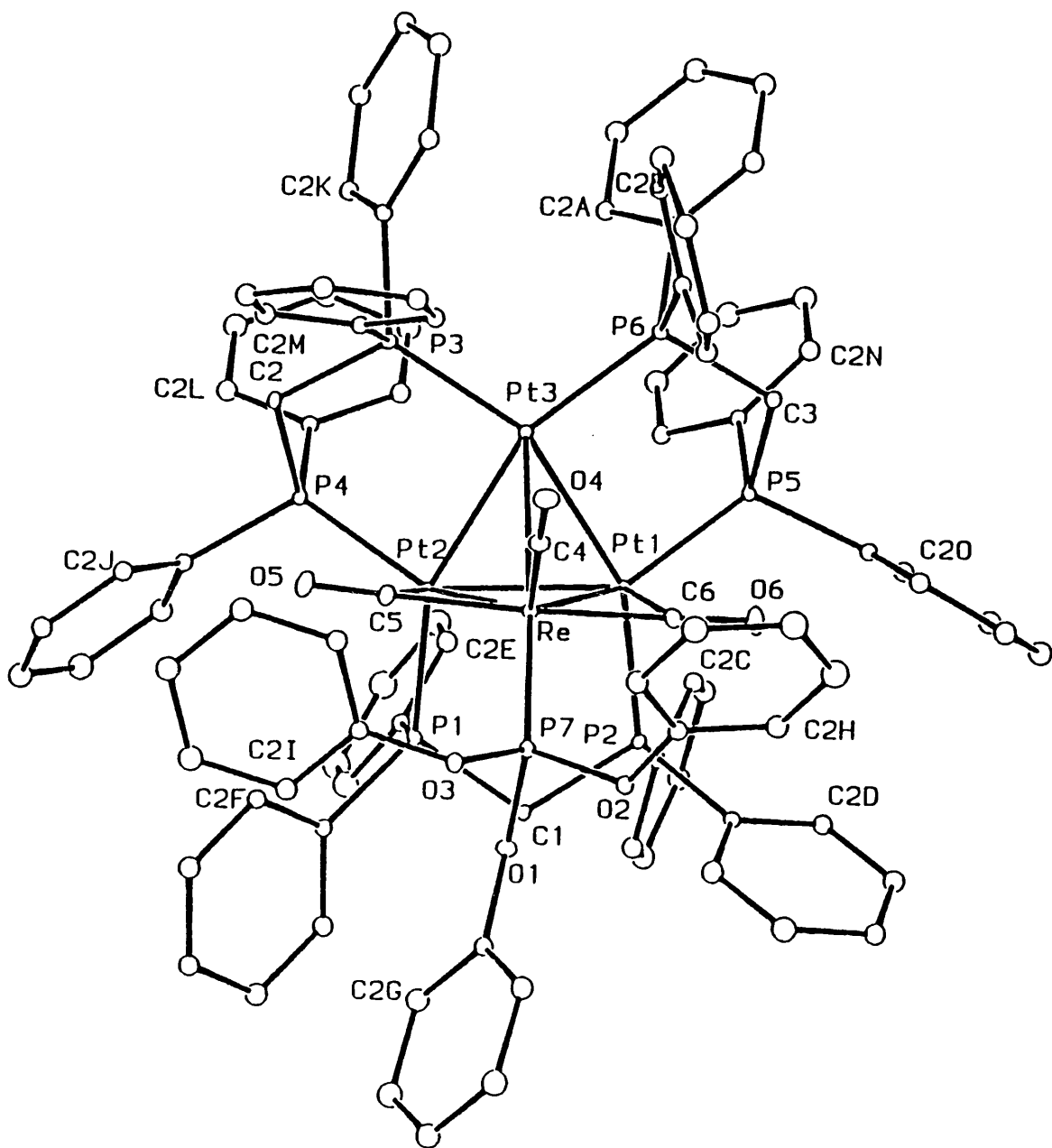


Figure 2.2.7

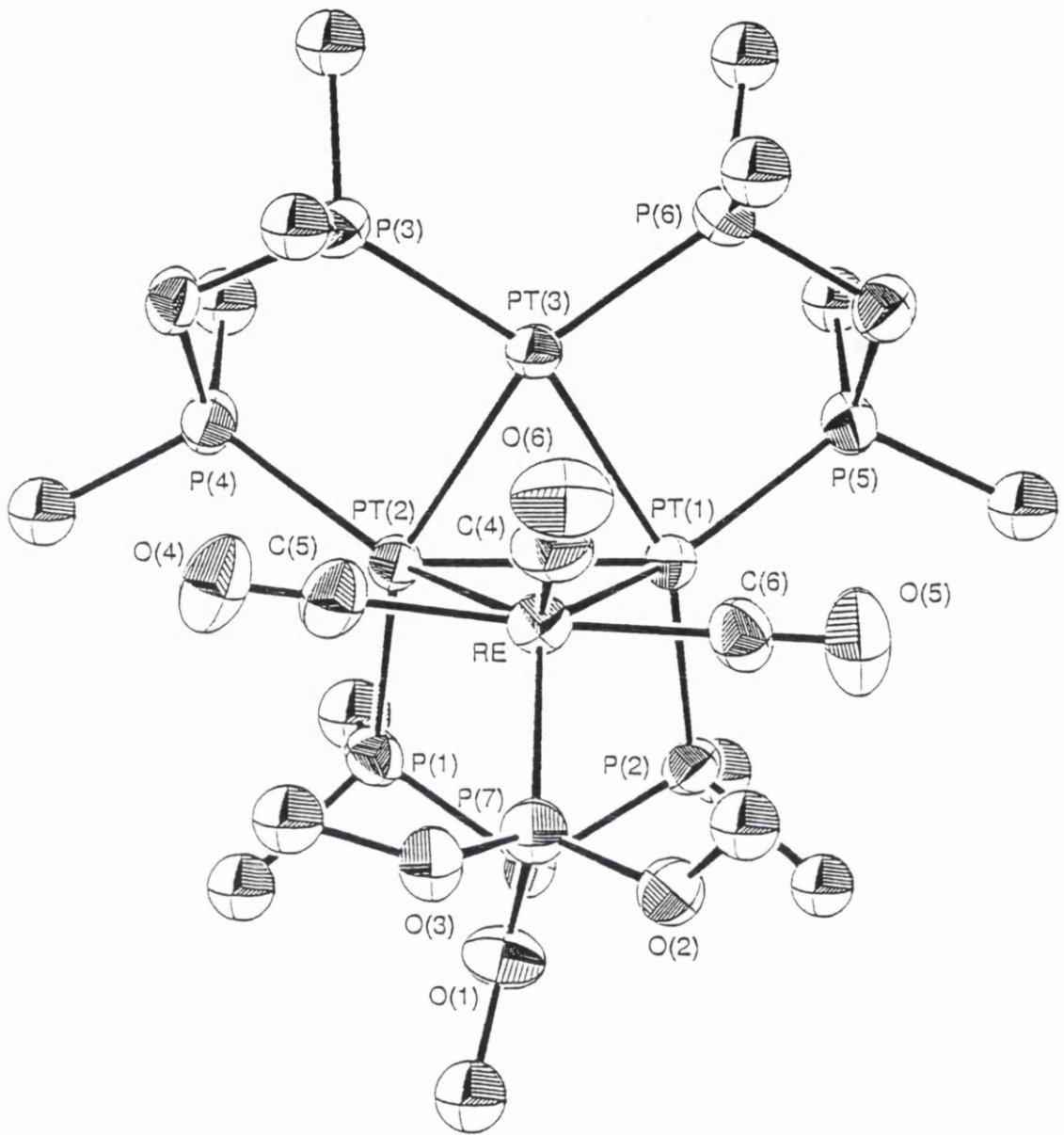


Figure 2.2.8

Table 2.2.7. Atomic fractional co-ordinates and isotropic displacement parameters(\AA^2) for compound **8**

Atom	x	y	z	U
Pt(1)	0.09857(2)	0.22934(2)	0.17596(1)	0.031
Pt(2)	0.16111(2)	0.22307(2)	0.30296(1)	0.031
Pt(3)	0.11056(2)	0.35599(2)	0.23544(1)	0.031
Re	0.29575(2)	0.23129(2)	0.19908(2)	0.037
P(1)	0.16276(16)	0.09659(12)	0.32031(10)	0.037
P(2)	0.10266(14)	0.10006(11)	0.17144(10)	0.035
P(3)	0.13759(15)	0.42667(11)	0.32465(10)	0.039
P(4)	0.10885(15)	0.28435(13)	0.40379(11)	0.038
P(5)	-0.02023(15)	0.30118(12)	0.10641(10)	0.037
P(6)	0.03969(15)	0.43991(12)	0.14921(10)	0.040
P(7)	0.43879(15)	0.13469(12)	0.17581(10)	0.042
P(8)	0.4465(2)	0.3500(2)	0.5820(2)	0.073
F(1)	0.3567(7)	0.3761(6)	0.5342(5)	0.163
F(2)	0.3749(9)	0.3201(7)	0.6307(5)	0.192
F(3)	0.4800(7)	0.2682(5)	0.5491(6)	0.178
F(4)	0.4089(8)	0.4290(6)	0.6187(6)	0.181
F(5)	0.5068(10)	0.3835(9)	0.5346(7)	0.253
F(6)	0.5314(9)	0.3269(7)	0.6283(8)	0.257
O(1)	0.4342(4)	0.0488(3)	0.1972(3)	0.051
O(2)	0.4785(4)	0.1174(3)	0.0979(3)	0.050
O(3)	0.5462(4)	0.1339(3)	0.2048(3)	0.048
O(4)	0.3555(4)	0.2470(4)	0.3484(3)	0.069
O(5)	0.2423(5)	0.2316(5)	0.0479(3)	0.080
O(6)	0.4107(5)	0.3448(4)	0.1554(4)	0.075
O(S1)	0.8429(14)	0.2216(11)	0.6671(10)	0.256(8)
C(S1)	0.786(2)	0.221(1)	0.730(1)	0.21(1)
C(S2)	0.7022(14)	0.2167(11)	0.7784(9)	0.152(6)
C(1)	0.1840(6)	0.0432(4)	0.2396(4)	0.041
C(2)	0.1537(6)	0.3709(5)	0.4072(4)	0.043
C(3)	0.0179(6)	0.3874(5)	0.0751(4)	0.045
C(4)	0.3687(7)	0.3009(6)	0.1722(5)	0.056
C(5)	0.3273(6)	0.2394(5)	0.2959(4)	0.052
C(6)	0.2546(6)	0.2298(5)	0.1050(4)	0.051
C(A1)	-0.0818(6)	0.5131(5)	0.1614(6)	0.046(2)
C(A2)	-0.1334(4)	0.5129(6)	0.2223(5)	0.052(2)
C(A3)	-0.2280(6)	0.5650(4)	0.2322(3)	0.069(3)
C(A4)	-0.2711(6)	0.6174(4)	0.1811(5)	0.077(3)
C(A5)	-0.2195(4)	0.6176(5)	0.1201(4)	0.074(3)
C(A6)	-0.1248(7)	0.5655(3)	0.1103(4)	0.065(3)
C(B1)	0.1234(4)	0.4936(5)	0.1115(3)	0.049(2)
C(B2)	0.1088(7)	0.5713(3)	0.1262(6)	0.065(3)
C(B3)	0.1809(7)	0.6068(4)	0.1070(4)	0.084(3)
C(B4)	0.2676(4)	0.5645(4)	0.0731(3)	0.082(3)
C(B5)	0.2822(7)	0.4868(3)	0.0584(5)	0.076(3)
C(B6)	0.2101(8)	0.4513(4)	0.0776(4)	0.063(3)

C(C1)	-0.0110(4)	0.0692(5)	0.1845(4)	0.042(2)
C(C2)	-0.1030(5)	0.1244(3)	0.1753(3)	0.055(2)
C(C3)	-0.1900(5)	0.1045(5)	0.1878(5)	0.070(3)
C(C4)	-0.1850(4)	0.0293(4)	0.2096(3)	0.069(3)
C(C5)	-0.0930(5)	-0.0260(3)	0.2188(4)	0.077(3)
C(C6)	-0.0060(5)	-0.0060(5)	0.2063(6)	0.064(3)
C(D1)	0.1604(8)	0.0488(4)	0.0943(4)	0.040(2)
C(D2)	0.1007(6)	0.0428(5)	0.0421(6)	0.055(2)
C(D3)	0.1440(6)	0.0067(6)	-0.0171(4)	0.067(3)
C(D4)	0.2469(7)	-0.0234(4)	-0.0240(4)	0.064(3)
C(D5)	0.3067(5)	-0.0173(5)	0.0282(5)	0.087(3)
C(D6)	0.2634(7)	0.0188(7)	0.0874(3)	0.071(3)
C(E1)	0.0442(6)	0.0903(5)	0.3566(6)	0.049(2)
C(E2)	-0.0397(4)	0.1500(4)	0.3380(3)	0.062(3)
C(E3)	-0.1329(6)	0.1519(6)	0.3648(6)	0.095(4)
C(E4)	-0.1422(6)	0.0941(5)	0.4103(5)	0.108(4)
C(E5)	-0.0583(5)	0.0344(5)	0.4289(4)	0.114(5)
C(E6)	0.0350(7)	0.0325(7)	0.4021(7)	0.095(4)
C(F1)	0.2617(4)	0.0273(6)	0.3687(5)	0.044(2)
C(F2)	0.3285(6)	0.0566(3)	0.4005(4)	0.050(2)
C(F3)	0.4077(6)	0.0062(5)	0.4344(3)	0.066(3)
C(F4)	0.4200(4)	-0.0734(5)	0.4366(4)	0.060(2)
C(F5)	0.3532(6)	-0.1027(3)	0.4048(3)	0.072(3)
C(F6)	0.2740(6)	-0.0523(6)	0.3709(3)	0.060(2)
C(G1)	0.5118(7)	-0.0230(5)	0.2006(7)	0.051(2)
C(G2)	0.5040(8)	-0.0738(3)	0.2531(6)	0.078(3)
C(G3)	0.5779(5)	-0.1446(4)	0.2611(3)	0.094(4)
C(G4)	0.6597(6)	-0.1646(5)	0.2166(6)	0.086(3)
C(G5)	0.6676(7)	-0.1137(3)	0.1641(5)	0.096(4)
C(G6)	0.5937(4)	-0.0429(5)	0.1561(4)	0.074(3)
C(H1)	0.4980(4)	0.1704(4)	0.0518(4)	0.053(2)
C(H2)	0.4569(7)	0.1750(6)	-0.0112(3)	0.074(3)
C(H3)	0.4746(8)	0.2265(7)	-0.0601(4)	0.112(4)
C(H4)	0.5333(4)	0.2734(4)	-0.0461(3)	0.116(5)
C(H5)	0.5744(7)	0.2688(7)	0.0169(3)	0.102(4)
C(H6)	0.5568(8)	0.2173(8)	0.0658(4)	0.072(3)
C(I1)	0.5587(9)	0.1564(7)	0.2697(2)	0.050(2)
C(I2)	0.5710(8)	0.1028(5)	0.3230(4)	0.069(3)
C(I3)	0.5863(4)	0.1244(4)	0.3872(4)	0.088(3)
C(I4)	0.5894(7)	0.1995(6)	0.3981(2)	0.084(3)
C(I5)	0.5771(7)	0.2531(4)	0.3448(4)	0.076(3)
C(I6)	0.5618(5)	0.2315(6)	0.2806(4)	0.064(3)
C(J1)	0.1605(5)	0.2278(6)	0.4794(5)	0.045(2)
C(J2)	0.2510(4)	0.2291(3)	0.5039(2)	0.055(2)
C(J3)	0.2921(5)	0.1811(6)	0.5580(4)	0.064(3)
C(J4)	0.2428(5)	0.1317(5)	0.5878(4)	0.085(3)
C(J5)	0.1523(4)	0.1304(4)	0.5633(3)	0.097(4)
C(J6)	0.1111(6)	0.1784(7)	0.5092(5)	0.072(3)
C(K1)	0.0431(7)	0.5211(4)	0.3436(6)	0.044(2)
C(K2)	-0.0386(4)	0.5251(3)	0.3864(4)	0.052(2)

C(K3)	-0.1159(5)	0.5944(3)	0.3915(4)	0.065(3)
C(K4)	-0.1116(6)	0.6598(3)	0.3539(5)	0.066(3)
C(K5)	-0.0299(3)	0.6558(3)	0.3112(3)	0.075(3)
C(K6)	0.0474(6)	0.5865(3)	0.3060(5)	0.060(2)
C(L1)	-0.0248(6)	0.3267(5)	0.4235(6)	0.043(2)
C(L2)	-0.0587(5)	0.3443(7)	0.4894(5)	0.063(3)
C(L3)	-0.1580(7)	0.3854(5)	0.5027(3)	0.081(3)
C(L4)	-0.2234(6)	0.4089(4)	0.4501(5)	0.084(3)
C(L5)	-0.1894(6)	0.3914(6)	0.3843(4)	0.078(3)
C(L6)	-0.0902(8)	0.3503(4)	0.3710(4)	0.057(2)
C(M1)	0.2536(4)	0.4554(5)	0.3185(4)	0.044(2)
C(M2)	0.3021(5)	0.4653(3)	0.3755(3)	0.060(2)
C(M3)	0.3848(6)	0.4921(6)	0.3691(3)	0.071(3)
C(M4)	0.4191(4)	0.5089(4)	0.3057(3)	0.073(3)
C(M5)	0.3706(5)	0.4990(4)	0.2487(2)	0.067(3)
C(M6)	0.2878(7)	0.4722(7)	0.02551(3)	0.053(2)
C(N1)	-0.1482(6)	0.3447(4)	0.1399(6)	0.041(2)
C(N2)	-0.2180(6)	0.3973(4)	0.1004(3)	0.062(2)
C(N3)	-0.3161(4)	0.4267(6)	0.1238(5)	0.080(3)
C(N4)	-0.3445(5)	0.4035(4)	0.1868(5)	0.085(3)
C(N5)	-0.2747(5)	0.3509(4)	0.2263(3)	0.080(3)
C(N6)	-0.1766(5)	0.3215(6)	0.2029(6)	0.051(2)
C(O1)	-0.0414(9)	0.2569(6)	0.0270(3)	0.045(2)
C(O2)	-0.1236(7)	0.2303(3)	0.0213(4)	0.057(2)
C(O3)	-0.1340(5)	0.1918(5)	-0.0361(3)	0.074(3)
C(O4)	-0.0622(7)	0.1798(5)	-0.0879(3)	0.077(3)
C(O5)	0.0200(6)	0.2064(3)	-0.0822(4)	0.074(3)
C(O6)	0.0304(6)	0.2449(6)	-0.0248(3)	0.058(2)

Table 2.2.8. Selected bond distances (Å) and bond angles (°)

(a) bond distances

Pt(1) - Pt(2)	2.677(1)	Pt(1) - Pt(3)	2.635(1)	Pt(1) - Re	2.825(1)
Pt(1) - P(2)	2.298(2)	Pt(1) - P(5)	2.253(3)	Pt(2) - Pt(3)	2.603(1)
Pt(2) - Re	2.762(1)	Pt(2) - P(1)	2.268(3)	Pt(2) - P(4)	2.289(3)
Pt(2) - C(5)	2.428(9)	Pt(3) - Re	2.942(1)	Pt(3) - P(3)	2.307(2)
Pt(3) - P(6)	2.281(3)	Re - P(7)	2.255(3)	Re - C(4)	1.885(10)
Re - C(5)	1.998(9)	Re - C(6)	1.969(9)	P(1) - C(1)	1.851(8)
P(1) - C(E1)	1.814(9)	P(1) - C(F1)	1.831(9)	P(2) - C(1)	1.863(8)
P(2) - C(C1)	1.841(7)	P(2) - C(D1)	1.832(9)	P(3) - C(2)	1.869(8)
P(3) - C(K1)	1.841(8)	P(3) - C(M1)	1.843(7)	P(4) - C(2)	1.840(8)
P(4) - C(J1)	1.823(10)	P(4) - C(L1)	1.824(9)	P(5) - C(3)	1.858(9)
P(5) - C(N1)	1.830(9)	P(5) - C(O1)	1.852(8)	P(6) - C(3)	1.846(8)
P(6) - C(A1)	1.817(9)	P(6) - C(B1)	1.847(7)	P(7) - O(1)	1.598(6)
P(7) - O(2)	1.623(6)	P(7) - O(3)	1.625(6)	P(8) - F(1)	1.548(10)
P(8) - F(2)	1.558(12)	P(8) - F(3)	1.548(10)	P(8) - F(4)	1.542(11)
P(8) - F(5)	1.469(15)	P(8) - F(6)	1.478(15)	O(1) - C(G1)	1.410(11)
O(2) - C(H1)	1.373(10)	O(3) - C(I1)	1.388(9)	O(4) - C(5)	1.150(11)
O(5) - C(6)	1.147(11)	O(6) - C(4)	1.149(12)	O(S1) - C(S1)	1.45(4)
C(S1) - C(S2)	1.50(4)				

(b) bond angles

Pt(2) - Pt(1) - Pt(3)	58.7(1)	Pt(2) - Pt(1) - Re	60.2(1)
Pt(2) - Pt(1) - P(2)	96.6(1)	Pt(2) - Pt(1) - P(5)	142.0(1)
Pt(3) - Pt(1) - Re	65.1(1)	Pt(3) - Pt(1) - P(2)	155.1(1)
Pt(3) - Pt(1) - P(5)	91.9(1)	Re - Pt(1) - P(2)	107.3(1)
Re - Pt(1) - P(5)	132.2(1)	P(2) - Pt(1) - P(5)	108.6(1)
Pt(1) - Pt(2) - Pt(3)	59.8(1)	Pt(1) - Pt(2) - Re	62.6(1)
Pt(1) - Pt(2) - P(1)	93.5(1)	Pt(1) - Pt(2) - P(4)	139.0(1)
Pt(1) - Pt(2) - C(5)	107.0(3)	Pt(3) - Pt(2) - Re	66.4(1)
Pt(3) - Pt(2) - P(1)	152.3(1)	Pt(3) - Pt(2) - P(4)	92.0(1)
Pt(3) - Pt(2) - C(5)	83.6(3)	Re - Pt(2) - P(1)	109.7(1)
Re - Pt(2) - P(4)	136.3(1)	Re - Pt(2) - C(5)	44.7(3)
P(1) - Pt(2) - P(4)	106.1(1)	P(1) - Pt(2) - C(5)	113.5(3)
P(4) - Pt(2) - C(5)	97.8(3)	Pt(1) - Pt(3) - Pt(2)	61.5(1)
Pt(1) - Pt(3) - Re	60.6(1)	Pt(1) - Pt(3) - P(3)	155.1(1)
Pt(1) - Pt(3) - P(6)	94.8(1)	Pt(2) - Pt(3) - Re	59.4(1)
Pt(2) - Pt(3) - P(3)	93.8(1)	Pt(2) - Pt(3) - P(6)	155.6(1)
Re - Pt(3) - P(3)	110.2(1)	Re - Pt(3) - P(6)	115.6(1)
P(3) - Pt(3) - P(6)	109.6(1)	Pt(1) - Re - Pt(2)	57.2(1)
Pt(1) - Re - Pt(3)	54.3(1)	Pt(1) - Re - P(7)	126.6(1)
Pt(1) - Re - C(4)	133.2(3)	Pt(1) - Re - C(5)	115.6(3)
Pt(1) - Re - C(6)	61.2(3)	Pt(2) - Re - Pt(3)	54.2(1)
Pt(2) - Re - P(7)	124.0(1)	Pt(2) - Re - C(4)	136.0(3)
Pt(2) - Re - C(5)	58.7(3)	Pt(2) - Re - C(6)	118.4(3)

Pt(3) - Re - P(7) 177.6(1)
 Pt(3) - Re - C(5) 83.2(3)
 P(7) - Re - C(4) 85.8(3)
 P(7) - Re - C(6) 90.0(3)
 C(4) - Re - C(6) 89.9(4)
 Pt(2) - P(1) - C(1) 111.1(3)
 Pt(2) - P(1) - C(F1) 121.0(3)
 C(1) - P(1) - C(F1) 98.2(5)
 Pt(1) - P(2) - C(1) 108.8(3)
 Pt(1) - P(2) - C(D1) 115.7(3)
 C(1) - P(2) - C(D1) 103.2(4)
 Pt(3) - P(3) - C(2) 113.5(3)
 Pt(3) - P(3) - C(M1) 115.9(3)
 C(2) - P(3) - C(M1) 101.2(4)
 Pt(2) - P(4) - C(2) 109.1(3)
 Pt(2) - P(4) - C(L1) 120.0(4)
 C(2) - P(4) - C(L1) 101.7(4)
 Pt(1) - P(5) - C(3) 108.0(3)
 Pt(1) - P(5) - C(O1) 118.7(4)
 C(3) - P(5) - C(O1) 102.8(4)
 Pt(3) - P(6) - C(3) 112.2(3)
 Pt(3) - P(6) - C(B1) 113.1(3)
 C(3) - P(6) - C(B1) 101.3(4)
 Re - P(7) - O(1) 113.9(3)
 Re - P(7) - O(3) 122.4(3)
 O(1) - P(7) - O(3) 101.9(3)
 F(1) - P(8) - F(2) 85.7(6)
 F(1) - P(8) - F(4) 90.5(6)
 F(1) - P(8) - F(6) 178.6(7)
 F(2) - P(8) - F(4) 87.4(6)
 F(2) - P(8) - F(6) 94.4(8)
 F(3) - P(8) - F(5) 94.1(8)
 F(4) - P(8) - F(5) 89.9(8)
 F(5) - P(8) - F(6) 89.3(8)
 P(7) - O(2) - C(H1) 126.3(5)
 O(S1) - C(S1) - C(S2) 161.0(23)
 P(3) - C(2) - P(4) 111.4(4)
 Re - C(4) - O(6) 178.1(9)
 Pt(2) - C(5) - O(4) 111.9(6)
 Re - C(6) - O(5) 170.6(8)
 P(6) - C(A1) - C(A6) 121.6(8)
 P(6) - C(B1) - C(B6) 118.4(6)
 P(2) - C(C1) - C(C6) 121.6(6)
 P(2) - C(D1) - C(D6) 120.3(7)
 P(1) - C(E1) - C(E6) 124.3(7)
 P(1) - C(F1) - C(F6) 122.1(6)
 O(1) - C(G1) - C(G6) 123.7(10)
 O(2) - C(H1) - C(H6) 122.9(7)
 O(3) - C(I1) - C(I6) 120.1(8)
 P(4) - C(J1) - C(J6) 118.6(6)

Pt(3) - Re - C(4) 94.9(3)
 Pt(3) - Re - C(6) 92.3(3)
 P(7) - Re - C(5) 94.5(3)
 C(4) - Re - C(5) 90.5(4)
 C(5) - Re - C(6) 175.5(4)
 Pt(2) - P(1) - C(E1) 111.7(4)
 C(1) - P(1) - C(E1) 106.7(5)
 C(E1) - P(1) - C(F1) 106.6(5)
 Pt(1) - P(2) - C(C1) 122.2(3)
 C(1) - P(2) - C(C1) 101.9(4)
 C(C1) - P(2) - C(D1) 102.8(5)
 Pt(3) - P(3) - C(K1) 118.1(4)
 C(2) - P(3) - C(K1) 104.5(5)
 C(K1) - P(3) - C(M1) 101.4(4)
 Pt(2) - P(4) - C(J1) 115.6(4)
 C(2) - P(4) - C(J1) 103.0(4)
 C(J1) - P(4) - C(L1) 105.2(5)
 Pt(1) - P(5) - C(N1) 119.4(4)
 C(3) - P(5) - C(N1) 103.7(4)
 C(N1) - P(5) - C(O1) 102.2(5)
 Pt(3) - P(6) - C(A1) 120.7(4)
 C(3) - P(6) - C(A1) 101.6(5)
 C(A1) - P(6) - C(B1) 105.7(4)
 Re - P(7) - O(2) 120.1(3)
 O(1) - P(7) - O(2) 98.4(4)
 O(2) - P(7) - O(3) 95.9(3)
 F(1) - P(8) - F(3) 89.7(6)
 F(1) - P(8) - F(5) 90.5(7)
 F(2) - P(8) - F(3) 88.5(6)
 F(2) - P(8) - F(5) 175.3(8)
 F(3) - P(8) - F(4) 175.9(7)
 F(3) - P(8) - F(6) 91.6(7)
 F(4) - P(8) - F(6) 88.1(7)
 P(7) - O(1) - C(G1) 129.9(6)
 P(7) - O(3) - C(I1) 123.9(6)
 P(1) - C(1) - P(2) 112.2(4)
 P(5) - C(3) - P(6) 108.2(4)
 PT(2) - C(5) - RE 76.5(3)
 RE - C(5) - O(4) 171.4(8)
 P(6) - C(A1) - C(A2) 118.3(8)
 P(6) - C(B1) - C(B2) 120.8(6)
 P(2) - C(C1) - C(C2) 118.3(6)
 P(2) - C(D1) - C(D2) 119.7(8)
 P(1) - C(E1) - C(E2) 115.7(7)
 P(1) - C(F1) - C(F2) 117.8(7)
 O(1) - C(G1) - C(G2) 116.2(10)
 O(2) - C(H1) - C(H2) 117.1(7)
 O(3) - C(I1) - C(I2) 119.9(10)
 P(4) - C(J1) - C(J2) 121.2(6)
 P(3) - C(K1) - C(K2) 121.3(6)

P(3) - C(K1) - C(K6)	118.0(8)	P(4) - C(L1) - C(L2)	120.5(8)
P(4) - C(L1) - C(L6)	119.0(9)	P(3) - C(M1) - C(M2)	121.6(6)
P(3) - C(M1) - C(M6)	118.2(6)	P(5) - C(N1) - C(N2)	119.7(8)
P(5) - C(N1) - C(N6)	120.1(7)	P(5) - C(O1) - C(O2)	120.8(7)
P(5) - C(O1) - C(O6)	119.0(8)		

Table 2.2.9. Crystallographic data of the structure analysis of compound 8

Formula	$C_{98}H_{87}F_6O_7P_8Pt_3Re$
Formula wt	2509.99
Crystal system	triclinic
Space group	$P \bar{1}$
a Å	13.993(1)
b Å	17.868(1)
c Å	19.753(2)
α °	88.198(7)
β °	87.766(7)
γ °	72.344(4)
V Å ³	4702.9(7)
Z	2
F(0 0 0)	2428
D calc g cm ⁻³	1.772
T K	300
Crystal colour and habit	dark red opaque
Crystal size mm	0.33 x 0.25 x 0.15
Cell: reflections used θ range(°)	25 reflections 20.8< θ <22.9
μ (Mo-K α) cm ⁻¹	59.93
Transmission on F ²	0.75 → 1.20
Measured reflections	31620
Unique reflections	28432
Observed reflections $I \geq 3\sigma(I)$	14765
θ range °	2.4 - 30.5
Miller indices h	-20→0
k	-25→25
l	-28→28
Decay in mean standard (%)	2.2
R _{int}	0.031
No. of parameters	464
R(F)	0.0405
R _w (F)	0.0429
S	1.53
$\Delta\rho_{max}$ and $\Delta\rho_{min}$ eÅ ⁻³	1.19 → -0.94
Δ/σ_{max}	0.10

2.2.5. The structure of $[\text{Pt}_3\text{I}\{\text{Re}(\text{CO})_3\}(\mu\text{-dppm})_3]\text{CH}_2\text{Cl}_2 \cdot \text{H}_2\text{O}$, **9**

The molecular structure of $[\text{Pt}_3(\mu_3\text{-I})\{\text{Re}(\text{CO})_3\}(\mu\text{-dppm})_3]$, **9**, is illustrated in Figure 2.2.9 from the results of X-ray analysis. Selected bond lengths and angles are listed in Table 2.2.11. The structure of complex **9**, $\text{CH}_2\text{Cl}_2 \cdot \text{H}_2\text{O}$ shows that the addition of halide to the parent complex $[\text{Pt}_3\{\mu_3\text{-Re}(\text{CO})_3\}(\mu\text{-dppm})_3]^+$, **4**, (Xiao, Puddephatt, Manojlovic-Muir & Muir, 1993) occurs at the Pt_3 site and not at the Re centre. Also, addition of iodide evidently changes the electron count of the cluster complex from 54 in **4** to 60 in **9**.

The structure of **9** contains a triangular Pt_3 unit capped by a $\text{Re}(\text{CO})_3$ fragment to form a distorted tetrahedral Pt_3Re cluster in which Pt atoms and CO groups complete a highly distorted octahedral coordination geometry around the Re centre [C-Re-C 84.1(5)-85.3(5), Pt-Re-Pt 56.0(1)-57.1(1)°]. The other face of the Pt_3 cluster is capped by a weakly bonded iodide ligand, resulting in a trigonal bipyramidal $[\text{Pt}_3(\mu_3\text{-I})(\mu_3\text{-Re})]$ core with approximate C_3 symmetry. The Pt_3 triangle is edge-bridged by three dppm ligands to form a $\text{Pt}_3(\mu\text{-dppm})_3$ fragment with an essentially planar Pt_3P_6 skeleton. All three $\text{Pt}_2\text{P}_2\text{C}$ rings adopt an envelope conformation with the methylenic carbon atom at the flap. Two flaps lie on the iodo side and one on the Re side the Pt_3 plane (see Figure 2.2.10). Such a conformation of the $\text{Pt}_3(\mu\text{-dppm})_3$ fragment is characterized by different numbers of axial and equatorial phenyl groups on the opposite faces of the Pt_3 cluster (Puddephatt, Manojlovic-Muir & Muir, 1990). The iodide ligand adds to the face associated with lower steric hindrance. The conformation results in approximate C_s symmetry of the $[\text{Pt}_3(\mu_3\text{-I})\{\mu_3\text{-Re}(\text{CO})_3\}(\mu\text{-dppm})_3]$ unit, the mirror plane passing through the Pt(2), Re, I and C(2) atoms and bisecting the Pt(1)-Pt(3) bond (see Figure 2.2.10).

The Pt-P and Re-C bond lengths are unexceptional (see Table 2.2.11). In the Pt₃Re core both the Pt-Pt [2.586(1), 2.598(1), 2.613(1) Å] and Pt-Re [2.728(1), 2.739(1), 2.771(1) Å] distances display small variations. Mean Pt-Pt [2.60 Å in **9** and **4**] and Pt-Re [2.75 Å in **9** and 2.67 Å in **4**] distances show that the addition of the iodide donor to the Pt₃ cluster in **9** has no effect on Pt-Pt bonding, but causes lengthening of the Pt-Re bonds. In contrast, addition of the P(OPh)₃ donor to the Re site in **8** (Xiao, Hao, Puddephatt, Manojlovic-Muir Muir & Torabi, 1995b) lengthens both Pt-Pt and Pt-Re bonds (mean values 2.64 and 2.80 Å respectively), and the effect on the Pt-Re bonds is substantially higher than in **9**. The Pt-I distances in **9** (see Table 2.2.11), which also display small variations, are much longer than the Pt-I bonds [2.806(2)-2.825(2) Å] in [Pt(μ₃-I)Me₃]₄ (Allman & Kucharczyk, 1983) where no direct Pt-Pt bonding is observed. It is, however, interesting to compare them with analogous distances in the molecular structures of the closely related complexes [Pd₃(μ₃-I)(μ₃-CO)(μ-dppm)₃]⁺² (Lloyd, Manojlovic-Muir Muir & Puddephatt, 1993) and [Au₃(μ₃-I)(μ₃-AuI)(μ-dppm)₃] (van der Veldon, Bour, Pet, Bosman & Noordik, 1983) in which the Re(CO)₃ fragment is replaced, respectively, by CO and AuI units. In all three complexes the M-(μ₃-I) distances are too long to be ascribed to normal covalent bonds. Nevertheless, the Pd-I [2.591(1)-3.083(1) Å], Pt-I [3.113(1)-3.343(1) Å] and Au-μ₃I [3.132(2)-3.668(2) Å] distances follow very roughly the order of the metal atom radii, Pd < Pt < Au and both the Pd-I and Au-(μ₃-I) distances are considered indicative of some degree of covalency (Lloyd, Manojlovic-Muir Muir & Puddephatt, 1993; van der Veldon, Bour, Pet, Bosman & Noordik, 1983). It would thus appear that some covalent character in Pt-I bonds in **9** cannot be completely excluded.

Experimental

A black, needle-like crystal of $9 \cdot \text{CH}_2\text{Cl}_2 \cdot \text{H}_2\text{O}$ was used in this analysis. The crystallographic data are given in Table 2.2.12. The unit cell constants were determined by a least squares treatment of the setting angles of 25 reflections. The final atomic co-ordinates and displacement parameters are listed in Table 2.2.10. The absorption correction was made at the end of isotropic refinement, using the empirical method of Walker and Stuart (1983). The positions of the platinum and rhenium atoms were determined from a Patterson function and those of the remaining non-hydrogen atoms from the subsequent Fourier difference syntheses. The eleven carbon and hydrogen atoms of each phenyl group were refined as a rigid body. In the CH_2 groups the hydrogen atoms were allowed to ride on the related carbon atoms. All non-hydrogen atoms in the metal complex, 9, were refined with anisotropic and those in the solvent molecules with isotropic, displacement parameters. No allowance was made for scattering of the hydrogen atoms of $\text{C}_2\text{H}_2\text{Cl}_2$ and H_2O molecules. All calculations were performed using the GX program package.

Captions to Figures

Figure 2.2.9. A view of the molecular structure of $[\text{Pt}_3\text{I}\{\text{Re}(\text{CO})_3\}(\mu\text{-dppm})_3]$, **9**, with atoms represented by spheres of arbitrary size. In the phenyl rings carbon atoms are numbered in sequences $\text{C}(n_1)\dots\text{C}(n_6)$, starting with the P-substituted atoms and the ring labels indicate the position of the $\text{C}(n_2)$ atoms. The hydrogen atoms are omitted for clarity.

Figure 2.2.10. A view of the inner core of **9**, with displacement ellipsoids showing 50% probability.

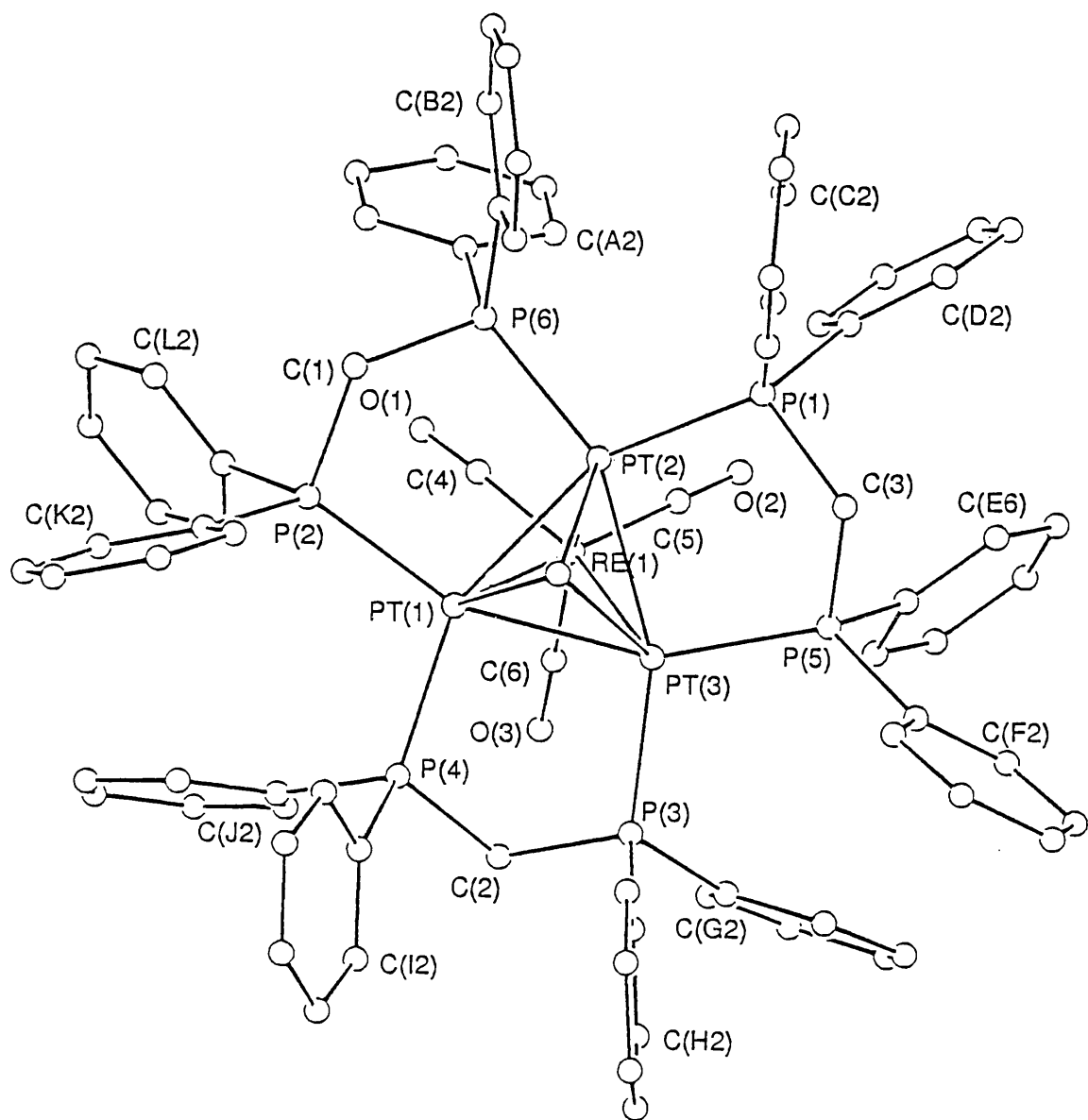


Figure 2.2.9

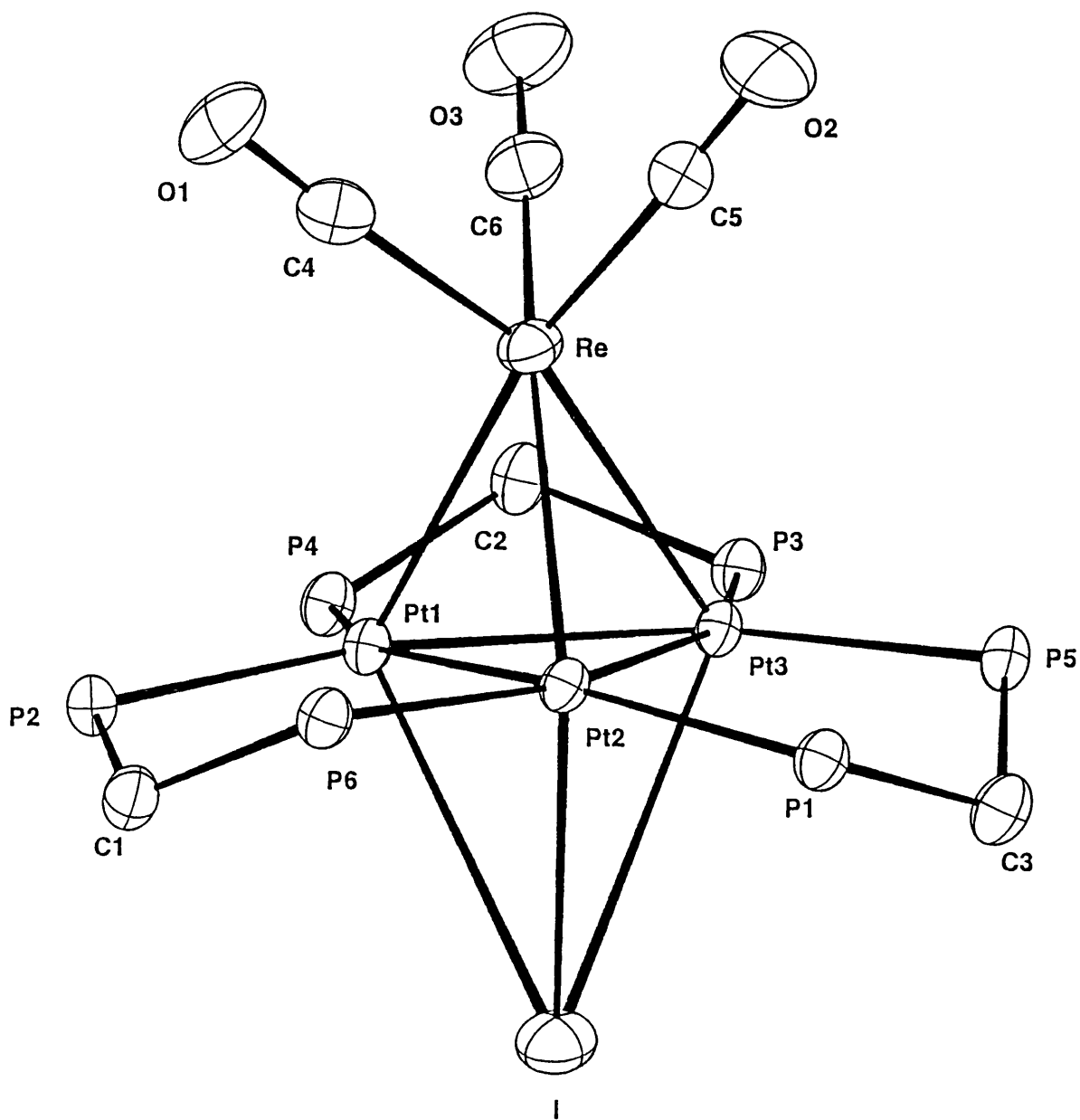


Figure 2.2.10

Table 2.2.10.

Atomic fractional co-ordinates and isotropic replacement parameters (\AA^2) for compound 9

Atom	x	y	z	U
Pt(1)	0.13055(1)	0.17229(2)	0.09200(2)	0.027
Pt(2)	0.09864(1)	0.27702(2)	0.12092(2)	0.027
Pt(3)	0.14642(1)	0.19153(2)	0.20692(2)	0.027
Re(1)	0.18542(1)	0.27467(2)	0.15567(2)	0.037
I	0.04361(2)	0.15004(4)	0.10935(4)	0.054
CL(1)	0.1130(3)	0.2690(5)	0.6968(5)	0.263(4)
CL(2)	0.0359(3)	0.2159(5)	0.7070(5)	0.267(4)
P(1)	0.07402(8)	0.33616(12)	0.17986(11)	0.033
P(2)	0.09668(8)	0.18906(12)	-0.01508(11)	0.031
P(3)	0.18981(8)	0.10092(12)	0.24955(11)	0.031
P(4)	0.16879(8)	0.07501(12)	0.11432(11)	0.033
P(5)	0.13727(8)	0.24237(12)	0.28437(11)	0.035
P(6)	0.06567(8)	0.32040(12)	0.02274(11)	0.032
O(1)	0.2075(3)	0.3406(4)	0.0605(4)	0.074
O(2)	0.2309(3)	0.3969(5)	0.2352(5)	0.093
O(3)	0.2765(3)	0.2175(5)	0.2077(4)	0.084
O(4)	0.5050(7)	0.1112(11)	0.2983(9)	0.25(1)
C(1)	0.0551(3)	0.2540(5)	-0.0341(4)	0.037
C(2)	0.2110(3)	0.0735(5)	0.1960(4)	0.037
C(3)	0.0847(3)	0.2863(5)	0.2492(5)	0.042
C(4)	0.1977(3)	0.3170(5)	0.0949(5)	0.044
C(5)	0.2132(4)	0.3512(6)	0.2056(5)	0.056
C(6)	0.2411(4)	0.2400(6)	0.1879(5)	0.056
C(7)	0.0575(10)	0.2447(14)	0.6676(13)	0.20(1)
C(A1)	0.0970(3)	0.3857(5)	0.0077(3)	0.039
C(A2)	0.1193(3)	0.4309(3)	0.0554(4)	0.058
C(A3)	0.1455(4)	0.4785(5)	0.0487(4)	0.072
C(A4)	0.1494(2)	0.4809(4)	-0.0056(3)	0.081
C(A5)	0.1271(3)	0.4356(4)	-0.0533(4)	0.073
C(A6)	0.1009(4)	0.3880(6)	-0.0466(4)	0.053
C(B1)	0.0102(3)	0.3541(7)	-0.0106(6)	0.038
C(B2)	-0.0021(3)	0.4136(5)	-0.0435(3)	0.069
C(B3)	-0.0451(3)	0.4331(4)	-0.0720(5)	0.103
C(B4)	-0.0757(3)	0.3930(6)	-0.0677(5)	0.083
C(B5)	-0.0635(2)	0.3335(4)	-0.0348(3)	0.058
C(B6)	-0.0205(3)	0.3140(5)	-0.0062(6)	0.052
C(C1)	0.0150(3)	0.3528(7)	0.1470(6)	0.043
C(C2)	-0.0010(3)	0.4153(5)	0.1228(2)	0.056
C(C3)	-0.0449(3)	0.4277(4)	0.0962(5)	0.074
C(C4)	-0.0729(2)	0.3775(6)	0.0939(5)	0.070
C(C5)	-0.0568(3)	0.3151(4)	0.1181(3)	0.059
C(C6)	-0.0129(3)	0.3026(5)	0.1447(6)	0.052
C(D1)	0.0980(5)	0.4172(5)	0.2154(5)	0.042
C(D2)	0.0814(3)	0.4557(6)	0.2465(4)	0.072
C(D3)	0.1012(4)	0.5152(4)	0.2743(6)	0.100

C(D4)	0.1377(4)	0.5362(5)	0.2707(4)	0.106
C(D5)	0.1543(3)	0.4977(5)	0.2395(5)	0.091
C(D6)	0.1345(5)	0.4382(3)	0.2119(7)	0.055
C(E1)	0.1775(4)	0.3058(6)	0.3295(3)	0.037
C(E2)	0.2193(4)	0.2961(3)	0.3390(6)	0.050
C(E3)	0.2516(3)	0.3406(5)	0.3753(5)	0.065
C(E4)	0.2421(3)	0.3948(5)	0.4023(2)	0.068
C(E5)	0.2003(4)	0.4045(3)	0.3928(6)	0.074
C(E6)	0.1680(3)	0.3600(6)	0.3564(5)	0.052
C(F1)	0.1318(3)	0.1959(3)	0.3462(4)	0.053
C(F2)	0.1595(4)	0.2056(7)	0.4093(4)	0.071
C(F3)	0.1520(5)	0.1733(7)	0.4539(3)	0.096
C(F4)	0.1167(3)	0.1313(3)	0.4354(3)	0.142
C(F5)	0.0890(5)	0.1216(7)	0.3724(4)	0.151
C(F6)	0.0965(5)	0.1539(7)	0.3278(3)	0.083
C(G1)	0.2386(4)	0.1177(7)	0.3256(3)	0.039
C(G2)	0.2769(3)	0.1414(3)	0.3292(4)	0.052
C(G3)	0.3100(2)	0.1622(5)	0.3861(4)	0.066
C(G4)	0.3049(3)	0.1593(6)	0.4394(3)	0.067
C(G5)	0.2666(3)	0.1356(2)	0.4359(4)	0.076
C(G6)	0.2335(3)	0.1148(6)	0.3789(4)	0.053
C(H1)	0.1694(3)	0.0226(3)	0.2656(3)	0.036
C(H2)	0.1978(3)	-0.0273(6)	0.3008(4)	0.049
C(H3)	0.1820(3)	-0.0868(5)	0.3111(5)	0.062
C(H4)	0.1379(3)	-0.0963(3)	0.2862(3)	0.076
C(H5)	0.1095(3)	-0.0463(6)	0.2511(5)	0.074
C(H6)	0.1253(3)	0.0131(5)	0.2407(6)	0.053
C(I1)	0.1395(4)	-0.0049(5)	0.1028(4)	0.038
C(I2)	0.1602(3)	-0.0633(7)	0.1322(4)	0.057
C(I3)	0.1376(3)	-0.1229(5)	0.1180(5)	0.081
C(I4)	0.0942(3)	-0.1241(4)	0.0744(3)	0.082
C(I5)	0.0735(3)	-0.0657(6)	0.0450(5)	0.069
C(I6)	0.0961(3)	-0.0060(4)	0.0592(6)	0.054
C(J1)	0.1983(3)	0.0600(3)	0.0688(5)	0.035
C(J2)	0.2398(4)	0.0838(5)	0.0887(3)	0.049
C(J3)	0.2588(3)	0.0787(5)	0.0499(3)	0.059
C(J4)	0.2363(3)	0.0499(3)	-0.0087(4)	0.065
C(J5)	0.1948(3)	0.0261(5)	-0.0286(3)	0.056
C(J6)	0.1758(3)	0.0312(6)	0.0102(4)	0.046
C(K1)	0.0635(4)	0.1217(5)	-0.0688(3)	0.035
C(K2)	0.0741(3)	0.0948(5)	-0.1126(4)	0.054
C(K3)	0.0492(3)	0.0439(2)	-0.1516(5)	0.073
C(K4)	0.0139(3)	0.0198(4)	-0.1467(3)	0.066
C(K5)	0.0033(2)	0.0467(4)	-0.1029(4)	0.061
C(K6)	0.0281(4)	0.0976(3)	-0.0640(5)	0.046
C(L1)	0.1280(3)	0.2167(4)	-0.0538(4)	0.039
C(L2)	0.1085(3)	0.2458(7)	-0.1126(6)	0.058
C(L3)	0.1331(3)	0.2631(5)	-0.1415(4)	0.080
C(L4)	0.1772(3)	0.2512(3)	-0.1116(4)	0.095
C(L5)	0.1967(3)	0.2221(6)	-0.0528(5)	0.081

C(L6)	0.1721(3)	0.2049(5)	-0.0239(4)	0.056
-------	-----------	-----------	------------	-------

Table 2.2.11. Selected bond distances (Å) and bond angles (°)

(a) bond distances

Pt(1) - Pt(2)	2.613(1)	Pt(1) - Pt(3)	2.586(1)	Pt(1) - Re(1)	2.728(1)
Pt(1) - I	3.283(1)	Pt(1) - P(2)	2.304(3)	Pt(1) - P(4)	2.274(3)
Pt(2) - Pt(3)	2.598(1)	Pt(2) - RE(1)	2.739(1)	Pt(2) - I	3.113(1)
Pt(2) - P(1)	2.301(3)	Pt(2) - P(6)	2.262(3)	Pt(3) - Re(1)	2.777(1)
Pt(3) - I	3.343(1)	Pt(3) - P(3)	2.272(3)	Pt(3) - P(5)	2.275(3)
Re(1) - C(4)	1.905(11)	Re(1) - C(5)	1.905(13)	Re(1) - C(6)	1.857(12)
Cl(1) - C(7)	1.79(4)	Cl(2) - C(7)	1.57(4)	P(1) - C(3)	1.829(10)
P(1) - C(C1)	1.857(9)	P(1) - C(D1)	1.838(12)	P(2) - C(1)	1.836(10)
P(2) - C(K1)	1.850(11)	P(2) - C(L1)	1.824(10)	P(3) - C(2)	1.846(10)
P(3) - C(G1)	1.856(10)	P(3) - C(H1)	1.832(8)	P(4) - C(2)	1.823(10)
P(4) - C(I1)	1.844(11)	P(4) - C(J1)	1.849(10)	P(5) - C(3)	1.844(11)
P(5) - C(E1)	1.824(12)	P(5) - C(F1)	1.840(8)	P(6) - C(1)	1.816(10)
P(6) - C(B1)	1.842(11)	O(1) - C(4)	1.137(14)	O(2) - C(5)	1.144(16)
O(3) - C(6)	1.185(15)	P(6) - C(A1)	1.844(9)		

(b) bond angles

Pt(2) - Pt(1) - Pt(3)	60.0(1)	Pt(2) - Pt(1) - Re(1)	61.7(1)
Pt(2) - Pt(1) - I	62.5(1)	Pt(2) - Pt(1) - P(2)	97.1(1)
Pt(2) - Pt(1) - P(4)	153.8(1)	Pt(3) - Pt(1) - Re(1)	62.9(1)
Pt(3) - Pt(1) - I	68.3(1)	Pt(3) - Pt(1) - P(2)	156.6(1)
Pt(3) - Pt(1) - P(4)	93.8(1)	Re(1) - Pt(1) - I	118.5(1)
Re(1) - Pt(1) - P(2)	112.2(1)	Re(1) - Pt(1) - P(4)	109.1(1)
I - Pt(1) - P(2)	98.2(1)	I - Pt(1) - P(4)	109.2(1)
P(2) - Pt(1) - P(4)	109.0(1)	Pt(1) - Pt(2) - Pt(3)	59.5(1)
Pt(1) - Pt(2) - Re(1)	61.2(1)	Pt(1) - Pt(2) - I	69.3(1)
Pt(1) - Pt(2) - P(1)	154.8(1)	Pt(1) - Pt(2) - P(6)	95.7(1)
Pt(3) - Pt(2) - Re(1)	62.7(1)	Pt(3) - Pt(2) - I	71.0(1)
Pt(3) - Pt(2) - P(1)	97.5(1)	Pt(3) - Pt(2) - P(6)	155.1(1)
Re(1) - Pt(2) - I	124.1(1)	Re(1) - Pt(2) - P(1)	120.0(1)
Re(1) - Pt(2) - P(6)	105.9(1)	I - Pt(2) - P(1)	94.6(1)
I - Pt(2) - P(6)	103.2(1)	P(1) - Pt(2) - P(6)	107.2(1)
Pt(1) - Pt(3) - Pt(2)	60.5(1)	Pt(1) - Pt(3) - Re(1)	61.0(1)
Pt(1) - Pt(3) - I	65.8(1)	Pt(1) - Pt(3) - P(3)	97.4(1)
Pt(1) - Pt(3) - P(5)	154.6(1)	Pt(2) - Pt(3) - Re(1)	61.2(1)
Pt(2) - Pt(3) - I	61.7(1)	Pt(2) - Pt(3) - P(3)	157.9(1)
Pt(2) - Pt(3) - P(5)	94.4(1)	Re(1) - Pt(3) - I	115.1(1)
Re(1) - Pt(3) - P(3)	108.4(1)	Re(1) - Pt(3) - P(5)	112.6(1)
I - Pt(3) - P(3)	112.9(1)	I - Pt(3) - P(5)	99.8(1)
P(3) - Pt(3) - P(5)	107.7(1)	Pt(1) - Re(1) - Pt(2)	57.1(1)
Pt(1) - Re(1) - Pt(3)	56.0(1)	Pt(1) - Re(1) - C(4)	104.6(4)
Pt(1) - Re(1) - C(5)	166.3(4)	Pt(1) - Re(1) - C(6)	106.1(4)
Pt(2) - Re(1) - Pt(3)	56.2(1)	Pt(2) - Re(1) - C(4)	111.9(3)
Pt(2) - Re(1) - C(5)	110.0(4)	Pt(2) - Re(1) - C(6)	157.7(4)

Pt(3) - Re(1) - C(4)	160.2(4)	Pt(3) - Re(1) - C(5)	114.2(4)
Pt(3) - Re(1) - C(6)	103.1(4)	C(4) - Re(1) - C(5)	84.1(5)
C(4) - Re(1) - C(6)	85.3(5)	C(5) - Re(1) - C(6)	84.9(5)
Pt(1) - I - Pt(2)	48.1(1)	Pt(1) - I - Pt(3)	45.9(1)
Pt(2) - I - Pt(3)	47.3(1)	Pt(2) - P(1) - C(3)	108.1(4)
Pt(2) - P(1) - C(C1)	119.3(4)	Pt(2) - P(1) - C(D1)	121.2(5)
C(3) - P(1) - C(C1)	101.3(5)	C(3) - P(1) - C(D1)	101.6(5)
C(C1) - P(1) - C(D1)	102.3(7)	Pt(1) - P(2) - C(1)	108.2(3)
Pt(1) - P(2) - C(K1)	120.1(3)	Pt(1) - P(2) - C(L1)	120.1(4)
C(1) - P(2) - C(K1)	100.2(5)	C(1) - P(2) - C(L1)	104.6(4)
C(K1) - P(2) - C(L1)	101.0(5)	Pt(3) - P(3) - C(2)	108.7(3)
Pt(3) - P(3) - C(G1)	114.3(5)	Pt(3) - P(3) - C(H1)	122.2(4)
C(2) - P(3) - C(G1)	105.1(5)	C(2) - P(3) - C(H1)	102.5(4)
C(G1) - P(3) - C(H1)	102.3(5)	Pt(1) - P(4) - C(2)	110.9(4)
Pt(1) - P(4) - C(I1)	118.7(4)	Pt(1) - P(4) - C(J1)	115.3(3)
C(2) - P(4) - C(I1)	104.9(4)	C(2) - P(4) - C(J1)	104.2(5)
C(I1) - P(4) - C(J1)	101.2(5)	Pt(3) - P(5) - C(3)	109.2(4)
Pt(3) - P(5) - C(E1)	115.7(4)	Pt(3) - P(5) - C(F1)	123.2(3)
C(3) - P(5) - C(E1)	105.5(6)	C(3) - P(5) - C(F1)	98.7(5)
C(E1) - P(5) - C(F1)	102.2(4)	Pt(2) - P(6) - C(1)	109.5(4)
Pt(2) - P(6) - C(A1)	114.8(3)	Pt(2) - P(6) - C(B1)	120.7(5)
C(1) - P(6) - C(A1)	107.3(4)	C(1) - P(6) - C(B1)	97.9(6)
C(A1) - P(6) - C(B1)	104.8(5)	P(2) - C(1) - P(6)	118.1(5)
P(3) - C(2) - P(4)	111.4(6)	P(1) - C(3) - P(5)	114.2(6)
Re(1) - C(4) - O(1)	175.9(9)	Re(1) - C(5) - O(2)	178.0(11)
Re(1) - C(6) - O(3)	179.1(11)	Cl(1) - C(7) - CL(2)	126.7(18)
P(6) - C(A1) - C(A2)	117.0(6)	P(6) - C(A1) - C(A6)	122.9(7)
C(A2) - C(A1) - C(A6)	120.0(9)	C(A1) - C(A2) - C(A3)	119.9(9)
P(6) - C(B1) - C(B2)	122.9(8)	P(6) - C(B1) - C(B6)	116.8(10)
P(1) - C(C1) - C(C2)	119.4(9)	P(1) - C(C1) - C(C6)	120.5(10)
P(1) - C(D1) - C(D2)	121.9(11)	P(1) - C(D1) - C(D6)	118.1(9)
P(5) - C(E1) - C(E2)	117.4(8)	P(5) - C(E1) - C(E6)	122.5(10)
P(5) - C(F1) - C(F2)	122.4(8)	P(5) - C(F1) - C(F6)	117.5(6)
P(3) - C(G1) - C(G2)	122.5(6)	P(3) - C(G1) - C(G6)	116.9(9)
P(3) - C(H1) - C(H2)	120.6(8)	P(3) - C(H1) - C(H6)	119.4(7)
P(4) - C(I1) - C(I2)	122.2(9)	P(4) - C(I1) - C(I6)	117.5(7)
P(4) - C(J1) - C(J2)	121.7(7)	P(4) - C(J1) - C(J6)	117.8(7)
P(2) - C(K1) - C(K2)	120.9(9)	P(2) - C(K1) - C(K6)	119.1(8)
P(2) - C(L1) - C(L2)	121.8(7)	P(2) - C(L1) - C(L6)	118.1(7)

Table 2.2.12. Crystallographic data for the structure analysis of compound 9

Formula	$C_{79}H_{70}Cl_2IO_4P_6Pt_3Re$
Formula wt	2238.5
Crystal system	monoclinic
Space group	C2/c
a Å	34.911(4)
b Å	19.965(6)
c Å	24.101(3)
β °	117.98(1)
V Å ³	14835(5)
Z	8
F(0 0 0)	8496
D calc g cm ⁻³	2.004
T K	292
Crystal colour and habit	black needle
Crystal size mm	0.42 x 0.10 x 0.03
Cell: reflections used θ range(°)	25 reflections 10.9< θ <20.8
μ (Mo-K α) cm ⁻¹	80.10
Transmission on F ²	0.872 → 1.187
Measured reflections	21882
Unique reflections	21565
Observed reflections $I \geq 3\sigma(I)$	10848
θ range °	2.1 - 30.0
Miller indices h	49→0
k	28→0
l	33→-33
Decay in mean standard (%)	6
R _{int}	0.034
No. of parameters	701
R(F)	0.0393
R _w (F)	0.0420
S	1.37
$\Delta\rho_{max}$ and $\Delta\rho_{min}$ eÅ ⁻³	1.57 → -1.87
Δ/σ_{max}	0.057

2.2.6. The structure of $[\text{Pt}_3\text{Re}(\text{CO})_2\{\text{P}(\text{OMe})_3\}(\mu_3\text{-O})_2(\mu\text{-dppm})_3][\text{AsF}_6]$, **10**

Oxidation of the complex $[\text{Pt}_3\{\text{Re}(\text{CO})_3\}(\mu\text{-dppm})]^+$, **4**, with oxidants such as Me_3NO , PhIO , O_2 or H_2O_2 under mild conditions gives a series of oxo clusters of $[\text{Pt}_3\text{Re}(\text{CO})_3\{\mu_3\text{-O}\}_n(\mu\text{-dppm})_3]^+$ ($n=1$: **11**, $n=2$: **5** and $n=3$: **12**). Cluster complex **5** reacts slowly with some ligands by substitution of a carbonyl ligand at the rhenium centre, for example with $\text{P}(\text{OMe})_3$ to give the new dioxo species $[\text{Pt}_3\{\mu_3\text{-Re}(\text{CO})_3\}\{\text{P}(\text{OMe})_3\}(\mu_3\text{-O})_2(\mu\text{-dppm})_3]^+$, **10**, (see scheme 2.3.3), the reaction taking over 20 hours to complete (Xiao, Hao, Puddephatt, Manojlovic-Muir & Muir, 1995) or $\text{P}(\text{OPh})_3$ gives a similar reaction.

The molecular structure of **10** is presented in Figures 2.2.11 and 2.2.12. and Tables 2.2.13 - 2.2.15. **10** was initially formulated as a $[\text{PF}_6]^-$ salt. Three data collections on different samples gave structures with identical cations but with anions which could either be pure $[\text{AsF}_6]^-$ or disordered $[\text{PF}_6]^-/[\text{AsF}_6]^-$. None of the experiments were consistent with $[\text{PF}_6]^-$. Eventually the problem was traced to a faulty batch of $[\text{PF}_6]^-$. The results only of the most satisfactory data set are presented here. The anion has been modelled satisfactorily as pure $[\text{AsF}_6]^-$.

The crystals contain $[\text{Pt}_3\text{Re}(\text{CO})_2\{\text{P}(\text{OMe})_3\}(\mu_3\text{-O})_2(\mu\text{-dppm})_3]^+$ cluster cations based on a very distorted tetrahedral arrangement of metal atoms, with each edge of the Pt_3 triangle bridged by a dppm ligand and with two Pt_2Re triangles capped by triply bridging oxygen atoms. The $\text{Pt}_3\text{Re}(\text{CO})_2\{\text{P}(\text{OMe})_3\}_6$ skeleton approximates to C_s symmetry, the mirror plane passing through the $\text{Pt}(3)\text{Re}$ $\text{P}(7)$ atoms and bisecting the $\text{Pt}(1)\text{-Pt}(2)$ bond (see Figure 2.2.11).

Addition of two μ_3 -oxo ligands to **4** causes a substantial disruption of the Pt-Pt bonding [2.8150(8), 3.0824(9) and 3.1338(9) Å]. In **10** the smallest Pt(1)-Pt(2) distance [2.8150(8) Å] is about 0.2 Å longer than the Pt-Pt bond lengths in **4** while

the Pt(1)-Re and Pt(2)-Re distances [2.7794(9) 2.8353(9) Å] are only slightly longer than the corresponding distances in **4**; nevertheless, these distances still remain in the accepted ranges of Pt-Pt (2.6-2.8 Å) and Pt-Re (2.7-2.9 Å) single bond distances [2.631(2) Å] (Douglas, Manojlovic-Muir, Muir, Rashidi, Anderson & Puddephatt, 1987). The Pt(3)-Pt(1) and Pt(3)-Pt(2) distances [3.1338(9) and 3.0824(9) Å] are very long and outside the normal range of Pt-Pt covalent bond distances. They are on the border line between weak bonding interactions and non-bonding contacts: a Pt-Pt distance as long as 3.075 Å has been regarded as evidence of weak metal-metal bonding but is best regarded as non-bonding in the present case (Ciani, Moret, Sirone, Beringhell, D'Alfonso & Pergola, 1990). The Pt(3)-Re distance [3.253(3) Å] is clearly a non-bonding contact. Thus, in **10** the atoms are held by normal covalent bonds in the Pt(1) Pt(2) Re triangle only, whereas in **4** they are held by six bonds coinciding with all edges of the Pt₃Re tetrahedron [Pt-Pt 2.593(1)-2.611(1) Å and Pt-Re 2.649(1)-2.685(1) Å].

In **10** the μ_3 -oxo ligands bind to the Pt₂Re triangles in nearly symmetrical fashion. The Pt-O bonds [2.025(10)-2.042(10) Å] are slightly shorter than the Re-O bonds [2.135(10)-2.158(10) Å], but both are in agreement with bond lengths observed in **5** (Xiao, Hao, Puddephatt, Manojlovic-Muir & Muir, 1995) and previous work. However, clusters containing two μ_3 -oxo ligands are rare for the late transition metals (Bottomley & Sutin, 1988). Examples of M₃(μ_3 -O) groups are found in [Ir₃(μ_2 -I)(μ_3 -O)₂(COD)₃], where COD=1, 5-cyclooctadiene (Cotton, Lahuerta, Sanua & Schwotzer, 1985) and [Pt₄(μ_3 -O)₂Cl₂(DMSO)₆], where DMSO=dimethyl sulphoxide (Betz & Bino, 1988).

The latitudinal Pt₃P₆ skeleton is approximately planar in [Pt₃(μ_3 -CO)(μ -dppm)₃]⁺² (Puddephatt, Manojlovic-Muir & Muir, 1990), whereas in **10** it is severely distorted (see Table 2.2.14). The Pt-P bonds are bent out of the Pt₃ plane and away from the μ_3 -oxo bridges (see Figure 2.2.12), the displacements of the P atoms

ranging from 0.606 to 1.103 Å. The Pt-P bonds lengths fall into two groups: the three bonds roughly trans to μ_3 -O atoms [2.204(4)-2.240(4) Å] are shorter than the other three [2.232(4)-2.306(4) Å]. There is a non-bonding contact between a methyl group of P(OMe)₃ and O(2) [3.318(3) Å] and between carbonyl groups and μ_3 -oxo groups [3.082(2)-3.086(2) Å].

Experimental

The crystal selected for analysis was red. All X-ray measurements were made at 20°C using a small needle crystal. The final atomic co-ordinates and displacement parameters are listed in Table 2.2.13. The crystallographic data and unit cell constants are given in Table 2.2.15. They were determined by a least squares treatment of 25 reflections. The absorption correction was made at the end of isotopic refinement using the empirical methods of Walker and Stuart (1983). The structure was solved by direct methods (Sheldrick, 1986) and refined by full matrix least-squares on F^2 . All non hydrogen atoms were assigned anisotropic displacement parameters. All refinement calculations were performed using the SHELXL-93 programme package (Sheldrick, 1993). Arsenic, all fluorine atoms, all methyl carbon atom and four carbon atoms of ring 2 have large displacement parameters, (see Table 2.2.13) This suggests positional disorder for these atoms. Attempts to model this disorder were not successful.

Captions to Figures

Figure 2.2.11. A view of the molecular structure of $[\text{Pt}_3\text{Re}(\text{CO})_2\{\text{P}(\text{OMe})_3\}(\mu\text{-O})_2(\mu\text{-dppm})_3]^+$, **10**, with atoms represented by spheres of arbitrary size. In the phenyl rings carbon atoms are numbered in sequences $\text{C}(n_1)\dots\text{C}(n_6)$, starting with the P-substituted atoms and the ring labels indicate the position of the $\text{C}(n_2)$ atoms. The hydrogen atoms are omitted for clarity.

Figure 2.2.12. A View of the inner core of **10**, with displacement ellipsoid showing 50% probability

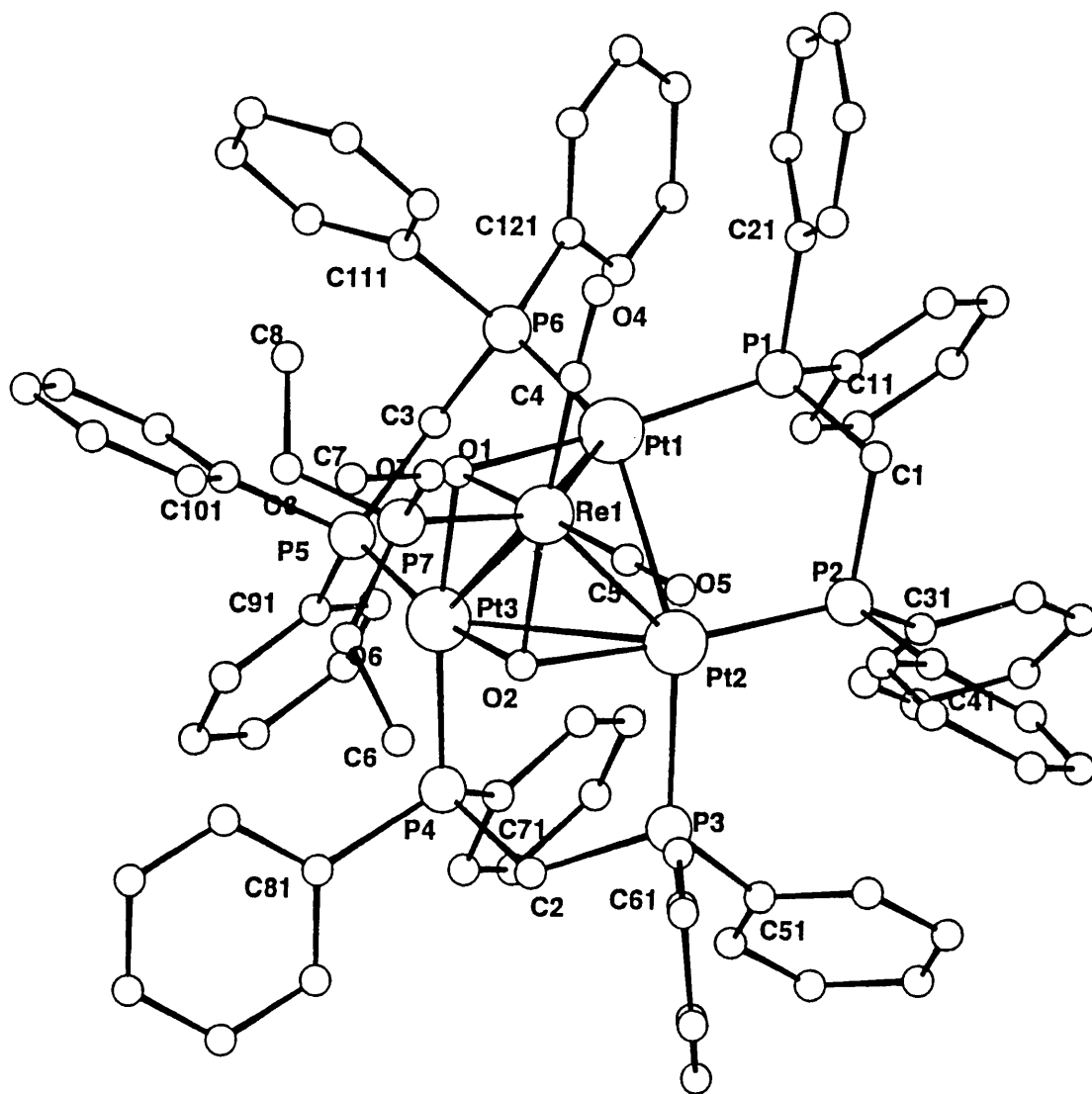


Figure 2.2.11

Table 2.2.13.

Atomic fractional co-ordinates and isotropic replacement parameters (\AA^2) for compound 10

Atom	x	y	z	U
Pt(1)	1769(1)	2600(1)	8301(1)	34(1)
Pt(2)	2316(1)	1490(1)	8813(1)	33(1)
Pt(3)	1725(1)	1383(1)	7608(1)	33(1)
Re	5470(1)	1747(1)	8597(1)	39(1)
P(1)	2417(3)	3176(2)	8936(2)	39(1)
P(2)	3074(3)	2001(2)	9459(2)	40(1)
P(3)	2963(3)	5290(2)	8805(2)	35(1)
P(4)	2623(3)	5890(2)	7518(2)	34(1)
P(5)	1924(3)	1908(2)	6846(2)	38(1)
P(6)	1734(3)	3163(2)	7516(2)	38(1)
P(7)	-7310(3)	1314(2)	8330(2)	55(1)
As(1)	5727(2)	1787(1)	1874(1)	104(1)
F(1)	5569(8)	1137(4)	2133(5)	183(4)
F(2)	4786(6)	1984(6)	1983(5)	180(4)
F(3)	6047(8)	2046(5)	2441(4)	182(4)
F(4)	5883(8)	2437(4)	1615(5)	183(4)
F(5)	6666(6)	1589(6)	1765(5)	180(4)
F(6)	5405(8)	1527(5)	1307(4)	182(4)
O(1)	9340(6)	2075(5)	7827(4)	39(3)
O(2)	1403(6)	1053(5)	8332(4)	37(3)
O(4)	-4330(10)	2863(7)	8982(6)	83(4)
O(5)	1860(9)	1253(6)	9719(5)	68(4)
O(6)	-7770(10)	5790(7)	8223(6)	89(5)
O(7)	-1447(9)	1420(7)	8742(6)	78(4)
O(8)	-1200(9)	1471(7)	7753(6)	77(4)
C(1)	2614(11)	2765(7)	9577(7)	45(4)
C(2)	2725(10)	1440(7)	8151(5)	32(4)
C(3)	2245(10)	2709(7)	7005(6)	39(4)
C(4)	-5600(12)	2432(9)	8818(8)	58(5)
C(5)	3290(11)	1452(8)	9278(7)	51(5)
C(6)	-2540(22)	1160(15)	8472(13)	145(12)
C(7)	-2293(16)	1148(12)	8660(10)	105(8)
C(8)	-1339(17)	2105(12)	7628(11)	106(9)
C(11)	3469(6)	3525(5)	8853(5)	43(4)
C(12)	3993(8)	3275(5)	8475(5)	65(5)
C(13)	4808(8)	3517(7)	8421(5)	83(7)
C(14)	5100(7)	4009(7)	8745(6)	97(8)
C(15)	4576(9)	4259(6)	9123(6)	101(8)
C(16)	3761(8)	4017(6)	9177(5)	70(6)
C(21)	1766(8)	3843(5)	9124(5)	39(4)
C(22)	1215(10)	3801(6)	9542(5)	101(8)
C(23)	7370(10)	4314(9)	9681(6)	134(11)
C(24)	8100(10)	4870(7)	9403(7)	106(9)
C(25)	1360(11)	4912(5)	8985(7)	123(10)
C(26)	1838(9)	4399(7)	8845(5)	82(7)

C(31)	4214(6)	2164(5)	9421(5)	48(4)
C(32)	4628(7)	1928(5)	8985(4)	41(4)
C(33)	5498(7)	2041(6)	8941(4)	58(5)
C(34)	5953(6)	2390(6)	9332(5)	84(7)
C(35)	5540(8)	2626(7)	9768(5)	82(7)
C(36)	4670(8)	2513(6)	9812(4)	72(6)
C(41)	2975(7)	1631(5)	1011(4)	41(4)
C(42)	2157(6)	1404(6)	1018(4)	65(5)
C(43)	2002(6)	1068(6)	1064(5)	79(6)
C(44)	2665(8)	9580(7)	1103(4)	62(5)
C(45)	3483(7)	1185(6)	1096(4)	82(7)
C(46)	3638(6)	1522(5)	1049(5)	53(5)
C(51)	4102(5)	4500(5)	8961(4)	40(4)
C(52)	4710(7)	3180(5)	8590(3)	47(4)
C(53)	5578(6)	3210(5)	8753(4)	85(5)
C(54)	5838(5)	5460(6)	9286(4)	59(5)
C(55)	5230(7)	5870(5)	9656(3)	52(5)
C(56)	4362(6)	5840(5)	9494(4)	44(4)
C(61)	2501(7)	-5800(4)	9233(4)	40(4)
C(62)	1731(7)	6000(4)	9467(5)	56(5)
C(63)	1358(6)	-3960(6)	9772(5)	69(6)
C(64)	1756(8)	-9700(5)	9844(5)	74(6)
C(65)	2526(7)	-1087(4)	9610(5)	65(5)
C(66)	2899(6)	-6310(5)	9305(4)	49(4)
C(71)	3684(5)	8480(4)	7384(4)	33(4)
C(72)	3950(6)	1400(4)	7632(4)	45(4)
C(73)	4763(7)	1634(4)	7554(4)	55(5)
C(74)	5309(5)	1317(5)	7229(5)	57(5)
C(75)	5043(6)	7660(5)	6980(4)	56(5)
C(76)	4230(6)	5310(4)	7058(4)	42(4)
C(81)	2304(8)	-3100(5)	7047(5)	46(4)
C(82)	2790(7)	-5670(6)	7008(5)	58(5)
C(83)	2507(9)	-1040(5)	6660(6)	83(7)
C(84)	1738(10)	-9770(6)	6352(5)	96(8)
C(85)	1252(8)	-4410(7)	6392(6)	98(8)
C(86)	1534(7)	3200(5)	6739(5)	72(6)
C(91)	2728(6)	1657(5)	6385(4)	43(4)
C(92)	2506(6)	1155(5)	6053(5)	58(5)
C(93)	3093(8)	9210(5)	5706(4)	70(6)
C(94)	3902(7)	1188(6)	5691(5)	72(6)
C(95)	4123(6)	1690(5)	6023(5)	59(5)
C(96)	3536(7)	1924(4)	6370(4)	47(4)
C(101)	9750(7)	1964(6)	6395(5)	47(4)
C(102)	1019(7)	2237(7)	5895(5)	65(5)
C(103)	2880(10)	2273(7)	5542(4)	88(7)
C(104)	-4860(8)	2036(8)	5698(6)	107(9)
C(105)	-5290(7)	1762(7)	6203(7)	111(9)
C(106)	2010(9)	1726(6)	6551(5)	73(6)
C(111)	6700(6)	3353(6)	7225(4)	43(4)
C(112)	1000(8)	3433(6)	7570(4)	71(6)

C(113)	-8080(7)	3590(6)	7362(5)	75(6)
C(114)	-9660(6)	3666(6)	6809(5)	87(7)
C(115)	-3070(8)	3586(6)	6463(4)	72(6)
C(116)	5110(7)	3430(6)	6672(4)	59(5)
C(121)	2282(7)	3910(4)	7467(5)	39(4)
C(122)	1815(5)	4455(5)	7512(5)	60(5)
C(123)	2232(8)	5025(4)	7520(5)	74(6)
C(124)	3116(8)	5050(4)	7484(6)	85(7)
C(125)	3584(6)	4505(6)	7440(5)	73(6)
C(126)	3167(6)	3935(5)	7431(5)	53(5)

Table 2.2.14. Selected bond distances (Å) and bond angles (°)

(a) bond distances

Pt(1)-O(1)	2.042(10)	Pt(1)-P(1)	2.204(4)	Pt(1)-P(6)	2.293(4)
Pt(1)-Re(1)	2.7794(9)	Pt(1)-Pt(2)	2.8150(8)	Pt(1)-Pt(3)	3.1338(9)
Pt(2)-O(2)	2.032(10)	Pt(2)-P(2)	2.225(4)	Pt(2)-P(3)	2.306(4)
Pt(2)-Re(1)	2.8353(9)	Pt(2)-Pt(3)	3.0824(4)	Pt(3)-O(2)	2.025(10)
Pt(3)-O(1)	2.031(10)	Pt(3)-P(4)	2.232(4)	Pt(3)-P(5)	2.240(4)
Pt(3)-Re(1)	3.252(3)	Re(1)-C(4)	1.85(2)	Re(1)-C(5)	1.86(2)
Re(1)-O(2)	2.135(10)	Re(1)-O(1)	2.158(10)	Re(1)-P(7)	2.264(5)
P(1)-C(11)	1.830(10)	P(1)-C(21)	1.837(11)	P(1)-C(1)	1.83(2)
P(2)-C(41)	1.816(9)	P(2)-C(1)	1.83(2)	P(2)-C(31)	1.823(10)
P(3)-C(51)	1.805(8)	P(3)-C(61)	1.826(9)	P(3)-C(2)	1.841(14)
P(4)-C(71)	1.798(8)	P(4)-C(81)	1.824(10)	P(4)-C(2)	1.839(14)
P(5)-C(101)	1.807(11)	P(5)-C(91)	1.832(9)	P(5)-C(3)	1.83(2)
P(6)-C(111)	1.816(10)	P(6)-C(3)	1.82(2)	P(6)-C(121)	1.831(9)
P(7)-O(7)	1.58(2)	P(7)-O(6)	1.61(2)	P(7)-O(8)	1.60(2)
As(1)-F(1)	1.566(7)	As(1)-F(2)	1.567(7)	As(1)-F(5)	1.567(7)
As(1)-F(6)	1.567(7)	As(1)-F(3)	1.567(7)	As(1)-F(4)	1.567(7)
O(4)-C(4)	1.18(2)	O(5)-C(5)	1.21(2)	O(6)-C(6)	1.41(3)
O(7)-C(7)	1.45(3)	O(8)-C(8)	1.42(3)		

(b) bond angles

O(1)-Pt(1)-P(1)	166.6(3)	O(1)-Pt(1)-P(1)	79.8(3)
P(1)-Pt(1)-P(6)	107.2(2)	O(1)-Pt(1)-Re(1)	50.4(3)
P(1)-Pt(1)-Re(1)	118.42(11)	P(6)-Pt(1)-Re(1)	126.42(11)
O(1)-Pt(1)-Pt(2)	87.4(3)	P(1)-Pt(1)-Pt(2)	92.45(11)
P(1)-Pt(1)-Pt(2)	145.44(11)	Re(1)-Pt(1)-Pt(2)	60.9(2)
O(1)-Pt(1)-Pt(3)	39.6(3)	P(1)-Pt(1)-Pt(3)	149.06(11)
P(6)-Pt(1)-Pt(3)	88.76(11)	Re(1)-Pt(1)-Pt(3)	66.41(2)
Pt(2)-Pt(1)-Pt(3)	62.14(2)	O(2)-Pt(2)-P(2)	167.1(3)
O(2)-Pt(2)-P(3)	82.6(3)	P(2)-Pt(2)-P(3)	103.6(2)
O(2)-Pt(2)-Pt(1)	86.9(3)	P(2)-Pt(2)-Pt(1)	92.20(11)
P(3)-Pt(2)-Pt(1)	151.74(10)	O(2)-Pt(2)-Re(1)	48.73(3)
P(2)-Pt(2)-Re(1)	120.56(11)	P(3)-Pt(2)-Re(1)	126.59(11)
Pt(1)-Pt(2)-Re(1)	58.93(2)	O(2)-Pt(2)-Pt(3)	40.5(3)
P(2)-Pt(2)-Pt(3)	148.25(12)	P(3)-Pt(2)-Pt(3)	91.75(10)
Pt(1)-Pt(2)-Pt(3)	64.01(2)	Re(1)-Pt(2)-P(3)	66.52(2)
O(2)-Pt(3)-O(1)	80.3(4)	O(2)-Pt(3)-P(4)	90.7(3)
O(1)-Pt(3)-P(4)	170.2(3)	O(2)-Pt(3)-P(5)	168.8(3)
O(1)-Pt(3)-P(5)	88.5(3)	P(4)-Pt(3)-P(5)	100.5(2)
O(2)-Pt(3)-Pt(3)	40.6(3)	O(1)-Pt(3)-Pt(2)	80.6(3)
P(4)-Pt(3)-Pt(2)	90.07(10)	P(5)-Pt(3)-P(2)	136.96(11)
O(2)-Pt(3)-Pt(1)	78.7(3)	O(1)-Pt(3)-Pt(1)	39.8(3)
P(4)-Pt(3)-Pt(1)	134.67(11)	P(5)-Pt(3)-Pt(1)	92.32(11)
Pt(2)-Pt(3)-Pt(1)	53.85(2)	C(4)-Re(1)-C(5)	83.0(8)

C(4)-Re(1)-O(2)	171.2(7)	C(5)-Re(1)-O(2)	101.2(6)
C(4)-Re(1)-O(1)	100.2(6)	C(5)-Re(1)-O(1)	174.3(6)
O(2)-Re(1)-O(1)	75.1(4)	C(4)-Re(1)-P(7)	87.7(6)
C(5)-Re(1)-P(7)	85.3(6)	O(2)-Re(1)-P(7)	100.3(3)
O(1)-Re(1)-P(7)	99.5(3)	C(4)-Re(1)-Pt(1)	85.5(6)
C(5)-Re(1)-Pt(1)	129.4(5)	O(2)-Re(1)-Pt(1)	85.9(3)
O(1)-Re(1)-Pt(1)	46.8(3)	P(7)-Re(1)-Pt(1)	143.27(14)
C(4)-Re(1)-Pt(2)	127.4(6)	C(5)-Re(1)-Pt(2)	89.6(5)
O(2)-Re(1)-Pt(2)	45.6(3)	O(1)-Re(1)-Pt(2)	84.7(3)
P(7)-Re(1)-Pt(2)	143.63(14)	Pt(1)-Re(1)-Pt(2)	60.17(2)
C(11)-P(1)-C(21)	102.8(6)	C(11)-P(1)-C(1)	101.1(7)
C(21)-P(1)-C(1)	103.0(7)	C(11)-P(1)-Pt(1)	121.8(4)
C(21)-P(1)-Pt(1)	112.7(4)	C(1)-P(1)-Pt(1)	113.2(6)
C(41)-P(2)-C(1)	101.3(7)	C(41)-P(2)-C(31)	105.6(6)
C(1)-P(2)-C(31)	103.2(7)	C(41)-P(2)-Pt(2)	110.7(4)
C(1)-P(2)-Pt(2)	111.3(6)	C(31)-P(2)-Pt(2)	122.4(4)
C(51)-P(3)-C(61)	103.3(5)	C(51)-P(3)-C(2)	106.8(6)
C(61)-P(3)-C(2)	97.8(6)	C(51)-P(3)-Pt()	120.6(4)
C(61)-P(3)-Pt(2)	115.4(4)	C(2)-P(3)-Pt(2)	110.3(5)
C(71)-P(4)-C(81)	109.1(5)	C(71)-P(4)-C(2)	106.7(6)
C(81)-P(4)-C(2)	99.8(6)	C(71)-P(4)-Pt(3)	111.9(4)
C(81)-P(4)-Pt(3)	118.4(4)	C(2)-P(4)-Pt(3)	109.7(5)
C(101)-P(5)-C(91)	101.5(6)	C(81)-P(5)-C(3)	105.9(7)
C(91)-P(5)-C(3)	102.9(6)	C(101)-P(5)-Pt(3)	113.9(4)
C(91)-P(5)-Pt(3)	120.9(4)	C(3)-P(5)-Pt(3)	110.2(5)
C(111)-P(6)-C(3)	105.9(7)	C(111)-P(6)-C(121)	101.3(5)
C(3)-P(6)-C(121)	101.5(6)	C(111)-P(6)-Pt(1)	115.5(4)
C(3)-P(6)-Pt(1)	108.5(5)	C(121)-P(6)-Pt(1)	122.3(4)
O(7)-P(7)-O(6)	102.9(8)	O(7)-P(7)-O(8)	104.2(8)
O(6)-P(7)-O(8)	92.7(8)	O(7)-P(7)-Re(1)	113.4(6)
O(6)-P(7)-Re(1)	119.0(6)	O(8)-P(7)-Re(1)	121.4(6)
Pt(3)-O(1)-Pt(1)	100.6(4)	Pt(3)-O(1)-Re(1)	101.8(4)
Pt(1)-O(1)-Re(1)	82.8(4)	Pt(3)-O(2)-Pt(2)	98.9(4)
Pt(3)-O(2)-Re(1)	102.8(4)	Pt(2)-O(2)-Re(1)	85.7(4)
C(6)-O(6)-P(7)	127.0(2)	C(7)-O(7)-P(7)	121.8(14)
C(8)-O(8)-P(7)	117.0(14)	P(2)-C(1)-P(1)	110.1(9)
P(4)-C(2)-P(3)	121.3(8)	P(6)-C(3)-P(5)	121.9(9)
O(4)-C(4)-Re(1)	177.02(2)	O(5)-C(5)-Re(1)	179.0(2)

Table 2.2.15. Crystallographic data for the structure analysis of compound 10

Formula	$C_{80}H_{75}O_7F_6AsP_7Pt_3Re$
Formula wt	2325.58
Crystal system	monoclinic
Space group	$P2_1/c$
a Å	15.614(2)
b Å	21.550(2)
c Å	24.810(2)
β °	93.518(10)
V Å ³	8332.5(13)
Z	4
F(0 0 0)	4448
D calc g cm ⁻³	1.854
T K	293
Crystal colour and habit	red needle elongated along c
Crystal size mm	0.44 x 0.25 x 0.12
Cell: reflections used θ range(°)	25 reflections 17.5< θ <21.3
$\mu(Mo-K\alpha)$ cm ⁻¹	70.60
Transmission on F ²	0.45 → 1.00
Measured reflections	11093
Unique reflections	10443
Observed reflections $I \geq 3\sigma(I)$	8916
θ range °	2.2 - 23.5
Miller indices h	-17→16
k	-7 →22
l	-6 → 26
Decay in mean standard (%)	8.7
R _{int}	0.0353
No. of parameters	335
R(F ²)	0.0501
R _w (F)	0.1331
S	1.07
$\Delta\rho_{max}$ and $\Delta\rho_{min}$. eÅ ⁻³	3.194 → -1.822 located near Re, Pt and AsF ₆
Δ/σ max.	0.16

2.2.7. The unsuccessful analysis of $[\{\text{Pt}(\text{PPr}_3)_3\}_3(\mu\text{-CO})_3](\mu_3\text{-ReO}_3)$, 16

The red complex 16 was synthesized during attempts to add ReO_3 groups to a triplatinum triangle stabilised by three bridging carbonyl groups and by the mono-tertiary phosphine PPr_3^i . The complex was thus expected to contain a tetrahedral Pt_3Re unit.

The crystals diffracted well. They proved to be monoclinic, space group either $C2/c$ or Cc . The cell volume suggested that four Pt_3Re clusters were present. $C2/c$ would require the Pt_3Re unit to possess diad symmetry incompatible with an ordered tetrahedral skeleton.

Many attempts have been made to solve this structure without success. A model in $C2/c$ based on a Pt_4 tetrahedron with diad symmetry linked to an $[\text{ReO}_4]^-$ anion gives a moderately encouraging R-value (0.15) but the resulting maps are not informative.

Twining, not unlikely since $a \approx c$ and $\beta = 120^\circ$, or other systematic error must be explain this failure. It is unlikely that the heavy atom skeleton originally proposed from chemical and spectroscopic data is correct and this is a further complication. For further detail see Table 2.2.16.

Table 2.2.16. Crystallographic data for the structure analysis of compound 16

Formula	$C_{38}H_{84}O_{10}P_4Pt_4Re_2$
Formula wt	1977.69
Crystal system	monoclinic
Space group	C2/c
a Å	23.147(2)
b Å	12.0140(9)
c Å	23.022(2)
β °	119.920(9)
V Å ³	5548.9(8)
Z	4
F(0 0 0)	3656
D calc g cm ⁻³	2.376
T K	294
Crystal colour and habit	red
Cell: reflections used θ range(°)	25 reflections 16.2< θ <21.2
μ (Mo-K α) cm ⁻¹	145.51
Measured reflections	8739
Unique reflections	8075
θ range °	2.45 - 30.0
Miller indices h	-28→32
k	-16 →2
l	-32→0
Decay in mean standard (%)	12
R(F ²)	0.1484
R _w (F)	0.3651
S	2.527

The crystals are metrically hexagonal. However, the Laue symmetry is no higher than 2/m

Chapter 2.3. Chemistry of binuclear Pt-Re complexes

2.3.1. Introduction

As we have seen, although dinuclear transition metal complexes stabilised by dppm have been extensively studied, very little was known about corresponding trinuclear $M_3(\text{dppm})_3$ species prior to 1983 (Manojlovic-Muir, Muir, Lloyd & Puddephatt, 1983). Since then the chemistry and structural characterisation of such complexes particularly for platinum, has become an active area of research. Especially, this has been prompted by the consideration that the behaviour of these trinuclear complexes offers a model for that of metal surfaces. Additionally, there has been a continuing theoretical debate on the nature of the metal-metal bonding in cluster compounds. In this chapter the structural results described above are used, together with published material from other laboratories, to review current knowledge of the chemical behaviour of platinum-rhenium heterometallic cluster compounds. Some consideration is also given to the properties of heterogeneous Pt/Re catalysts.

2.3.2. Chemical reactions

There are several synthetic routes to Pt-Re cluster complexes, and the most frequently used method starts from zero-valent platinum compounds, which are highly reactive and can readily form metal-metal bonds by reaction with $\text{Re} - \text{X}$ or $\text{Re} = \text{X}$ species. According to Xiao & Puddephatt (1995), the earliest binuclear Pt-Re complex was prepared by the reaction of a Pt(0) complex with a mononuclear alkylidene complex.

The parent complex $[\text{Pt}_3\{\mu_3\text{-Re}(\text{CO})_3\}(\mu_3\text{-dppm})_3]^+$, **4**, was obtained by the treatment of $[\text{Pt}_3(\mu_3\text{-CO})(\mu_3\text{-dppm})_3]^{+2}$, **3**, with $[\text{Re}(\text{CO})_5]^-$. **4** is a unsaturated compound. It can be oxidized and it also reacts with neutral or ionic species; the identity of the products of these reactions has been established by X-ray diffraction, as described in the previous chapter.

(a) Oxidation by dioxygen

Reaction scheme 2.1.1 shows the formation of the parent $[\text{Pt}_3\{\mu_3\text{-Re}(\text{CO})_3\}(\mu_3\text{-dppm})_3]^+$, **4**, from **3** and the results of stepwise oxidation of **4**. The structure of **4** has been reported (Xiao, Puddephatt Manojlovic-Muir & Muir, 1993). The complexes **5**, **6** and **7** have been characterised in this laboratory (Xiao, Hao, Puddephatt Manojlovic-Muir & Muir, 1995; Xioa, Puddephatt Manojlovic-Muir, Muir & Torabi, 1994; Hao, Xioa, Vittal, Puddephatt, Manojlovic-Muir, Muir & Torabi, 1996). The structures of **11** and **12** are based on chemical and spectroscopic evidence only (Xiao, Hao, Puddephatt, Manojlovic-Muir & Muir, 1995).

The first step in these oxidation reactions is the addition of two 4-electron ($\mu_3\text{-oxo}$) ligands to two Pt_2Re triangles. This step is the first example of oxidative addition of O_2 to a transition metal cluster to form a bis($\mu_3\text{-oxo}$) species. Remarkably, it leads to a 4-electron oxidation of the cluster and to an increase in its electron count by 8-electrons from 54 in **4** to 62 in **5**. The platinum oxidation state is zero and that of rhenium is one in **4**, but in **5** contains a Pt(II), two Pt(I) and one Re(I) ions.

The second step occurs with loss of the two $\mu\text{-oxo}$ ligands, and replacement by three oxygen atoms of the carbonyl groups. The electron count changes from 62 in **5** back to 54 in **6** and **7** with regeneration of the metal-metal bonds. **6** and **7** are remarkable in that they provide a unique example of a cluster containing metals in

widely different oxidation states: zero for platinum but seven for rhenium. **6** has the ability to encapsulate a loosely bound $[\text{ReO}_4]^-$ anion but in **7** there is no connection between the cation and the $[\text{PF}_6]^-$ anion. Although only the dioxo species **5** has been fully characterised there is some evidence for transient formation of the mono- and trioxo-species **11** and **12**.

The existence of two cluster complexes, **4** and **6**, with the same geometry but widely divergent metal oxidation states is unprecedented and offers an opportunity to study cluster chemistry as a function of the oxidation states of rhenium.

(b) Addition of neutral ligands.

Triphenylphosphite, $[\text{P}(\text{OPh})_3]$, reacts with **4** to give the 56-electron cluster $[\text{Pt}_3\text{Re}(\text{CO})_3\text{P}(\text{OPh})_3](\mu_3\text{-dppm})_3]^+$, **8**, by selective addition to the rhenium centre, contrasting with its previously established addition to the Pt_3 centre in **4** (Xiao, Hao, Puddephatt, Manojlovic-Muir, Muir & Torabi, 1995b). In contrast phosphite reacts with the electron-rich 62-electron complex **5** by replacing a carbonyl group ligand at the rhenium centre to give the a 62-electron cluster $[\text{Pt}_3\text{Re}(\text{CO})_2\{\text{P}(\text{OMe})_3\}(\mu\text{-O})_2(\mu_3\text{-dppm})_3]^+$, **10**. Scheme 2.3.2 shows these reactions.

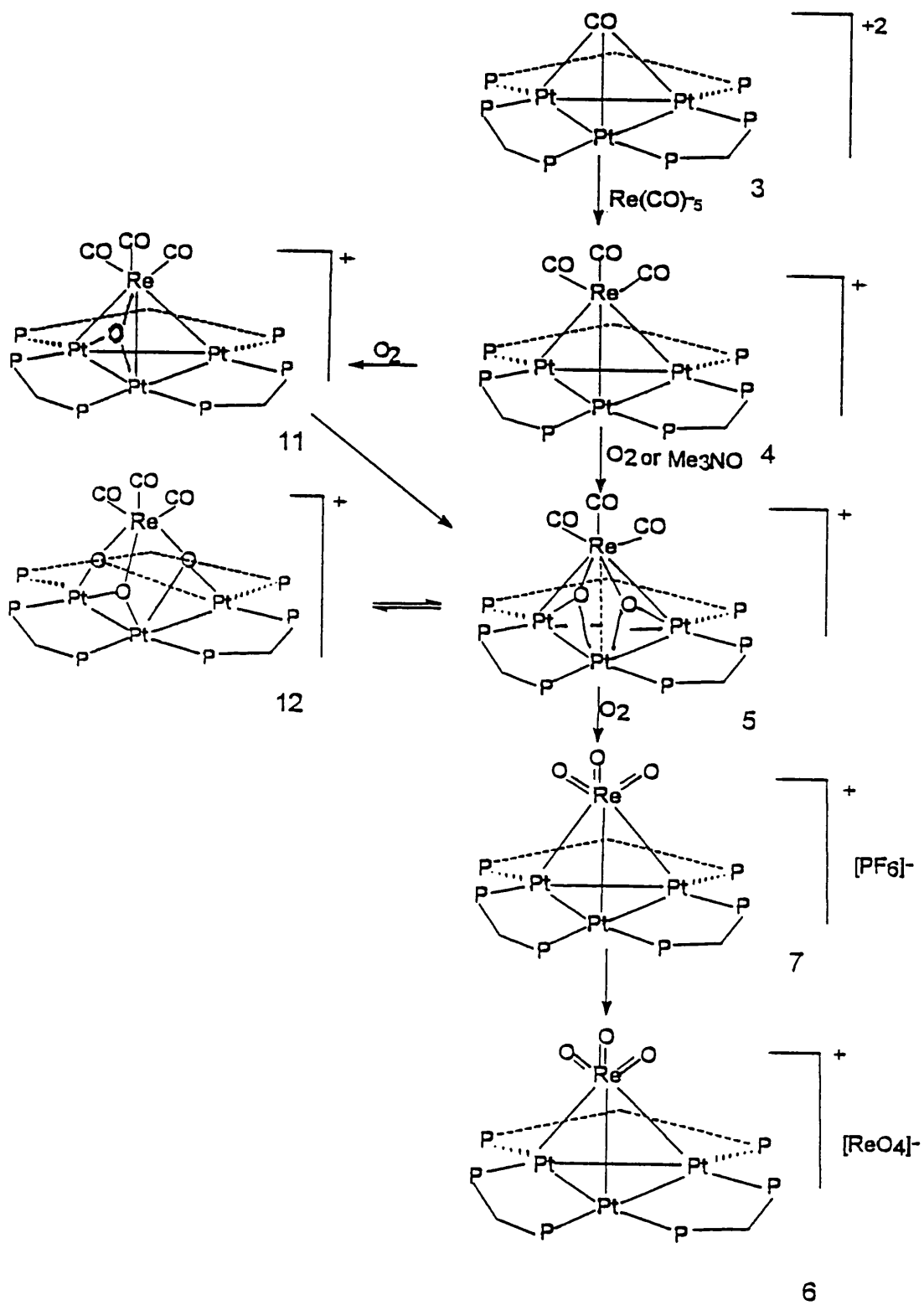
(c) Anion addition.

Halide ion adds to **4** in the same way as it adds to $[\text{Pd}_3(\mu_3\text{-CO})(\mu_3\text{-dppm})_3]^{+2}$, (Lloyd, Manojlovic-Muir, Muir and Puddephatt, 1993). It binds weakly to the Pt_3 centre to form a complex with a trigonal-bipyramidal Pt_3ReX core ($\text{X} = \text{Cl}, \text{Br}$ or I), such as $[\text{Pt}_3(\mu_3\text{-I})\{(\mu_3\text{-Re})(\text{CO})_3\}(\mu_3\text{-dppm})_3]^+$, **9**, (Xiao, Hao, Puddephatt, Manojlovic-Muir, Muir & Torabi, 1995a). Also, it is possible that halide reacts with

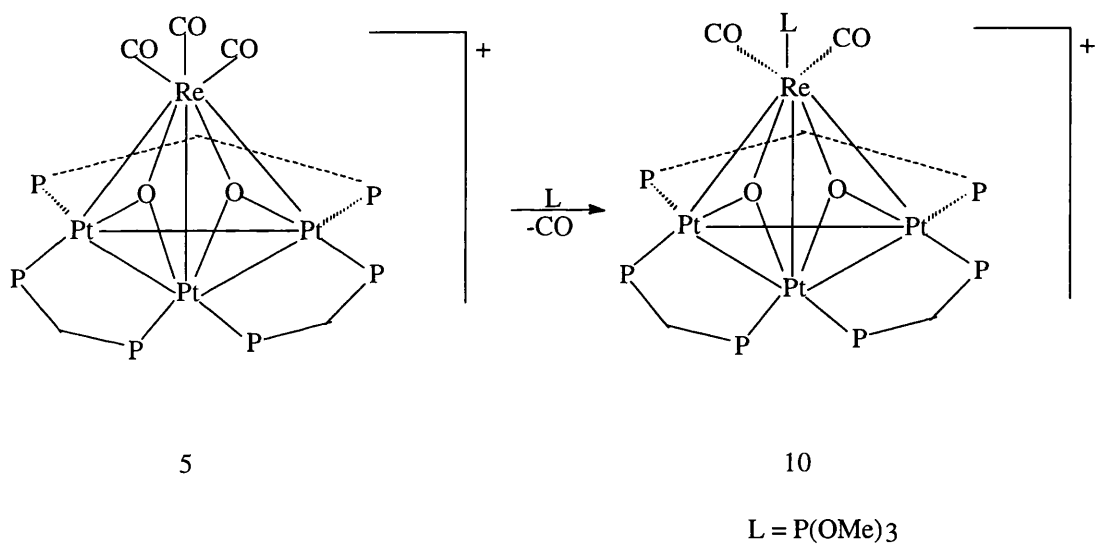
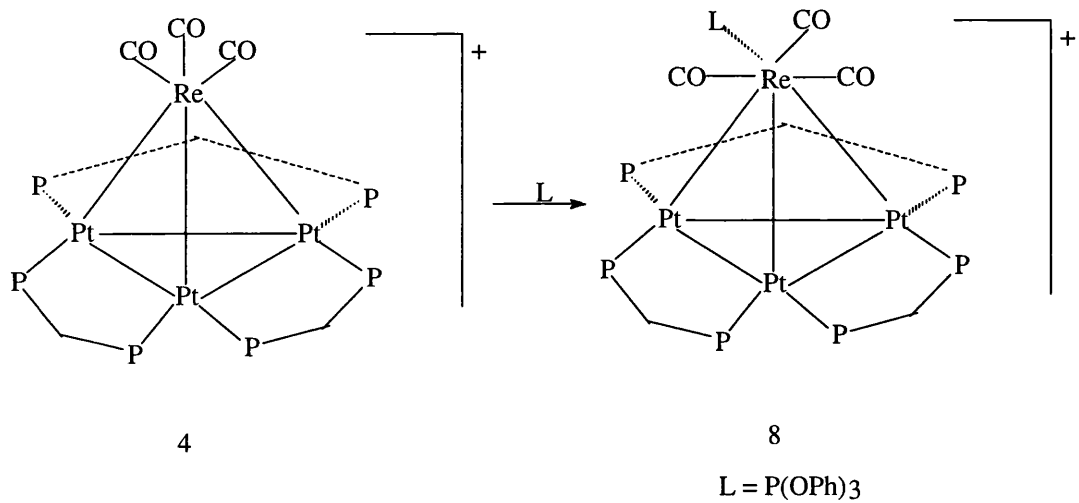
7 to give $[\text{Pt}_3\text{X}(\text{Re}-\text{O}_3)(\mu_3\text{-dppm})_3]$, **13** (see Scheme 2.3.3) (Xiao, Hao, Puddephatt, Manojlovic-Muir, Muir & Torabi, 1995a).

(d) Addition of Sulphur.

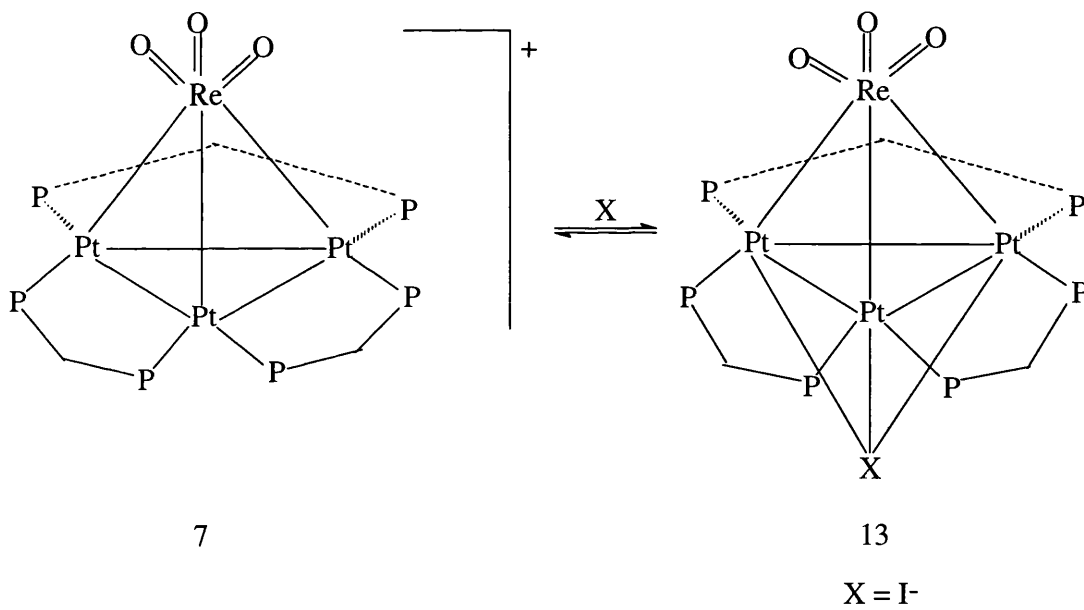
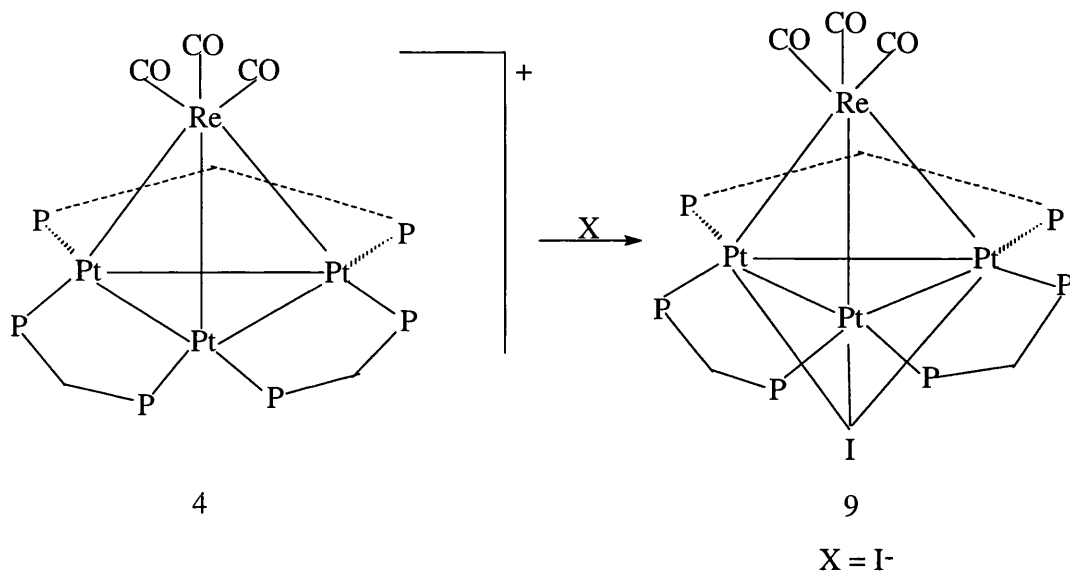
In a way similar to oxidation, the cluster **4** can be sulphided. Thus when treated in 1:1 mole ratio with propene sulphide, **4** is converted to the terminal monosulphide cluster **14** and then is converted to the disulphide cluster **15** on further reaction with propene sulphide (Xiao & Puddephatt, 1995). Cluster **15** is analogous to the dioxo cluster **5**. It is indefinitely stable in air and does not add further sulphur atoms. In contrast clusters **14** is slowly oxidized in air with loss of the sulphide ligand to give **5**. Scheme 2.3.4 shows these sulphide reactions. The $\mu_3\text{-S}$ moiety is the most frequently observed coordination mode for sulphur in cluster complexes (Hao, Xiao, Vittal, & Puddephatt, 1994).



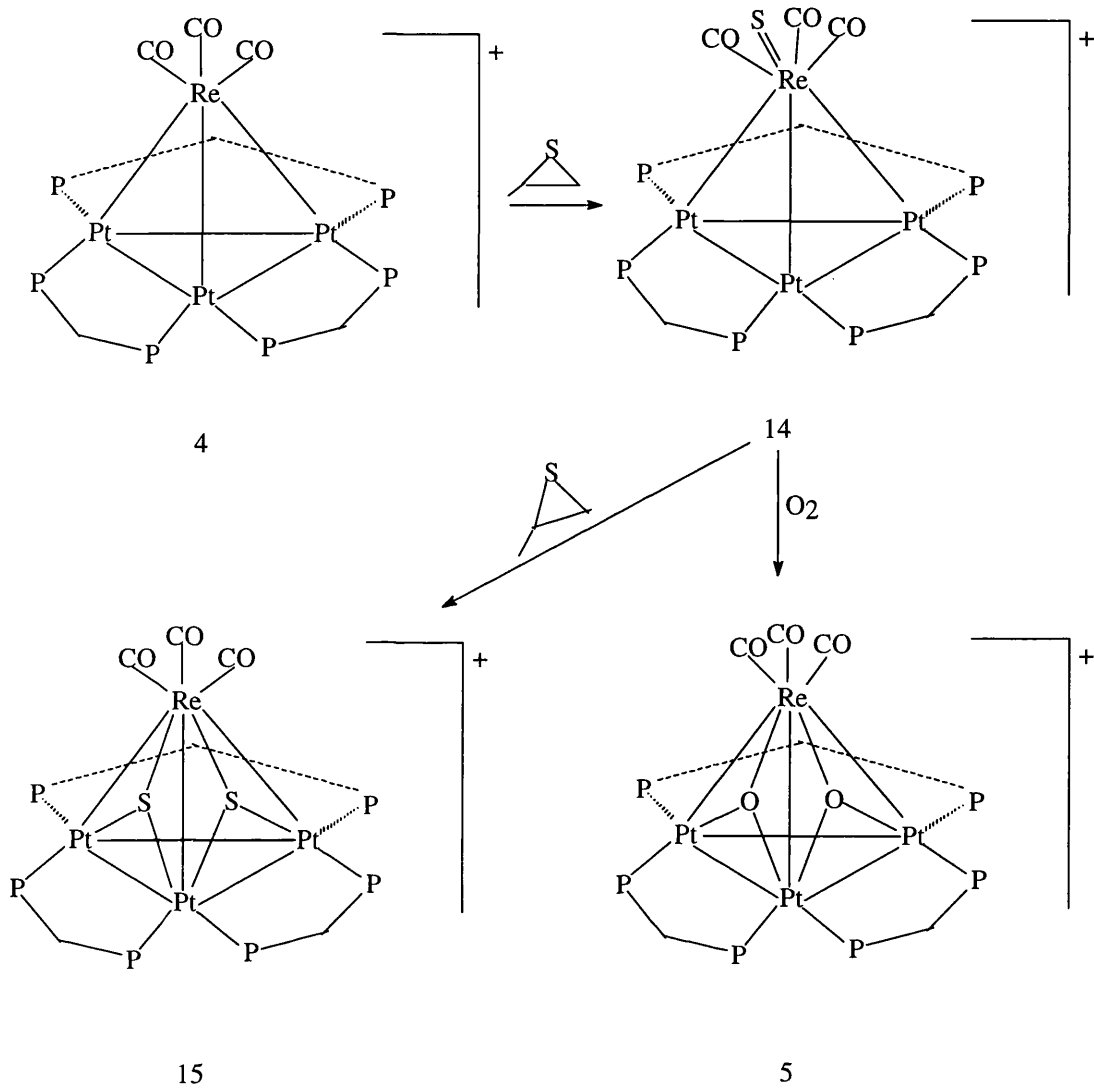
Scheme 2.3.1. Reaction with dioxxygen



Scheme 2.3.2. Reaction with neutral ligands



Scheme 2.3.3. Reaction with halide ligands



Scheme 2.3.4. Reaction with sulphur ligands

2.3.3. Current views on bonding in platinum rhenium clusters.

For most transition metal cluster complexes it has been long known that the geometry of the cluster is related to the number of skeletal electron pairs required to fill all the bonding metal-metal molecular orbitals (Mason, Thomas and Mingos, 1973). The theoretical basis of the polyhedral skeletal electron-pair theory has been discussed by Mingos & Forsyth (1977) and by Johnson (1980) and Mingos (1984). The important role played by terminal and bridging ligands in stabilising clusters has been recognized.

This theory successfully explained the geometry of many metal clusters, particularly those containing conical $M(\text{CO})_3$ and $M(\eta^5\text{-C}_5\text{H}_5)$ fragments (Evans & Mingos, 1982), because of their isolobal relationship (Hoffman, 1982) to main group fragments such as B-H and CH_2 (Elian, Chen, Hoffman & Mingos 1976; Mingos, 1977).

In its initial form the theory was not usually applicable to platinum clusters and attempts to remedy this deficiency still continue. The polyhedral skeletal electron pair theory was extended by Evans and Mingos (1982) to cover the non-conical ML_2 fragments which are found in many platinum clusters. They studied the electronic and structural features of triangular platinum clusters by extended Huckel molecular orbital calculations. The prevalence of planar triangular clusters with a 42 electron count was rationalised and the way in which the cluster bonding orbitals are markedly stabilised by a edge-bridging ligands has been discussed (Mealli, 1985). In such clusters, the metal p orbitals play a minor role, but out-of-plane capping carbonyl ligands induce a greater role for these p orbitals and facilitate the formation of clusters with electron counts from 42 to 48 electrons (Evans, 1988).

Attempts to explain trends in Pt-Pt and Pt-Re bond lengths and adduct formation by Pt/Re clusters are based on considering the interaction of $\text{Pt}_3(\text{dppm})_3$ with an appropriate rhenium fragment such as $\text{Re}(\text{CO})_3^+$ or $\text{Re}(\text{CO})_4^+$. The molecular

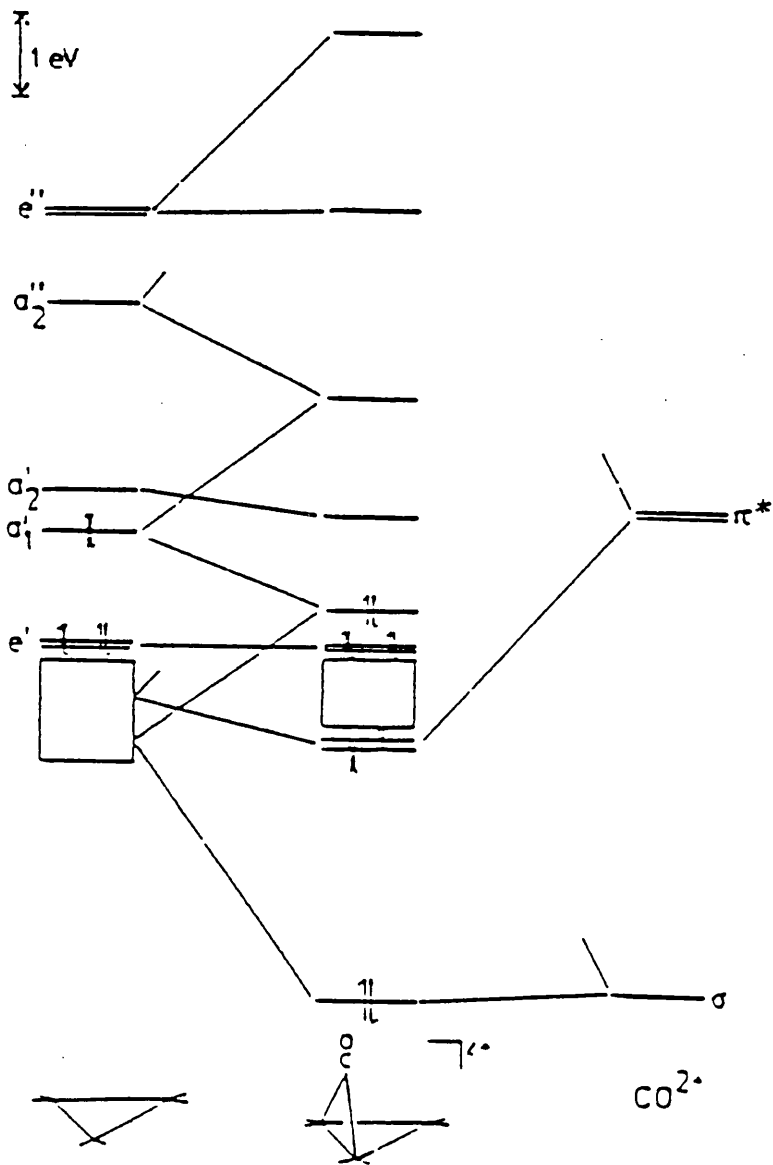


Figure 2.3.1. Molecular orbital diagram for interaction of $[\text{Pt}_3(\mu_3\text{-CO})(\mu_3\text{-dppm})_3]^{+2}$, considering it to be formed from $[\text{Pt}_3(\mu_3\text{-dppm})_3]$ and CO^{2+} (Evans, 1988).

orbitals of latitudinal $\text{Pt}_3(\text{dppm})_3$ have been extensively discussed by Evans (1988). According to Evans the cluster orbitals of D_{3h} $\text{Pt}_3(\text{dppm})_3$ comprise 18 metal d and σ -Pt-P orbitals plus three Pt-Pt bonding orbitals of a^+e^- symmetry, the a^- orbital being the HOMO (Figure 2.3.1). Thus 42 electrons are required to fill all bonding MOs. Figure 2.3.1 also shows how a $\mu_3\text{-CO}_2^+$ capping ligand (with three acceptor $\sigma+\pi^*$ orbitals) stabilises the system though the highest occupied MOs remain the a_1 HOMO and the two degenerate orbitals.

The fragments $\text{Re}(\text{CO})_3^+$ and ReO_3^+ can both be regarded as 12-electron units. Moreover they possess three $a+e$ type acceptor orbitals and thus can be regarded as isolobal with CO^{2+} . The bonding in $[\text{Pt}_3\{\text{Re}(\text{CO})_3\}(\mu\text{-dppm})_3]^+$ and in $[\text{Pt}_3(\text{ReO}_3)(\mu\text{-dppm})_3]^+$ thus is comparable with that of the $\mu_3\text{-CO}^{2+}$ complex shown in Figure 2.3.1. Despite the difference in rhenium oxidation states the 54 electrons possessed by each complex are just sufficient to fill all the bonding MOs. The three filled $a+e$ orbitals of the Pt_3 triangle donate to Re which thereby attains an 18-electron configuration, whereas each Pt atom has only 16 electrons. Detailed calculations (Xiao, Vittal, Puddephatt, Manojlovic-Muir & Muir, 1993) support these arguments and suggest Pt \rightarrow Re donation is greater in the ReO_3 complex. Mean bond lengths confirm the similarity of the two clusters (Table 2.3.1) the Pt-Re bonds are longer, rather than shorter, in the ReO_3 complex.

Addition of $\text{P}(\text{OPh})_3$ to Re rather than Pt is surprising given this bonding scheme, since the 16-electron Pt atoms have empty acceptor p-orbitals, whereas all Re-based orbitals are full. Once it is accepted that $[\text{Pt}_3\{\text{Re}(\text{CO})_3\text{P}(\text{OPh})_3\}(\mu\text{-dppm})_3]^+$ carries the additional phosphite ligand on Re then it is qualitatively clear that the Pt-Re bonds must weaken since a 14-electron ReL_4^+ fragment has only two acceptor orbitals. As can be seen from Table 2.3.1 this expectation is fulfilled: the Pt-Re distances are on average longer in the $\text{P}(\text{OPh})_3$ adduct (and are also irregular). There is also a slight lengthening of the mean Pt-Re bond length.

Even greater disruption of the cluster skeleton is found in the $(\mu_3\text{-O})_2$ dioxo complex. The addition of two 4-electron capping groups to the $\text{Re}(\text{CO})_3^+$ parent complex gives a 62-electron species. A tetrahedral M_4 cluster can accommodate only 60 electrons in bonding or non-bonding orbitals and anti-bonding orbitals are filled by any additional electrons. In this case (Table 2.3.1) the mean metal-metal distances are very long and consistent only with very weak metal-metal bonding.

Earlier work on the $\text{P}(\text{OPh})_3$ and other addition adducts of $[\text{Pt}_3\{\text{Re}(\text{CO})_3\}(\mu\text{-dppm})_3]^+$ indicated that the unsaturation was centred on Re rather than the platinum. However, I^- (and related anions) add μ_3 to Pt rather than to Re. This can be explained by overlap of filled I^- orbitals with the unstable acceptor Pt p-orbitals. Formally the anion transforms three electron pairs to the three empty p_z platinum orbitals, giving a 60 electron count; the unfavourable energy of these metal p-orbitals explains the weakness of the Pt-I bonding. Addition of I^- has no effect on the Pt-Pt distances but may slightly lengthen the Pt-Re bonds.

In summary, current bonding theories are useful in rationalising trends in metal-metal bond lengths. They are less helpful when attempting to predict whether platinum or rhenium will be the site of nucleophilic attack.

Table 3.2.1

Mean Pt-Pt and Pt-Re bond lengths (Å)
in platinum and rhenium cluster complexes

Reference	Complex	Electrons	Pt-Pt	Pt-Re
a	$[\text{Pt}_3\{\text{Re}(\text{CO})_3\}(\mu\text{-dppm})_3]^+$	54	2.604	2.673
b	$[\text{Pt}_3(\text{ReO}_3)(\mu\text{-dppm})_3][\text{ReO}_4]$	54	2.602	2.726
c	$[\text{Pt}_3(\text{ReO}_3)(\mu\text{-dppm})_3][\text{PF}_6]$	54	2.612	2.701
d	$[\text{Pt}_3\{\text{Re}(\text{CO})_3\text{P}(\text{OPh})_3\}(\mu\text{-dppm})_3]^+$	56	2.638	2.843
e	$[\text{Pt}_3\{\text{Re}(\text{CO})_3\}(\mu_3\text{-O})_2(\mu\text{-dppm})_3]^+$	62	3.000	2.975
f	$[\text{Pt}_3\text{Re}(\text{CO})_2\{\text{P}(\text{OMe})_3\}(\mu_3\text{-O})_2(\mu\text{-dppm})_3]^+$	62	3.010	2.955
g	$[\text{Pt}_3\{\text{Re}(\text{CO})_3\}(\mu_3\text{-I})(\mu\text{-dppm})_3]$	60	2.599	2.748

References

- (a). Xiao, J., Vittal, J. J., Puddephatt, R. J., Manojlovic-Muir, Lj. & Muir, K. W. (1993). *J. Amer. Chem. Soc.* 115, 7882-7883.
- (b). Xiao, J., Puddephatt, R. J., Manojlovic-Muir, Lj., Muir, K. W. & Torabi, A. A. (1994). *J. Amer. Chem. Soc.* 116, 1129-1130.
- (c). Hao, L., Xiao, J., Puddephatt, R. J., Manojlovic-Muir, Lj., Muir, K. W. & Torabi, A. A. (1996). *Inorg. Chem.* 35, 658-666.
- (d). Xiao, J., Hao, L., Puddephatt, R. J., Manojlovic-Muir, Lj., Muir, K. W. & Torabi, A. A. (1994). *J. Chem. Soc. Chem. Commun.* 2221-2222.
- (e). Xiao, J., Hao, L., Puddephatt, R. J., Manojlovic-Muir, Lj. & Muir, K. W. (1995). *J. Amer. Chem. Soc.* 117, 6316-6326.
- (f). 2.3.6. Compound **10**
- (g). Xiao, J., Hao, L., Puddephatt, R. J., Manojlovic-Muir, Lj., Muir, K. W. & Torabi, A. A. (1995). *Organometallics*, 14, 2194-2201.

2.2.4. Bimetallic Pt-Re catalysis.

Introduction

Several types of clusters have been of interest in catalysis. One type consists of a combination a group 8 metal and a group 11 metal, such as ruthenium-copper and osmium-copper (Sinfeld, 1973); other interesting types of bimetallic clusters include a combination of two group 9 or 10 metals, e.g. platinum-iridium and iridium-rhodium (Garten & Sinfeld, 1980; Sinfeld, Via & Lytle, 1982); or a combination of two group 11 metals, such as silver-copper or gold-copper (Meitzner, Via, Lytle & Sinfelt, 1985).

The combination of platinum and rhenium provides an example of still another type, comprising a group 10 metal and a metal from group 7. Such catalysts have been developed and widely used in petroleum refining to production aromatic hydrocarbons for automotive fuels (Sinfelt, 1987).

Use of Pt/Re

Among industrial bimetallic catalysts, oxide-supported Pt-Re catalysts have received the most attention, due to their use in naphtha reforming for the production of gasoline with high octane number (anti-knock quality). Some of the reactions which can be catalysed by Pt/Re/Al₂O₃ are shown in Figure 3.3.2. Platinum is the metal of choice because it is the only one that has activity for the desired reactions, such as hydrogenolysis of paraffins. Since platinum is expensive, it is imperative in the development of an economical industrial process to minimize its amount and maximize its dispersion. Alumina is the support of choice because it is inexpensive and is easily prepared with the desired physical properties. The original reforming catalyst is based on alumina-supported platinum (Gates, 1992). The addition of

rhenium significantly improves the life time and selectivity for aromatics of the catalysts (Xiao & Puddephatt, 1995). As an example, in the conversion of methyl cyclopentane to benzene and C1-C6 alkanes over Pt/Al₂O₃ or Pt-Re/Al₂O₃ the benzene/alkane ratio after 24 hours is greater with the bimetallic catalyst (Carter, McVick, Weissmann, Kmak & Sinfelt, 1982). The oxidation state of platinum in the reduced catalysts is widely accepted to be zero. However, the oxidation state of rhenium in the reduced catalysts has been debated for a long time and still the issue is not resolved (Huang, Fryer, Park, Stirling & Webb, 1994; Chen, Ni, Zang, Lin, Luo & Chen, 1994; Purnell, Chang & Gates, 1993). Pt-Re/Al₂O₃ catalysts work at low pressure and low pressure increases the selectivity for aromatic production. Different oxidation states give different characteristics to rhenium: for example, rhenium in oxidation state zero is known to chemisorb CO strongly while Re(IV) surface sites do not chemisorb CO (Chen, Ni, Zang, Lin, Luo & Chen, 1994).

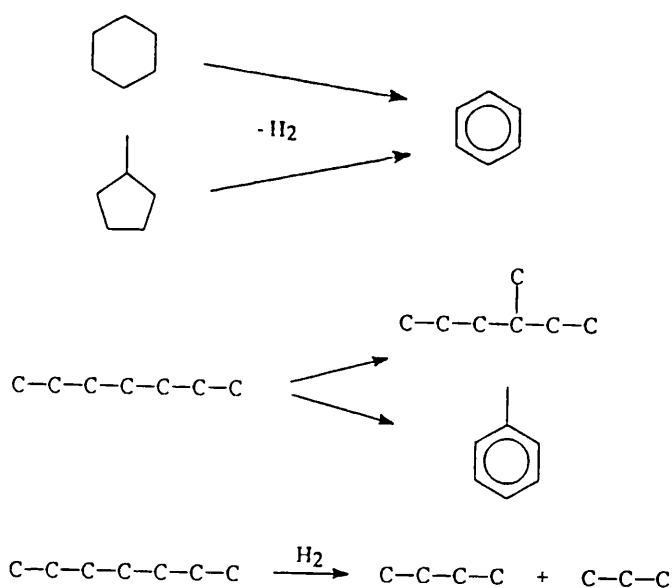


Figure 2.3.2. Typical reactions in catalytic reforming (Xiao & Puddephatt, 1995)

Conclusion

The Pt/Re cluster chemistry presented in this thesis suggests some possible rules, which may be applicable to the behaviour Pt/Re catalysts.

(1). The presence of rhenium makes the cluster much more susceptible to oxidation than a pure platinum cluster would be.

(2). Oxidation occurs in a stepwise manner and mainly (though not exclusively) involves rhenium. Re shows all oxidation states between I to VII whereas, platinum is mainly zero valent, though Pt(I) and Pt(II) are found.

(3). As noted in the previous sections chemical behaviour of platinum-rhenium clusters can be strongly influenced by the rhenium oxidation state (compare addition of L to 4 and 5, Scheme 2.3.2).

Though the nature of the support catalysts is still debated (2) seems to apply platinum is zero valent whereas rhenium is in a position oxidation state. Application of (3) to the catalyst, i.e. the idea that the rhenium oxidation state might control chemical behaviour has only the status of a hypothesis at present.

References

- Albright, T. A., Burdett, J. K. & Whangbo, M. -H. (1985). *Orbital Interactions in Chemistry*, Wiley, New York.
- Allman, R. & Kucharczyk, D. (1983). *Z. Krist.* 165, 227-232.
- Ara, I., Fanwick, P. E. & Walton, R. A. (1992). *Inorg. Chem.* 31, 3211-3215.
- Betz, P. & Bino, A. (1988). *J. Amer. Chem. Soc.* 110, 602-603.
- Bottomley, F. & Sutin, L. (1988). *Adv. Organomet. Chem.* 28, 339-396.
- Bradford, A. M., Douglas, G., Manojlovic-Muir, Lj., Muir, K. W. & Puddephatt, R. J. (1990). *Organometallics*, 9, 409-416.
- Brown, M. P., Cooper, S. J., Frew, A. A., Manojlovic-Muir, Lj., Muir, K. W., Puddephatt, R. J., Seddon, K. R. & Thomson, M. A. (1981). *Inorg. Chem.* 20, 1500-1507.
- Bruce, M. I., Hamphrey, M. G., Snow, M. R., Tiekink, E. R. T. & Wallis, R. C. (1986). *J. Organomet. Chem.* 314, 311-322.
- Carr, S. W., Fontaine, X. L. R., Shaw, B. L. & Thornton-Pett, M. (1988). *J. Chem. Soc. Dalton Trans.* 769-774.
- Garten, R. L. & Sinfelt, J. H. (1980). *J. Catal.* 62, 127-139
- Carter, Y. L., McVick, G. B., Weissmann, W., Kmak, W. S. & Sinfelt, J. H. (1982). *Appl. Catal.* 3, 327-346.
- Chakravarty, A. R., Cotton, F. A., Diebold, M. P., Lewis, D. B. & Roth, W. J. (1986). *J. Amer. Chem. Soc.* 108, 971-976.
- Chen, L., Ni, Y., Zang, J., Lin, L., Luo, X. & Chen, S. (1994). *J. Catal.* 145, 132-140
- Ciani, G., Moret, M., Sironi, A., Beringhelli, T., D'Alfonso, G. & Pergola, R. D. (1990). *J. Chem. Soc. Chem. Commun.* 1668-1670.

Ciani, G., Moret, M., Sironi, A., Antogmazza, P., Beringhelli, T., D'Alfonso, G., Pergola, R. D. & Minoja, A. (1991). *J. Chem. Soc. Chem. Commun.* 1255-1257.

Clucas, J. A., Harding, M. M., Nicholls, A. K. & Smith, A. K. (1985) *J. Chem. Soc. Dalton Trans.* 1835-1842.

Colombie, A., Bonnet, J. J., Fomperine, P., Lavigne, G. & Sunshine, S. (1986). *Organometallics*, 5, 1154-1159.

Colton, R. (1976). *Aust. J. Chem.* 29, 1833-1835.

Cotton, F., Lahuerta, P., Sanau, M. & Schwatzer, W. (1985). *J. Amer. Chem. Soc.* 107, 8284-8285.

Cotton, F. A. & Wilkinson, G. (1986). *Advanced Inorganic Chemistry*, Fifth edition, John Wiley and Sons.

Cowie, M. & Dwight, S. K. (1979). *Inorg. Chem.* 18, 1209-1214.

Degnan, H. A., Herrmann, W. A. & Herdtweck, E. (1990). *Chem. Ber.* 123, 1347-1349.

Dilworth, J. R., Ibrahim, B. K., Khan, S. R., Hursthouse, M. B & Karaulov, A. A. (1990). *Polyhedron*, 9, 1323-1329.

Domingos, A., Marcalo, J., Parclo, A. Pires de Matos, A & Santos, I. (1993). *Inorg. Chem.* 32, 5114-5118.

Douglas, G., Jennings, M. C., Manojlovic-Muir, Lj., Muir, K. W. & Puddephatt, R. J. (1989). *J. Chem. Soc. Chem. Comm.* 159-161.

Douglas, G., Manojlovic-Muir, Lj., Muir, K. W., Rashidi, M., Anderson, C. M. & Puddephatt, R. J. (1987). *J. Amer. Chem. Soc.* 109, 6527-6528.

Elian, M., Chen, M. M., L. Hoffman, R. & Mingos, D. M. P. (1976). *Inorg. Chem.* 15, 1148-1155.

Evans, D. G. (1988). *J. Organomet. Chem.* 352, 397-413.

Evans, D. G. & Mingos, D. M. P. (1982). *J. Organomet. Chem.* 240, 321-327.

Ferguson, G., Lloyd, B. R., Manojlovic-Muir, Lj., Muir, K. W. & Puddephatt, R. J. (1983). *Inorg. Chem.* 25, 4190-4197.

Ferguson, G., Lloyd, B. R. & Puddephatt, R. J. (1986). *Organometallics*, 5, 344-348.

Fischer, V. D., Krebs, B. & Hoppe, R. (1982). *Z. anorg. allg. Chem.* 491, 73-82.

Gates, B. C. (1992). *Catalytic Chemistry*, Wiley, New York.

Haung, Z., Fryer, J. R., Park, C., Stirling, D. & Webb, G. (1994). *J.Catal.* 148, 478-492.

Herrmann, W. A., Kuhn, F. E., Romao, C. C., Huy, H. T., Wang, M., Fischer, R. W., Kirprof, P. & Scherer, W. (1993). *Chem. Ber.* 126, 45-50.

Herrmann, W. A., Serrano, R. A. & Bock, H. (1984). *Angew. Chem. Int. Ed. Engl.* 23, 383-385.

Hao, L., Xiao, J., Vittal, J. J. & Puddephatt, R. J. (1994). *J. Chem. Soc.Chem. Commun.* 2183-2184.

Hao, L., Xiao, J., Vittal, J. J., Puddephatt, R. J., Manojlovic-Muir, Lj., Muir, K. W. & Torabi, A. A. (1996). *Inorg.Chem.* 35, 658-666.

Hoffman, R. (1982). *Angew. Chem. Int. Ed. Engl.* 21, 711-724.

Hoffman, DM. & Hoffmann, R. (1981). *Inorg. Chem.* 20, 3543-3555.

Johnson, B.F.G. (1980). *Transition metal clusters*, Ed. J. Wiley Chichester.

Johnson, K. A. & Gladfelter, W. L. (1992). *Organometallics*, 11, 2534-2542.

Lloyd, B. R., Manojlovic-Muir, Lj., Muir, K. W. & Puddephatt, R. J. (1993). *Organometallics*, 12, 1231-1237.

Lugan, N., Bonnet, J. J. & Ibers, J. A. (1985). *J. Amer. Chem. Soc.* 107, 4484-4491.

Mallinson, P. R. & Muir, K. W. (1985). *J. Appl. Crystallogr.* 18, 51-53.

Manojlovic-Muir, Lj. & Muir, K. W. (1982). *Chem. Soc. Chem. Commun.* 1155-1156

Manojlovic-Muir, Lj., Muir, K. W., Lloyd, B. R. & Puddephatt, R. J. (1983). *J. Chem. Soc. Chem. Comm.* 1336-1337.

Manojlovic-Muir, Lj., Muir, K. W. & Solomun, T. (1979). *Acta cryst.* B35, 1237-1239.

- Manojlovic-Muir, Lj., Brandes, D. A. & Puddephatt, R. J. (1987). *J. Organomet. Chem.* 332, 201-211.
- Manojlovic-Muir, Lj., Muir, K. W., Rennie, M. -A., Xiao, J. & Puddephatt, R. J. (1993). *J. Organomet. Chem.* 462, 235-241.
- Mason, K., Thomas, K. M. & Mingos, D. M. P. (1973). *J. Amer. Chem. Soc.* 95, 3802-3804.
- McAuliffe, C. A. & Levason, W. (1979). *Phosphine, arsine and stibine complexes of transition elements.* Elsevier, Amsterdam.
- Mealli, C. (1985). *J. Amer. Chem. Soc.* 107, 2245-2253.
- Meitzner, G., Via, G. H., Lytle, F. W. & Sinfelt, J. H. (1985). *J. Chem. Phys.* 83, 4793-4799.
- Mingos, D. M. P. (1977). *Adv. Organomet. Chem.* 15, 1-51.
- Mingos, D. M. P. (1984). *Acc. Chem. Res.* 17, 311-319.
- Mingos, D. M. P. & Forsyth, M. I. (1977). *J. Chem. Soc. Dalton Trans.* 610-616.
- Mingos, D. M. P. & Wardle, R. W. M. (1985). *Transition Met. Chem.* 10, 441-459.
- Mirza, H. A., Vittal, J. J. & Puddephatt, R. J. (1993). *Inorg. Chem.* 32, 1327-1332.
- Molen (1990). *Crystallographic program package, Enraf-Nonius, Delft, The Netherlands.*
- Okawara, R. & Matsumura, J. (1976). *Adv. Organomet. Chem.* 14, 187-202.
- Okuda, J., Herdtweck, E. & Herrmann, W. A. (1988). *Inorg. Chem.* 27, 1254-1257.
- Olmstead, M. M., Lee, C. L. & Balch, A. L. (1982). *Inorg. Chem.* 21, 2712-2716.
- Powell, J., Brewer, J. C., Gulia, G. & Sawyer, J. F. (1992). *J. Chem. Soc. Dalton Trans.* 2503-2516.
- Pringle, P. J. & Shaw, B. L. (1982) *J. Chem. Soc. Chem. Comm.* 581-583.
- Puddephatt, R. J., Manojlovic-Muir, Lj. & Muir, K. W. (1990). *Polyhedron*, 9, 2767-2802.
- Puddephatt, R. J., Thomson, M. A., Manojlovic-Muir, Lj., Muir, K. W., Frew, A. A. & Brown, M. P. (1981). *J. Chem. Soc. Chem. Comm*, 805-806.

Puddephatt, R. J. (1983). *Chem. Soc. Rev.* 12, 99-127.

Qi, J., Fanwick, P. E. & Walton, R. A. (1990). *Inorg. Chem.* 29, 457-462.

Rogers, D. (1981). *Acta Crystallogr.* A37, 734-741.

Sanger, A. R. (1981). *J. Chem. Soc. Dalton Trans.* 228-233.

Shaik, S., Hoffmann, R., Fisel, C. R. & Summerville, R. H. (1980). *J. Amer. Chem. Soc.* 102, 4555-4572.

Sheldrick, G. M. (1985). SHELXS-86, Program for solution of crystal structures; University of Geottingen, Germany.

Sheldrick, G. M. (1993). SHELXL-93, Program for refinement of crystal structures; University of Geottingen, Germany.

Shriver, D. F., Kaesz, H. D. & Adams, R. D. (1990). *The chemistry of metal cluster complexes*, VCH, New York.

Sinfelt, J. H. (1987). *Acc. Chem. Res.* 20, 134-139

Sinfelt, J. H. (1973). *J. Catal.* 29, 308-315

Sinfelt, J. H., Via, G. H. & Lytle, F.W. (1982). *J. Chem. Phys.* 76, 2279-2789

Stern, E. W. & Maples, P. K. (1972). *J. Catal.* 27, 120-133.

Tolman, C. A. (1977). *Chem. Rev.* 77, 313-348.

Tsany, B. W., Reibenspies, J. & Martell, A. E. (1993). *Inorg. Chem.* 23, 988-994.

van der Veldon, J., W. A. Bour, J. J., Pet, R., Bosman, W. P. & Noordik, J. H. (1983). *Inorg. Chem.* 22, 3112-3131

Walker, N. & Stuart, D. (1983). *Acta Crystallogr.* A39, 158-166.

Xiao, J., Hao, L., Puddephatt, R. J., Manojlovic-Muir, Lj., Muir, K. W. & Torabi, A. A. (1995a). *Organometallics*, 14, 2194-2201.

Xiao, J., Hao, L., Puddephatt, R. J., Manojlovic-Muir, Lj., Muir, K. W. & Torabi, A. A. (1995b). *Organometallics*, 14, 4183-4193.

Xiao, j., Hao, L., Puddephatt, R. J., Manojlovic-Muir, Lj., Muir, K. W. & Torabi, A. A. (1994). *J. Chem. Soc. Chem. Commun.* 2221-2222.

Xiao, J. & Puddephatt, R. J. (1995). *Coordination. Chem. Rev.* 143, 457-500.

Xiao, J., Kristof, E. Vittal, J. J. & Puddephatt, R. J. (1995). *J. Organometal.* 490, 1-6.

Xiao, J., Vittal, J. J. & Puddephatt, R. J. (1993). *J. Chem. Soc. Chem. Commun.* 167-169.

Xiao, J., Puddephatt, R. J., Manojlovic-Muir, Lj, Muir, K. W. & Torabi, A. A. (1994). *J. Amer. Chem. Soc.* 116, 1129-1130.

Xiao, J., Vittal, J. J., Puddephatt, R. J., Monojlovic-Muir, Lj. & Muir, K. W. (1993). *J. Amer. Chem. Soc.* 115, 6316-6326.

Xiao, J., Vittal, J. J., Puddephatt, R. J., Manojlovic-Muir, Lj. & Muir, K. W. (1993). *J. Amer. Chem. Soc.* 115, 7882-7883.

Section 3

Stereochemical studies of some organic compounds

Introduction

The following three chapters deal with structures of relatively simple organic molecules. In general, the structures of such molecules are easily established by spectroscopic methods and bond lengths can usually be predicted to ca. 0.02 Å from average values obtained from database studies. Diffraction methods are, however, needed to establish preferred conformations or the relative stereochemistry of molecules with several chiral centres.

The latter consideration applies to chapters 3.1 and 3.2, both of which are concerned with the structures of Diels-Alder adducts. The Diels-Alder reaction constitutes one of the most popular synthetic methods for the construction of six-membered and polycyclic ring systems and is therefore of fundamental interest in organic chemistry. Chapter 3.1 is concerned with the formation of dihydro-oxazine diastereoisomers and the structural studies were required in order to develop synthetic routes to optically pure products of known stereochemistry. In recent years there has been increasing interest in the development of special physical (e.g. high pressure, choice of solvent) and catalytic methods (Lewis acids e.g. TiCl_4 or AlCl_3) for the purpose of improving the rate and selectivity of $[4\pi+2\pi]$ Diels-Alder cycloadditions (Pindur, Lutz & Otto, 1993). The structures discussed in chapter 3.2 illustrate how the course of a Diels-Alder reaction may be effected by the presence or absence of a catalyst.

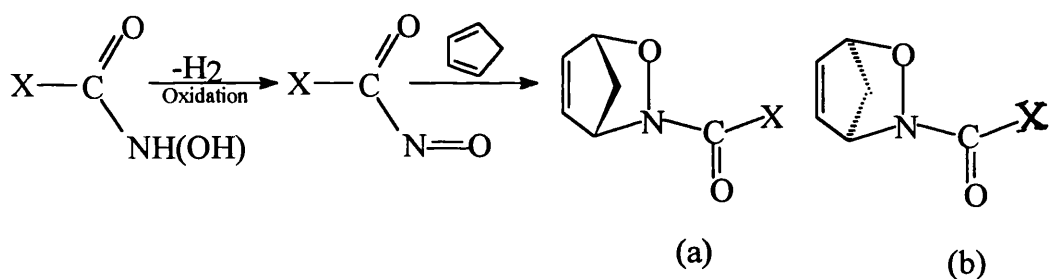
The conformations of the anti-cancer drugs described in chapter 3.3 were determined to see if they helped explain the biological activity of the drugs.

Chapter 3.1 Cycloadducts of Chiral Acylnitroso Compounds

3.1.1 Introduction

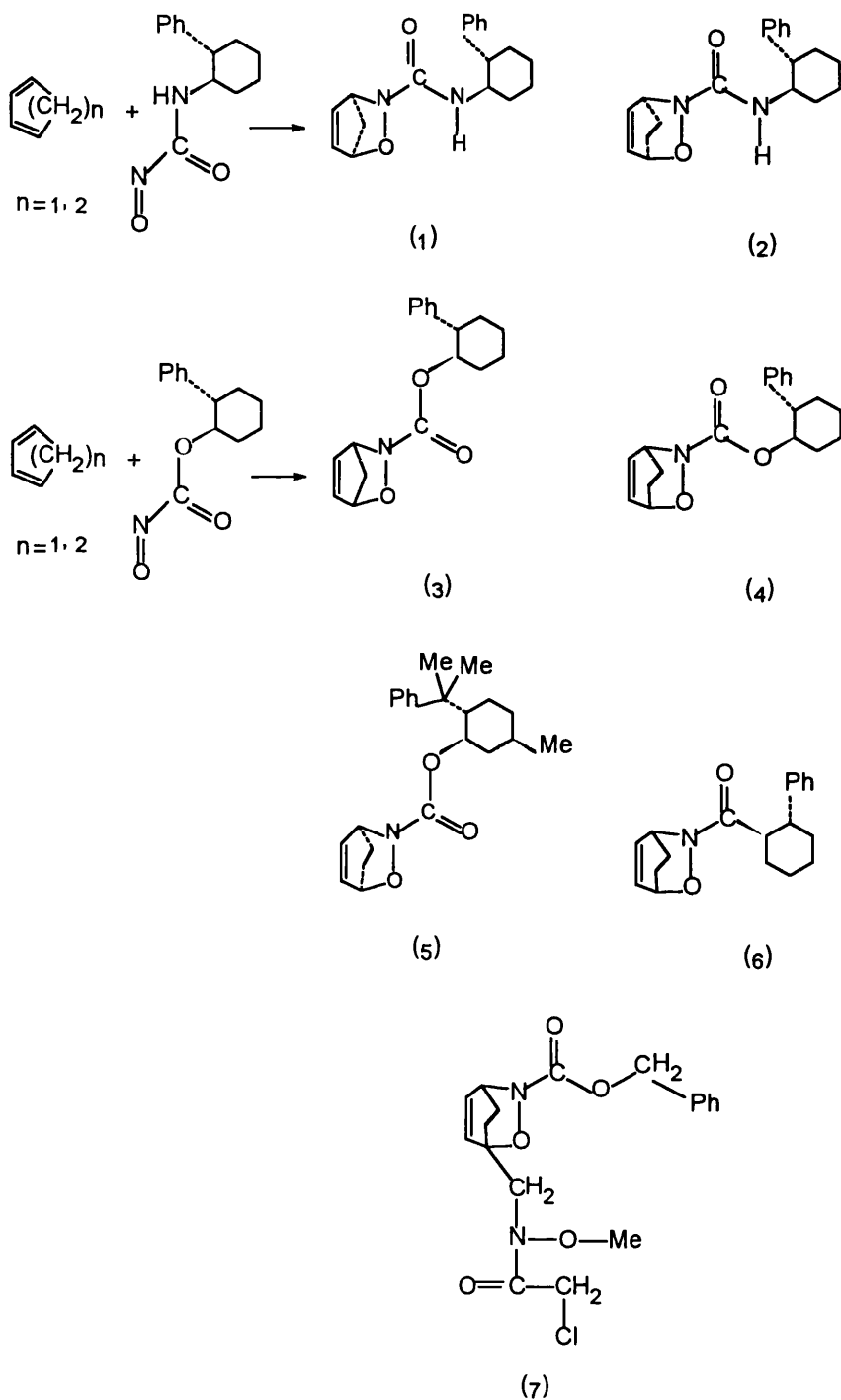
Diels-Alder cyclo-addition of nitroso compounds to conjugated dienes is known to be an effective route to dihydro-oxazines which in turn have synthetic applications in the preparation of several types of cyclo-nitroso compound (Kirby, McGuinan, Mackinnon, McLean & Sharma, 1985). Recently, Professor Kirby and his co-workers in this department have used hydroxamic acids, XCONHOH, to generate the required nitroso compounds (Kirby & Nazeer, 1993). Hydroxamic acids are easily oxidized to give acyl-nitroso compounds, XCONO (X = R, RO, or RR'N), as transient intermediates which can be immediately trapped by conjugated dienes to give compounds containing the required dihydro-oxazine ring system (Reaction 3.1.1). Chiral centres are normally formed in this reaction and the product is racemic.

Reaction 3.1.1



If X in reaction 3.1.1 is chiral then the products (a) and (b) are diastereoisomers, i.e. chemically distinct compounds, which may be formed in different amounts. Their separation, followed by removal of the acyl side-chain,

Scheme 3-1-1



would give optically pure forms of the dihydro-oxazine ring system. The ultimate synthetic objective is thus to prepare optically pure dihydro-oxazine compounds of known absolute configuration. The X-ray structural studies described here were undertaken in the hope that they might, besides establishing the steric course of particular reactions, indicate rules which would allow the stereochemistry of such reactions to be more generally predicted. The work described here is concerned with reactions in which the starting point is normally a racemic hydroxamic acid. In consequence both products (a) and (b) in reaction 3.1.1 are formed as racemates. In general the reactions show significant asymmetric induction, i.e. either (a) or (b) preponderates. The particular reactions involved are presented in Scheme 3.1.1. They involve nitroso compounds containing acyl groups derived from racemic *trans*-2-phenyl-cyclohexylamine reacting with cyclopentadiene or cyclohexadiene to give **1** and **2**. *trans*-2-Phenyl-cyclohexanol similarly gives rise to **3** and **4**, an optically pure hydroxamic acid gives **5**, whereas **6** is again obtained from a racemic starting compound. The X-ray analyses described here were undertaken mainly in order to define the stereochemistries of the products **1** - **6**. In each case the major product of the reaction was therefore selected for investigation. The results permit the absolute stereochemistries of the products of reactions using optically pure starting materials to be predicted. In addition, a search of the Cambridge Data Base revealed only one structural study of a dihydro-oxazine, **7**, (Baldwin et al., 1984). The results of the structure analyses of **1** - **6** therefore represent a considerable increase in structural knowledge concerning this unusual functional group. A detailed structural comparison of compound **7** with **1** - **6** is not possible because of the limited information available in the report of Baldwin et al., (1984).

3.1.2 Results and Discussion

The structures of compounds **1** - **6** have been determined by X-ray diffraction analysis and are shown in Figures 3.1.1 - 3.1.6. It should be noted here that the asymmetric unit of **2** contains two crystallographically independent molecules with nearly identical conformations. Key stereochemical parameters are summarised in Table 3.1.1. The addition of a diene to the N=O bond of a hydroxamic acid creates a bicyclic residue in which the chiral bridgehead carbon atoms necessarily have opposite configurations, i.e. RS or SR. All the compounds except **5** are racemic and the enantiomer shown in Figures 3.1.1 - 3.1.6 (and described in Tables 3.1.1 & 3.1.2) is in each case the one in which the torsion angle ϕ_1 [Ph-C-C-X, X = O=N-C(O)NH, O=N-C(O)O or O=N-C(O)], which defines the relationship of the two cyclohexane ring substituents, is ca. -60° . The torsion angles ϕ_2 [O-N-C=O] and ϕ_3 [N-O-C-CH₂] then define the stereochemistries of the hydroxamate and bicyclic systems as shown in Scheme 3.1.1. For compound **5** which is chiral the known absolute structure of the starting material was assumed to apply since the diffraction experiment did not allow experimental determination of the absolute structure.

For the hexadiene adducts **2** and **4** - **6** co-crystallisation of two diastereoisomeric products is by no means unlikely since one isomer can formally be converted to the other by interchanging CH₂-CH₂ and CH=CH units. The relevant C=C and C-C bond lengths (Table 3.1.1) suggest that only in the case of **6** does the crystal contain a mixture of diastereoisomers.

The signs of the ϕ_3 torsion angles show no obvious pattern. Thus, while the structure analyses establish the stereochemistry of the addition reactions which produce **1** - **6** they do not allow predictions to be made with confidence concerning related reactions. In the pentadiene adducts **1** and **3** ϕ_3 is smaller than the corresponding values for the remaining compounds, all of which are formed from

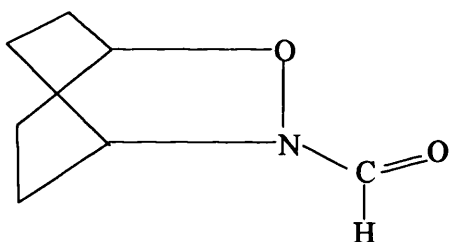
hexadiene. This reflects the greater ring strain imposed by the presence of one, rather than two, bridging methylene groups.

The O-N-C(O)R (R=O,NH,C) hydroxamate residues in the compounds are all roughly planar. The O-N-C=O torsion angle, ϕ_2 , is either near zero (*cis*) or 180° (*trans*). The *trans* configurations of **1** and **2** permit the formation of an intramolecular N-H...O hydrogen bond. Otherwise **4** and **6** adopt *trans* arrangements whereas **3** and **5** are *cis*. Except when one arrangement is more favourable for hydrogen bonding the results suggest that *trans* and *cis* O-N-C=O stereochemistries are about equally probable. Figures 3.1.7. and 3.1.8 show views of the crystal packing and hydrogen bonding for compounds **1** and **2**. In both structures the N-H proton is involved in hydrogen bonding to acceptor oxygen atoms (see Table 3.1.2). In **1** N(2)-H(2) forms an intramolecular hydrogen bond with O(1) [H(2)...O(1) 2.2 Å], locking the molecule into the *trans* O-N-C=O conformation, but also donates to an oxygen atom in a neighbouring molecule [H(2)...O(2ⁱ) 2.1 Å i: -x, 2-y, 1-z]; this bifurcated bond thereby links the molecules into ribbons running parallel to a. In **2** there are no intermolecular hydrogen bonds but the *trans* - O-N-C=O unit in each molecule is again associated with an intramolecular hydrogen bond [H(21)...O(11) 2.1 Å, H(22)...O(12) 2.0 Å]. The three-centre hydrogen bond involving the N-H substituent in **1** displays distances and angles in the ranges considered typical for such bifurcated hydrogen bonds (Steiner & Saenger, 1992; Pirard, Baudoux, & Durant, 1995).

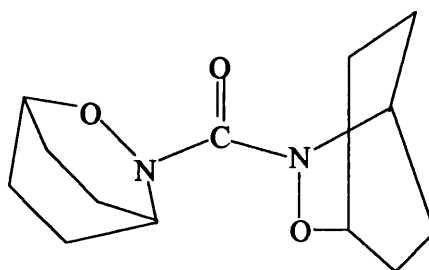
The stereochemistry of the oxazine nitrogen atom, N(1), is pyramidal in each of the compounds. This is obvious from the sum of the valence angles at N(1), ΣN , for **1** - **6** given in Table 3.1.1. This confirms the conclusion of Baldwin et al. (1984), who remarked on the pyramidal character of the oxazine nitrogen atom in **7**. A number of authors (Thiessen, Levy & Flaigo, 1978; Nesterova, Porai-Koshits & Moev, 1981; Nelsen, Thompson-Colon, Kirste, Rosenhouse & Kaftory, 1987;

Nelsen, Thompson-Colon & Kaftory, 1989) have suggested that in similar compounds electronic arrangements favour sp^3 hybridisation at nitrogen.

Bond lengths in the ONC(O)R units of **1** - **6** are compared in Table 3.1.3. Values for **6** cannot be regarded as reliable since the crystal is probably composed of two diastereoisomers. The C=O bonds (d) appear to have lengths which are intermediate between the values typical of a carboxylic ester [1.196 Å] and these found in ureas (e.g., 1-hydroxy-1-methylurea and 1-hydroxy-3-methylurea)[1.259(1) and 1.256(11) Å] (Nielsen, Frydenveny & Larsen, 1993). The exocyclic C=O bond lengths in the saturated oxazine compounds **8** and **9** of 1.223 and 1.211 Å (Nelsen, Thompson-Colon, Kirste, Rosenhouse & Kaftory, 1987; Nelsen, Thompson-Colon & Kaftory, 1989) are closely comparable to the values in **1** - **6**.



(8)



(9)

The lengths of the oxazine-N-C(carbonyl) bonds are slightly longer than the accepted values for a $\text{N}_{sp^3}\text{-C}_{sp^2}$ single bond [1.376 Å], as is also the case in **9** [N-C 1.384, 1.389 Å] and related structures (Thiessen, Levy & Flaigo, 1978). A much shorter $\text{N}_{sp^3}\text{-C}_{sp^2}$ distance is found in compound **8** [1.319 Å]. The oxazine N-O bonds (e) have a mean length of 1.43 Å, c.f. 1.41 and 1.448 & 1.444 Å in **8** and **9**, somewhat shorter than the accepted value [1.463 Å] for a $\text{C}_2\text{N-OC}$ bond where the nitrogen has sp^3 hybridisation but longer than that found where the nitrogen atom is

planar [1.397 Å]. The oxazine N-C(bridgehead) bonds (g) are, if anything, longer than is typical for N_{sp3}-C_{sp3} distances [1.469 Å]. The three bonds radiating from the oxazine nitrogen atom thus have lengths consistent with bond orders close to one and with the pyramidal hybridisation of the nitrogen atom.

3.1.3 Experimental

Crystallographic data for **1** - **6** are summarised in Table 3.1.4 - 3.1.6. The fractional co-ordinates for non-hydrogen atoms for compounds **1** - **6** are given in Table 3.1.7. The experimental and computational procedures used have been described in Section 1. All structures were solved by direct methods (Sheldrick, 1985). For compound **1** eight reflections suspected of serious systematic error ($\Delta/\sigma > 8$) were excluded from the refinement. For **2** and **3** a full hemisphere (two asymmetric units) of data was collected. The crystal of **3** decomposed during the experiment and data with $\theta > 24.5^\circ$ were excluded from the refinement because decomposition was substantial at high angles. The final full matrix least squares refinement on F included anisotropic displacement parameters for all elements except hydrogen. Additional material available in Volume 2 includes hydrogen atom co-ordinates and observed and calculated structure factors. All calculations were performed with the GX package (Mallinson & Muir, 1985).

Table 3.1.1. Stereochemical parameters for compounds **1 - 6** (Å, °)

	1	2	3	4	5	6	
space group	P2 ₁ /a	Cc	P2 ₁ /c	P2 ₁ /c	P2 ₁	Pna2 ₁	
ϕ_1	-52.7(4)	-56.9(7)	-57.6(7)	-56.4(5)	-63.2(4)	-52.1(5)	-61.1(5)
ϕ_2	165.9(5)	-167.0(9)	-164.8(9)	14.3(6)	-158.9(7)	-19.4(6)	169.9(7)
ϕ_3	40.8(4)	69.0(7)	70.6(7)	-36.7(5)	-68.7(4)	69.0(5)	-63.9(5)
C = C	1.288(8)	1.318(1)	1.300(11)	1.302(9)	1.305(7)	1.312(7)	1.390(8)
C - C	-	1.515(11)	1.504(10)	-	1.528(7)	1.515(8)	1.426(12)
ΣN	329	333	334	329	339	338	354

Notes:

1. The *trans* stereochemistry of the 1, 2-substituted cyclohexane ring is defined by the Ph-C-C-R torsion angle ϕ_1 . Compounds **1**, **2**, **3**, **4** & **6** crystallise in achiral space groups. The enantiomers shown in Figures 3.1.1 - 3.1.6 and described here have $\phi_1 \cong -60^\circ$.
2. The O-N-C=O torsion angle ϕ_2 defines the relationship of the nitroso and carbonyl oxygen atoms.
3. The configuration of the dihydro-oxazine ring system is defined by torsion angle $\phi_3 = \text{N-O-C-C}_b$ where C_b is a methylene carbon derived from the diene.
4. Each compound has a C=C double bond in the dihydro-oxazine ring. Here its length is compared with CH₂-CH₂ distances, where both CH₂ are derived from hexa-1, 3-diene.
5. ΣN is the sum of valency angles subtended at the oxazine nitrogen atom.

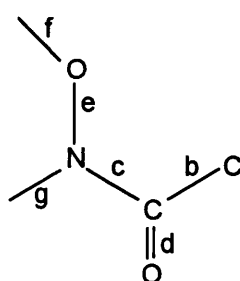
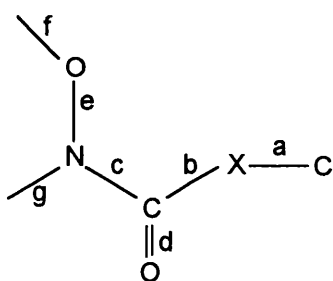
Table 3.1.2. Characteristics of the hydrogen bonds (Å) and angles (°) in **1** and **2**

Compound	D-H...A	D-H	D...A	H...A	D-H...A
1	N(2)-H(2)...O(1)	0.96	2.593(4)	2.20	103
1	N(2)-H(2)...O(2 ⁱ)	0.96	2.973(5)	2.15	143
2	N(21)-H(21)...O(11)	0.96	2.530(6)	2.09	106
2	N(22)-H(22)...O(12)	0.96	2.564(8)	2.01	105

Symmetry code: (i); -x, 2-y, 1-z

Table 3.1.3. Selected bond lengths in the ONC(O)R unit of **1** - **6** (Å)*

	1	2	3	4	5	6	
a	1.454(5)	1.461(10)	1.464(10)	1.462(6)	1.464(5)	1.452(6)	-
b	1.319(5)	1.332(10)	1.327(10)	1.316(7)	1.340(6)	1.340(6)	1.510(7)
c	1.410(5)	1.438(10)	1.417(10)	1.426(7)	1.385(6)	1.395(6)	1.342(6)
d	1.231(5)	1.227(10)	1.251(9)	1.202(7)	1.203(5)	1.192(6)	1.223(6)
e	1.455(5)	1.410(8)	1.426(8)	1.430(6)	1.428(5)	1.435(5)	1.437(5)
f	1.482(6)	1.461(9)	1.464(11)	1.486(7)	1.471(6)	1.471(6)	1.457(6)
g	1.507(6)	1.532(10)	1.500(10)	1.534(8)	1.474(6)	1.486(6)	1.469(6)

* In this table the bonds referred to by the letters **a**, **b**, **c**, **d**, **e**, **f** & **g** are defined as follows.

Captions to Figures.

Figure 3.1.1. A view of a molecule of the compound 1. 50% probability ellipsoids are displayed except for hydrogen atoms which are represented by spheres of arbitrary radius. In cyclohexane and phenyl rings the carbon atoms are in the sequence Ca(n), Ca(n+1)...Ca(n+5) and Cb(n), Cb(n+1)...Cb(n+5) respectively; only the Ca(n), Ca(n+1) and Cb(n), Cb(n+1) are labelled.

Figure 3.1.2. A view of two independent molecules of the compound 2. 50% probability ellipsoids are displayed except for hydrogen atoms which are represented by spheres of arbitrary radius. In cyclohexane and phenyl rings the carbon atoms are in the sequence Ca(n), Ca(n+1)...Ca(n+5) and Cb(n), Cb(n+1)...Cb(n+5) respectively; only the Ca(n), Ca(n+1) and Cb(n), Cb(n+1) are labelled

Figure 3.1.3. A view of a molecule of the compound 3. 50% probability ellipsoids are displayed except for hydrogen atoms which are represented by spheres of arbitrary radius. In cyclohexane and phenyl rings the carbon atoms are in the sequence Ca(n), Ca(n+1)...Ca(n+5) and Cb(n), Cb(n+1)...Cb(n+5) respectively; only the Ca(n), Ca(n+1) and Cb(n), Cb(n+1) are labelled.

Figure 3.1.4. A view of a molecule of the compound 4. 50% probability ellipsoids are displayed except for hydrogen atoms which are represented by spheres of arbitrary radius. In cyclohexane and phenyl rings the carbon atoms are in the sequence Ca(n), Ca(n+1)...Ca(n+5) and Cb(n), Cb(n+1)...Cb(n+5) respectively; only the Ca(n), Ca(n+1) and Cb(n), Cb(n+1) are labelled.

Figure 3.1.5. A view of a molecule of the compound 5. 50% probability ellipsoids are displayed except for hydrogen atoms which are represented by spheres of arbitrary radius. In cyclohexane and phenyl rings the carbon atoms are in the sequence Ca(n), Ca(n+1)...Ca(n+5) and Cb(n), Cb(n+1)...Cb(n+5) respectively; only the Ca(n), Ca(n+1) and Cb(n), Cb(n+1) are labelled.

Figure 3.1.6. A view of a molecule of the compound **6**. 50% probability ellipsoids are displayed except for hydrogen atoms which are represented by spheres of arbitrary radius. In cyclohexane and phenyl rings the carbon atoms are in the sequence Ca(n), Ca(n+1)...Ca(n+5) and Cb(n), Cb(n+1)...Cb(n+5) respectively; only the Ca(n), Ca(n+1) and Cb(n), Cb(n+1) are labelled.

Figure 3.1.7. A view down b of the packing and hydrogen bonding for compound **1**.

Figure 3.1.8. A view down b of the packing and hydrogen bonding for compound **2**.

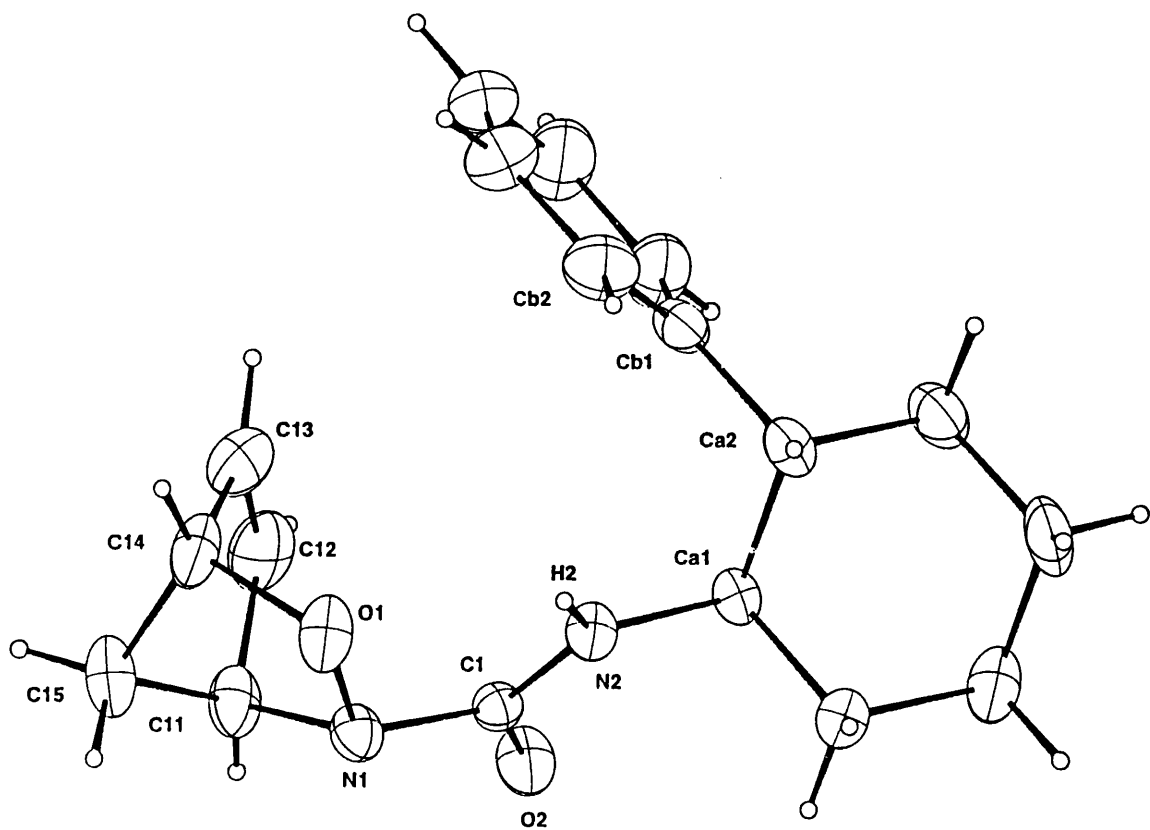


Figure 3.1.1

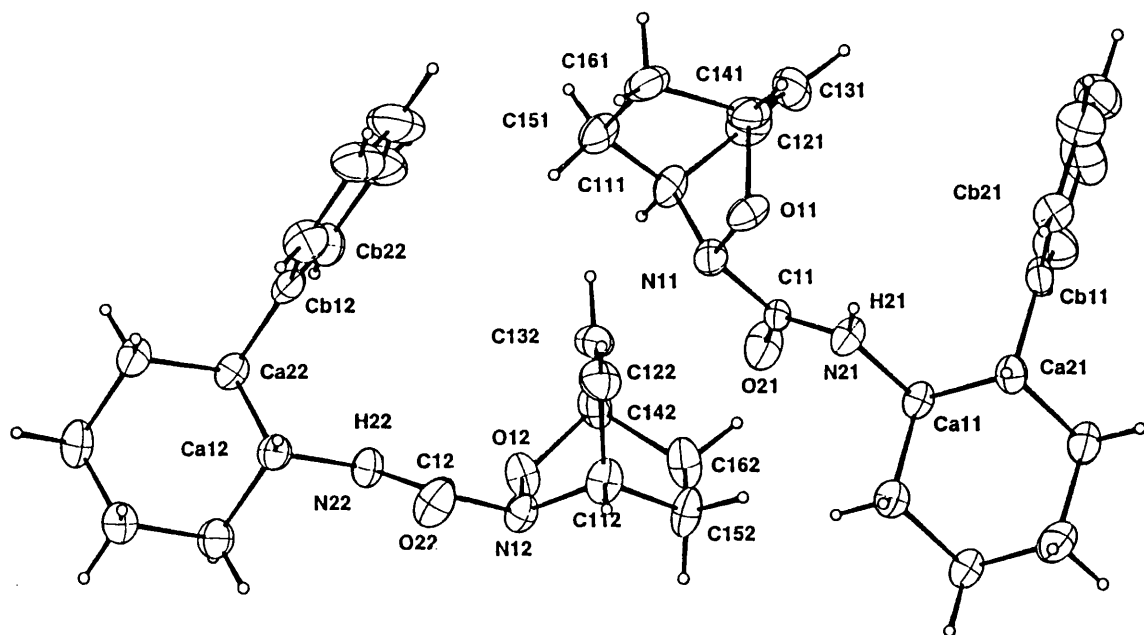


Figure 3.1.2

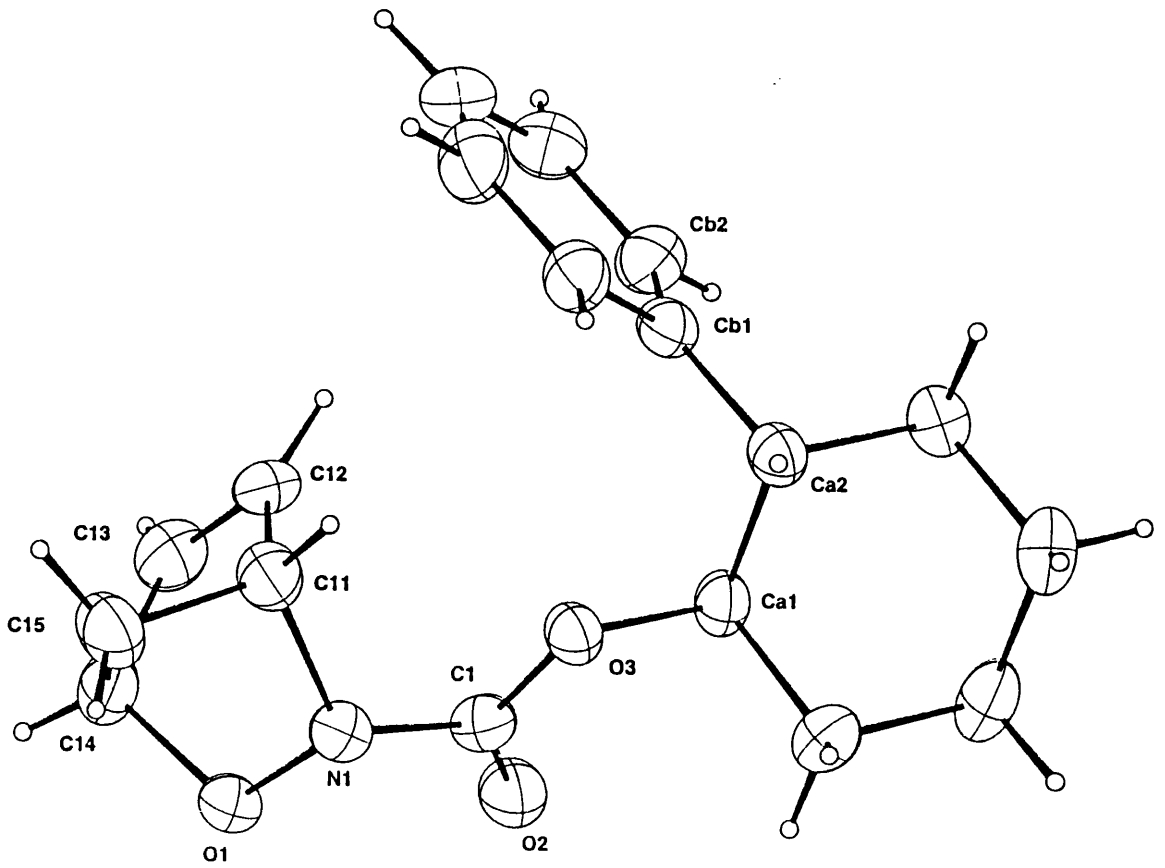


Figure 3.1.3

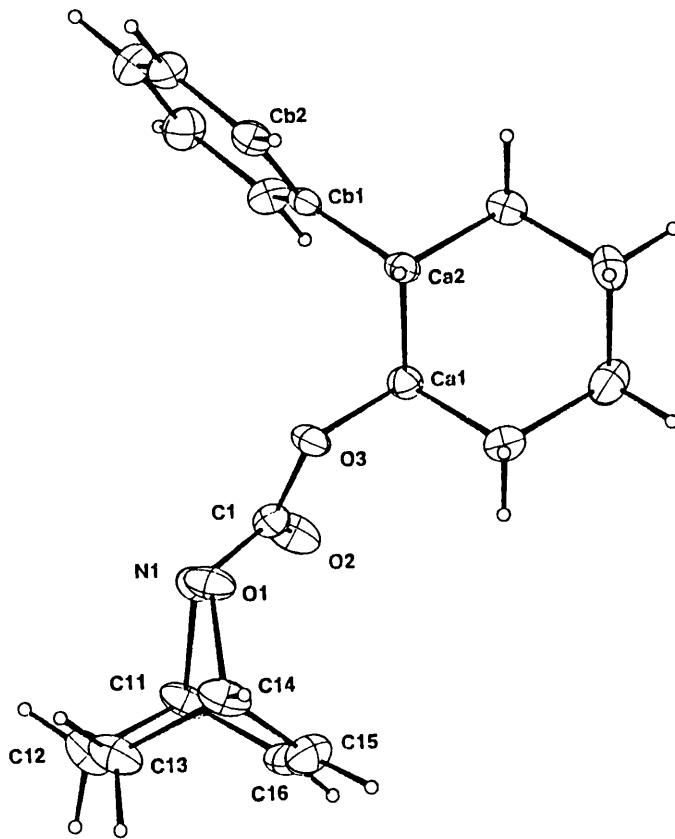


Figure 3.1.4

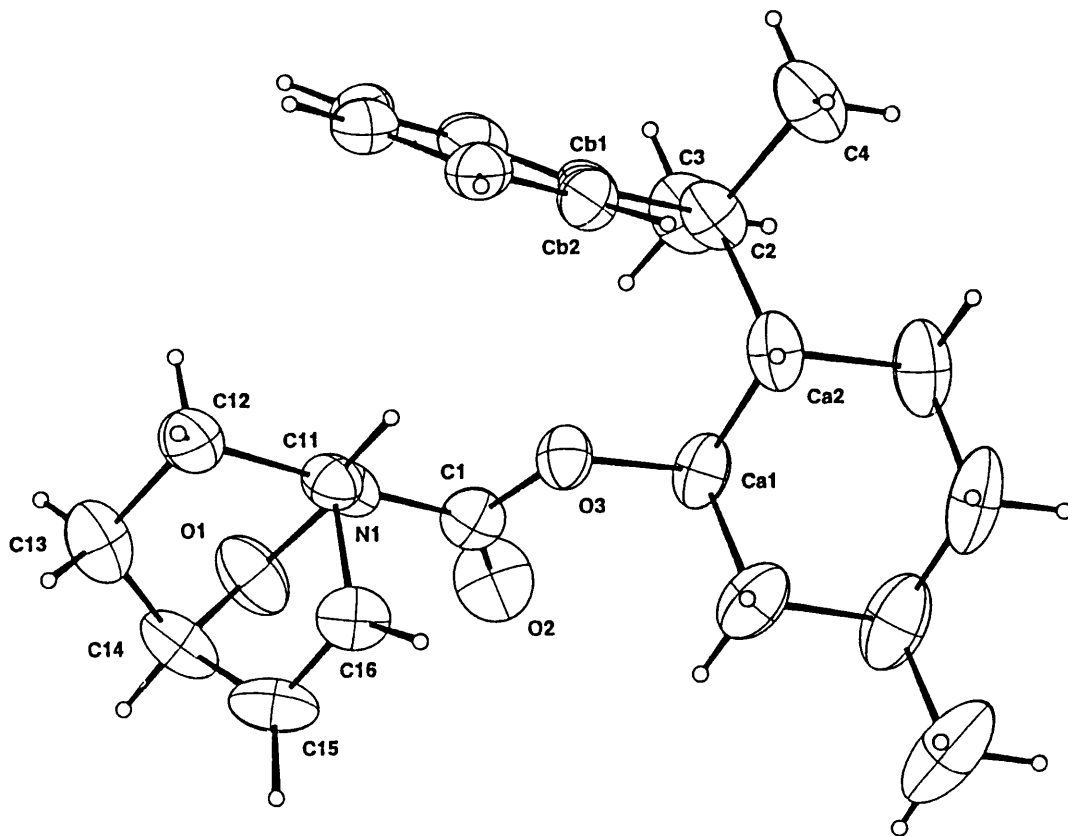


Figure 3.1.5

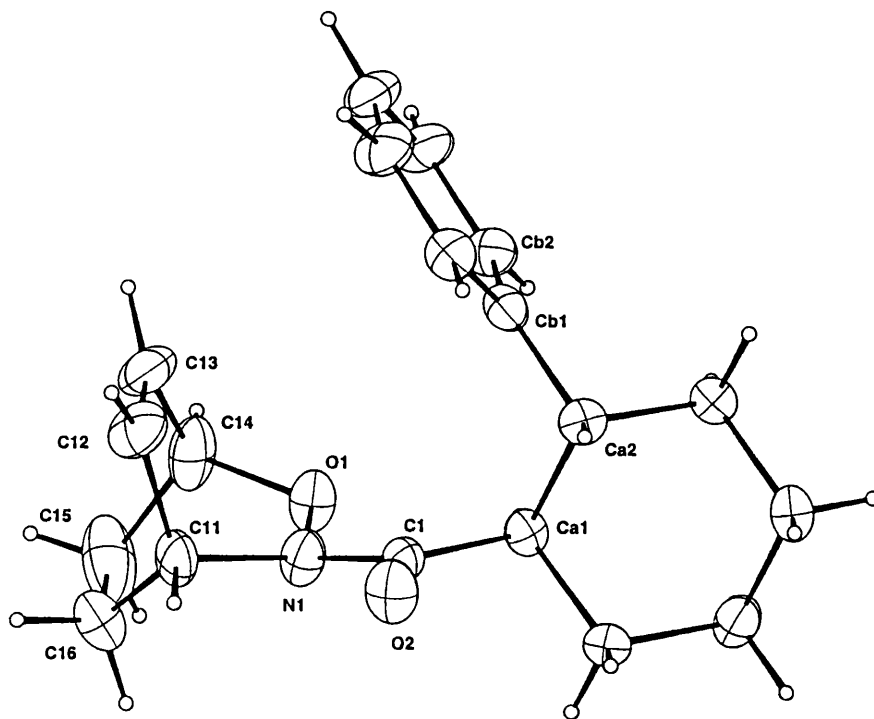


Figure 3.1.6

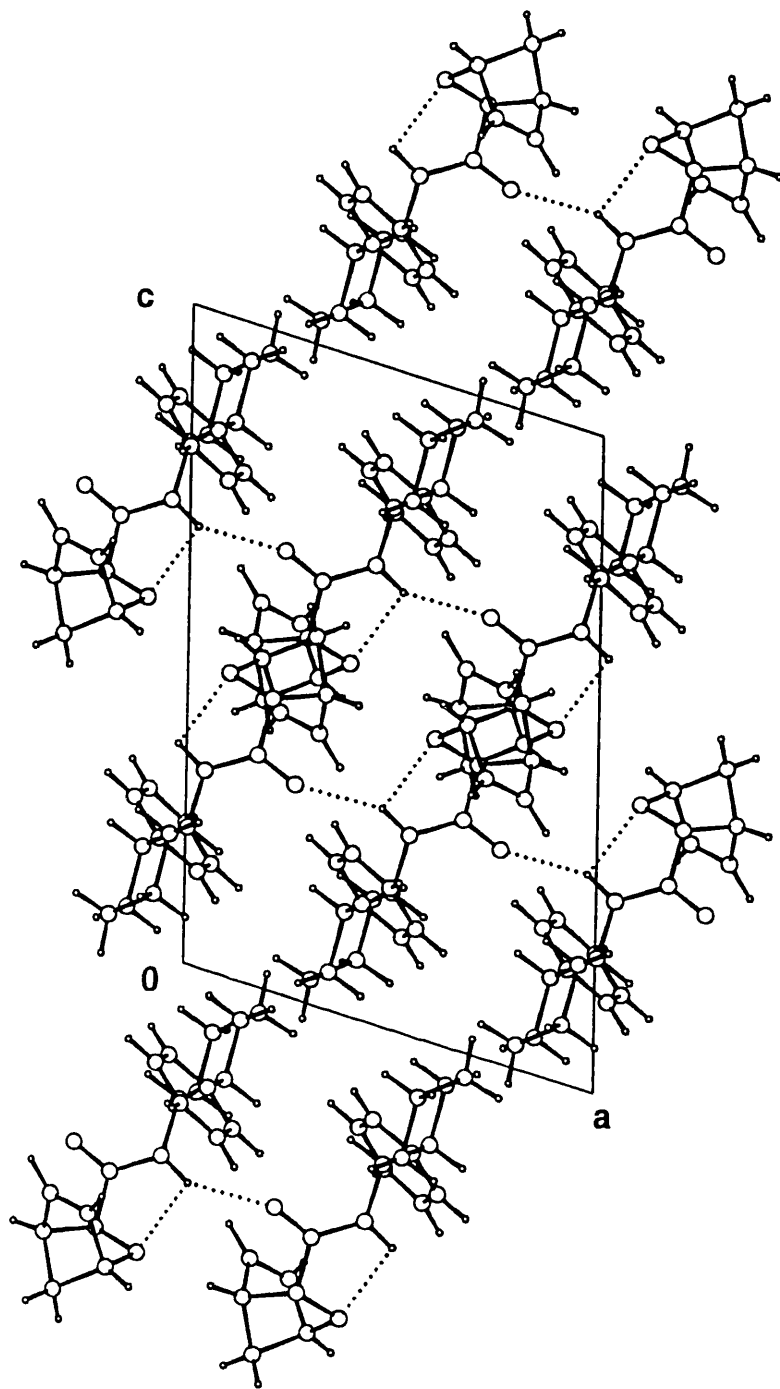


Figure 3.1.7

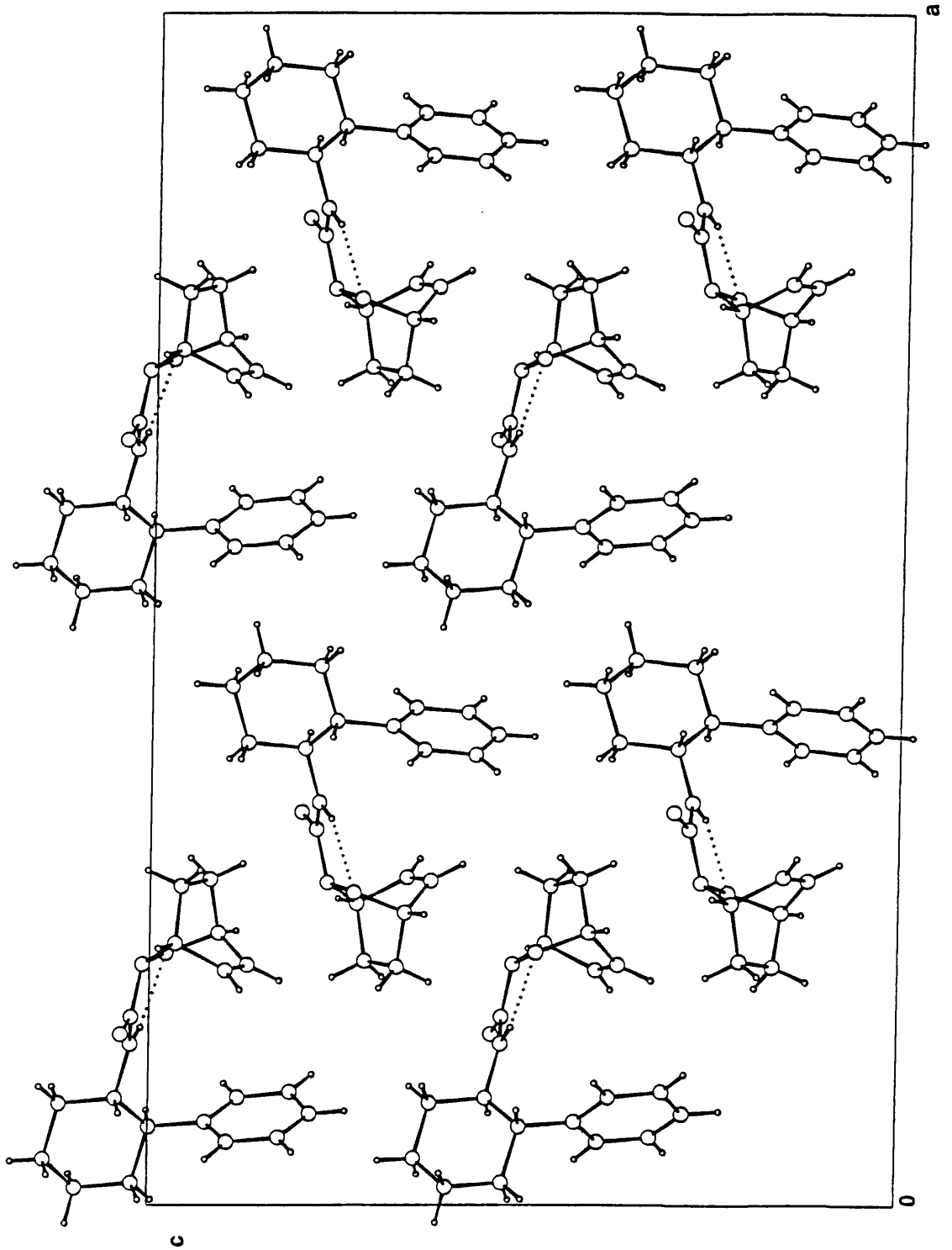


Figure 2.1.8

142a

Table 3.1.4. Crystallographic details of the structure analyses of compounds 1 and 2

Formula	$C_{18}H_{22}N_2O_2$	$C_{19}H_{24}N_2O_2$
Formula wt	298.39	312.41
Crystal system	monoclinic	monoclinic
Space group	$P2_1/a$	Cc
a Å	10.157(2)	31.1495(18)
b Å	10.543(2)	5.5988(5)
c Å	15.617(2)	19.3637(15)
β °	107.085(14)	90.94(6)
V Å ³	1598.6(5)	3376.6(5)
Z	4	8
F(0 0 0)	640	1344
D calc g cm ⁻³	1.240	1.229
T K	295	295
Crystal colour and habit	colourless, needle	colourless, needle
Crystal size mm	0.38 x 0.20 x 0.15	0.54 x 0.29 x 0.15
Cell: reflections used θ range(°)	25 reflections 11.3< θ <20.9	15 reflections 5.4< θ <13.2
μ (Mo-K α) cm ⁻¹	0.76	0.75
Measured reflections	3821	5911
Unique reflections	3612	5909
Observed reflections $I \geq 3\sigma(I)$	1619	3251
θ range °	2.7 - 27.4	2.5 - 25.0
Miller indices h	-13 \rightarrow 0	0 \rightarrow 6
k	-13 \rightarrow 0	-18 \rightarrow 18
l	-19 \rightarrow 20	-22 \rightarrow 22
Decay in mean standard (%)	1.7	1.9
R _{int}	0.024	-
No. of parameters	200	414
R(F)	0.061	0.056
R _w (F)	0.078	0.071
S	2.9	2.4
$\Delta\rho_{max}$ and $\Delta\rho_{min}$ eÅ ⁻³	0.30 \rightarrow -0.28	0.25 \rightarrow -0.20
Δ/σ_{max}	0.024	0.023
Extinction coefficient	256(113)	588(97)

Table 3.1.5. Crystallographic details of the structure analyses of compounds **3** and **4**

Formula	$C_{18}H_{21}O_3N$	$C_{19}H_{23}O_3N$
Formula wt	299.37	313.40
Crystal system	monoclinic	monoclinic
Space group	$P2_1/c$	$P2_1/c$
a Å	10.708(2)	15.640(6)
b Å	9.591(1)	9.819(4)
c Å	15.470(2)	11.324(8)
β °	95.129(14)	109.81(6)
V Å ³	1582.4(4)	1634.0(5)
Z	4	4
F(0 0 0)	640	672
D calc g cm ⁻³	1.257	1.272
T K	295	293
Crystal colour and habit	colourless block	colourless block
Crystal size mm	0.53 x 0.53 x 0.30	0.42 x 0.18 x 0.10
Cell: reflections used θ range(°)	25 reflections 11.5< θ <18.2	25 reflections 12.4< θ <20.6
μ (Mo-K α) cm ⁻¹	0.80	0.80
Measured reflections	2655	4659
Unique reflections	2549	2280
Observed reflections $I \geq 3\sigma(I)$	1161	1108
θ range °	3.0 - 24.5	2.7 - 27.4
Miller indices h	-12 → 12	-10 → 10
k	0 → 11	0 → 12
l	0 → 17	-16 → 17
Decay in mean standard (%)	50	1
R _{int}	0.055	0.038
No. of parameters	199	208
R(F)	0.066	0.045
R _w (F)	0.073	0.043
S	2.9	1.7
$\Delta\rho_{max}$ and $\Delta\rho_{min}$ eÅ ⁻³	0.30 → -0.29	0.19 → -0.24
Δ/σ_{max}	0.12	0.051

Table 3.1.6. Crystallographic details of the structure analyses of compounds 5 and 6

Formula	$C_{23}H_{32}O_3N$	$C_{19}H_{23}O_2N$
Formula wt	370.5	297.4
Crystal system	monoclinic	orthorhombic
Space group	$P2_1$	$Pna2_1$
a Å	6.0973(1)	21.1332(1)
b Å	20.1094(5)	12.7566(2)
c Å	9.1098(2)	5.9446(3)
β °	105.5(14)	-
V Å ³	1065.7(4)	1602.6(5)
Z	2	4
F(0 0 0)	402	640
D calc g cm ⁻³	1.154	1.232
T K	294	295
Crystal colour and habit	colourless plate	colourless plate
Crystal size mm	0.32 x 0.25 x 0.20	0.51 x 0.22 x 0.18
Cell: reflections used θ range(°)	25 reflections 8.3< θ <18.1	25 reflections 9.7< θ <19.1
μ (Mo-K α) cm ⁻¹	0.70	0.74
Measured reflections	3993	1544
Unique reflections	1934	1544
Observed reflections $I \geq 3\sigma(I)$	1047	894
θ range °	2.4 - 25.0	2.5 - 25.0
Miller indices h	0 \rightarrow 7	0 \rightarrow 7
k	0 \rightarrow 23	0 \rightarrow 15
l	-10 \rightarrow 10	0 \rightarrow 25
Decay in mean standard (%)	2	1.4
R_{int}	0.030	-
No. of parameters	243	198
R(F)	0.037	0.038
R_w (F)	0.034	0.042
S	1.8	1.6
$\Delta\rho_{max}$ and $\Delta\rho_{min}$. eÅ ⁻³	0.10 \rightarrow -0.13	0.15 \rightarrow -0.16
Δ/σ_{max}	0.033	0.091

Table 3.1.7. Atomic fractional coordinates and equivalent isotropic displacement parameters (\AA^2) for compounds 1 - 6

(a) compound 1

Atom	x	y	z	U
O(1)	0.1041(3)	0.8712(3)	0.4637(2)	0.053
O(2)	0.2658(3)	0.7109(3)	0.3268(2)	0.054
N(1)	0.2083(3)	0.7895(3)	0.4457(2)	0.042
N(2)	0.0461(3)	0.7739(3)	0.3044(2)	0.040
C(1)	0.1747(4)	0.7578(4)	0.3541(2)	0.035
C(11)	0.3390(4)	0.8656(5)	0.4783(3)	0.053
C(12)	0.3232(6)	0.9733(5)	0.4162(3)	0.072
C(13)	0.2274(7)	1.0448(5)	0.4285(4)	0.076
C(14)	0.1813(5)	0.9878(5)	0.5008(3)	0.058
C(15)	0.3131(5)	0.9285(5)	0.5601(3)	0.064
C(A1)	0.0048(4)	0.7469(4)	0.2089(2)	0.042
C(A2)	-0.1071(4)	0.8388(4)	0.1569(2)	0.044
C(A3)	-0.1444(5)	0.8073(5)	0.0577(3)	0.062
C(A4)	-0.1887(6)	0.6704(5)	0.0375(3)	0.074
C(A5)	-0.0773(7)	0.5802(5)	0.0900(3)	0.078
C(A6)	-0.0401(5)	0.6106(4)	0.1900(3)	0.059
C(B1)	-0.0667(4)	0.9762(4)	0.1774(3)	0.046
C(B2)	-0.1289(5)	1.0472(5)	0.2289(3)	0.069
C(B3)	-0.0926(7)	1.1729(6)	0.2485(4)	0.085
C(B4)	0.0012(8)	1.2297(5)	0.2151(4)	0.089
C(B5)	0.0648(7)	1.1604(6)	0.1646(4)	0.093
C(B6)	0.0313(6)	1.0347(5)	0.1463(3)	0.072

(b) compound 2

Atom	x	y	z	U
O(11)	0.2616	0.2023(8)	0.2258*	0.048
N(11)	0.2697(2)	-0.0118(11)	0.2621(3)	0.044
O(21)	0.3290(2)	-0.2325(10)	0.2978(3)	0.062
N(21)	0.3372(2)	0.1618(10)	0.2740(3)	0.046
C(11)	0.3147(2)	-0.0401(14)	0.2776(4)	0.039
C(111)	0.2521(2)	-0.2263(12)	0.2214(5)	0.046
C(121)	0.2742(3)	-0.2200(16)	0.1539(5)	0.065
C(131)	0.2715(3)	-0.0132(17)	0.1216(5)	0.068
C(141)	0.2444(3)	0.1529(15)	0.1566(4)	0.059
C(151)	0.2041(3)	-0.1741(13)	0.2103(4)	0.055
C(161)	0.1993(3)	0.0503(15)	0.1671(5)	0.063

C(A11)	0.3826(2)	0.1735(13)	0.2941(4)	0.047
C(A21)	0.4057(2)	0.3613(12)	0.2510(4)	0.042
C(A31)	0.4524(3)	0.3792(16)	0.2736(4)	0.061
C(A41)	0.4572(3)	0.4272(18)	0.3507(5)	0.078
C(A51)	0.4350(3)	0.2438(17)	0.3932(4)	0.073
C(A61)	0.3875(2)	0.2250(15)	0.3708(4)	0.059
C(B11)	0.4012(3)	0.3138(14)	0.1748(4)	0.047
C(B21)	0.3815(3)	0.4828(16)	0.1322(5)	0.061
C(B31)	0.3773(3)	0.4531(23)	0.0618(6)	0.092
C(B41)	0.3942(4)	0.2490(25)	0.0325(6)	0.101
C(B51)	0.4132(4)	0.0833(19)	0.0732(7)	0.087
C(B61)	0.4170(3)	0.1147(16)	0.1439(5)	0.069
O(12)	0.2110(2)	0.2375(7)	0.4780(4)	0.044
N(12)	0.2017(2)	0.4611(10)	0.5097(4)	0.044
O(22)	0.1429(2)	0.6890(9)	0.5380(3)	0.059
N(22)	0.1349(2)	0.2855(10)	0.5247(4)	0.042
C(12)	0.1575(2)	0.4866(13)	0.5242(4)	0.038
C(112)	0.2187(3)	0.6599(12)	0.4660(5)	0.047
C(122)	0.1963(3)	0.6475(15)	0.3990(5)	0.056
C(132)	0.2008(3)	0.4411(18)	0.3691(4)	0.065
C(142)	0.2276(3)	0.2722(14)	0.4084(5)	0.053
C(152)	0.2667(2)	0.6104(13)	0.4586(5)	0.054
C(162)	0.2726(3)	0.3783(15)	0.4199(5)	0.061
C(A12)	0.0898(2)	0.2792(13)	0.5446(4)	0.043
C(A22)	0.0660(2)	0.1013(12)	0.4992(4)	0.040
C(A32)	0.0188(3)	0.0857(14)	0.5217(4)	0.057
C(A42)	0.0149(3)	0.0295(15)	0.5975(5)	0.069
C(A52)	0.0389(3)	0.1974(17)	0.6414(4)	0.066
C(A62)	0.0855(2)	0.2167(15)	0.6206(4)	0.058
C(B12)	0.0696(2)	0.1605(13)	0.4242(4)	0.043
C(B22)	0.0900(3)	-0.0027(13)	0.3800(5)	0.053
C(B32)	0.0947(3)	0.0432(20)	0.3100(5)	0.086
C(B42)	0.0766(4)	0.2589(21)	0.2826(5)	0.091
C(B52)	0.0566(3)	0.4102(15)	0.3250(6)	0.071
C(B62)	0.0527(3)	0.3668(15)	0.3943(5)	0.061

*Fixed to defined origin

(c) compound 3

Atom	x	y	z	U
O(1)	0.6475(4)	0.1601(4)	0.7630(2)	0.062
O(2)	0.8169(4)	0.1950(4)	0.8951(3)	0.070
O(3)	0.7017(3)	0.0634(4)	0.9795(2)	0.050
N(1)	0.6184(4)	0.1138(5)	0.8467(3)	0.052
C(1)	0.7255(5)	0.1279(5)	0.9078(4)	0.050
C(11)	0.5716(5)	-0.0360(6)	0.8307(4)	0.061
C(12)	0.6825(6)	-0.1169(6)	0.8092(4)	0.063
C(13)	0.7127(6)	-0.0712(7)	0.7346(4)	0.073

C(14)	0.6176(6)	0.0379(6)	0.7057(4)	0.067
C(15)	0.5011(7)	-0.0127(7)	0.7433(5)	0.077
C(A1)	0.8043(5)	0.0595(6)	1.0485(3)	0.049
C(A2)	0.7792(5)	-0.0661(6)	1.1048(3)	0.051
C(A3)	0.8805(6)	-0.0712(7)	1.1819(4)	0.065
C(A4)	0.8867(6)	0.0640(8)	1.2333(4)	0.074
C(A5)	0.9073(7)	0.1878(7)	1.1763(4)	0.079
C(A6)	0.8065(6)	0.1964(6)	1.0992(4)	0.070
C(B1)	0.7675(5)	-0.1992(6)	1.0529(3)	0.053
C(B2)	0.8717(5)	-0.2643(7)	1.0226(4)	0.069
C(B3)	0.8577(8)	-0.3844(8)	0.9739(5)	0.088
C(B4)	0.7436(10)	-0.4421(7)	0.9528(5)	0.096
C(B5)	0.6418(8)	-0.3807(9)	0.9819(5)	0.090
C(B6)	0.6532(6)	-0.2601(7)	1.0313(4)	0.068

(d) compound 4

Atom	x	y	z	U
O(1)	0.05406(19)	0.22346(33)	0.79740(26)	0.042
O(2)	0.2356(2)	0.1212(3)	0.7097(3)	0.052
O(3)	0.21591(19)	0.14715(30)	0.89671(29)	0.035
N(1)	0.0937(3)	0.1527(4)	0.7186(3)	0.033
C(1)	0.1874(3)	0.1420(5)	0.7710(5)	0.034
C(11)	0.0600(3)	0.2092(5)	0.5885(4)	0.040
C(12)	-0.0432(3)	0.1977(5)	0.5428(5)	0.052
C(13)	-0.0794(3)	0.2846(6)	0.6274(5)	0.055
C(14)	0.0019(3)	0.3414(5)	0.7302(4)	0.044
C(15)	0.0576(4)	0.4228(5)	0.6740(5)	0.053
C(16)	0.0878(3)	0.3546(6)	0.5974(5)	0.046
C(A1)	0.3142(3)	0.1614(5)	0.9588(4)	0.032
C(A2)	0.3373(3)	0.0964(4)	1.0877(4)	0.031
C(A3)	0.4380(3)	0.1237(5)	1.1628(4)	0.045
C(A4)	0.4613(3)	0.2739(5)	1.1709(5)	0.058
C(A5)	0.4361(4)	0.3356(5)	1.0407(6)	0.059
C(A6)	0.3361(3)	0.3109(5)	0.9659(5)	0.046
C(B1)	0.3181(3)	-0.0544(5)	1.0856(4)	0.028
C(B2)	0.2786(3)	-0.1094(5)	1.1677(4)	0.035
C(B3)	0.2670(3)	-0.2479(5)	1.1744(5)	0.044
C(B4)	0.2936(3)	-0.3352(5)	1.0990(5)	0.047
C(B5)	0.3314(3)	-0.2826(5)	1.0162(5)	0.046
C(B6)	0.3438(3)	-0.1439(5)	1.0093(4)	0.039

(e) compound 5

Atom	x	y	z	U
O(1)	0.5716(5)	0.6057	0.3125(4)	0.087
O(2)	0.4743(6)	0.4802(2)	0.2530(4)	0.091
O(3)	0.1018(5)	0.5053(2)	0.1595(3)	0.061
N(1)	0.3498(6)	0.5883(3)	0.2183(4)	0.062
C(1)	0.3227(10)	0.5195(3)	0.2185(5)	0.064
C(2)	-0.1673(8)	0.4648(3)	-0.1419(5)	0.071
C(3)	0.0484(8)	0.4412(3)	-0.1866(6)	0.092
C(4)	-0.3733(9)	0.4441(3)	-0.2749(6)	0.098
C(5)	-0.0842(15)	0.3126(4)	0.4380(10)	0.165
C(11)	0.1728(8)	0.6298(3)	0.2589(5)	0.060
C(12)	0.2387(10)	0.7017(3)	0.2418(5)	0.084
C(13)	0.4684(11)	0.7168(3)	0.3518(7)	0.100
C(14)	0.5520(9)	0.6532(3)	0.4322(6)	0.085
C(15)	0.3900(12)	0.6262(3)	0.5127(5)	0.094
C(16)	0.1856(8)	0.6154(3)	0.4224(5)	0.073
C(A1)	0.0381(8)	0.4356(3)	0.1420(6)	0.068
C(A2)	-0.1773(8)	0.4304(3)	0.0124(6)	0.071
C(A3)	-0.2475(9)	0.3565(3)	-0.0023(8)	0.106
C(A4)	-0.2655(13)	0.3291(3)	0.1530(10)	0.118
C(A5)	-0.0537(12)	0.3382(3)	0.2860(9)	0.109
C(A6)	0.0148(8)	0.4097(3)	0.2948(6)	0.084
C(B1)	-0.1754(8)	0.5403(3)	-0.1295(5)	0.060
C(B2)	-0.3422(8)	0.5708(3)	-0.0748(5)	0.065
C(B3)	-0.3630(9)	0.6386(3)	-0.0665(5)	0.071
C(B4)	-0.2165(11)	0.6795(3)	-0.1176(6)	0.079
C(B5)	-0.0486(10)	0.6506(4)	-0.1735(6)	0.084
C(B6)	-0.0312(8)	0.5825(3)	-0.1804(5)	0.070

(f) compound 6

Atom	x	y	z	U
O(1)	0.09481(15)	0.0445(3)	0.3204**	0.052
O(2)	0.0899(2)	0.2219(3)	-0.1269(7)	0.060
N(1)	0.0854(2)	0.0844(3)	0.0968(8)	0.051
C(1)	0.0890(2)	0.1884(3)	0.0659(9)	0.038
C(11)	0.0999(3)	0.0064(4)	-0.0774(10)	0.056
C(12)	0.1674(3)	-0.0221(5)	-0.0521(11)	0.066
C(13)	0.1791(3)	-0.0598(5)	0.1633(12)	0.077
C(14)	0.1210(3)	-0.0608(4)	0.3009(11)	0.069
C(15)	0.0717(4)	-0.1266(5)	0.1876(18)	0.108
C(16)	0.0603(3)	-0.0875(5)	-0.0336(17)	0.087
C(A1)	0.0861(2)	0.2606(3)	0.2670(9)	0.037
C(A2)	0.1469(2)	0.3263(3)	0.2763(9)	0.040
C(A3)	0.1424(2)	0.4089(3)	0.4612(10)	0.049
C(A4)	0.0841(2)	0.4775(3)	0.4347(10)	0.057

C(A5)	0.0248(2)	0.4126(3)	0.4297(11)	0.054
C(A6)	0.0280(2)	0.3312(3)	0.2422(10)	0.045
C(B1)	0.2060(2)	0.2597(3)	0.3022(9)	0.043
C(B2)	0.2175(2)	0.2032(4)	0.4960(10)	0.050
C(B3)	0.2718(2)	0.1449(4)	0.5181(11)	0.060
C(B4)	0.3165(2)	0.1434(4)	0.3534(12)	0.061
C(B5)	0.3059(2)	0.1975(4)	0.1571(11)	0.063
C(B6)	0.2511(2)	0.2553(4)	0.1325(9)	0.050

****Fixed to define origin**

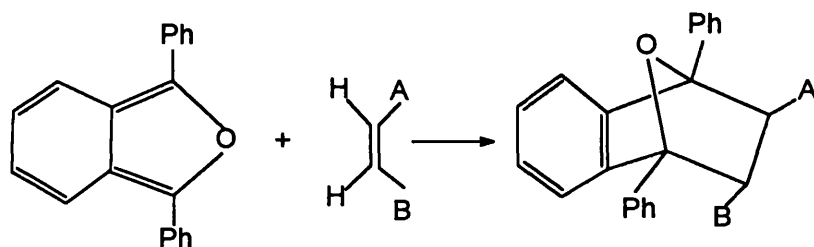
Chapter 3.2. Normal and Catalysed Diels-Alder Reaction of Ferrocenylethylenes

3.2.1 Introduction

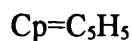
The Diels-Alder addition of ferrocenyl-substituted alkenes to 1, 3-diphenylisobenzofuran (Reaction 3.2.1) has recently been studied by Dr. Knox and Professor Toma and their co-workers at Strathclyde University and Comenius University (Bratislava, Slovakia). Chromatography and recrystallisation of the products of several of these reactions in each case gave one pure isomer of the adduct. The stereochemistry of the adducts is difficult to establish by spectroscopic methods and the problem is further complicated in that the starting alkenes are either a mixture of (E) and (Z) isomers or are of undetermined stereochemistry. Accordingly, the crystal structures of a representative group of adducts, compounds **10**, **11**, **12** and **13**, have been determined in order to define the stereochemistry of the addition reaction.

In general, Diels-Alder addition does not require the presence of catalyst. However, when $A=C(O)CH_3$ (compound **10**) or $C(O)Ph$ (compound **11**) the addition only occurs in the presence of $AlCl_3$ (i.e. the so called catalysed Diels-Alder reaction, see Kagan & Riant, 1992). Under these circumstances it was considered possible that the course of the reaction might not be that shown in reaction 3.2.1. Since the formation of stable ferrocenyl cations (see Cotton & Wilkinson, 1986, page 1176) is known to occur in the presence of aluminium trichloride, the possibility that adducts **10** and **11** were not the final products could not be ruled out and ring opening or rearrangement to give products with seven- or eight-membered rings was considered possible. These considerations also prompted the decision to determine the structures of **10** and **11** by diffraction methods.

Reaction 3.2.1



A	B
10 C(O)CH ₃ ,	C ₅ H ₄ Fe(C ₅ H ₅)
11 C(O)Ph,	C ₅ H ₄ Fe(C ₅ H ₅)
12 C(O)C ₅ H ₄ FeCp,	H
13 NO ₂ ,	C ₅ H ₄ Fe(C ₅ H ₅)

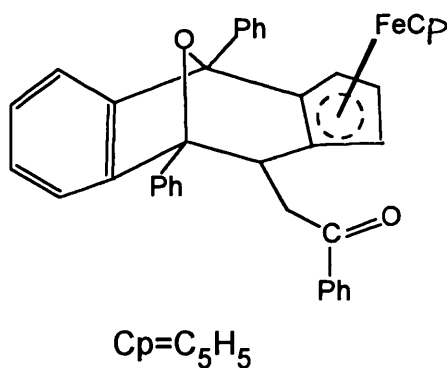


3.2.2 Results and discussion

Compounds **10**, **12** and **13** are the result of normal Diels-Alder addition of an alkene to 1, 3-diphenylisobenzofuran (Figures 3.2.1, 3.2.3 and 3.2.4). They have similar structures in which the substituted furan ring and the alkene have fused to form an oxygen-bridged six-membered ring. With respect to the bridging oxygen atom substituent A (Reaction 3.2.1) is found to be *exo* in **10**, **12** and **13** and B to be *endo* (in **10** and **13** only). It would thus appear that a substituent with oxygen β to the bridged six-membered ring prefers to be *exo* and the bulky ferrocenyl group may be found both in *endo* (**10** and **13**) or *exo* (**12**) sites. The stereochemistry of compounds **10**, **12** and **13** is that expected from addition of E-CH₃C(O)CH=CHC₅H₄Fe(C₅H₅), CH₂=CH₂C(O)C₅H₄Fe(C₅H₅) and E-(NO₂)CH=CHC₅H₄Fe(C₅H₅) respectively to 1, 3-diphenylisobenzofuran.

Compound **11** has a different structure. The four carbon atoms of the diene are now incorporated into an oxygen-bridged seven-membered ring with two

cyclopentadienyl carbon atoms and C(13), originally an alkene sp^2 carbon atom. Inserting the ferrocenyl unit into the central bicyclic ring system produces five- and six-membered rings which both contain the bridging oxygen atom O(1) (Figure 3.2.2). The six-membered ring thus formed, O(1)-C(11)-C(E2)-C(E1)-C(13)-C(12), adopts an envelope conformation with O(1) at the flap and near zero endocyclic torsion angles across C(13)-C(E1) and C(E1)-C(E2) [$0.5(7)^\circ$ and $1.3(7)^\circ$, see Table 3.2.2]: the ring puckering parameters [$Q=0.614(7)$ Å, $\theta=53.7(7)^\circ$, $\varphi=358(1)^\circ$] are also quite typical for envelope conformations (Cremer & Pople, 1975, Boeyens, 1978). The Ph-C(O)-CH₂ group lies on the opposite side of the C(11), C(E2), C(E1) and C(13) plane from O(1), with torsion angle O(1)-C(12)-C(13)-C(1) equal to $-160.6(8)^\circ$ (Table 3.2.2). **11** crystallises in the orthorhombic space group $P2_12_12_1$ and the results suggest that the crystal studied was optically pure, being built of molecules in which the chiral carbon atoms C(11), C(12) and C(13) have absolute configurations R, S and R. It has not been established whether the bulk sample was optically pure or whether resolution only occurred on crystallisation.



Compounds **10**, **12** and **13** consist of a single diastereoisomer in racemic form with the A substituent in an exo position (Figure 3.2.1, 3.2.3 and 3.2.4). All figures and torsion angles refer to molecules in which the O(1)-C(12)-C(13)-C(1) or -N(1) torsion angle is positive. Chiral carbon atoms C(11), C(12) and C(13) have

absolute configurations S,R and R in **10**, **12** and **13**; C(14) has absolute configuration R in **10** and S in **13**. Crystals of **10** and **13** each contain two independent molecules which are structurally and conformationally nearly identical (see Figures 3.2.1 and 3.2.4 and Table 3.2.2).

The diphenylisobenzofuran units in all four compounds are closely comparable except for the orientations of the phenyl rings attached to the bridgehead carbon atoms; in **10** and **13** O(1) lies close to the plane of both phenyl rings [O(1)-C-C_{ar}-C_{ar} = 5.5(4), 12.6(4), 7.2(4) and 9.1(2)° in **10** and 6.7(10), -6.7(10)°, 11.1(8) and -5.4(9)° in **13**] whereas in **11** the oxygen atom is close to the plane of ring (C) and away from ring (D) and in **12** vice versa [see torsion angles O(1)-C(11)-C_{ar}-C_{ar} and O(1)-C(12)-C_{ar}-C_{ar} for **11** and **12** in Table 3.2.2 and Figures 3.2.2 and 3.2.3]. It seems ring (D) in **11** and ring (C) in **12** twist away from O(1) by about 90°. The tendency of bridgehead phenyl groups to approach co-planarity with the bridging oxygen atoms leads to intramolecular O...H contacts of 2.3 - 2.5 Å (Table 3.2.1.b) which are shorter than the sum of the van der Waals radii (2.72 Å, Bondi, 1964).

Bond lengths in the isobenzofuran units of **10** - **13** are compared in Table 3.2.1. In general corresponding bond lengths in the four structures agree with each other and with accepted values. Thus bond (a) (see Table 3.2.1.a) is somewhat shorter than the carbon-carbon (C-C=O) bond lengths for aldehydes and ketones [1.510 - 1.511 Å], (d) and (g) with means of 1.565 and 1.570 Å respectively are longer than the average C-C bond length in an unsaturated cyclohexane ring (1.509 Å) but are comparable with the typical C₃C-CHC₂ mean distance of 1.556 Å (International Tables, Vol. C, 1992). In **13** (e) and (f) are shorter than typical C_{sp3}-C_{sp2} bond lengths (1.535 Å). The bridging O-C bonds are slightly longer than O-C_{sp3} bonds in general (1.426 Å) and the C-O-C angles are about 100° (see Table 3.2.2).

Individual Fe-C bond lengths in ferrocenyl units are given in Table 3.2.3. They appear to be appreciably shorter than the accepted mean for such distances (2.080 Å) but they compare well with the value of 2.045 Å found in the ordered low temperature form of ferrocene itself (Seiler & Dunitz, 1978) and with a similar mean value (2.044 Å) recently obtained by Scott, Rief, Diebold & Brintzinger (1993) in a substituted ferrocene. In **13** the values are especially short, in some cases less than 2.000 Å.

The C(E1)-C(PE)-C(PF)-C(F1) torsion angles, where C(PE) and C(PF) are the centroids of cyclopentadienyl rings (E) and (F) are shown in Table 3.2.2. This angle is zero for eclipsed rings and 36° if they are staggered. In compounds **10**, **11** and **13** these angles [-9.2, -6.9° in **10**, -1.7° in **11** and -3.2, -12.8° in **13**] indicate an eclipsed ferrocene conformation in each compound and agree well with the value of 9° found in the ordered low temperature form of ferrocene itself (Seiler & Dunitz, 1979) and more recently in C₆₀(ferrocene)₂ (Crane, Hitchcock, Kroto, Taylor & Walton, 1992) In **12** where the torsion angle is 18° the conformation is intermediate between staggered and eclipsed. The cyclopentadienyl rings in each compound are very nearly parallel, with C(CE)-Fe-C(CF) angles close to 180° (see Table 3.2.2).

3.2.3 Experimental

The crystallographic data for compounds **10** - **13** are given in Table 3.2.4 and 3.2.5. The fractional co-ordinates and equivalent isotropic displacement parameters (Å²) are given in Table 3.2.6. The experimental and computational methods employed have already been described (see Section 1). Corrections for absorption were considered unnecessary for compounds **10**, **12** and **13**. For **11** an empirical correction based on Ψ -scans was applied using the MOLEN package

(Enraf-Nonius, 1992). The transmission factors were in the range 0.930 - 0.997. The structures were solved either by heavy atom (Patterson) or direct methods using SHELXS (Sheldrick, 1985). For compounds **10**, **12** and **13** the final full matrix least squares refinement on F was performed on a VAX 3000/60 with the GX package (Mallinson & Muir, 1985).

The structure of **11** was refined by full matrix least squares on F^2 and included an extinction coefficient of 0.0017(4); the calculations were performed on a PC 486-33 machine using SHELXL-93 (Sheldrick, 1993). Disordered ring F was modelled as two rigid pentagonal groups of carbon atoms with carbon atom site occupancies of a half and C-C bond lengths of 1.42 Å. Five pairs of carbon atoms were each constrained to have similar U_{ij} parameters and for one such pair a restraint to near isotropic behaviour was necessary. The absolute configuration was confirmed by refinement of the Flack parameter to $x=0.056(4)$ (Flack, 1983; Bernardinelli & Flack, 1985).

Anisotropic displacement parameters for non-hydrogen atoms, hydrogen atom co-ordinates, a geometry listing and observed and calculated structure factors are available.

Captions to Figures.

Figure 3.2.1. A view of one of the two independent molecules of the compound 10. 50% probability ellipsoids are displayed except for hydrogen atoms which are represented by spheres of arbitrary radius. In phenyl and cyclopentadienyl rings the carbon atoms are in the sequence C(n), C(n+1)...C(n+5) and C(n), C(n+1)...C(n+4) respectively; only C(n) and C(n+1) are labelled.

Figure 3.2.2. A view of a molecule of the compound 11. 50% probability ellipsoids are displayed except for hydrogen atoms which are represented by spheres of arbitrary radius. In phenyl and cyclopentadienyl rings the carbon atoms are in the sequence C(n), C(n+1)...C(n+5) and C(n), C(n+1)...C(n+4) respectively; only C(n) and C(n+1) are labelled.

Figure 3.2.3. A view of a molecule of the compound 12. 50% probability ellipsoids are displayed except for hydrogen atoms which are represented by spheres of arbitrary radius. In phenyl and pentadienyl rings the carbon atoms are in the sequence C(n), C(n+1)...C(n+5) and C(n), C(n+1)...C(n+4) respectively; only C(n) and C(n+1) are labelled

Figure 3.2.4. A view of one of the two independent molecules of the compound 13. 50% probability ellipsoids are displayed except for hydrogen atoms which are represented by spheres of arbitrary radius. In phenyl and cyclopentadienyl rings the carbon atoms are in the sequence C(n), C(n+1)...C(n+5) and C(n), C(n+1)...C(n+4) respectively; only C(n) and C(n+1) are labelled.

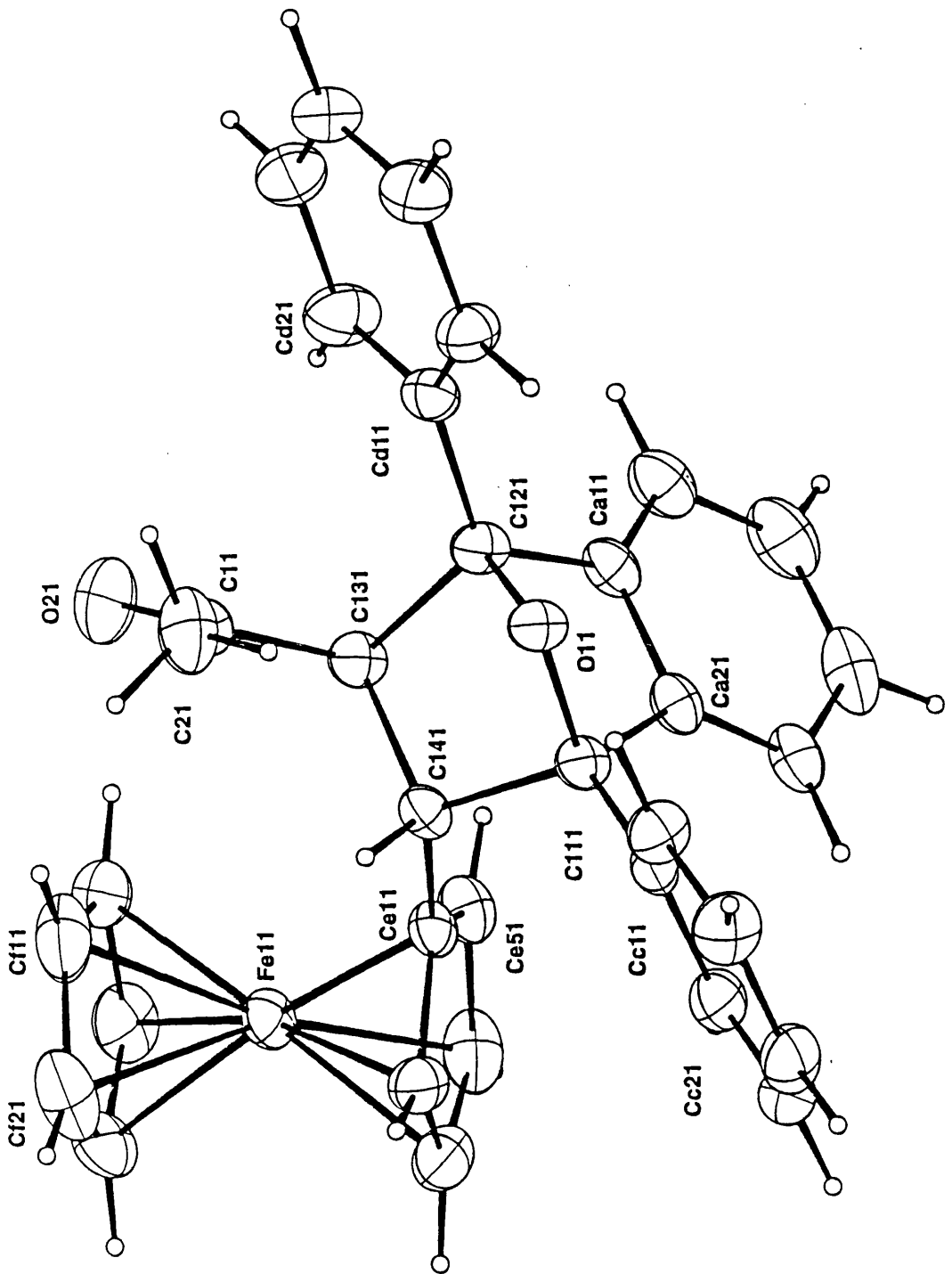


Figure 3.2.1

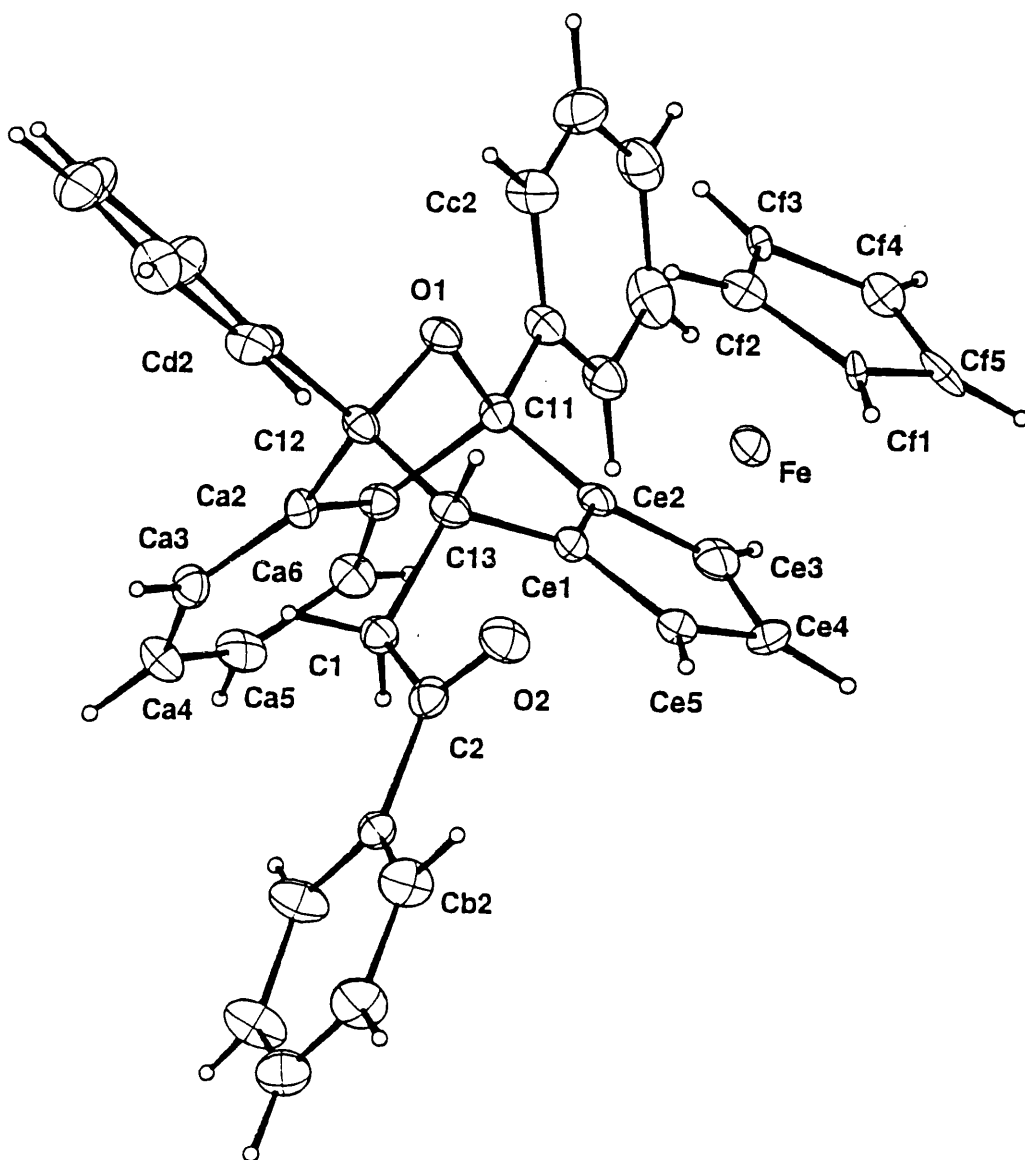


Figure 3.2.2

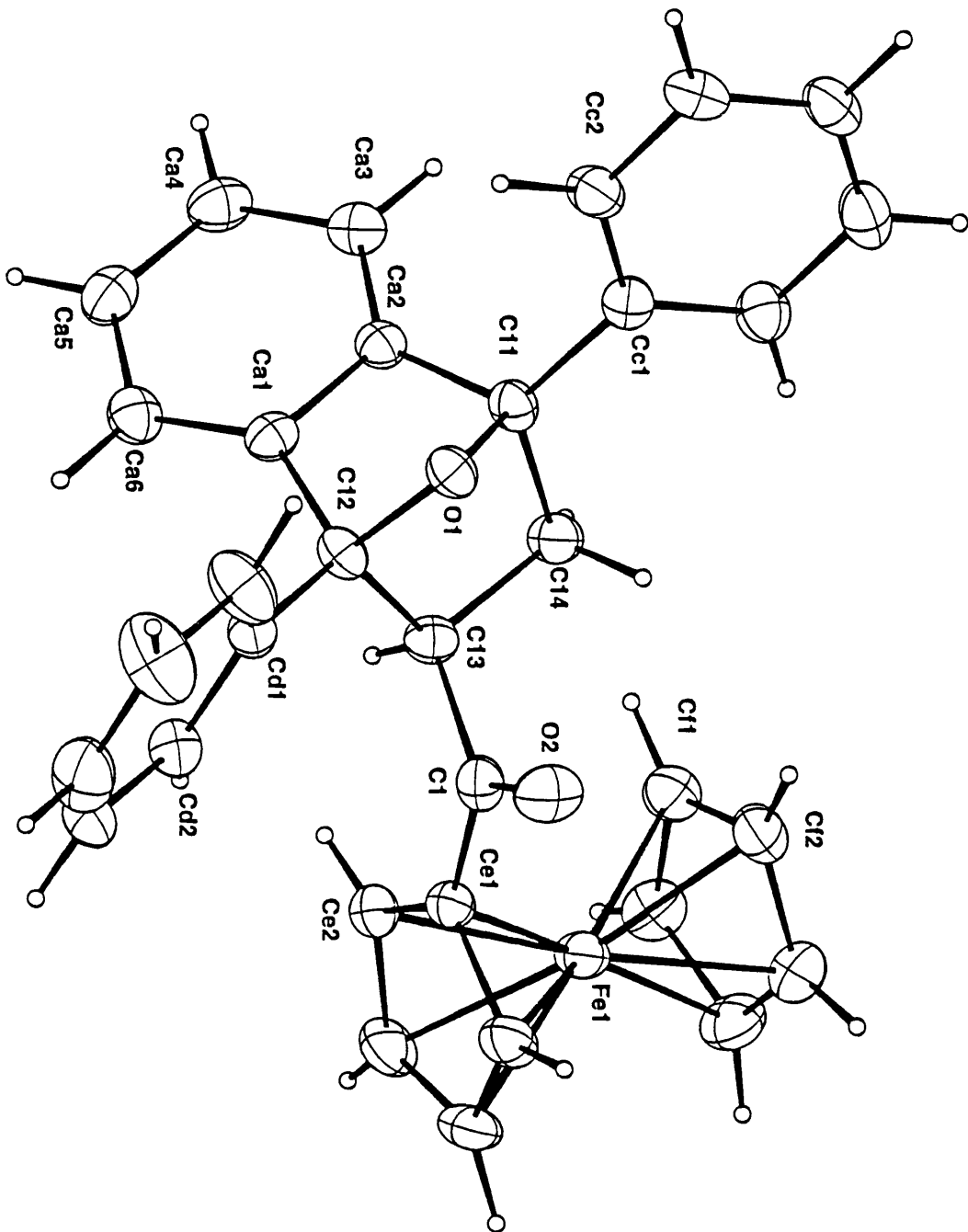


Figure 3.2.3

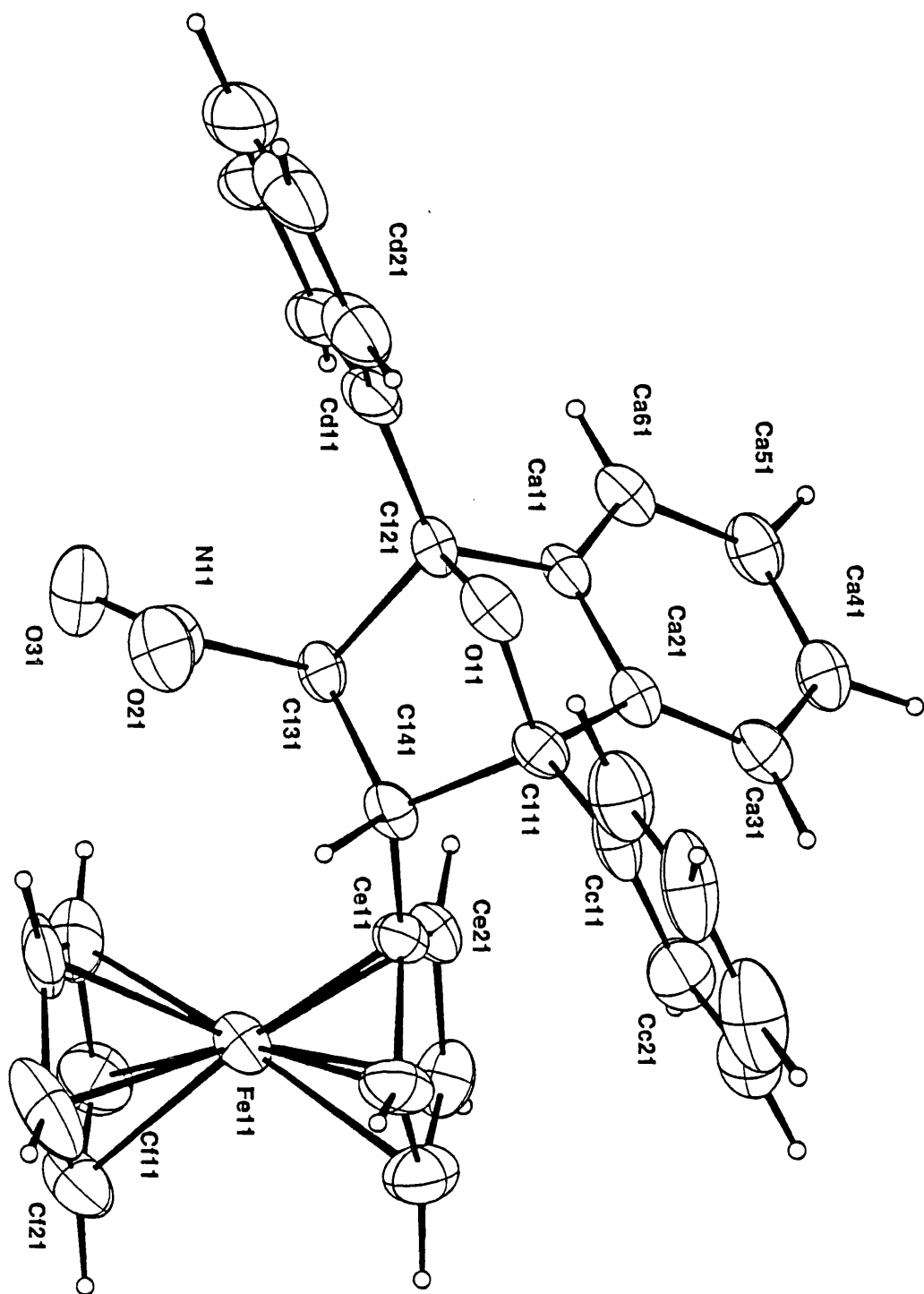


Figure 3.2.4

Table 3.2.1. Selected bond lengths in the isobenzofuran units of **10** - **13** (Å)*

(a) bond lengths

	10		11	12	13	
a	1.463(7)	1.486(7)	1.496(11)	1.459(6)	1.148(12)	1.168(13)
b	1.208(6)	1.212(6)	1.224(10)	1.216(5)	1.216(14)	1.203(14)
c	1.514(6)	1.509(6)	1.535(11)	1.522(5)	1.430(13)	1.411(13)
d	1.580(6)	1.583(6)	1.505(11)	1.567(6)	1.570(13)	1.553(12)
e	1.530(6)	1.514(6)	1.536(11)	1.534(6)	1.430(13)	1.436(12)
f	1.524(6)	1.523(6)	1.531(10)	1.519(6)	1.424(13)	1.417(12)
g	1.594(6)	1.594(5)	1.535(11)	1.536(6)	1.565(15)	1.562(13)
h	1.503(6)	1.495(5)	-	-	1.472(12)	1.483(12)
i	1.442(5)	1.440(5)	1.451(9)	1.464(5)	1.435(11)	1.435(11)
j	1.448(5)	1.449(5)	1.464(9)	1.452(5)	1.407(12)	1.412(11)
k	1.553(6)	1.554(6)	1.508(11)	1.539(6)	1.523(13)	1.522(13)
l	-	-	1.421(11)	-	-	-

(b) intramolecular contacts between bridging oxygen atom O(1) and H atoms of phenyl rings attached to bridgehead C atoms.

	10		11	12	13	
O(1)...H	2.34	2.37	2.34	2.43	2.42	2.31
O(1)...H	2.38	2.36	-	-	2.47	2.45

* The definition of bonds denoted by the letters **a** - **l** is shown below. In the nitro-substituted compound **13** **a** and **b** are N-O bonds and **c** is a N-C bond.

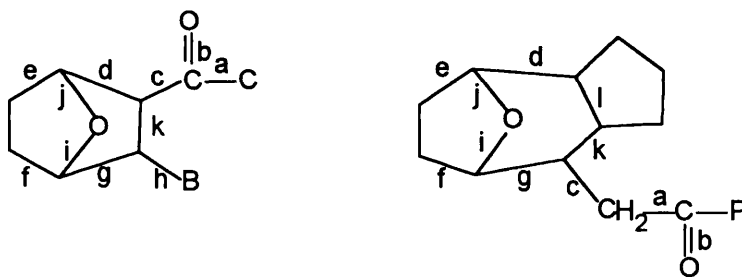


Table 3.2.2. Selected torsion and bond angles for compounds **10** - **13** (°)

	10		11	12	13	
O(1)-C(12)-C(13)-C(1)	91.2(4)	92.1(4)	-160.6(8)	91.1(4)	94.5(8)	94.5(8)
O(1)-C(11)-C(14)-C(E1)	163.8(4)	166.7(4)	-	-	164.3(10)	160.4(10)
C(1)-C(13)-C(14)-C(E1)	109.3(4)	108.5(3)	-	-	108.3(9)	110.6(9)
O(1)-C(11)-C(C1)-C(C2)	5.5(4)	7.2(4)	1.6(18)	124.0(5)	6.7(10)	11.1(8)
O(1)-C(12)-C(D1)-C(D2)	12.6(4)	9.1(4)	125.7(22)	23.2(4)	-6.7(10)	-5.4(9)
O(1)-C(11)-C(E2)-C(E1)	-	-	33.3(7)	-	-	-
O(1)-C(12)-C(13)-C(E1)	-	-	-37.8(6)	-	-	-
C(E1)-C(PE)-C(PF)-C(F1)	-9.2	-6.9	-1.7	-18.0	-3.2	-12.8
C(13)-C(E1)-C(E2)-C(11)	-	-	0.5(7)	-	-	-
C(12)-C(13)-C(E1)-C(E2)	-	-	1.3(7)	-	-	-
C(11)-O(1)-C(12)	98.5(3)	98.2(3)	106.4(5)	97.6(3)	102.0(7)	100.3(6)
C(PE)-Fe-C(PF)	176.8	177.2	173.2	177.4	176.9	176.1

C(PE) and C(PF) are the centroids of cyclopentadienyl rings E and F.

Table 3.2.3. Selected bond distances in the ferrocenyl units of **10** - **13** (Å)

	10		11		12	13	
Fe-C(E1)	2.068(4)	2.055(4)	2.048(8)	-	2.021(5)	2.033(9)	2.044(9)
Fe-C(E2)	2.040(5)	2.049(5)	2.033(8)	-	2.024(5)	1.968(9)	1.953(10)
Fe-C(E3)	2.017(5)	2.030(5)	2.032(8)	-	2.049(5)	1.926(11)	1.909(12)
Fe-C(E4)	2.031(5)	2.030(5)	2.034(8)	-	2.054(5)	2.017(12)	2.004(13)
Fe-C(E5)	2.053(5)	2.037(4)	2.024(9)	-	2.042(5)	2.014(11)	2.024(11)
Fe-C(F1)	2.055(5)	2.038(5)	2.074(17)	1.990(3)	2.039(5)	2.005(14)	2.023(13)
Fe-C(F2)	2.030(6)	2.041(6)	2.047(13)	2.035(18)	2.053(5)	2.012(13)	2.034(14)
Fe-C(F3)	2.023(5)	2.038(5)	2.057(19)	2.0521(18)	2.053(5)	1.918(14)	2.009(13)
Fe-C(F4)	2.034(6)	2.034(5)	2.090(14)	2.021(13)	2.046(5)	1.965(16)	1.914(16)
Fe-C(F5)	2.036(6)	2.029(16)	2.100(16)	1.984(15)	2.029(5)	2.020(13)	1.930(11)

Table 3.2.4. Crystallographic details of the structure analyses of compounds **10** and **11**

	$C_{34}H_{28}O_2Fe$	$C_{39}H_{30}O_2Fe$
Formula	$C_{34}H_{28}O_2Fe$	$C_{39}H_{30}O_2Fe$
Formula wt	525.54	586.48
Crystal system	triclinic	orthorhombic
Space group	$P \bar{1}$	$P2_12_12_1$
a Å	11.7283(9)	10.150(22)
b Å	13.4212(9)	14.508(19)
c Å	17.6187(9)	19.742(29)
α °	78.182(5)	90
β °	70.708(5)	90
γ °	86.779(6)	90
V Å ³	2561.9(3)	2907(8)
Z	4	4
F(0 0 0)	1100	1224
D calc g cm ⁻³	1.362	1.340
T K	295	292
Crystal colour and habit	orange plate	yellow plate
Crystal size mm	0.20 x 0.20 x 0.10	0.28 x 0.18 x 0.02
Cell: reflections used θ range(°)	25 reflections 17.5< θ <20.8	15 reflections 3.6< θ <15.4
$\mu(Mo-K\alpha)$ cm ⁻¹	6.15	5.5
Measured reflections	9450	3932
Unique reflections	9450	3902
Observed reflections $I \geq k\sigma(I)$	4915 (k=3)	1820 (k=2)
θ range °	2.27 - 25.0	2.26 - 25.0
Miller indices h	0 → 13	-1 → 12
k	-15 → 15	-2 → 17
l	-19 → 20	-2 → 23
Decay in mean standard (%)	2.0	2.5
R_{int}	0.026	0.031
No. of parameters	667	377
R(F)	0.0412	0.048
$R_w(F)$	0.0413	0.119
S	1.46	1.04
$\Delta\rho_{max}$ and $\Delta\rho_{min}$ eÅ ⁻³	0.29 → -0.31	0.33 → -0.25
Δ/σ_{max}	0.006	0.42
Extinction coefficient		0.0017(4)

Table 3.2.5. Crystallographic details of the structure analyses of compounds **12** and **13**

Formula	$C_{33}H_{26}O_2Fe$	$C_{32}H_{25}NO_3Fe$
Formula wt	497.4	511.4
Crystal system	monoclinic	monoclinic
Space group	$P2_1/c$	$P2_1/c$
a Å	9.7048(12)	18.940(9)
b Å	15.6885(18)	11.464(6)
c Å	16.0012(9)	24.523(12)
β °	91.869(13)	112.19(4)
V Å ³	2432.5(4)	4950.9(4)
Z	4	8
F(0 0 0)	1036	2128
D calc g cm ⁻³	1.358	1.372
T K	291	290
Crystal colour and habit	reddish plate	bright orange plate
Crystal size mm	0.18 x 0.10 x 0.09	0.61 x 0.14 x 0.04
Cell: reflections used θ range(°)	25 reflections 8.0< θ <20.8	14 reflections 9.9< θ <17.0
μ (Mo-K α) cm ⁻¹	6.44	6.36
Measured reflections	5650	9145
Unique reflections	5451	7805
Observed reflections $I \geq 3\sigma(I)$	2250	2700
θ range °	2.27 - 25.0	2.79 - 23.83
Miller indices h	-11 → 11	-20 → 20
k	-18 → 2	-1 → 12
l	-2 → 18	-27 → 2
Decay in mean standard (%)	1.8	1.7
R _{int}	0.03	0.036
No. of parameters	325	667
R(F)	0.039	0.0476
R _w (F)	0.039	0.0417
S	1.46	1.65
$\Delta\rho_{max}$ and $\Delta\rho_{min}$ eÅ ⁻³	0.22 → -0.32	0.36 → -0.29
Δ/σ_{max}	0.006	0.095

Table 3.2.6. Atomic fractional co-ordinates and equivalent isotropic displacement parameters (\AA^2) for compounds **10** - **13**

(a) compound **10**

Atom	x	y	z	U
Fe(11)	0.13223(5)	0.64485(4)	0.74363(4)	0.047
O(11)	0.0693(2)	1.0554(2)	0.7502(2)	0.041
O(21)	0.3138(3)	0.9097(3)	0.5635(2)	0.091
C(11)	0.2267(4)	0.9491(3)	0.6049(3)	0.056
C(21)	0.1466(5)	1.0145(4)	0.5684(3)	0.077
C(111)	0.0180(3)	0.9624(3)	0.8061(2)	0.039
C(121)	0.1957(3)	1.0290(3)	0.7313(3)	0.042
C(131)	0.1989(3)	0.9286(3)	0.6970(3)	0.044
C(141)	0.0706(3)	0.8836(3)	0.7470(2)	0.040
C(A11)	0.2032(4)	0.9927(3)	0.8177(3)	0.047
C(A21)	0.0905(4)	0.9509(3)	0.8649(3)	0.043
C(A31)	0.0675(4)	0.9076(3)	0.9465(3)	0.054
C(A41)	0.1606(5)	0.9087(3)	0.9791(3)	0.072
C(A51)	0.2725(5)	0.9484(4)	0.9314(4)	0.079
C(A61)	0.2963(4)	0.9916(3)	0.8494(3)	0.063
C(C11)	-0.1169(3)	0.9689(3)	0.8396(2)	0.041
C(C21)	-0.1845(4)	0.8916(3)	0.9003(3)	0.053
C(C31)	-0.3086(4)	0.8978(4)	0.9326(3)	0.061
C(C41)	-0.3660(4)	0.9817(4)	0.9031(3)	0.068
C(C51)	-0.3012(4)	1.0587(4)	0.8427(3)	0.065
C(C61)	-0.1763(4)	1.0526(3)	0.8106(3)	0.052
C(D11)	0.2760(4)	1.1159(3)	0.6755(3)	0.047
C(D21)	0.3963(4)	1.0994(3)	0.6350(3)	0.068
C(D31)	0.4690(4)	1.1782(5)	0.5809(3)	0.074
C(D41)	0.4218(5)	1.2730(4)	0.5666(3)	0.071
C(D51)	0.3034(5)	1.2908(3)	0.6066(3)	0.070
C(D61)	0.2295(4)	1.2122(3)	0.6614(3)	0.056
C(E11)	0.0652(4)	0.7740(3)	0.7896(2)	0.041
C(E21)	-0.0291(4)	0.7040(3)	0.8028(3)	0.051
C(E31)	-0.0063(5)	0.6112(3)	0.8498(3)	0.064
C(E41)	0.1009(5)	0.6229(3)	0.8664(3)	0.069
C(E51)	0.1453(4)	0.7229(3)	0.8292(3)	0.053
C(F11)	0.2073(7)	0.6762(4)	0.6180(3)	0.080
C(F21)	0.1184(5)	0.5990(5)	0.6441(4)	0.090
C(F31)	0.1532(5)	0.5187(4)	0.6945(3)	0.073
C(F41)	0.2620(5)	0.5440(4)	0.7013(3)	0.070

C(F51)	0.2951(5)	0.6421(4)	0.6547(3)	0.072
Fe(12)	0.37369(5)	0.26594(4)	0.25967(4)	0.044
O(12)	0.4002(2)	0.6778(2)	0.2553(2)	0.039
O(22)	0.2009(3)	0.4475(2)	0.4574(2)	0.074
C(12)	0.2842(4)	0.4994(3)	0.4077(3)	0.047
C(22)	0.3785(5)	0.5405(4)	0.4326(3)	0.071
C(112)	0.4453(3)	0.6129(3)	0.1963(2)	0.039
C(122)	0.2757(3)	0.6426(3)	0.2878(2)	0.040
C(132)	0.2908(3)	0.5249(3)	0.3188(2)	0.037
C(142)	0.4146(3)	0.5046(3)	0.2565(2)	0.037
C(A12)	0.2460(4)	0.6498(3)	0.2095(2)	0.041
C(A22)	0.3531(3)	0.6314(3)	0.1512(2)	0.040
C(A32)	0.3571(4)	0.6296(3)	0.0723(3)	0.054
C(A42)	0.2509(5)	0.6466(3)	0.0534(3)	0.065
C(A52)	0.1435(4)	0.6633(3)	0.1128(3)	0.069
C(A62)	0.1397(4)	0.6652(3)	0.1918(3)	0.053
C(C12)	0.5760(3)	0.6345(3)	0.1489(2)	0.042
C(C22)	0.6351(4)	0.5862(3)	0.0836(3)	0.051
C(C32)	0.7554(4)	0.6058(3)	0.0399(3)	0.056
C(C42)	0.8207(4)	0.6707(4)	0.0610(3)	0.063
C(C52)	0.7643(4)	0.7178(3)	0.1257(3)	0.066
C(C62)	0.6428(4)	0.7003(3)	0.1693(3)	0.053
C(D12)	0.2017(3)	0.7021(3)	0.3498(2)	0.040
C(D22)	0.2485(4)	0.7880(3)	0.3615(2)	0.048
C(D32)	0.1794(4)	0.8429(3)	0.4183(3)	0.060
C(D42)	0.0622(4)	0.8134(3)	0.4629(3)	0.061
C(D52)	0.0139(4)	0.7283(4)	0.4521(3)	0.063
C(D62)	0.0831(4)	0.6726(3)	0.3959(3)	0.056
C(E12)	0.4213(3)	0.4169(3)	0.2147(2)	0.039
C(E22)	0.3346(4)	0.3892(3)	0.1826(3)	0.050
C(E32)	0.3808(5)	0.3094(3)	0.1408(3)	0.060
C(E42)	0.4974(5)	0.2876(3)	0.1454(3)	0.062
C(E52)	0.5233(4)	0.3531(3)	0.1916(3)	0.052
C(F12)	0.3142(6)	0.2344(3)	0.3847(3)	0.069
C(F22)	0.4078(5)	0.1696(4)	0.3553(3)	0.071
C(F32)	0.3736(5)	0.1142(3)	0.3072(3)	0.065
C(F42)	0.2580(5)	0.1445(4)	0.3072(3)	0.069
C(F52)	0.2209(5)	0.2198(4)	0.3548(3)	0.067

(b) compound 11

Atom	x	y	z	U
Fe(1)	0.92191(12)	0.29200(7)	0.81430(6)	0.048
O(1)	0.7476(5)	0.3068(3)	0.6658(2)	0.037
O(2)	0.4976(6)	0.3022(4)	0.8961(3)	0.059
C(1)	0.5005(7)	0.2191(5)	0.7928(3)	0.039
C(2)	0.4572(18)	0.2357(5)	0.8642(4)	0.043
C(11)	0.8256(7)	0.2220(5)	0.6690(4)	0.035
C(12)	0.6164(7)	0.2830(5)	0.6893(4)	0.036
C(13)	0.6187(7)	0.2748(5)	0.7668(3)	0.037
C(A1)	0.7230(8)	0.1517(5)	0.6446(4)	0.037
C(A2)	0.6013(7)	0.1874(5)	0.6573(3)	0.034
C(A3)	0.4882(8)	0.1371(5)	0.6429(4)	0.044
C(A4)	0.5019(9)	0.0481(5)	0.6169(4)	0.048
C(A5)	0.6252(10)	0.0136(5)	0.6051(4)	0.052
C(A6)	0.7390(9)	0.0630(5)	0.6198(10)	0.047
C(B1)	0.3579(8)	0.1712(5)	0.946(4)	0.039
C(B2)	0.3024(9)	0.1224(6)	0.9563(4)	0.062
C(B3)	0.2113(10)	0.1340(7)	0.9848(4)	0.071
C(B4)	0.1740(9)	0.0551(7)	0.9519(5)	0.062
C(B5)	0.2287(10)	0.0334(6)	0.8915(5)	0.068
C(B6)	0.3183(9)	0.0924(5)	0.8916(5)	0.062
C(C1)	0.9473(8)	0.2308(5)	0.6265(4)	0.041
C(C2)	0.9719(8)	0.3087(6)	0.5898(4)	0.051
C(C3)	1.0861(11)	0.3181(6)	0.5521(5)	0.065
C(C4)	1.1740(10)	0.2471(7)	0.5500(5)	0.063
C(C5)	1.1494(10)	0.1672(7)	0.5845(5)	0.066
C(C6)	1.0374(8)	0.1595(6)	0.6228(4)	0.049
C(D1)	0.5217(8)	0.3545(5)	0.6617(4)	0.036
C(D2)	0.4388(8)	0.4082(5)	0.7018(4)	0.047
C(D3)	0.3534(9)	0.7414(5)	0.6716(5)	0.059
C(D4)	0.3516(9)	0.4836(6)	0.6035(6)	0.063
C(D5)	0.4330(10)	0.4318(5)	0.5633(4)	0.064
C(D6)	0.5162(9)	0.3678(6)	0.5928(4)	0.057
C(E1)	0.7466(8)	0.2313(5)	0.7889(4)	0.036
C(E2)	0.8481(7)	0.2047(5)	0.7433(4)	0.036
C(E3)	0.9417(9)	0.1605(5)	0.7814(5)	0.051
C(E4)	0.9112(11)	0.1613(5)	0.8512(5)	0.055
C(E5)	0.7865(8)	0.2060(6)	0.8552(4)	0.046
C(F11)	0.9439(15)	0.4050(13)	0.8776(6)	0.040
C(F21)	0.8953(12)	0.4319(12)	0.8131(8)	0.048

C(F31)	0.9902(16)	0.4046(14)	0.7637(5)	0.049
C(F41)	1.0975(11)	0.3638(12)	0.7977(9)	0.059
C(F51)	1.0689(14)	0.3629(13)	0.8681(7)	0.058
C(f12)	0.9010(13)	0.4148(15)	0.8582(8)	0.059
C(F22)	0.9188(15)	0.4274(13)	0.7875(8)	0.058
C(F32)	1.0419(16)	0.3880(14)	0.7693(5)	0.040
C(f42)	1.1001(11)	0.3510(12)	0.8288(8)	0.048
C(f52)	1.0130(15)	0.3675(12)	0.8837(5)	0.049

(c) compound 12

Atom	x	y	z	U
Fe(1)	0.31525(5)	0.15169(4)	0.45771(4)	0.042
O(1)	0.0856(2)	0.3875(2)	0.1976(2)	0.038
O(2)	0.3548(3)	0.2997(2)	0.2769(2)	0.055
C(1)	0.2818(4)	0.2996(3)	0.3374(3)	0.038
C(11)	-0.0233(4)	0.3238(2)	0.2064(2)	0.037
C(12)	0.1007(4)	0.4111(3)	0.2851(2)	0.038
C(13)	0.1297(3)	0.3228(3)	0.3279(2)	0.037
C(14)	0.0500(4)	0.2624(3)	0.2679(3)	0.042
C(A1)	-0.0497(4)	0.4313(3)	0.3043(2)	0.037
C(A2)	-0.1269(4)	0.3749(2)	0.2550(2)	0.036
C(A3)	-0.2680(4)	0.3720(3)	0.2587(3)	0.045
C(A4)	-0.3318(4)	0.4280(3)	0.3123(3)	0.050
C(A5)	-0.2549(4)	0.4847(3)	0.3612(3)	0.050
C(A6)	-0.1107(4)	0.4861(3)	0.3586(3)	0.045
C(C1)	-0.0716(4)	0.2898(3)	0.1229(3)	0.038
C(C2)	-0.1228(4)	0.3458(3)	0.0631(3)	0.047
C(C3)	-0.1692(5)	0.3174(3)	-0.0139(3)	0.052
C(C4)	-0.1658(5)	0.2315(3)	-0.0324(4)	0.052
C(C5)	-0.1165(6)	0.1750(3)	0.0264(4)	0.055
C(C6)	-0.0706(5)	0.2039(3)	0.1043(3)	0.048
C(D1)	0.2051(4)	0.4811(3)	0.2976(3)	0.039
C(D2)	0.2694(4)	0.4946(3)	0.3743(3)	0.050
C(D3)	0.3643(4)	0.5603(3)	0.3857(3)	0.063
C(D4)	0.3959(4)	0.6113(3)	0.3201(3)	0.073
C(D5)	0.3310(4)	0.5997(3)	0.2443(3)	0.085
C(D6)	0.2359(4)	0.5342(3)	0.2330(3)	0.065
C(E1)	0.3350(4)	0.2739(3)	0.4200(3)	0.037
C(E2)	0.2626(4)	0.2695(3)	0.4975(3)	0.044
C(E3)	0.3497(5)	0.2308(3)	0.5582(3)	0.053
C(E4)	0.4754(4)	0.2113(3)	0.5212(3)	0.055
C(E5)	0.4684(4)	0.2377(3)	0.4367(3)	0.048
C(F1)	0.1394(4)	0.0899(3)	0.4194(3)	0.053
C(F2)	0.2421(5)	0.0770(3)	0.3607(3)	0.057
C(F3)	0.3545(5)	0.0372(3)	0.4010(3)	0.060
C(F4)	0.3223(5)	0.0245(3)	0.4862(3)	0.059

C(F5)	0.1888(4)	0.0580(3)	0.4973(3)	0.057
-------	-----------	-----------	-----------	-------

(d) compound 13

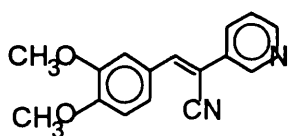
Atom	x	y	z	U
Fe(11)	0.04897(7)	0.79025(11)	0.33992(6)	0.053
O(11)	0.3421(3)	0.6262(5)	0.4106(2)	0.053
O(21)	0.3101(3)	0.8108(6)	0.4866(3)	0.070
O(31)	0.2808(4)	0.9638(7)	0.4320(3)	0.080
N(11)	0.2849(4)	0.8586(8)	0.4385(4)	0.055
C(111)	0.2674(5)	0.5773(8)	0.3792(4)	0.045
C(121)	0.3349(4)	0.7326(8)	0.3781(3)	0.043
C(131)	0.2608(4)	0.7851(7)	0.3835(3)	0.041
C(141)	0.2161(4)	0.6776(7)	0.3880(3)	0.043
C(A11)	0.3066(4)	0.6848(8)	0.3151(4)	0.041
C(A21)	0.2651(5)	0.5870(9)	0.3160(4)	0.041
C(A31)	0.2318(5)	0.5206(8)	0.2668(5)	0.055
C(A41)	0.2412(5)	0.5521(9)	0.2148(4)	0.054
C(A51)	0.2828(5)	0.6506(10)	0.2140(4)	0.058
C(A61)	0.3151(5)	0.7191(8)	0.2630(4)	0.049
C(C11)	0.2564(6)	0.4600(9)	0.4006(4)	0.054
C(C21)	0.1908(6)	0.3979(10)	0.3727(4)	0.070
C(C31)	0.1806(7)	0.2899(10)	0.3932(5)	0.086
C(C41)	0.2348(9)	0.2436(11)	0.4413(6)	0.109
C(C51)	0.3003(8)	0.3040(13)	0.4705(5)	0.093
C(C61)	0.3122(6)	0.4129(11)	0.4501(5)	0.079
C(D11)	0.4040(5)	0.8059(10)	0.4008(4)	0.058
C(D21)	0.4654(6)	0.7798(10)	0.4515(5)	0.078
C(D31)	0.5273(7)	0.8553(16)	0.4719(6)	0.108
C(D41)	0.5294(10)	0.9554(18)	0.4423(9)	0.142
C(D51)	0.4704(8)	0.9793(12)	0.3926(6)	0.111
C(D61)	0.4078(5)	0.9077(11)	0.3716(4)	0.076
C(E11)	0.1339(4)	0.6760(7)	0.3483(4)	0.043
C(E21)	0.1019(4)	0.7168(7)	0.2896(3)	0.046
C(E31)	0.0224(6)	0.6912(9)	0.2659(4)	0.059
C(E41)	0.0063(5)	0.6309(9)	0.3102(5)	0.070
C(E51)	0.0746(5)	0.6211(8)	0.3596(5)	0.066
C(F11)	-0.0140(6)	0.9356(11)	0.3158(5)	0.083
C(F21)	-0.0363(6)	0.8741(11)	0.3544(6)	0.089
C(F31)	0.0268(9)	0.8620(13)	0.4077(5)	0.110
C(F41)	0.0887(6)	0.9202(13)	0.3999(7)	0.101
C(F51)	0.0621(9)	0.9643(10)	0.3425(8)	0.103
Fe(12)	0.45474(7)	0.97168(11)	0.15736(6)	0.057
O(12)	0.1560(3)	1.1082(5)	0.0956(2)	0.038
O(22)	0.1890(4)	0.9399(7)	0.0150(3)	0.083
O(32)	0.2297(5)	0.7866(7)	0.0668(4)	0.100
N(12)	0.2202(5)	0.8904(9)	0.0625(4)	0.060
C(112)	0.2288(4)	1.1647(7)	0.1239(3)	0.036

C(122)	0.1725(4)	1.0016(7)	0.1289(3)	0.034
C(132)	0.2447(4)	0.9603(7)	0.1178(4)	0.041
C(142)	0.2839(4)	1.0738(7)	0.1128(3)	0.038
C(A12)	0.2040(4)	1.0506(8)	0.1919(4)	0.037
C(A22)	0.2396(5)	1.1555(9)	0.1892(4)	0.039
C(A32)	0.2750(5)	1.2228(8)	0.2377(4)	0.050
C(A42)	0.2715(5)	1.1829(10)	0.2904(4)	0.056
C(A52)	0.2353(5)	1.0821(10)	0.2939(4)	0.061
C(A62)	0.2021(5)	1.0134(8)	0.2452(5)	0.052
C(C12)	0.2278(5)	1.2841(8)	0.0999(4)	0.044
C(C22)	0.2935(6)	1.3490(8)	0.1147(4)	0.066
C(C32)	0.2900(6)	1.4611(10)	0.0928(5)	0.080
C(C42)	0.2227(8)	1.5083(8)	0.0577(5)	0.080
C(C52)	0.1575(6)	1.4456(10)	0.0439(4)	0.075
C(C62)	0.1593(6)	1.3329(8)	0.0646(4)	0.059
C(D12)	0.1062(4)	0.9205(7)	0.1125(3)	0.036
C(D22)	0.0360(5)	0.9506(7)	0.0739(4)	0.046
C(D32)	-0.0233(5)	0.8692(10)	0.0580(4)	0.057
C(D42)	-0.0117(5)	0.7609(9)	0.0805(5)	0.063
C(D52)	0.0590(5)	0.7305(8)	0.1201(4)	0.063
C(D62)	0.1187(5)	0.8114(8)	0.1366(4)	0.055
C(E12)	0.3667(4)	1.0790(7)	0.1522(4)	0.043
C(E22)	0.4002(5)	1.0302(8)	0.2096(4)	0.056
C(E32)	0.4780(5)	1.0648(11)	0.2324(5)	0.072
C(E42)	0.4929(6)	1.1303(9)	0.1906(6)	0.086
C(E52)	0.4234(5)	1.1405(9)	0.1411(4)	0.061
C(F12)	0.4386(9)	0.8212(11)	0.1426(8)	0.110
C(F22)	0.5153(8)	0.8212(11)	0.1786(6)	0.096
C(F32)	0.5451(6)	0.8941(12)	0.1484(7)	0.098
C(F42)	0.4912(10)	0.9173(12)	0.0937(6)	0.104
C(F52)	0.4239(6)	0.8584(13)	0.0891(6)	0.093

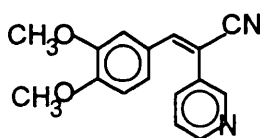
Chapter 3.3. The conformations of some anti-cancer drugs

3.3.1. Introduction

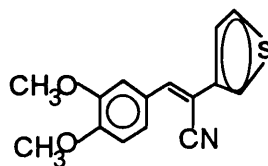
In the last ten years there has been a great effort to understand the signaling pathways that control both cell division and the growth and proliferation of cancerous cells. It is now established that enzymes known as protein tyrosine kinases (PTKs) play a key role in growth-related processes by catalyzing the phosphorylation of tyrosine in intracellular protein substrates. This has led to the search for selective PTK inhibitors in the hope of generating potential chemotherapeutic agents to use in the treatment of cancer. The synthesis and biological screening of compounds thought to have potential as chemotherapeutic agents is of interest to Professor Robins and his co-workers in this department. Compounds **14** -**16**, whose structures are described here, were prepared by Professor Robins and Mr. M. Lear.



(14)



(15)



(16)

Compound **14** has been shown to have significant anti-cancer activity in mice. Furthermore, it readily undergoes isomerisation to the *cis* isomer (**15**). Both (**14**) and (**15**) possess biological activity, but at present it is believed that the *trans* isomer is 2.5 times more active than the *cis* isomer. (Lear, 1995). As part of studies directed to understanding the biological activity of such compounds the solid state conformations displayed by **14**, its *cis* isomer **15** and the related thiophenyl species **16** have been determined by single crystal X-ray analysis.

In the course of this work the conformations displayed by substituted *cis* and *trans* stilbenes have been systematically considered by means of a search of the Cambridge Structural Database. In addition a limited use has been made of molecular mechanics calculations to assess the stereochemical rigidity of these molecules. In the following discussion of the structures of 1,2-diphenylethenes and similar molecules the terms *cis* and *trans* define the relationship of the aromatic rings with respect to the double bond; they are preferred to *Z* and *E* which do not always clearly indicate the relationship of the two rings.

3.3.2. Results and Discussion

Single crystal X-ray analyses (Figures 3.3.1 - 3.3.3) have been carried out for compounds **14** - **16** in order to confirm the pattern of substitution at the central double bond of each molecule and to examine the conformation that it adopts in the solid state. In crystals of the *cis*-isomer there are two independent molecules (A and B). In both isomers of the pyridyl compound and also in the thiophenyl compound **16** the atoms of the $(\text{MeO})_2\text{C}_6\text{H}_3\text{C}=\text{CCN}$ units (excluding the hydrogen atoms) are coplanar to within 0.16 Å. As expected, the pyridyl and thiophenyl rings are each planar to within 0.01 Å. The *trans* isomers (pyridyl and thiophenyl) adopt an approximately flat conformation in which the angle between the $(\text{MeO})_2\text{C}_6\text{H}_3=\text{CCN}$ unit and the pyridyl or thiophenyl ring, measured by the C(1)-C(2)-C(21)-C(22) or -(25) torsion angle, is only $-23.5(5)^\circ$ in **14** and $-26.9(2)^\circ$ in **16**. In the *cis*-isomer the pyridyl group twists about the C(2)-C(21) bond until it is nearly normal to the plane of the $(\text{MeO})_2\text{C}_6\text{H}_3=\text{CCN}$, unit, giving rise to C(1)-C(2)-C(21)-C(26) torsion angles of $75.3(3)$ and $75.0(3)^\circ$. The orientation of the pyridyl ring in the *cis*-isomer is therefore unfavorable for conjugation across C(2)-C(21) and this bond is slightly longer [by 0.039(6) Å] than the corresponding bond in the *trans* pyridyl isomer, with C(2)-C(3) shorter by 0.028(6) Å in compensation. The C(2)-C(21) bond

length in the thiophenyl compound is weaker [longer by 0.020(6) Å] than the corresponding bond in the *trans* pyridyl isomer, with C(2)-C(3) stronger [shorter by 0.018 Å] in compensation (see Table 3.3.1). The tendency of the methoxy substituents to lie in the plane of the phenyl ring ($\varphi = |\text{CH}_3\text{-O-C-C}| < 10.5^\circ$), suggests that there is an interaction between the oxygen atoms and the ring π -system (see Table 3.3.1). In all three crystals intermolecular contacts are consistent with normal van der Waals radii, the packing efficiency being slightly greater for compound **14** than for **15** [*trans/cis* density ratio 1.026]. The flat conformation adopted by the *trans* isomers involves steric strain: in addition to short intramolecular contacts between methyl and phenyl hydrogen atoms [H...H 2.30 - 2.36 Å] H(1) is wedged between H(12) and H(22) [H...H 2.10 - 2.28 Å] in **14** and between H(12) and H(25) [H...H 2.26 - 2.39 Å] in **16** and C(3) between H(16) and H(26) [C(3)...H 2.47 and 2.52 Å] in **14** and between H(16) and H(22) [C(3)...H 2.39 - 2.75] in **16** (see Figure 3.3.1 and 3.3.3). These strains are partly relieved by bond angle distortions, C(2)-C(1)-C(11) [$133.3(4)^\circ$ in **14** and $132.2(2)^\circ$ in **16**] being most obviously affected. *Trans*-stilbene shows similar angular distortions for the same reasons (Hoeksta, Meertens & Vos, 1975; Finder, Newton & Allinger, 1974; Bernstein, 1975). The bond angles in the *cis* isomer also distort to relieve overcrowding [C(2)-C(1)-C(11) = $131.9(3)^\circ$ and $131.6(3)^\circ$].

In order to compare the molecular conformations of compounds **14** - **16** with those of related molecules a search was made using the Cambridge Structural Database for stilbene-like compounds containing a central carbon double bond in which each carbon atom is attached via a single bond to a six-membered aromatic ring. The Ar-C=C-Ar torsion angle φ defines the configuration (*trans* or *cis*) at the central double bond. In this search 105 molecules were found with *trans* structures, φ ranging between 161° to 180° , while the *cis* configuration was found in 22 molecules with φ between 1.6 to 13.5° . In these molecules two C=C-C_{Ar}-C_{Ar} torsion angles, φ_1 and φ_2 , can be

used to define the conformational relationship of the two rings to the central C=C bond. The *trans* compounds tend to prefer symmetrical arrangements (see Figure 3.3.4): many of them are exactly centrosymmetric with ($\varphi_1 = -\varphi_2$) and some are close to C_2 point symmetry ($\varphi_1 = \varphi_2$); flat conformations, with both φ close to zero are popular. However, the range displayed by the φ_1 and φ_2 angles indicates conformation flexibility such that relatively little energy is required to deform such molecules from non-planarity. From Figure 3.3.4 the conformations displayed by **14** and **16**, although unsymmetrical, appear quite typical for *trans*-ArC=CAr molecules.

A similar analysis of *cis*-ArC=CAr molecules (see Figure 3.3.5) unsurprisingly suggests that their conformations are constrained because minimum non-bonded distances need to be preserved between the *cis* rings: all have at least one ring twisted out of conjugation with the C=C bond ($\varphi_2 > 45^\circ$), with the other ring twisted by variable amounts ($\varphi_1 = 15 - 90^\circ$). Compound **15** is distinguished from the other *cis* molecules represented in Figure 3.3.5 by the closeness to zero of φ_1 (filled circles). This conclusion is consistent with preliminary molecular mechanics calculations for *trans* and *cis* stilbene carried out with CHEMMOD (Tyler, 1994). In all cases φ_1 and φ_2 have the same sign and φ_2 always is greater than 40° . The planarity of the $(\text{MeO})_2\text{C}_6\text{H}_3\text{C}=\text{C}$ unit in the *cis* isomer is therefore untypical. It is possible that the tendency of the two methoxy groups to interact with the phenyl ring and electrophilic nature of the cyano group are responsible both for the unusual conformation adopted by **15** and for the biological activity. The structures studies do not appear to shed any light on the anti-cancer properties on **14** or on its facile isomerisation to **15**.

3.3.3. Experimental

Crystallographic data are given for compounds **14** - **16** in Table 3.3.2. More details about experimental and computational methods have already been described in Section 1. No absorption corrections were applied for these compounds. The structures were solved by direct methods using SHELXS (Sheldrick, 1986). The GX package (Mallinson & Muir, 1985) was used for all other calculations. Refinement was performed on F. The fractional co-ordinates for non-hydrogen atoms for compounds **14** - **16** are given in Table 3.3.3. Anisotropic U_{ij} were used for all non-hydrogen atoms. Anisotropic displacement parameters for non-hydrogen atoms, hydrogen atoms co-ordinates, a geometry listing and observed and calculated structure factors are available.

Table 3.3.1 Selected torsion and bond angles and bond distances for compounds **14- 16** ($^{\circ}$, \AA)

	14	15		16
C(1)-C(2)-C(21)-C(22)	-23.5(5)	-107.4(3)	-106.7(3)	152.1(3)
C(1)-C(2)-C(21)-C(26)*	156.5(6)	75.3(3)	76.0(3)	-26.9(2)
C(2)-C(1)-C(11)-C(16)	-2.7(5)	2.0(3)	0.5(2)	5.0(2)
C(18)-O(15)-C _{Ar} -C _{Ar}	4.4	-8.4(2)	-8.0(2)	-4.8(2)
C(17)-O(14)-C _{Ar} -C _{Ar}	10.3(5)	1.4(3)	4.3(3)	2.7(2)
C(2)-C(1)-C(11)	133.3(4)	131.9(3)	131.6(3)	132.2(2)
C(2)-C(3)	1.461(5)	1.433(3)	1.432(3)	1.443(3)
C(2)-C(21)	1.457(5)	1.497(3)	1.495(3)	1.477(3)
C(1)-C(2)	1.338(6)	1.341(3)	1.338(3)	1.341(3)

* In compound **16** C(25) takes the place of C(26).

Captions to Figures

Figure 3.3.1. A view of a molecule of the *trans* pyridyl isomer (**14**). 50% probability ellipsoids are displayed except for hydrogen atoms which are represented by spheres of arbitrary radius.

Figure 3.3.2. A view of one of the two independent molecules of the *cis* pyridyl isomer (**15**). 50% probability ellipsoids are displayed except for hydrogen atoms which are represented by spheres of arbitrary radius.

Figure 3.3.3. A view of a molecule of the *trans* thiophenyl isomer (**16**). 50% probability ellipsoids are displayed except for hydrogen atoms which are represented by spheres of arbitrary radius.

Figure 3.3.4. The conformations of 105 *trans*-Ar-C=C-Ar molecules obtained from the Cambridge structural database (open circles). In this figure and Figure 3.3.5 φ_1 (horizontal axis) and φ_2 (vertical axis) are C=C-Ar-Ar torsion angles in degrees defining the twisting of the Ar ring about the C=C bonds. Compound **14** is represented by a filled circle and compound **16** as a crossed circle.

Figure 3.3.5. The conformations of 22 *cis*-Ar-C=C-Ar molecules obtained from the Cambridge structural database (open circles). The two independent molecules of Compound **15** are represented by the filled circles.

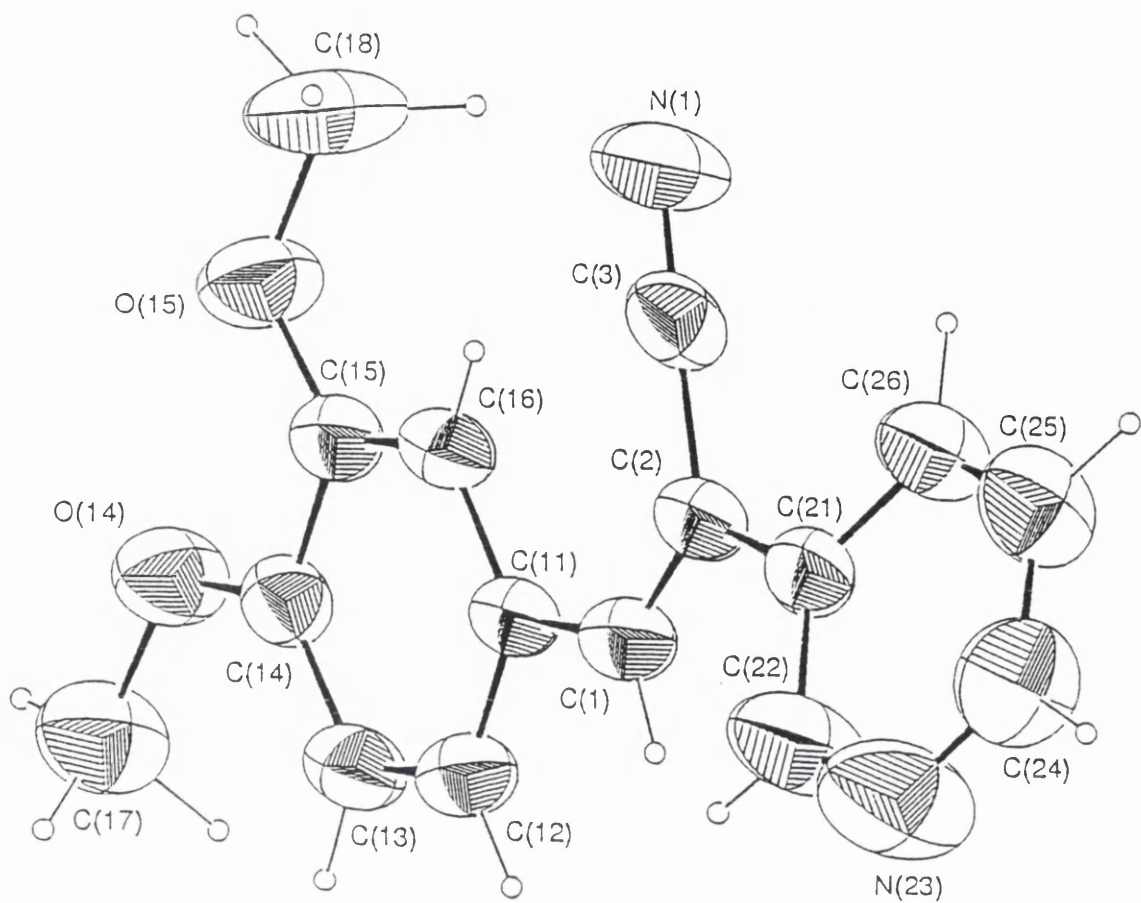


Figure 3.3.1

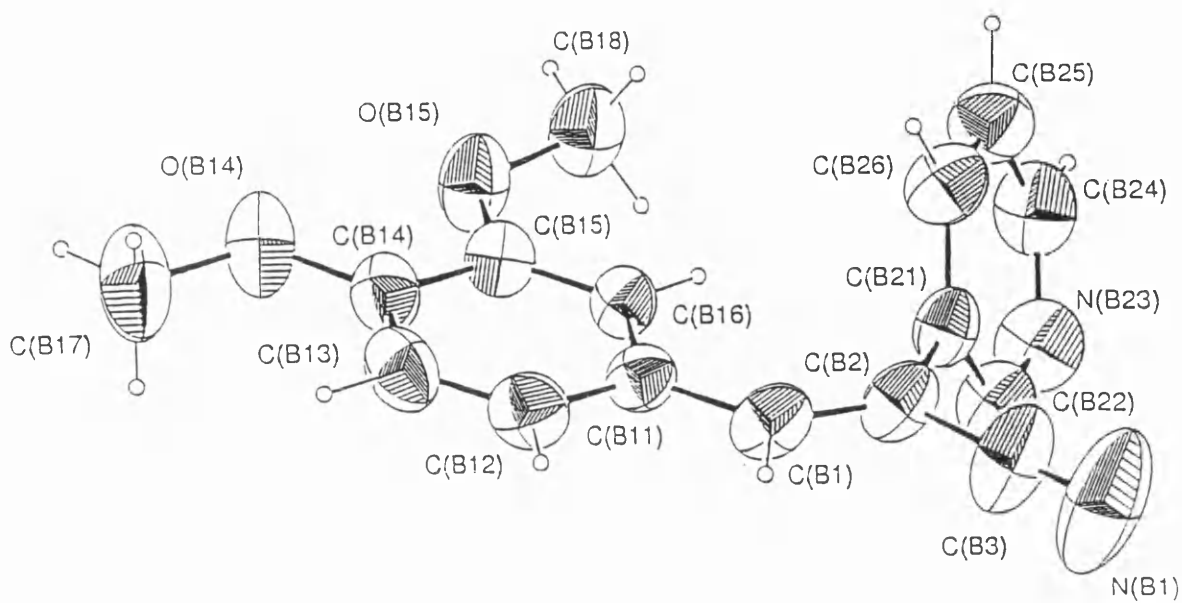


Figure 3.3.2

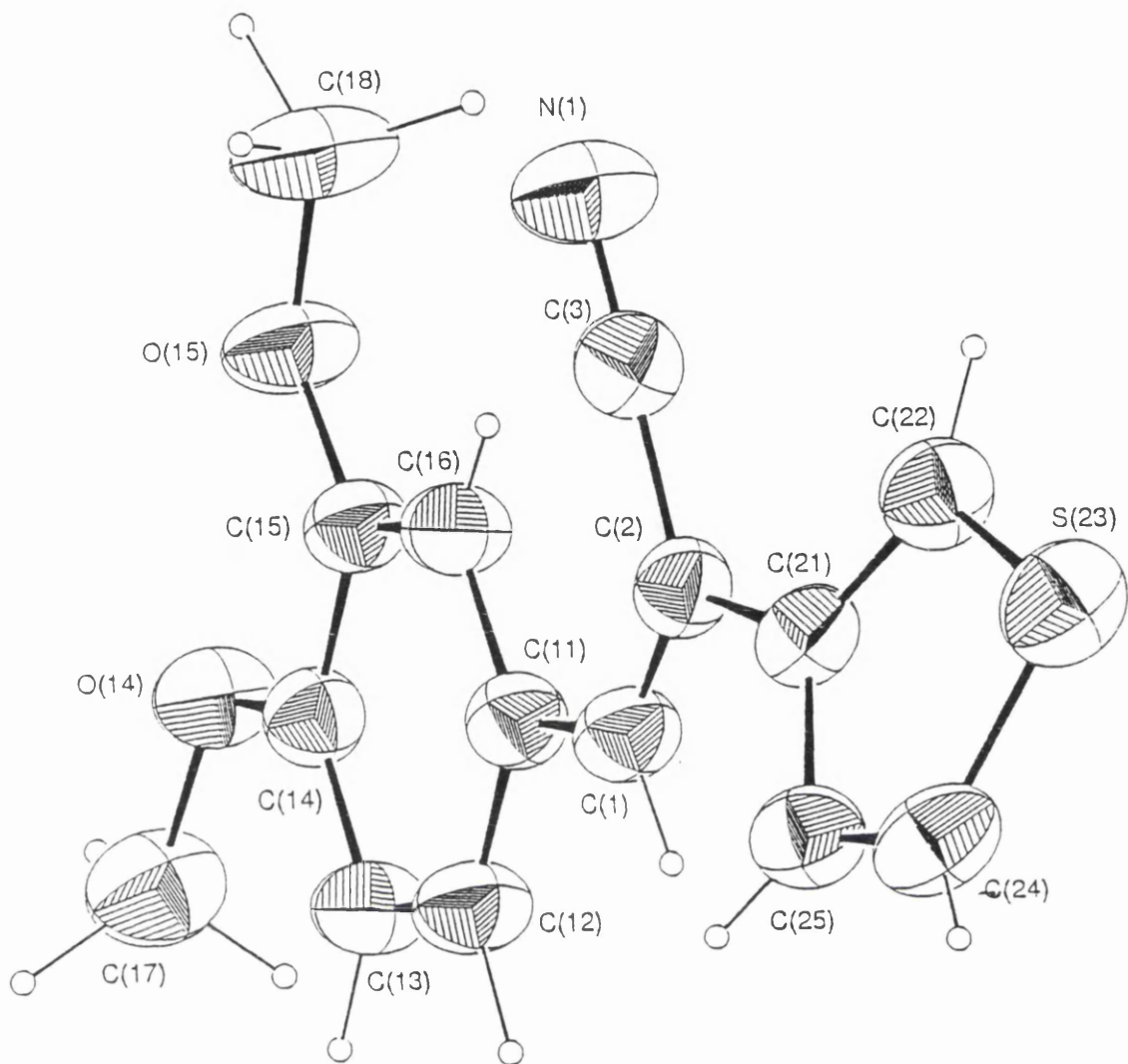


Figure 3.2.3

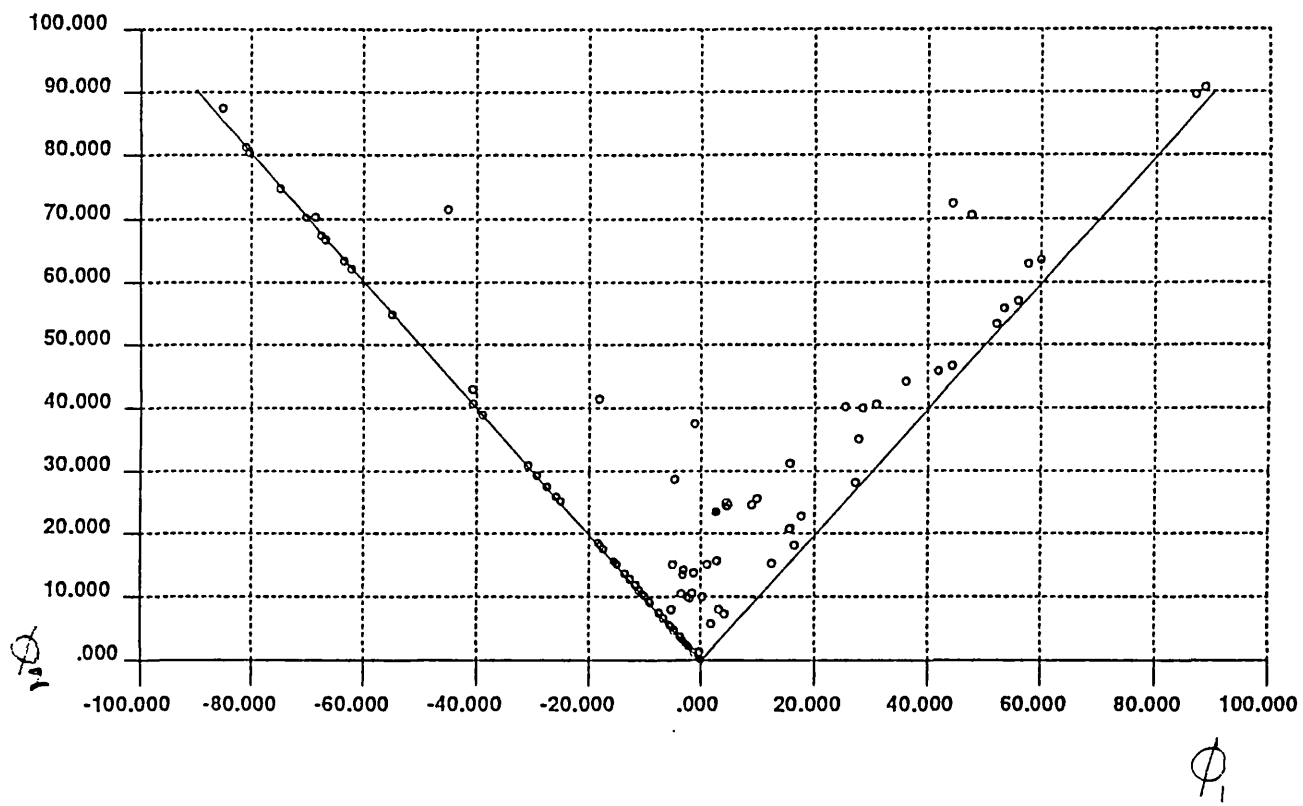


Figure 3.3.4

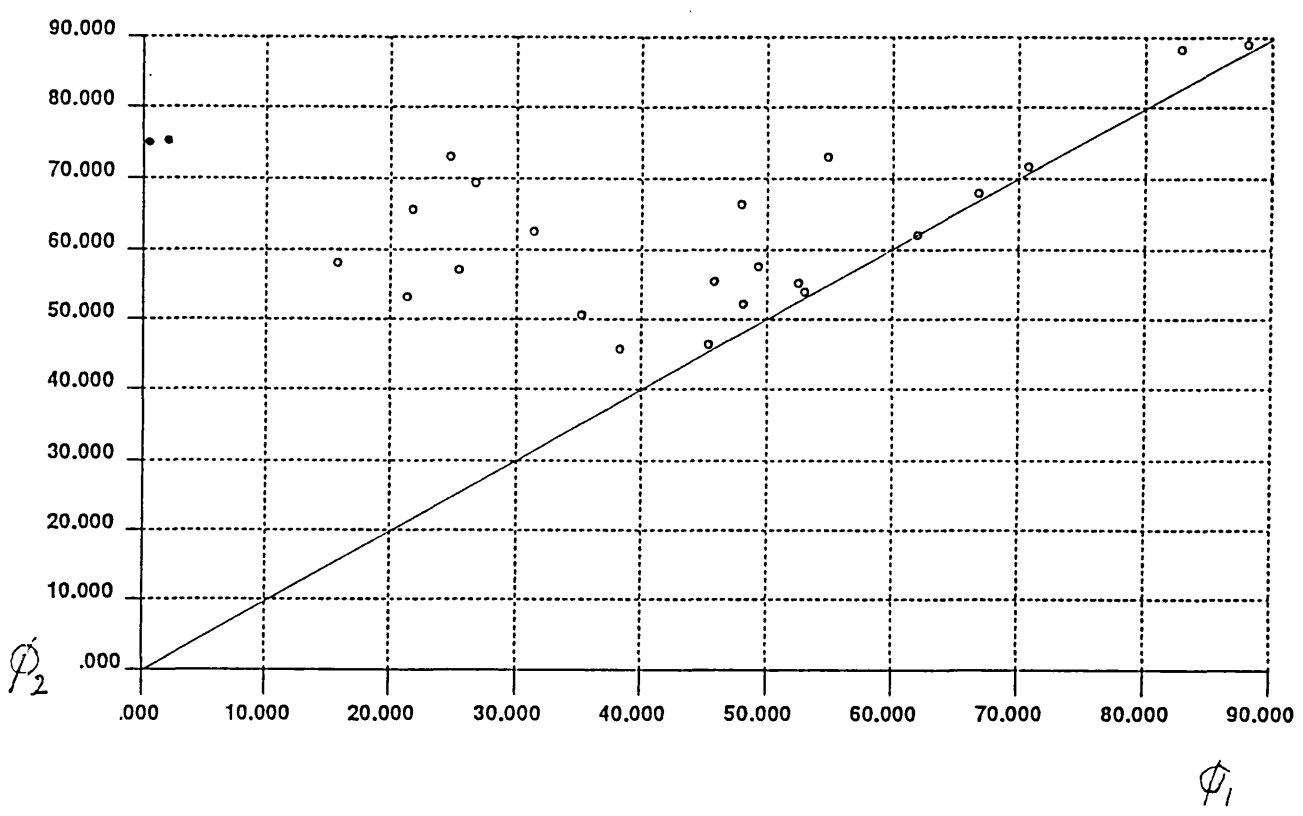


Figure 3.3.5

Table 3.3.2. Crystallographic details of the structure analyses of compounds 14 - 16

	C ₁₆ H ₁₄ N ₂ O ₂	C ₁₆ H ₁₄ N ₂ O ₂	C ₁₅ H ₁₃ NO ₂ S
Formula	C ₁₆ H ₁₄ N ₂ O ₂	C ₁₆ H ₁₄ N ₂ O ₂	C ₁₅ H ₁₃ NO ₂ S
Formula wt	266.30	266.30	271.34
Crystal system	orthorhombic	monoclinic	monoclinic
Space group	Pcab	P2 ₁ /c	P2 ₁ /n
a Å	8.0279(8)	9.7755(5)	10.5062(5)
b Å	26.0981(19)	25.6816(9)	11.0185(7)
c Å	13.3235(11)	11.4330(6)	12.4749(8)
β °	-	93.625(5)	107.363(43)
V Å ³	2791.4(5)	2864.53(23)	1378.32(14)
Z	8	8	4
F(0 0 0)	1120	1120	568
D calc g cm ⁻³	1.267	1.235	1.308
T K	296	297	295
Crystal colour and habit	colourless needle	colourless plate	pale yellow brick shaped
Crystal size mm	0.80 x 0.25 x 0.15	0.48 x 0.42 x 0.30	0.55 x 0.38 x 0.20
Cell: reflections used	25 reflections	25 reflections	25 reflections
θ range(°)	18<θ<25	18<θ<23	20.9<θ<22.9
μ(Mo-Kα) cm ⁻¹	0.79	0.77	2.21
Measured reflections	3607	8969	4388
Unique reflections	1607	8349	4020
Observed reflections I ≥ 3σ(I)	1292	3801	2610
θ range °	2.3 - 27.4	2.2 - 30	2.23 - 30
Miller indices h	0 → 10	0 → 13	-14 → 14
k	-33 → 0	-36 → 0	-15 → 0
l	-0 → 17	-16 → 16	0 → 17
Decay in mean standard (%)	2.8	10	1.3
R _{int}	-	0.022	0.067
No. of parameters	237	473	225
R(F)	0.057	0.042	0.044
R _w (F)	0.061	0.047	0.056
S	2.36	1.83	2.27
Δρ _{max.} and Δρ _{min.} eÅ ⁻³	0.17 → -0.20	0.13 → -0.22	0.26 → -0.25
Δ/σ _{max}	0.048	0.09	0.11

Table 3.3.3. Atomic fractional co-ordinates and equivalent isotropic displacement parameters (\AA^2) for compounds 14 - 16

(a) compound 14

Atom	x	y	z	U
N(1)	0.3244(6)	0.5215(1)	-0.1091(2)	0.086
N(23)	0.3028(6)	0.3501(2)	0.1660(3)	0.110
O(14)	-0.0116(3)	0.7149(1)	0.1800(2)	0.066
O(15)	0.1420(4)	0.6890(1)	0.0206(2)	0.075
C(1)	0.1469(5)	0.5073(1)	0.1287(3)	0.055
C(2)	0.2252(5)	0.4800(1)	0.0579(2)	0.049
C(3)	0.2790(5)	0.5044(1)	-0.0353(3)	0.057
C(11)	0.1030(5)	0.5612(1)	0.1377(2)	0.049
C(12)	0.0161(5)	0.5767(2)	0.2229(3)	0.055
C(13)	-0.0240(5)	0.6270(2)	0.2392(3)	0.055
C(14)	0.0194(5)	0.6643(1)	0.1712(3)	0.049
C(15)	0.1035(5)	0.6496(1)	0.0835(3)	0.051
C(16)	0.1431(6)	0.5996(2)	0.0687(3)	0.054
C(17)	-0.0864(9)	0.7326(2)	0.2706(4)	0.079
C(18)	0.2068(10)	0.6758(2)	-0.0763(4)	0.099
C(21)	0.2615(5)	0.4254(1)	0.0650(3)	0.050
C(22)	0.2734(7)	0.3999(2)	0.1556(3)	0.088
C(24)	0.3228(7)	0.3226(2)	0.0834(4)	0.085
C(25)	0.3190(6)	0.3442(2)	-0.0099(4)	0.073
C(26)	0.2892(5)	0.3953(2)	-0.0187(3)	0.063

(b) compound 15

Atom	x	y	z	U
N(A1)	0.7124(3)	0.3770(1)	0.0078(2)	0.134
N(A23)	1.16031(19)	0.46999(9)	-0.08413(17)	0.082
N(B1)	0.8357(3)	0.8051(1)	0.5535(2)	0.131
N(B23)	0.40167(16)	0.74334(7)	0.73463(16)	0.070
O(A14)	1.03853(14)	0.32933(6)	-0.70282(12)	0.077
O(A15)	1.13964(12)	0.40175(5)	-0.57068(10)	0.060
O(B14)	0.41490(14)	0.51628(6)	0.26324(12)	0.076
O(B15)	0.35567(14)	0.55280(5)	0.46305(11)	0.068
C(A1)	0.8280(2)	0.3545(1)	-0.2617(2)	0.057
C(A2)	0.8533(2)	0.3882(1)	-0.1733(2)	0.059
C(A3)	0.7754(3)	0.3813(1)	-0.0723(2)	0.087
C(A11)	0.88567(18)	0.34927(6)	-0.37523(16)	0.050
C(A12)	0.8338(2)	0.3101(1)	-0.4487(2)	0.058
C(A13)	0.8818(2)	0.3017(1)	-0.5578(2)	0.062
C(A14)	0.98412(18)	0.33313(7)	-0.59683(16)	0.056
C(A15)	1.03870(17)	0.37291(6)	-0.52404(15)	0.049
C(A16)	0.99096(18)	0.38060(7)	-0.41541(16)	0.050
C(A17)	0.9828(4)	0.2901(2)	-0.7817(3)	0.101
C(A18)	1.1860(2)	0.4470(1)	-0.5080(2)	0.059
C(A21)	0.95085(18)	0.43317(7)	-0.16612(15)	0.051
C(A22)	1.0699(2)	0.4309(1)	-0.0961(2)	0.068
C(A24)	1.1291(3)	0.5135(1)	-0.1436(2)	0.074

C(A25)	1.0134(3)	0.5196(1)	-0.2129(2)	0.077
C(A26)	0.9222(2)	0.4789(1)	-0.2251(2)	0.070
C(B1)	0.6805(2)	0.6985(1)	0.4256(2)	0.057
C(B2)	0.67751(19)	0.72556(7)	0.52531(17)	0.056
C(B3)	0.7657(3)	0.7699(1)	0.5393(2)	0.082
C(B11)	0.60667(18)	0.65241(6)	0.38423(15)	0.050
C(B12)	0.6361(2)	0.6319(1)	0.2762(2)	0.060
C(B13)	0.5739(2)	0.5872(1)	0.2325(2)	0.064
C(B14)	0.48077(19)	0.56130(7)	0.29645(16)	0.057
C(B15)	0.44875(18)	0.58116(7)	0.40587(15)	0.051
C(B16)	0.50933(18)	0.62602(7)	0.44776(16)	0.049
C(B17)	0.4374(4)	0.4958(2)	0.1488(3)	0.100
C(B18)	0.3335(3)	0.5676(1)	0.5799(2)	0.072
C(B21)	0.59313(18)	0.71614(6)	0.62785(15)	0.050
C(B22)	0.4835(2)	0.7487(1)	0.6465(2)	0.060
C(B24)	0.4301(2)	0.7045(1)	0.8083(2)	0.067
C(B25)	0.5375(2)	0.6707(1)	0.7995(2)	0.069
C(B26)	0.6214(2)	0.6769(1)	0.7075(2)	0.062

(c) compound 16

Atom	x	y	z	U
S(23)	0.08116(6)	0.29478(5)	-0.07237(4)	0.065
N(1)	0.06637(19)	0.13266(17)	0.31805(14)	0.071
O(14)	-0.22089(12)	0.47672(11)	0.64442(10)	0.056
O(15)	-0.06582(14)	0.30057(12)	0.63176(11)	0.061
C(1)	-0.11532(18)	0.40011(17)	0.23408(14)	0.049
C(2)	-0.04447(16)	0.31653(15)	0.19832(14)	0.045
C(3)	0.01851(17)	0.21529(17)	0.26732(14)	0.050
C(11)	-0.14338(17)	0.41649(16)	0.34062(14)	0.046
C(12)	-0.22720(18)	0.50996(18)	0.34963(15)	0.054
C(13)	-0.25657(19)	0.53300(17)	0.44892(16)	0.054
C(14)	-0.20052(16)	0.46261(15)	0.54269(14)	0.046
C(15)	-0.11501(16)	0.36645(15)	0.53550(13)	0.045
C(16)	-0.08712(18)	0.34410(17)	0.43678(14)	0.049
C(17)	-0.3120(3)	0.5686(2)	0.6554(2)	0.070
C(18)	0.0116(3)	0.1966(3)	0.6261(2)	0.081
C(21)	-0.02284(17)	0.31991(15)	0.08668(13)	0.045
C(22)	0.0847(2)	0.2718(2)	0.0636(2)	0.055
C(24)	-0.0679(2)	0.3681(2)	-0.1011(2)	0.057
C(25)	-0.1125(2)	0.3763(2)	-0.0106(1)	0.051

References

- Baldwin, J. E., Bailey, P. D., Gallacher, G., Otsuka, M., Singleton, K. A. & Mallace, P. M. (1984). *Tetrahedron*, 40, 3695-3708.
- Barnardinelli, G. & Flack, H. D. (1985). *Acta Cryst.* A41, 500 - 511.
- Bernstein, J. (1975). *Acta Cryst.* B31, 1268-1271.
- Boeyens, J. C. A. (1978). *J. Cryst Mol. Struct.* 8, 317 - 320.
- Bondi, A. (1964). *J. Phys. Chem.* 68, 441-451.
- Cotton, F. A. & Wilkinson, G. (1988). *Advanced Inorganic Chemistry*, Fifth edition, John Wiley and Sons.
- Crane, J. D., Hitchcock, P. B., Kroto, H. H., Taylor, R. & Walton, D. R. M. (1992). *J. Chem. Soc. Chem. Commun.* 1764 - 1765.
- Cremer, D. & Pople, J. A. (1975). *J. Amer. Chem. Soc.* 97, 1354 - 1358.
- Finder, C. J., Newton, M. G. & Allinger, N. L. (1974). *Acta Cryst.* B30, 411-415.
- Enraf-Nonius. (1992). *CAD4EXPRESS*, A program for controlling CAD4 diffractometers, Delft, The Netherlands
- Flack, H. D. (1983). *Acta Cryst.* A39, 876-881.
- Hoeksta, A., Meertens, P. & Vos, A. (1975). *Acta Cryst.* B31, 2813-2817.
- International Tables for Crystallography.* (1992). Kluwer Academic Publishers, Dordrecht, Vol. C, 685-791.
- Kagan, H. B. & Riant, O. (1992). *Chem. Rev.* 92, 1007-1358.
- Kirby, G. W., McGuinan, H., Mackinnon, J. W., M. McLean, D. & Sharma, P. P. (1985). *J. Chem. Soc. Perkin Trans. 1*, 1437-1442.
- Kirby, G. W. & Nazeer, M. (1993). *J. Chem. Soc. Perkin. Trans. 1*, 1397-1402.
- Lear, M. (1995). Private communication.
- Mallinson, P. R. & Muir, K. W. (1985). *J. Appl. Cryst.* 18, 51 - 53.
- Molen. (1990). *Crystallographic program package*, Enraf-Nonius, Delft, The Netherlands

- Nelsen, S. F., Thompson-Colon, J. A., Kirste, B., Rosenhouse, A. & Kaftory, M. (1987). *J. Amer. Chem. Soc.* 109, 7128-7136.
- Nelsen, S. F., Thompson-Colon, J. A. & Kaftory, M. (1989). *J. Amer. Chem. Soc.* 111, 2809-2815.
- Nesterova, Ya. M., Porai-koshits, M. A. & Moev, A. G. (1981). *Zh. Strukt. Khim.* 22, 111-115.
- Nielsen, B. B., Frydenveny, K. & Larsen, I. K. (1993). *Acta Cryst.* C49, 1018-1022.
- Pindur, U., Lutz, G. & Otto, C. (1993). *Chem. Rev.* 93, 742-761.
- Pirard, B., Baudoux, G. & Durant, F. (1995). *Acta Cryst.* B51, 103.
- Scott, P., Reif, U., Diebold, J & Brintzinger, H. H. (1993). *Organometallics* 12, 3094 - 3101.
- Seiler, P. & Dunitz, J. D. (1979). *Acta Cryst* B35, 2020 - 2032.
- Seiler, P. & Dunitz, J. D. (1978). *Acta Cryst* B35, 1069 - 1078.
- Sheldrick, G. M. SHELXL-93, A program for refining crystal structures. University of Gottingen, Germany, (1993).
- Sheldrick, G. M. (1985). SHELXS-86, Programme for the Solution of Crystal Structures. University of Gottingen, Germany.
- Steiner, T. H. & Saenger, W. (1992). *Acta Cryst.* B48, 819-827.
- Thiessen, W. E., Levy, H. A. & Flaigo, B. D. (1987). *Acta Cryst.* B34, 2495-2509.
- Tyler, K. (1994). Molecular mechanics calculations were carried out with the CHEMMOD Program, Version 5.3, Glasgow University.

Section 4

Miscellaneous compounds

Chapter 4.1. o-Tetramethoxy calix[4]arene silver(I) nitrate

4.1.1. Introduction

One of the most important areas in supramolecular chemistry is that which is concerned with the macrocyclic structures known as calixarenes. Calixarenes are cyclic molecules which contain a number of phenyl rings linked by methylene bridges. In one of the first deliberate attempts to prepare a calixarene the cyclic tetramer, called today p-tert-butyl calix[4]arene, was obtained in two steps from p-tert-butyl phenol and formaldehyde by Alois Ziegler & Erich Ziegler more than 50 years ago (see Vincens, Asfari & Harrowfield, 1994) though the first calixarenes were discovered earlier. Current interest in calixarenes arises from their ability to act as host molecules, since they display high affinity and high selectivity for cations (Lindoy, 1989, Atwood, Davies, & MacNicol, 1991, Gutsche, 1989). Although they are known to form complexes with transition, alkali and alkaline earth metals, in most cases the metals are firmly bound and the co-ordination is irreversible. There are numerous examples of calixarenes with nitrogen or phosphorus substituents (Roundhill, Georgiev & Yordanov, 1994). Chiral calixarenes are simply obtained by attachment of a chiral substituent.

The smallest calixarenes are the cyclic tetramers known as calix[4]arenes. These molecules are useful building blocks for more complex structures with different properties. Their abilities to act as hosts strongly depend on their conformation. Four different conformations have been recognised: (i) all four rings up (cone), (ii) three up and one down (partial cone), (iii) two up and two down (1, 2- alternate), and (iv) two up and two down "1, 3- alternate" (Gutsche, Dhowan, Levine, No & Bauer, 1983) (see Figure 4.1.1).

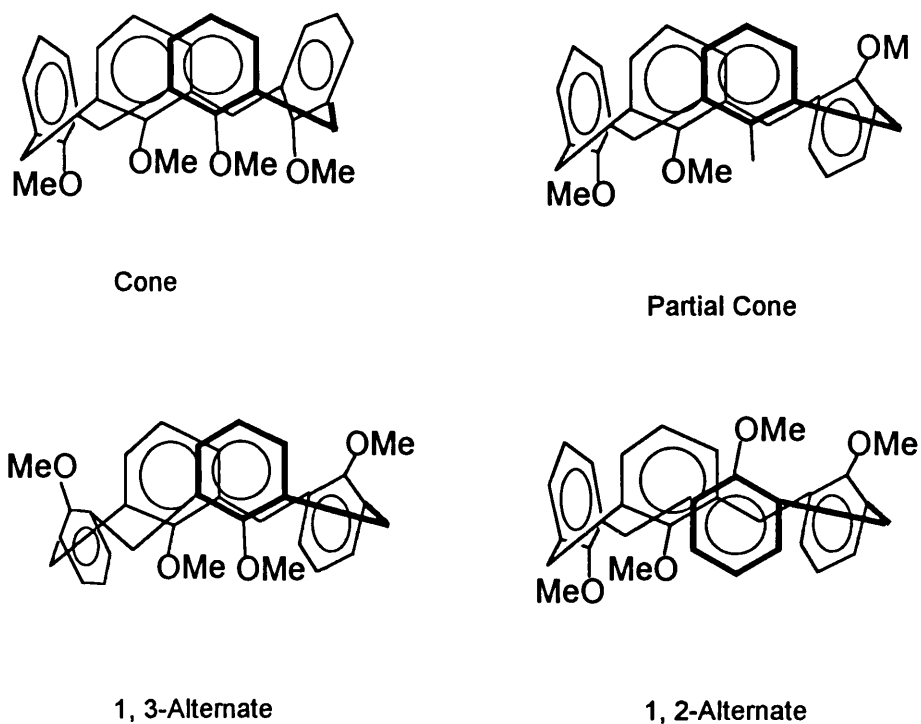
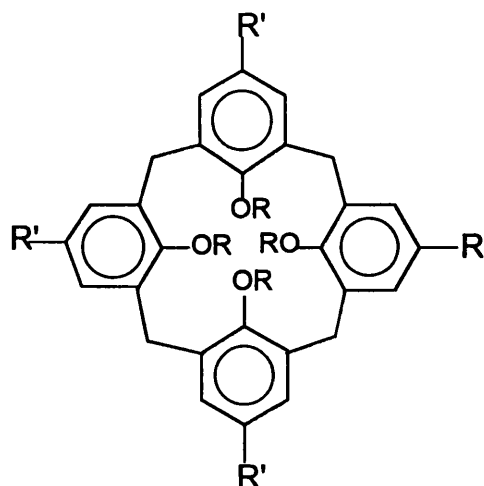


Figure (4.1.1). Conformation of calix[4]arene ethers.

Most calix[4]arenes with OH groups, such as compounds (a) and (b) (see Figure 4.1.2), exist preferentially in the cone conformation because of hydrogen-bonding effects. Calix[n]arenes are known to form complexes with transition metals and provide a unique polyphenoxo binding surface for transition metal ions (Corazza, Floriani, Chiesi-Villa & Guastini, 1990a and 1990b; Atwood, Orr, Mens, Hamada, Zhang, Bott & Robinson, 1992; Atwood, Bott, Jones & Raston, 1992). In this chapter *o*-tetramethoxy calix[4]arene silver(I) nitrate will be discussed.



- | | |
|----------------|------------------------------|
| (a) R=H, R'=H | (b) R=H, R'=Bu ^t |
| (c) R=Me, R'=H | (d) R=Me, R'=Bu ^t |

Figure 4.1.2. Different species of calix[4]arene.

4.1.2. Results and discussion

X-ray crystallography affords the best method for ascertaining conformations of calixarenes in the solid state. The product of the reaction of *o*-methoxyphenol with formaldehyde is compound (c) (see Figure 4.1.2). Then a suspension of AgNO₃ in solution of (c) in THF was stirred for 12 hours at room temperature to give a colourless solution of **1**. After a week of slow evaporation a colourless crystal of **1** appeared. This compound was prepared and crystallized by Professor Puddephatt's group at the University of Western Ontario.

X-ray analysis shows that in the crystal structure of **1** (Figure 4.1.3) the silver ion bonds both to the calix[4]arene and to an asymmetrically bidentate nitrate residue. The molecule has an approximate plane of symmetry which contains the AgNO₃ unit and bisects phenyl rings 1 and 3 of the calix[4]arene. Also, the calix[4]arene adopts a partial cone conformation, as shown by the signs of the CH₂-

C_{ar} torsion angles φ and χ defined in Figure 4.1.4. Using the convention of Uguzzoli and Andreotti (1992) the conformation symbol of **1** will be (+ -, + -, + +, - -) (see Table 4.1.2).

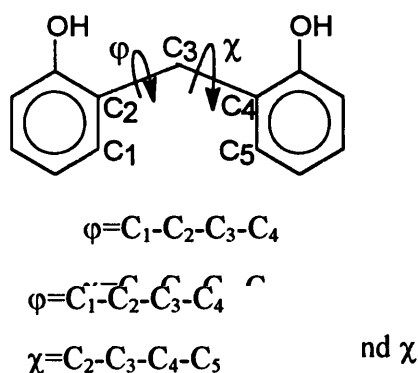


Figure 4.1.4. Torsion angles φ and χ

The conformation is such that rings 2 and 4 are nearly cofacial (dihedral angle $12.7 (2)^\circ$). The silver ion lies in the cleft between rings 2 and 4 and is bound to them through the edges C(23)-C(24) and C(44)-C(45); it is also attached to ring 3 through its methoxy oxygen atom, O(31). Phenyl ring 1 and its associated methoxy group protect the silver ion from further ligation but do not interact with it covalently: the Ag-O(11) contact of $3.989(3) \text{ \AA}$ roughly *trans* to O(2) is clearly nonbonding. The atoms of the calix[4]arene donor set [C(23), C(24), C(44), C(45), O(31)] are coplanar to within $0.005(5) \text{ \AA}$; the silver atom is displaced 0.30 \AA from this plane toward N, i.e. away from the interior of the calix[4]arene. The silver ion is thus attached to a rim of the calix[4]arene and does not completely occupy its central cavity as may be seen from Figure 4.1.5. This arrangement differs from that found in the silver triflate complex of deltaphane, where the silver atom lies at an average distance of 2.43 \AA from the three nearest carbon atoms (Kang, Hanson Eaton & Boekelheide, 1985). The term π -prismand is usually used to describe the shape of the cavity of a host defined by the planes of π -donor phenyl rings (Piere, Baret, Chautemps & Armand, 1981) and exploration of host-guest relationships and

of the interaction of the π -electron systems of π -cryptands has already begun. Species such as **1** are π -cryptands by the above definition. The partial cone conformation of **1** provides a particularly favorable environment for formation of a π -cryptand complex, since the silver can readily interact with four carbon atoms and one methoxy oxygen atom. Ag evidently prefers to lie on the rim rather than to occupy fully the cavity in such species. The only metal cation whose presence has been established in a calixarene cavity is Cs^+ (Harrowfield, Ogden, Richmond & White, 1991). The co-ordination of silver in **1** resembles that found in other silver complexes (e.g. silver triflate deltaphane and paracyclophane) (Gano, Subramaniam & Birnbaum, 1990): in all these compounds the silver atom is attached to one or more oxygen atoms of the counteranion and lies on the rim of a cavity defined by electron-rich phenyl rings to which it is linked by between three and six Ag-C π -bonds. The Ag atom is usually bound to the phenyl ring through a pair of adjacent carbons (i.e. through on edge), but in some compounds such as cofacial stilbenes, Ag binds both to edges and to a single ring carbon atom (Gano, Subramaniam & Birnbaum, 1990).

Bond lengths and angles and crystallographic data are given in Tables 4.1.2-3. The Ag-C distances [2.504(5) - 2.643(5) Å] in **1** are in agreement with accepted values, and fairly similar to those 2.54(2) - 2.67(2) Å found in the perchlorate salt of (paracyclophane) Ag^+ ; (Pierre, Baret, Chautempts & Armand) but are rather longer than the Ag-C bond lengths (2.41 to 2.48 Å) observed in deltaphane silver (I) triflate (Kang, Hansan, Eaton & Boekelheide, 1985). The Ag-O(31) bond length of 2.517(3) Å in **1** is similar to the average Ag-O distance in $[\text{Ag}([12]\text{crown-4})_2][\text{AsF}_6]$ (Jones, Gries, Grutzmacher, Reosky, Schimkowiak & Sheldrick, 1984) and in antibiotic X-206 silver salt, (in the range 2.5 to 2.8 Å) (Blount & Westley, 1971). The interaction of the silver cation with the nitrate group also appears normal: the Ag-O(2) and Ag-O(3) distances in **1** [(2.389(7) and 2.705(8) Å] are comparable with the Ag-O bond lengths in $\text{Ag}_2(\text{NO}_3)_2$ where the shortest such distance is 2.384

Å and with others of 2.63, 2.702 and 2.760 Å in solid silver nitrate (Meyer, Rimsky & Cheralier, 1978).

Bond lengths and angles within the calix[4]arene residue in **1** are in agreement with accepted values (Gallagher, Ferguson, Bohmer & Kraft, 1994). In particular, the C(23)-C(24) and C(44)-C(45) bond lengths [1.391(7) and 1.383(7) Å] do not differ significantly from the mean $C_{Ar}-C_{Ar}$ bond length; nor are the C(31)-O(31) and O(31)-C(37) distances of 1.394(5) and 1.451(6) Å exceptional.

To summarise: investigation has shown that calix[4]arenes have four phenyl rings arranged around a central cavity and form unusually stable silver(I) complexes which can be considered as π -cryptands. The electron-rich calix[4]arene in **1** adopts the partial cone conformation, thereby forming a suitable cavity to host the silver ion. The ability of the calix[4]arene to act as a host to silver(I) is strongly influenced by the electronic effects of its substituent. The binding of silver(I) is relatively weak and can easily be removed by competition with stronger cations.

4.1.3. Experimental

Crystallographic data are given for compound **1** in Table 4.1.3. The structure was solved by Patterson and Fourier methods. The fractional co-ordinates for non-hydrogen atoms, anisotropic parameters, and hydrogen atom co-ordinates and observed and calculated structure factors are available in the published paper (Xu, Puddephatt, Muir & Torabi, 1994). The U (isotropic) displacement parameters for the oxygen atoms of NO_3^- suggest slight positional disorder of the nitrate anion. Empirical absorption corrections were performed by the method of Walker & Stuart (1983) at the end of the isotropic refinement. All calculations were made with the GX package (Mallinson & Muir, 1985).

Captions to Figures

Figure 4.1.3. A view of the o-tetramethoxy calix[4]arene silver(I) nitrate molecule. 50% probability ellipsoids are displayed except for hydrogen atoms which are represented by spheres of arbitrary radius.

Figure 4.1.5. Space-filling diagram for the o-tetramethoxy calix[4]arene silver(I) nitrate.

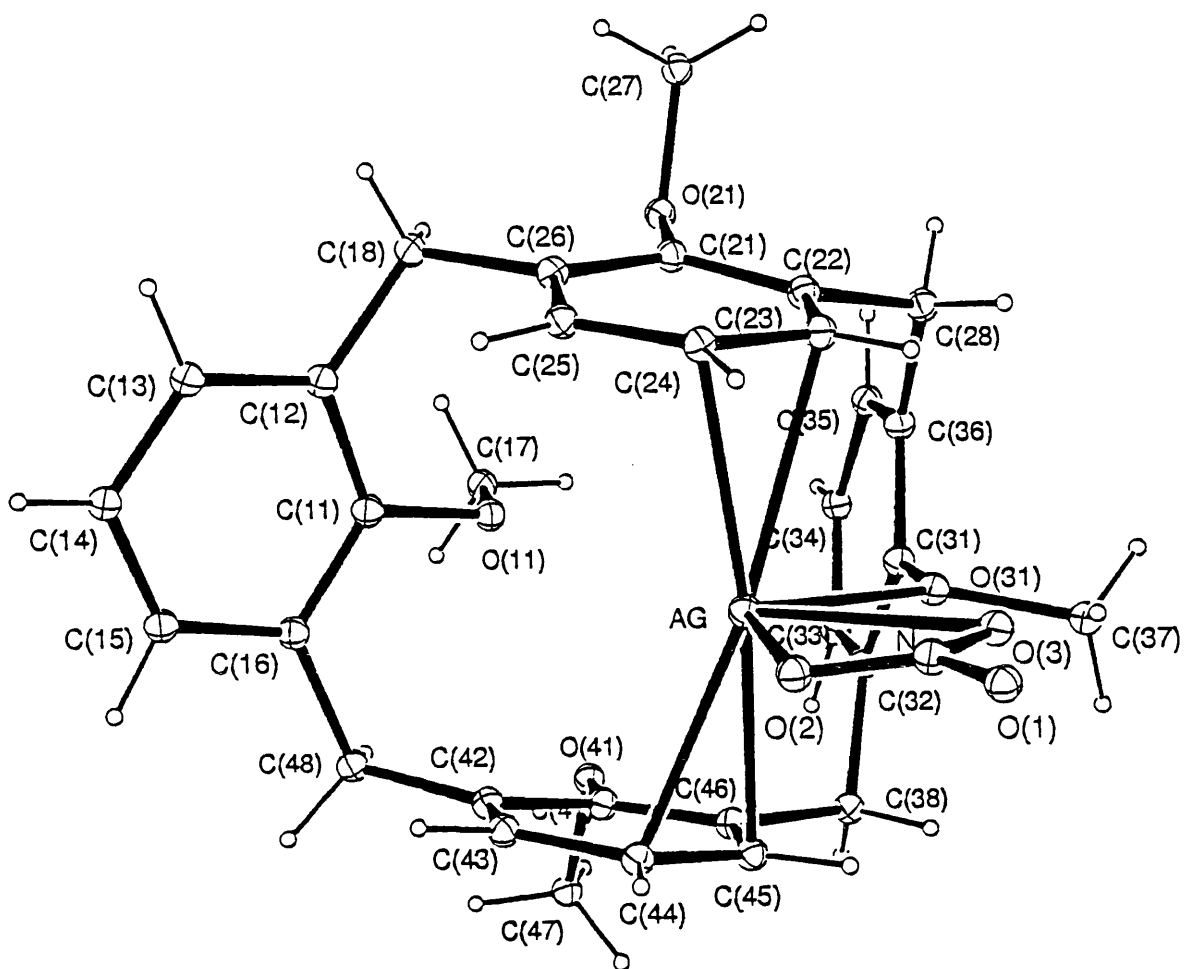


Figure 4.1.3

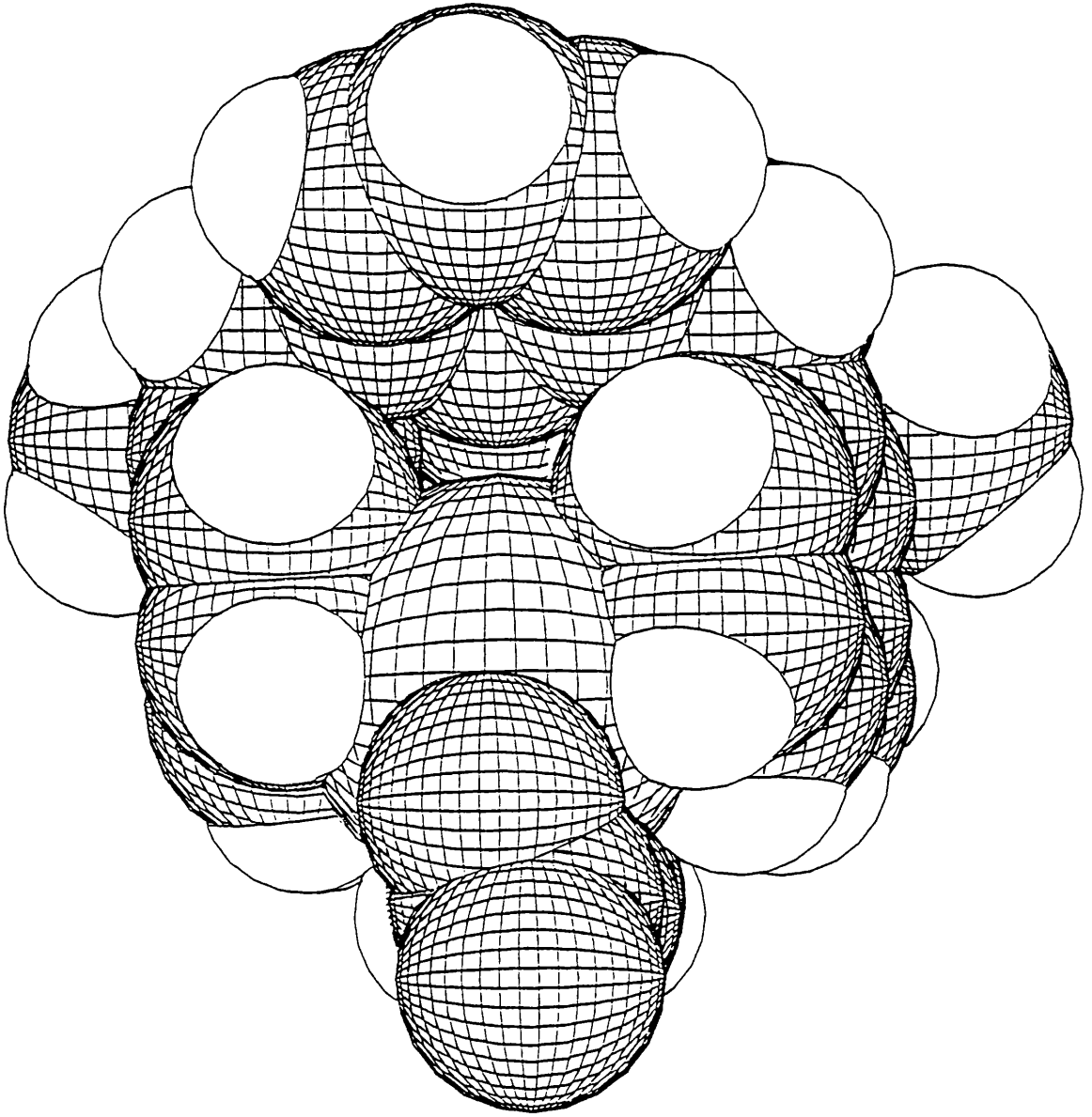


Figure 4.1.5

Table 4.1.1. Fractional atomic coordinates and isotropic displacement parameters (\AA^2) for compound 1

Atom	x	y	z	U
Ag	0.12277(4)	0.19027(2)	0.23204(3)	0.054
O(1)	-0.1482(6)	0.3199(3)	0.2376(4)	0.128
O(2)	0.0007(7)	0.2688(3)	0.1691(6)	0.176
O(3)	-0.0718(7)	0.2521(3)	0.3177(7)	0.193
O(11)	0.4303(3)	0.0901(1)	0.2029(2)	0.045
O(21)	0.5290(3)	0.1284(1)	0.4781(3)	0.048
O(31)	0.0617(3)	0.1317(1)	0.4006(3)	0.043
O(41)	0.2184(3)	-0.0008(1)	0.1505(3)	0.050
N	-0.0731(5)	0.2835(2)	0.2429(4)	0.065
C(11)	0.4915(4)	0.1161(2)	0.1120(4)	0.047
C(12)	0.5862(4)	0.1557(2)	0.1387(4)	0.051
C(13)	0.6447(5)	0.1810(2)	0.0451(6)	0.070
C(14)	0.6087(7)	0.1668(3)	-0.0679(6)	0.080
C(15)	0.5124(6)	0.1296(3)	-0.0903(4)	0.072
C(16)	0.4505(5)	0.1026(2)	-0.0019(4)	0.055
C(17)	0.4969(5)	0.0432(2)	0.2464(4)	0.063
C(18)	0.6171(4)	0.1728(2)	0.2622(5)	0.056
C(21)	0.4525(4)	0.1686(2)	0.4242(4)	0.039
C(22)	0.3311(4)	0.1814(2)	0.4714(3)	0.040
C(23)	0.2585(5)	0.2238(2)	0.4206(4)	0.048
C(24)	0.3008(5)	0.2498(2)	0.3216(5)	0.054
C(25)	0.4160(5)	0.2316(2)	0.2688(4)	0.056
C(26)	0.4933(4)	0.1914(2)	0.3220(4)	0.046
C(27)	0.6179(5)	0.1500(2)	0.5681(4)	0.065
C(28)	0.2744(5)	0.1475(2)	0.5656(3)	0.048
C(31)	0.1332(4)	0.0855(2)	0.4345(3)	0.038
C(32)	0.1054(4)	0.0370(2)	0.3805(4)	0.043
C(33)	0.1776(5)	-0.0078(2)	0.4168(4)	0.052
C(34)	0.2783(6)	-0.0039(2)	0.5031(5)	0.059
C(35)	0.3076(5)	0.0457(2)	0.5536(4)	0.051
C(36)	0.2361(4)	0.0918(2)	0.5207(3)	0.041
C(37)	-0.0572(5)	0.1401(2)	0.4650(5)	0.063
C(38)	0.0038(5)	0.0336(2)	0.2778(4)	0.050
C(41)	0.1589(4)	0.0474(2)	0.1155(3)	0.040
C(42)	0.2124(5)	0.0781(2)	0.0281(4)	0.045
C(43)	0.1505(5)	0.1256(2)	-0.0040(4)	0.052
C(44)	0.0369(5)	0.1434(2)	0.0482(4)	0.050
C(45)	-0.0128(4)	0.1134(2)	0.1380(4)	0.045
C(46)	0.0500(4)	0.0651(2)	0.1743(3)	0.040
C(47)	0.1693(6)	-0.0471(2)	0.0874(6)	0.079
C(48)	0.3412(6)	0.0615(2)	-0.0257(4)	0.063

Table 4.1.2. Selected bond distances (Å) and bond angles (°)

(a) bond distances

Ag - O(2)	2.389(7)	Ag - O(3)	2.705(8)	Ag - O(31)	2.517(3)
Ag - C(23)	2.643(5)	Ag - C(24)	2.504(5)	Ag - C(44)	2.527(5)
Ag - C(45)	2.549(5)	O(1) - N	1.174(8)	O(2) - N	1.209(9)
O(3) - N	1.157(10)	O(11) - C(11)	1.393(6)	O(11) - C(17)	1.418(7)
O(21) - C(21)	1.385(6)	O(21) - C(27)	1.440(6)	O(31) - C(31)	1.394(6)
O(31) - C(37)	1.451(6)	O(41) - C(41)	1.383(6)	O(41) - C(47)	1.432(7)
C(11) - C(12)	1.389(7)	C(11) - C(16)	1.395(7)	C(12) - C(13)	1.398(8)
C(12) - C(18)	1.501(8)	C(13) - C(14)	1.379(10)	C(14) - C(15)	1.351(10)
C(15) - C(16)	1.387(8)	C(16) - C(48)	1.513(8)	C(18) - C(26)	1.522(7)
C(21) - C(22)	1.396(6)	C(21) - C(26)	1.382(7)	C(22) - C(23)	1.390(7)
C(22) - C(28)	1.502(6)	C(23) - C(24)	1.391(7)	C(24) - C(25)	1.407(8)
C(25) - C(26)	1.387(7)	C(28) - C(36)	1.514(7)	C(31) - C(32)	1.371(7)
C(31) - C(36)	1.409(6)	C(32) - C(33)	1.377(7)	C(32) - C(38)	1.530(7)
C(33) - C(34)	1.389(8)	C(34) - C(35)	1.382(8)	C(35) - C(36)	1.391(7)
C(38) - C(46)	1.513(7)	C(41) - C(42)	1.387(7)	C(41) - C(46)	1.385(6)
C(42) - C(43)	1.370(7)	C(42) - C(48)	1.519(8)	C(43) - C(44)	1.387(7)
C(44) - C(45)	1.383(7)	C(45) - C(46)	1.405(7)		

(b) torsion and bond angles

C(43)-C(42)-C(48)-C(16)	60.2(6)	C(15)-C(16)-C(48)-C(42)	-119.8(7)
C(13)-C(12)-C(18)-C(26)	120.4(7)	C(12)-C(18)-C(26)-C(25)	-54.2(5)
C(23)-C(22)-C(28)-C(36)	107.2(6)	C(22)-C(28)-C(36)-C(35)	108.6(6)
C(33)-C(32)-C(38)-C(46)	-111.2(6)	C(32)-C(38)-C(46)-C(45)	-109.9(6)
O(2) - Ag - O(3)	44.0(3)	O(2) - Ag - O(31)	124.0(2)
O(2) - Ag - C(23)	103.5(2)	O(2) - Ag - C(24)	89.8(2)
O(2) - Ag - C(44)	88.1(2)	O(2) - Ag - C(45)	102.6(2)
O(3) - Ag - O(31)	80.7(2)	O(3) - Ag - C(23)	83.1(2)
O(3) - Ag - C(24)	92.0(2)	O(3) - Ag - C(44)	109.7(3)
O(3) - Ag - C(45)	101.1(2)	O(31) - Ag - C(23)	71.6(2)
O(31) - Ag - C(24)	102.5(2)	O(31) - Ag - C(44)	107.1(2)
O(31) - Ag - C(45)	75.7(2)	C(23) - Ag - C(24)	31.2(2)
C(23) - Ag - C(44)	166.9(2)	C(23) - Ag - C(45)	145.9(2)
C(24) - Ag - C(44)	145.5(2)	C(24) - Ag - C(45)	166.2(2)
C(44) - Ag - C(45)	31.6(2)	Ag - O(2) - N	110.9(5)
Ag - O(3) - N	95.3(5)	C(11) - O(11) - C(17)	115.0(4)
C(21) - O(21) - C(27)	111.8(4)	Ag - O(31) - C(31)	122.9(3)
Ag - O(31) - C(37)	123.1(3)	C(31) - O(31) - C(37)	113.7(4)
C(41) - O(41) - C(47)	113.9(4)	O(1) - N - O(2)	127.6(6)
O(1) - N - O(3)	122.4(6)	O(2) - N - O(3)	109.4(7)
O(11) - C(11) - C(12)	118.7(4)	O(11) - C(11) - C(16)	118.2(5)
C(12) - C(11) - C(16)	123.0(5)	C(11) - C(12) - C(13)	117.1(5)
C(11) - C(12) - C(18)	121.2(5)	C(13) - C(12) - C(18)	121.6(5)

C(12) - C(13) - C(14)	120.6(6)	C(13) - C(14) - C(15)	120.6(6)
C(14) - C(15) - C(16)	121.9(6)	C(11) - C(16) - C(15)	116.7(5)
C(11) - C(16) - C(48)	120.7(5)	C(15) - C(16) - C(48)	122.5(5)
C(12) - C(18) - C(26)	111.9(4)	O(21) - C(21) - C(22)	117.9(4)
O(21) - C(21) - C(26)	119.4(4)	C(22) - C(21) - C(26)	122.5(4)
C(21) - C(22) - C(23)	117.4(4)	C(21) - C(22) - C(28)	121.5(4)
C(23) - C(22) - C(28)	120.9(4)	Ag - C(23) - C(22)	110.5(3)
Ag - C(23) - C(24)	68.9(3)	C(22) - C(23) - C(24)	121.1(5)
Ag - C(24) - C(23)	79.9(3)	Ag - C(24) - C(25)	102.9(4)
C(23) - C(24) - C(25)	119.6(5)	C(24) - C(25) - C(26)	119.7(5)
C(18) - C(26) - C(21)	122.9(5)	C(18) - C(26) - C(25)	118.1(5)
C(21) - C(26) - C(25)	118.9(5)	C(22) - C(28) - C(36)	111.0(4)
O(31) - C(31) - C(32)	119.8(4)	O(31) - C(31) - C(36)	117.3(4)
C(32) - C(31) - C(36)	122.9(4)	C(31) - C(32) - C(33)	118.1(5)
C(31) - C(32) - C(38)	120.8(5)	C(33) - C(32) - C(38)	121.0(5)
C(32) - C(33) - C(34)	121.3(5)	C(33) - C(34) - C(35)	119.7(5)
C(34) - C(35) - C(36)	120.9(5)	C(28) - C(36) - C(31)	120.6(4)
C(28) - C(36) - C(35)	122.0(4)	C(31) - C(36) - C(35)	117.1(4)
C(32) - C(38) - C(46)	111.1(4)	O(41) - C(41) - C(42)	120.3(4)
O(41) - C(41) - C(46)	118.2(4)	C(42) - C(41) - C(46)	121.5(4)
C(41) - C(42) - C(43)	118.5(5)	C(41) - C(42) - C(48)	120.9(5)
C(43) - C(42) - C(48)	120.5(5)	C(42) - C(43) - C(44)	121.9(5)
Ag - C(44) - C(43)	104.5(4)	Ag - C(44) - C(45)	75.1(3)
C(43) - C(44) - C(45)	119.2(5)	Ag - C(45) - C(44)	73.3(3)
Ag - C(45) - C(46)	106.3(3)	C(44) - C(45) - C(46)	120.2(5)
C(38) - C(46) - C(41)	120.0(4)	C(38) - C(46) - C(45)	121.3(4)
C(41) - C(46) - C(45)	118.7(4)	C(16) - C(48) - C(42)	111.9(5)

Table 4.1.3. Crystallographic data of the structure analysis of compound 1 (tetra-*o*-methoxycalix[4]arene silver nitrate)

Formula	$C_{32}H_{32}O_4 \cdot AgNO_3$
Formula wt	650.48
Crystal system	monoclinic
Space group	$P2_1/c$
a Å	10.0693(7)
b Å	24.6923(10)
c Å	11.4950(4)
β °	92.609(4)
V Å ³	2855.09(25)
Z	4
F(0 0 0)	1336
D calc g cm ⁻³	1.513
T K	300.5
Crystal colour and habit	light yellow block
Crystal size mm	0.35 x 0.45 x 0.45
Cell: reflections used θ range(°)	25 reflections 20.8< θ <23.2
μ (Mo-K α) cm ⁻¹	7.45
Transmission on F	0.78 → 1.44
Measured reflections	9304
Unique reflections	9092
Observed reflections $I \geq 3\sigma(I)$	4563
θ range °	0 - 30.33
Miller indices h	0→14
k	-35 →0
l	-16→16
Decay in mean standard (%)	1.5
R_{int}	0.027
No. of parameters	370
R(F)	0.0524
R_w (F)	0.0638
S	2.56
$\Delta\rho_{max}$ and $\Delta\rho_{min}$. eÅ ⁻³	1.1 → -1.0
Δ/σ_{max}	0.08

4.2. The structure of a seven co-ordinate tungsten(II) complex:



4.2.1. Introduction

This compound belongs to a group of mononuclear tungsten(II) complexes which contain the potentially bidentate ligands S_2PMe_2 and norbornadiene (NBD). Assuming an ethylenic bond occupies a single co-ordination site, the metal may either be seven co-ordinate with an 18-electron configuration or six co-ordinate with a 16-electron configuration. X-ray analysis is often the only reliable way of establishing which type of co-ordination occurs in a particular complex. In the case of $[\text{W}(\text{S}_2\text{PMe}_2)_2(\text{CO})(\text{C}_7\text{H}_8)]$, **2**, (see Figure 4.2.1 and Table 4.2.2) the tungsten atom proves to be seven co-ordinate. A notable feature of the chemistry of divalent tungsten is its affinity for inorganic π -donor ligands, such as Cl, Br, I, O, S, or four electron π -donor alkynes (Templeton, Winston & Word, 1981) and for diolefins (e.g. norbornadiene, cyclooctadiene, cyclooctatetraene) (Braterman, Davidson & Sharp, 1976). A mixture of $[\text{WBr}_2(\text{CO})_2(\text{NBD})]$ (50 mg) and NaS_2PMe_2 (30 mg) in Et_2O (8 cm^3) was stirred at room temperature for 20 hours to give an orange solution. After centrifuging the mixture was treated with hexane (15 cm^3) and concentrated in vacuum to give orange red crystal of **2**. The norbornadiene (NBD) derivatives are very stable (Cotton & Meadows, 1984). Preparation, crystallisation and spectroscopic characterisation of this compound has been done by Dr Davidson and his co-workers at Heriot Watt University.

4.2.2. Results and discussion

Important bond distances and angles in **2** are listed in Table 4.2.2. Compounds with six co-ordinate tungsten were described as distorted octahedral by e.g. Cotton & Meadows (1984); Carlton, Davidson, Vasapolla, Douglas & Muir (1993) but in compound **2** the metal co-ordination polyhedron is a distorted

pentagonal bipyramid; the tungsten atom is bonded to all four available donor sulphur atoms, to the π -acid ligand CO and to both double bonds of norbornadiene. The equatorial plane contains the centroids of the two double bonds of norbornadiene and three sulphur atoms; the axial sites are occupied by S(11) (Figure 4.2.1) and by the carbonyl group. The angle S(11)-W-CO is $162.9(4)^\circ$; angles subtended at tungsten by adjacent equatorial donor atoms are in the range $63.8(1)^\circ$ - $77.9(1)^\circ$ and axial - W- equatorial angles are $77.5(1)^\circ$ - $105.5(1)^\circ$ (the angles reported above were calculated by taking the midpoints of double bonds of norbornadiene as polyhedron vertices). The r.m.s. displacement from the equatorial plane is 0.049 \AA .

A survey of the Cambridge Structural Database gave W-S bond distances in 20 structures containing sulphur bonded to six co-ordinate tungsten; the great majority of these bonds are shorter than that in **2**. Thus, W-S bond distances are $2.565(4) - 2.654(4) \text{ \AA}$ in **2**, compared with the mean value of 2.466 \AA derived for such distances. Also bridging W - S bond distances in two different polymorphs of $[\text{W}_2\text{S}_4\{\text{S}_2\text{P}(\text{OEt})_2\}_2]$ and in $[\text{W}_2\text{S}_4(\text{S}_2\text{CNEt}_2)_2]$ (Drew, Hobson, Mumba, Rice & Turp, 1987) are $2.473(5) - 2.498(6) \text{ \AA}$, $2.430(9) - 2.480(10) \text{ \AA}$, and $2.429(9) - 2.448(9) \text{ \AA}$ respectively and in $[\text{W}(\text{SC}_6\text{H}_2\text{Pr}^i\text{-}2,4,6)_2(\text{CO})_2(\text{PMePh})_2]$ (Burrow, Lough, Morris, Hill, Hughes, Lane & Richards, 1991) they are $2.460(2)$ and $2.395(2) \text{ \AA}$. This bond length dramatically shortens in $[\text{WBr}_2(\text{SC}_6\text{F}_5)(\text{CO})(\text{NBD})]$ (Carlton, Davidson, Vasapolla, Douglas, Muir, 1993) to $2.322(5)^\circ$ where W is six co-ordinate. The metal-(C=C) bond distances in **2** [$2.265(13) - 2.334(12) \text{ \AA}$] are shorter than both the accepted mean value of 2.430 \AA for such distances and the corresponding distances in $[\text{W}(\text{CO})_4(\text{NBD})]$ [$2.403(6) - 2.419(5) \text{ \AA}$], (Grevels, Jacke, Betz, Kruger & Tsay, 1989), but there is no significant difference in metal-(C=C) bond distances with the $[\text{WBr}_2(\text{SC}_6\text{F}_5)(\text{CO})(\text{NBD})]$ complex (Carlton, Davidson, Vaspolla, Douglas & Muir, 1993). In contrast the W - CO distance in **2** [$1.923(13)$] seems slightly shorter than either the mean value for W - CO bond distance of 2.003 \AA or the value of $2.040(18) - 1.975(19)$ in

[WBr₂(S₂C₆F₅)(CO)₂(NBD) (Carlton, Davidson, Vasapolla, Douglas & Muir, 1993).

4.2.3. Experimental

Crystallographic data and the fractional co-ordinates for non-hydrogen atoms are given in Tables 4.2.1 and 4.2.3. The structure was solved by Patterson and Fourier methods. The final full-matrix least squares refinement on F included anisotropic displacement parameters for all elements except hydrogen. Absorption corrections have been done by Gaussian quadrature over the crystal volume. All calculations were performed with the GX package (Mallinson & Muir, 1985). Additional material available includes hydrogen atom co-ordinates and observed and calculated structure factors.

Caption to Figure

Figure 4.2.1. A view of the $[\text{W}(\text{S}_2 \text{PMe}_2)_2(\text{CO})(\text{C}_7\text{H}_8)]$ molecule. 50% probability ellipsoids are displayed except for hydrogen atoms which are represented by spheres of arbitrary radius.

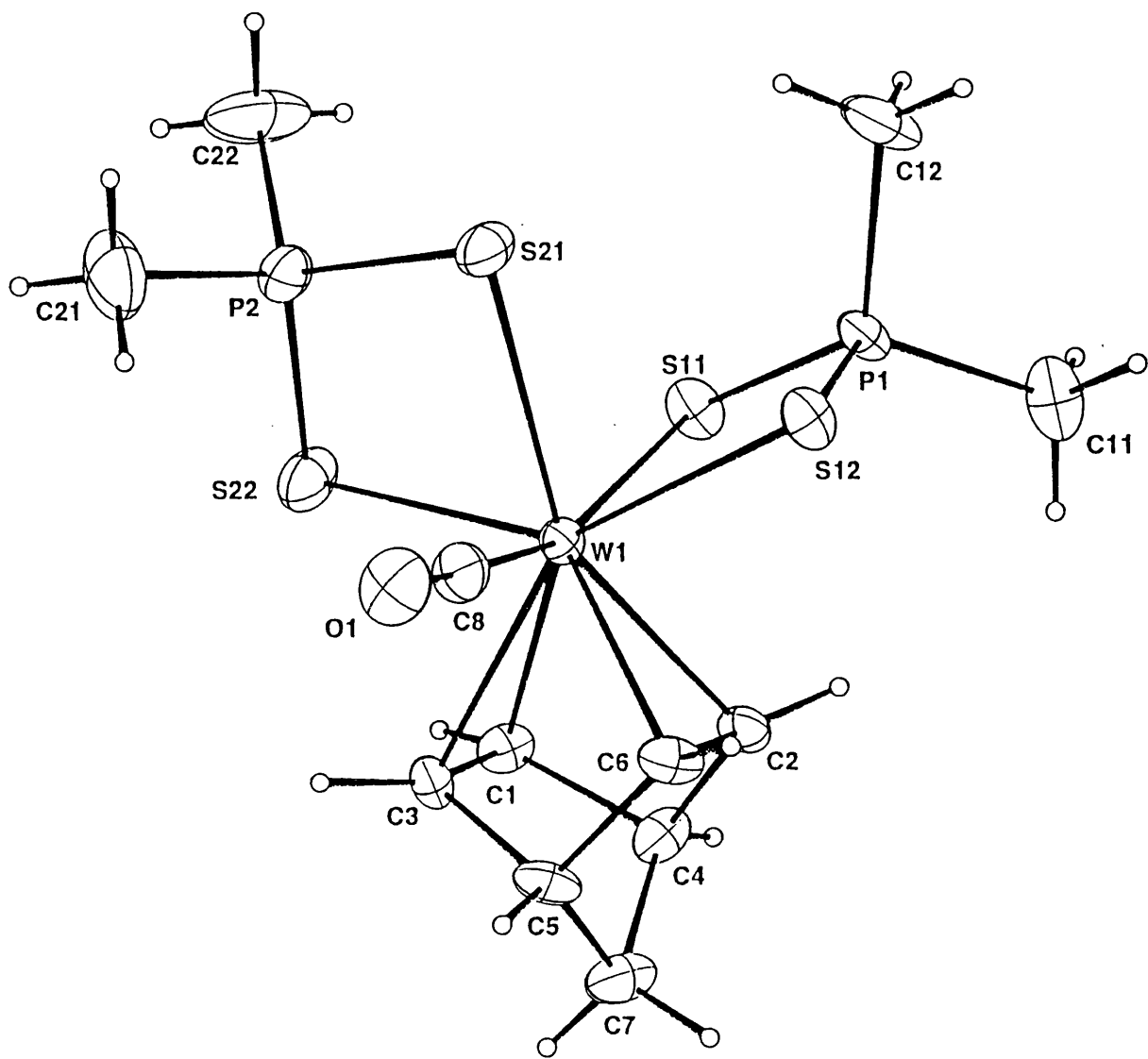


Figure 4.2.1

Table 4.2.1. Atomic fractional co-ordinates and isotropic displacement parameters (\AA^2) for compound **2** [$\text{W}(\text{S}_2\text{PMe}_2)_2(\text{CO})(\text{C}_7\text{H}_8)$]

Atom	x	y	z	U
W	0.17780(3)	0.09177(5)	0.21950(4)	0.025
S(11)	0.0075(2)	0.0992(4)	0.2973(2)	0.037
S(12)	0.2422(2)	0.2217(4)	0.3706(2)	0.036
S(21)	0.2461(3)	-0.0872(4)	0.3498(2)	0.044
S(22)	0.0987(3)	-0.1309(3)	0.1541(3)	0.049
P(1)	0.0946(2)	0.2000(3)	0.4025(2)	0.033
P(2)	0.1816(3)	-0.2290(3)	0.2619(3)	0.040
O	0.4053(7)	0.0284(11)	0.1830(8)	0.059
C(1)	0.0689(9)	0.1303(12)	0.0796(8)	0.034
C(2)	0.1334(10)	0.3025(13)	0.1776(8)	0.035
C(3)	0.1717(9)	0.1107(13)	0.0582(8)	0.035
C(4)	0.0563(9)	0.2829(13)	0.0843(9)	0.038
C(5)	0.2217(9)	0.2470(14)	0.0540(9)	0.041
C(6)	0.2372(9)	0.2796(14)	0.1576(8)	0.039
C(7)	0.1221(11)	0.3289(14)	0.0114(10)	0.050
C(8)	0.3190(10)	0.0572(13)	0.1955(9)	0.041
C(11)	0.0353(10)	0.3574(15)	0.4237(11)	0.053
C(12)	0.1088(13)	0.1159(17)	0.5151(10)	0.063
C(21)	0.2766(13)	-0.3324(19)	0.2214(12)	0.076
C(22)	0.1000(14)	-0.3349(20)	0.3148(14)	0.093

Table 4.2.2. Selected bond distances (Å) and bond angles (°)

(a) bond distances

W - S(11)	2.615(3)	W - S(12)	2.565(4)	W - S(21)	2.654(4)
W - S(22)	2.584(4)	W - C(1)	2.283(12)	W - C(2)	2.265(13)
W - C(3)	2.334(12)	W - C(6)	2.289(14)	W - C(8)	1.923(13)
S(11) - P(1)	2.003(5)	S(12) - P(1)	2.026(5)	S(21) - P(2)	2.000(6)
S(22) - P(2)	1.992(6)	P(1) - C(11)	1.814(15)	P(1) - C(12)	1.822(16)
P(2) - C(21)	1.777(18)	P(2) - C(22)	1.76(2)	O - C(8)	1.182(16)
C(1) - C(3)	1.412(16)	C(1) - C(4)	1.558(19)	C(2) - C(4)	1.539(17)
C(2) - C(6)	1.421(17)	C(3) - C(5)	1.527(19)	C(4) - C(7)	1.532(19)
C(5) - C(6)	1.517(18)	C(5) - C(7)	1.551(19)		

(b) bond angles

S(11) - W - S(12)	77.5(1)	S(11) - W - S(21)	84.6(2)
S(11) - W - S(22)	83.3(2)	S(11) - W - C(1)	87.5(3)
S(11) - W - C(2)	84.3(4)	S(11) - W - C(3)	123.0(3)
S(11) - W - C(6)	120.1(4)	S(11) - W - C(8)	162.9(4)
S(12) - W - S(21)	74.2(2)	S(12) - W - S(22)	143.9(2)
S(12) - W - C(1)	136.5(4)	S(12) - W - C(2)	76.8(3)
S(12) - W - C(3)	139.7(4)	S(12) - W - C(6)	80.1(4)
S(12) - W - C(8)	94.5(4)	S(21) - W - S(22)	73.8(2)
S(21) - W - C(1)	145.3(4)	S(21) - W - C(2)	150.6(3)
S(21) - W - C(3)	135.9(4)	S(21) - W - C(6)	139.3(3)
S(21) - W - C(8)	78.7(4)	S(22) - W - C(1)	71.7(4)
S(22) - W - C(2)	131.5(4)	S(22) - W - C(3)	76.2(4)
S(22) - W - C(6)	135.8(4)	S(22) - W - C(8)	95.3(4)
C(1) - W - C(2)	61.0(5)	C(1) - W - C(3)	35.6(4)
C(1) - W - C(6)	72.6(5)	C(1) - W - C(8)	108.3(5)
C(2) - W - C(3)	72.0(5)	C(2) - W - C(6)	36.4(5)
C(2) - W - C(8)	108.7(5)	C(3) - W - C(6)	59.6(5)
C(3) - W - C(8)	72.7(5)	C(6) - W - C(8)	72.4(5)
W - S(11) - P(1)	87.3(2)	W - S(12) - P(1)	88.2(2)
W - S(21) - P(2)	89.5(2)	W - S(22) - P(2)	91.7(2)
S(11) - P(1) - S(12)	107.1(2)	S(11) - P(1) - C(11)	112.7(5)
S(11) - P(1) - C(12)	113.5(6)	S(12) - P(1) - C(11)	112.0(5)
S(12) - P(1) - C(12)	107.7(6)	C(11) - P(1) - C(12)	103.9(8)
S(21) - P(2) - S(22)	104.1(3)	S(21) - P(2) - C(21)	114.0(6)
S(21) - P(2) - C(22)	111.7(7)	S(22) - P(2) - C(21)	109.5(7)
S(22) - P(2) - C(22)	111.9(7)	C(21) - P(2) - C(22)	105.8(9)
W - C(1) - C(3)	74.2(7)	W - C(1) - C(4)	100.5(8)
C(3) - C(1) - C(4)	104.8(10)	W - C(2) - C(4)	101.8(8)
W - C(2) - C(6)	72.7(8)	C(4) - C(2) - C(6)	105.8(10)
W - C(3) - C(1)	70.2(7)	W - C(3) - C(5)	100.0(8)
C(1) - C(3) - C(5)	106.9(11)	C(1) - C(4) - C(2)	96.4(10)
C(1) - C(4) - C(7)	101.5(10)	C(2) - C(4) - C(7)	103.1(10)
C(3) - C(5) - C(6)	98.1(10)	C(3) - C(5) - C(7)	100.6(10)
C(6) - C(5) - C(7)	103.5(11)	W - C(6) - C(2)	70.9(8)
W - C(6) - C(5)	102.3(9)	C(2) - C(6) - C(5)	105.8(10)
C(4) - C(7) - C(5)	94.0(11)	W - C(8) - O	175.9(12)

Table 4.2.3. Crystallographic details for $W(S_2PMe_2)_2(CO)(C_7H_8)$

Formula	$C_{12}H_{20}OP_2S_4W$
Formula weight	554.34
Crystal system	monoclinic
Space group	$P2_1/a$
a Å	12.737(3)
b Å	10.138(2)
c Å	14.496(4)
β °	100.054(18)
V Å ³	1843.3(6)
Z	4
F(0 0 0)	1072
D calc g cm ⁻³	1.997
T K	305
Crystal colour and habit	orange-red block
Crystal size mm	0.33 x 0.33 x 0.23
Cell: reflections used θ range (°)	20 15.6 < θ < 24.1
$\mu(Mo-K\alpha)$ cm ⁻¹	70.03
Transmission on F ²	0.13474 - 0.28032
Measured reflections total	5826
Unique reflections	5344
Observed reflections $I \geq 3\sigma(I)$	2910
θ range °	3.1 - 30
Miller indices h	17 → 17
k	-14 → 0
l	0 → 20
Decay in mean standard (%)	2
R _{int}	0.042
No. of parameters	181
R(F)	0.048
R _w (F)	0.055
S	1.93
$\Delta\rho_{max}$ and $\Delta\rho_{min}$ eÅ ⁻³	1.46 → -1.34
Δ/σ_{max}	0.05

References

- Atwood, J. L., Davies, J. E. & MacNicol, D. D. (1991). *Inclusion Compounds*, Oxford University Press, New York, vol. 4.
- Atwood, J. L., Orr, G. W., Means, N. C., Hamada, F., Zhang, H., Bott S. G. & Robinson, K. D. (1992). *Inorg. Chem.* 31, 603-606.
- Atwood, J. L., Bott, S. G., Jones, C. & Raston, C. L. (1992). *J. Chem. Soc. Chem. Commun.* 1992, 1349-1351.
- Blount, J. F. & Westley, J. W. (1971). *J. Chem. Soc. Commun.* 927-928.
- Braterman, P. S., Davidson, J. L. & Sharp, D. W. A. (1976). *J. Chem. Soc. Dalton Trans.* 241-245.
- Burrow, T. E., Lough, A. J., Morris, R. H., Hill, A., Hughes, D. L., Lane, J. D. & Richards, R. L. (1991). *J. Chem. Soc. Dalton Trans.* 2519-2526.
- Carlton, L., Davidson, J. L., Vasapolla, G., Douglas, G. & Muir, K. W. (1993). *J. Chem. Soc. Dalton Trans.* 3341-3347.
- Corazza, F., Floriani, C., Chiesi-Villa, A. & Guastini, C. (1990a). *J. Chem. Soc. Chem. Commun.* 640-641.
- Corazza, F., Floriani, C., Chiesi-Villa, A. & Guastini, C. (1990b). *J. Chem. Soc. Chem. Commun.* 1083-1084.
- Cotton, F. A. & Meadows, J. H. (1984). *Inorg. Chem.* 23, 4688-4693.
- Davidson, J. L. & Vasapolla, G. (1983). *J. Organomet. Chem.* 241, C24-C26.
- Drew, M. G. B., Hobson, R. J., Mumba, P. P. E. M., Rice, D. A. & Turp, N. (1987). *J. Chem. Soc. Dalton Trans.* 1163-1167.
- Gallagher, J. F., Ferguson, G., Bohmer, V. & Kraft, D. (1994). *Acta Cryst. C* 50, 73-77.
- Gano, J. E., Subramaniam, G. & Birnbaum, R. (1990). *J. Org. Chem.* 55, 4760-4763.
- Grevels, F. W., Jacke, J., Betz, P., Kruger, C. & Tsay, Y. H. (1989). *Organometallics*, 8, 293-298.

- Gutsche, C. D. (1989). *Calixarenes*, The Royal Society Monographs in Supramolecular Chemistry, Cambridge University Press, Cambridge, UK.
- Gutsche, C. D., Dhowan, B., Levine, J. A., No, K. H. & Bauer, L. (1983). *J Tetrahedron*, 39, 409-426.
- Harrowfield, J. M., Ogden, M. I., Richmond, W. R. & White, A. H. (1991). *J. Chem. Soc. Chem. Commun.* 1159-1161.
- Jones, P. J., Gries, H., Grutzmacher, H., Reosky, H. W., Schimkowiak, J. & Sheldrick, G. M. (1984). *Angew. Chem.* 23, 376-376.
- Kang, H. C., Hanson, A. W., Eaton, B. & Boekelheide, V. (1985). *J. Amer. Chem. Soc.* 107, 1979-1985.
- Lindoy, L. F. (1989). *The Chemistry of Macrocyclic Ligand Complexes*, Cambridge University Press, Cambridge, U. K.
- Mallinson, P. & Muir, K. W. (1985). *J. Appl. Cryst.* 18, 51-53.
- Meyer, P. P., Rimsky, A. & Cheralier, R. (1978). *Acta Cryst.* B34, 1457-1462.
- Piere, J. L., Baret, P., Chautemps, P. & Armand, M. (1981). *J. Amer. Chem. Soc.* 103, 2986-2988.
- Roundhill, D. M., Georgiev, E. & Yordanov, A. (1994). *J. Incl. Pheno*, 19, 101-109.
- Templeton, J. L., Winston, P. B. & Word, B. C. (1981). *J. Amer. Chem. Soc.*, 103, 7713-7721.
- Ugozzoli, F & Andreetti, G. D. (1991). *J. Incl. Phenom.*, 13, 337-348.
- Vincens, J., Asfari, Z. & Harrowfield, J. M. (1994). *Calixarenes 50th Anniversary*, Kluwer Academic Publisher, Netherland.
- Walker, N. & Stuart, D. (1983). *Acta Cryst.* A39, 158-166.
- Xu, W., Puddephatt, R. J., Muir, K. W. & Torabi, A. A. (1994). *Organometallics*, 13, 3054-3062.

